

**UNIVERSIDADE FEDERAL DE SÃO CARLOS**

**CENTRO DE CIÊNCIAS EXATAS E DE TECNOLOGIA**

**DEPARTAMENTO DE QUÍMICA**

**PROGRAMA DE PÓS-GRADUAÇÃO EM QUÍMICA**

**“COVALENT MODIFICATION OF ANTIMICROBIAL AND ANTICANCER  
PEPTIDES FOR THE IMPROVEMENT OF THEIR FARMACOLOGICAL  
PROPERTIES.”**

**Fidel Ernesto Morales Vicente\***

Tese apresentada como parte dos requisitos para  
obtenção do título de DOUTOR EM CIÊNCIAS,  
área de concentração: QUÍMICA ORGÂNICA.

**Orientador: Prof. Dr. Márcio Weber Paixão**

**Co-orientador: Dra. Hilda Elisa Garay**

**\* bolsista CAPES e Convenio de cotutela entre a Universidade da Habana, Cuba e a  
Unversidade Federal de sao Carlos, Brasil**

**São Carlos - SP**

**2019**



UNIVERSIDADE FEDERAL DE SÃO CARLOS

Centro de Ciências Exatas e de Tecnologia  
Programa de Pós-Graduação em Química

Folha de Aprovação

Assinaturas dos membros da comissão examinadora que avaliou e aprovou a Defesa de Tese de Doutorado do candidato Fidel Ernesto Morales Vicente, realizada em 16/08/2019.

Prof. Dr. Márcio Weber Paixão  
UFSCar

Prof. Dr. Julio Zukerman Schpector  
UFSCar

Prof. Dr. Roberto Gomes de Souza Berlinck  
USP

Prof. Dr. Paulo Cezar Vieira  
UFSCar

Prof. Dra. Anita Jocelyne Marsaioli  
UNICAMP

*“El hombre razonable se adapta al mundo, el irrazonable trata de adaptar el mundo a sí mismo. Por tanto, todo el progreso depende del hombre irrazonable.”*

***R. F. Retamar”***

***To my love Roxy***

## **Acknowledgements**

Foremost, I would like to thank my family, especially my mother, my brother and my grandmother. Thank you for your support through all these years. I want also to thank Roxy, my friend and beautiful love, for all the patience and understanding during these years.

I also thank to my advisor Prof. Marcio Weber Paixão from the Centre of Excellence for Research in Sustainable Chemistry (CERSusChem), for being such a great teacher and always pleasant to be around. Especially, I want to show my eternal gratitude to my advisor in Cuba, Dra. Hilda Elisa Garay, head of the Laboratory of Peptides Synthesis at CIGB. I thank both for the opportunity that they gave me to develop this project.

Moreover, I would like to thank my lab mates. My thanks to Alexander (Fidel), Jose, Erlen, Sajjad Ali, Akbar Ali, Floyd, Wanderson, Sussette, Gustavo Piva, Radell, Barbara and all the colleagues in the lab.

Furthermore, I also thank my friends in Cuba: Gerardo, Elena and my students Yeslie, Irodiel, Erbio, Melaine, Xiomara and Asiel. Especially I want to show my eternal gratitude to the personal of the Laboratory of Peptide Synthesis, at the CIGB in Cuba.

I want to thank especially to professor Rosemeire Pietro at the Faculty of Pharmacy in Araraquara for the biological evaluation of the Cm-p5 mutant analogue. Also, my gratitude to professor Anselmo Otero for showing me the Cm-p5, for the biological test of the cyclic and dimeric analogues realized in Germany and all the personal of the laboratory of Core Facility for Functional Peptidomics in the Ulm University, Germany, directed by professor Ludger Standker.

Last but not least, I want to thank my friend and partner Pablo Eduardo Rosi from the Buenos Aires University in Argentina who in special show me the pHLIP peptide and the possible applications in the targeted delivery of drugs to tumors.

My sincere thanks to Coordenação de Aperfeiçoamento de Pessoal de Nível Superior - Brasil (CAPES), which provided the fellowships for my PhD studies at UFSCar and for the research period abroad, an experience that enriched me as a person and as a researcher. Also, my eternal acknowledgments to CIGB for the transmission of their knowledge, experience and financial support.

## List of Abbreviations

ACN	Acetonitrile	LUMO	lowest unoccupied molecular orbital
Aa	aminoacid	LCC	Liquid Column Chromatography
Alloc	Allyloxycarbonyl	MCR	Multicomponent reaction
Acm	acetamidomethyl	MAP	Multiantigenic peptide
Ac <sub>2</sub> O	Acetic anhydride	MIC	Minimal inhibitory concentration
ATCC	American Type Culture Collection	MOPS	3-morpholinopropane-1-sulfonic acid buffer
AMPs	Antimicrobial peptides	M38-A2	Reference Method for Broth Dilution Antifungal Susceptibility Testing of Filamentous Fungi
ALS	amyotrophic lateral sclerosis	MBHA	methylbenzhydrylamine
AMPs	antimicrobial peptides	MIC	minimal inhibitory concentration
ADME	absorption, distribution, metabolism, and excretion	ME	multiple sclerosis
ADCs	Antibody drug conjugate	NMR	nuclear magnetic resonance
Boc	tert-Butyloxycarbonyl	OxymaK	2-Cyano-2-(hydroxyimino)acetic acid ethyl ester, potassium sa
Bzl	benzoyl	OxymaPure or Oxyma	ethyl cyano-(hydroxyimino) acetate
Cm-p1	Cenchritis muricatus derived peptide one	PBS	phosphate-buffered saline
Cm-p3	Cenchritis muricatus derived peptide three	PAB	para-aminobenzyl
Cm-p4	Cenchritis muricatus derived peptide four	PABOH	para-aminobenzyl alcohol
Cm-p5	Cenchritis muricatus derived peptide five	PDCs	Peptide drug conjugates
CFZ	Carfilzomib	Py	pyridine
CFU	colony-forming unit	Pip	Piperidine
CD	circular dichroism	PEG	Polyethyleneglycol
<i>C. albicans</i>	<i>Candida albicans</i>	PyBOP	benzotriazol-1-yl-oxytripyrrolidinophosphonium hexafluorophosphate
<i>C. parapsilosis</i>	<i>Candida parapsilosis</i>	PPG	polypropyleneglycol
<i>C. auris</i>	<i>Candida auris</i>	Pbf	2,2,4,6,7-Pentamethyldihydrobenzofuran-5-sulfonyl
CIGB	Center for Genetic Engineering and Biotechnology	pK <sub>ar</sub>	logarithmic acid dissociation constant of the group at the lateral chain
CLSI	Clinical and Laboratory Standards Institute	pK <sub>br</sub>	logarithmic base dissociation constant of the group at the lateral chain
Cit	citruline	pK <sub>hr</sub>	logarithmic hydrolysis dissociation constant of the group at the lateral chain
Caproic acid	n-hexanoic acid	PPTS	Pyridinium para-toluene sulfonate
Cbz or Z	Carbobenzyloxy	<i>P. aeuginosa</i>	<i>Pseudomonas aeuginosa</i>
DIC	<i>N,N'</i> -Diisopropylcarbodiimide	pHLIP	pH Low Insertion Peptide
DIEA	Diisopropylethylamine	PBMCs	Peripheral Blood Mononuclear Cells

DMF	<i>N,N</i> -dimethylformamide	PTSA	para-toluenesulfonic acid
DMA	dimethylacetamide	QTOF-2	hybrid quadrupole time of flight mass spectrometer
DCC	dicyclohexylcarbodiimide	RP-HPLC	reversed phase high performance liquid chromatography
DHP resin	3,4-Dihydro-2H-pyran-2-yl-methoxymethyl polystyrene resin	RFU	relative fluorescence units
DMSO	dimethyl sulfoxide	Rink Resin or Am-Resin	4-(2',4'-Dimethoxyphenyl-Fmoc-aminomethyl)-phenoxy resin
DMEM	Dulbecco's modified Eagle's médium	RPMI	Roswell Park Memorial Institute Medium
DCM	Dichloromethane	SPC	Simple Point Charge (water model used)
EDC	1-Ethyl-3-(3-dimethylaminopropyl)carbodiimide	SAR	structure activity relationship
E1-Cb	Unimolecular elimination of the conjugate base	SAR	structure activity relationships
EDT	1,2-Ethanedithio	SPPS	Solid phase peptide synthesis
ESI-MS	Electrospray Ionisation Mass Spectrometry:	S <sub>N</sub> 2	Bimolecular nucleophilic substitution
ESI-HRMS	High resolution electrospray ionization mass spectrometry	S <sub>N</sub> Ar	Nucleophilic aromatic substitution
Fmoc	fluorenylmethoxycarbonyl	SDS	Sodium dodecylsulfate
HOBt	1-hydroxybenzotriazole	SAR	Structure activity relationship
HBTU	O-benzotriazo-1-yl- <i>N,N,N',N'</i> -tetramethyluroniumhexafluorophosphate	THF	tetrahydrofuran
HATU	1-[Bis(dimethylamino)methylene]-1H-1,2,3-triazolo[4,5-b]pyridinium 3-oxid hexafluorophosphate	TFA	Trifluoroacetic acid
HOAt	1-Hydroxy-7-azabenzotriazole	Trt	trityl
HOObt	Hydroxy-3,4-dihydro-4-oxo-1,2,3-benzotriazine	TBDPSCI	<i>t</i> -butyldiphenylsilylchloride
HOMO	Highest occupied molecular orbital	TIS	triisopropylsilane
HOSu	<i>N</i> -hydroxysuccinimide	TBTU	2-(1H-Benzotriazole-1-yl)-1,1,3,3-tetramethylammonium tetrafluoroborate
HMBA	<i>p</i> -hydroxymethylbenzoic acid	TIS	Triisopropylsilane
HIV	Human immunodeficiency virus	Tos or Ts	tosyl
hMDMs	human monocyte derived macrophages	THP-1 human cells	Human monocytic cell line derived from an acute monocytic leukemia patient.
HEPES	4-(2-hydroxyethyl)-1-piperazineethanesulfonic acid buffer	TFE	2,2,2-trifluoroethanol
Hcy	homo-cysteine	Ugi-4CR	Ugi four component reaction
Hph	homo-phenylalanine	YPD	Yeast Extract Peptone Dextrose
IMCR	Isocyanide multicomponent reaction	Z (2-Br)	2-bromo-carbobenzyloxy
<i>L. monocytogenes</i>	<i>Listeria monocytogenes</i>	Z (2-Cl)	2-chloro-carbobenzyloxy

## List of Tables

TABLE 1: SOME CHARACTERISTICS OF THE MOST USED POLYMER SUPPORTS. ....	12
TABLE 2: HELICAL PARAMETERS FOR NON-AMIDATED CM-P1, CM-P3, CMP4 AND CM-P5.....	19
TABLE 3: HELICAL PARAMETERS OF CM-P5 ANALOGUES.....	21
TABLE 4: BIOLOGICAL ACTIVITY MEASURED AS MINIMAL INHIBITORY CONCENTRATION (MIC) AGAINST DIFFERENT BACTERIA AND FUNGI FOR EACH SYNTHESIZED PEPTIDE. (NT: NOT TESTED) .....	22
TABLE 5: MINIMAL INHIBITORY CONCENTRATION (MIC) ( $\mu\text{g/mL}$ ) OF CM-P5 AND DERIVATIVES AGAINST THREE <i>CANDIDAS</i> , A GRAM-POSITIVE AND A GRAM-NEGATIVE BACTERIAL SPECIES.....	29
TABLE 6: AGAR DIFFUSION TEST (MM) OF CM-P5, CYSCYSCM-P5 CYCLIC MONOMER AND DIMERS AGAINST GRAM- POSITIVE AND GRAM-NEGATIVE BACTERIAL SPECIES. ....	41
TABLE 7: EFFECT OF DIFFERENT AMINOACIDS ON LOCAL PEPTIDE DYNAMIC .....	67
TABLE 8: HELICAL PARAMETERS FOR TWO INDEPENDENT HELICES AND A POSSIBLE TOTAL HELIX OF MELITTIN. <a href="http://heliquest.ipmc.cnrs.fr/cgi-bin/computparams.py">HTTP://HELIQUEST.IPMC.CNRS.FR/CGI-BIN/COMPUTPARAMS.PY</a> <sup>97</sup> .....	68
TABLE 9: HELICAL PARAMETERS FOR TWO INDEPENDENT HELICES AND A POSSIBLE TOTAL HELIX OF THE <i>N</i> - TERMINAL DOMAIN OF HISTONE H1E. <a href="http://heliquest.ipmc.cnrs.fr/cgi-bin/computparams.py">HTTP://HELIQUEST.IPMC.CNRS.FR/CGI-BIN/COMPUTPARAMS.PY</a> <sup>97</sup> .....	69
TABLE 10: ANTIFUNGAL ACTIVITY OF THE LIPIDATED ANALOGUES OF CM-P5. ....	72
TABLE 11: ANTIFUNGAL ACTIVITY OF DECANOIL AND PENTADECANOIL LIPIDATED ANALOGUES OF CM-P5.....	76
TABLE 12: THERMODYNAMICAL PROPERTIES OF ALA, GLY AND PRO CONTAINING PEPTIDES.....	79

## List of Charts

CHART 1: CD ANALYSIS IN WATER AND 10% SDS. SECONDARY STRUCTURE CONTENT (IN PERCENTAGE) CALCULATED WITH THE ONLINE PROGRAM BESTSEL ( <a href="http://bestsel.elte.hu">HTTP://BESTSEL.ELTE.HU</a> ). ....	29
CHART 2: <i>IN VITRO</i> CYTOTOXICITY OF CYSCYSCM-P5 CYCLIC MONOMER AND DIMERS AGAINST MACROPHAGES AND THP-1 HUMAN CELLS. ....	30
CHART 3: SIMULATION BY MOLECULAR DYNAMIC OF THE DISTANCE BETWEEN SULFUR ATOMS IN THE $\alpha$ -HELIX OF ACYCLIC PEPTIDE CYSCYSCM-P5.....	57

## List of Figures

FIGURE 1: COMMON COUPLING REAGENTS FOR PEPTIDES, A) CARBODIIMIDES, B) PHOSPHONIUM SALTS AND C) URONIUM SALTS. ....	8
FIGURE 2: MOST COMMON RACEMIZATION INHIBITORS. ....	10
FIGURE 3: SOME AMINO AND CARBOXYLATE PROTECTING GROUPS. ....	10
FIGURE 4: STABILIZATION OF THE $\alpha$ -HELIX OF A PEPTIDE BY SALT BRIDGE INTERACTIONS OF THE RESIDUES GLU(E) RED AND LYS(K) BLUE OF THE SIDE CHAIN SPACED AT $I, I+3$ AND $I, I+4$ AND BY HYDROGEN BONDS FORMED BETWEEN COI --- NH( $I+4$ ) (GREEN). <sup>64B</sup> .....	15
FIGURE 5: SCHIFFER-EDMUNDSON PROJECTIONS OF THE ANTIFUNGAL PEPTIDES CM-P1 (A), CM-P3 (B), CM-P4 (C) AND CM-P5 (D). ....	19
FIGURE 6: SCHIFFER-EDMUNDSON PROJECTION OF PEPTIDES ANALOGUES OF CM-P5. ....	21
FIGURE 7: DESIGNED CYCLIC ANALOGUES OF CM-P5. HELICAL WHEEL PROJECTION OF CYS CYS CM-P5 AND HELICOIDAL PARAMETERS. ....	25
FIGURE 8: PARALLEL (LEFT) AND ANTI-PARALLEL (RIGHT) DIMERIC CYS CYS CM-P5 .....	27
FIGURE 9: PROPOSED RELATIVE ORIENTATION OF $\mu$ HREL WITH RESPECT TO THE DIPOLE MOMENT OF CHARGED RESIDUES THAT MAXIMIZE THE RESULTANT DIPOLE MOMENT VECTOR NEEDED FOR OPTIMAL INTERACTION WITH ANTIMICROBIAL MEMBRANES (A). FORMATION (B), STABILIZATION (C) AND DESTABILIZATION (DUE TO NEGATIVELY CHARGED SODIUM ATOM) (D) OF SALT BRIDGES BETWEEN HIS AND GLU IN $I, I+4$ POSITIONS. .	41
FIGURE 10: RP-HPLC (CRUDE IN THE LEFT UPPER PANEL) (PURE IN THE RIGHT UPPER PANEL) AND ESI-HRMS (LOWER PANEL) OF CM-P5 PEPTIDE. ....	42
FIGURE 11: RP-HPLC (CRUDE IN THE LEFT UPPER PANEL) (PURE IN THE RIGHT UPPER PANEL) AND ESI-HRMS (LOWER PANEL) OF PEPTIDE 1. ....	43
FIGURE 12: RP-HPLC (CRUDE IN THE LEFT UPPER PANEL) (PURE IN THE RIGHT UPPER PANEL) AND ESI-HRMS (LOWER PANEL) OF PEPTIDE 2. ....	43
FIGURE 13: RP-HPLC (CRUDE IN THE LEFT UPPER PANEL) (PURE IN THE RIGHT UPPER PANEL) AND ESI-HRMS (LOWER PANEL) OF PEPTIDE 3. ....	44
FIGURE 14: RP-HPLC (CRUDE IN THE LEFT UPPER PANEL) (PURE IN THE RIGHT UPPER PANEL) AND ESI-HRMS (LOWER PANEL) OF PEPTIDE 4. ....	44
FIGURE 15: RP-HPLC (CRUDE IN THE LEFT UPPER PANEL) (PURE IN THE RIGHT UPPER PANEL) AND ESI-HRMS (LOWER PANEL) OF PEPTIDE 5. ....	45
FIGURE 16: RP-HPLC (CRUDE IN THE LEFT UPPER PANEL) (PURE IN THE RIGHT UPPER PANEL) AND ESI-HRMS (LOWER PANEL) OF PEPTIDE 6. ....	45
FIGURE 17: RP-HPLC (CRUDE IN THE LEFT UPPER PANEL) (PURE IN THE RIGHT UPPER PANEL) AND ESI-HRMS (LOWER PANEL) OF PEPTIDE 7. ....	46
FIGURE 18: RP-HPLC (CRUDE IN THE LEFT UPPER PANEL) (PURE IN THE RIGHT UPPER PANEL) AND ESI-HRMS (LOWER PANEL) OF PEPTIDE 8. ....	46
FIGURE 19: RP-HPLC (CRUDE IN THE LEFT UPPER PANEL) (PURE IN THE RIGHT UPPER PANEL) AND ESI-HRMS (LOWER PANEL) OF PEPTIDE 9. ....	47



FIGURE 20: RP-HPLC (CRUDE IN THE LEFT UPPER PANEL) (PURE IN THE RIGHT UPPER PANEL) AND ESI-HRMS (LOWER PANEL) OF PEPTIDE 10.....	47
FIGURE 21: RP-HPLC (CRUDE IN THE LEFT UPPER PANEL) (PURE IN THE RIGHT UPPER PANEL) AND ESI-HRMS (LOWER PANEL) OF THE PEPTIDE 11.....	48
FIGURE 22: RP-HPLC (CRUDE IN THE LEFT UPPER PANEL) (PURE IN THE RIGHT UPPER PANEL) AND ESI-HRMS (LOWER PANEL) OF PEPTIDE 12.....	48
FIGURE 23: RP-HPLC (CRUDE IN THE LEFT UPPER PANEL) (PURE IN THE RIGHT UPPER PANEL) AND ESI-HRMS (LOWER PANEL) OF PEPTIDE 13.....	49
FIGURE 24: RP-HPLC (CRUDE IN THE LEFT UPPER PANEL) (PURE IN THE RIGHT UPPER PANEL) AND ESI-HRMS (LOWER PANEL) OF PEPTIDE 14.....	49
FIGURE 25: RP-HPLC (UPPER PANEL) AND ESI-HRMS (LOWER PANEL) OF THE ACYCLIC CYS <sub>2</sub> CYS <sub>2</sub> CM-P <sub>5</sub> PEPTIDE.....	50
FIGURE 26: CHROMATOGRAPHIC EVOLUTION OF CYCLIZATION OF CYS <sub>2</sub> CYS <sub>2</sub> CM-P <sub>5</sub> PEPTIDE AT 0.5 mM.....	50
FIGURE 27: ESI-HRMS OF THE COMPOUNDS (ORDERED BY TIME RETENTION) FORMED DURING CYCLIZATION OF CYS <sub>2</sub> CYS <sub>2</sub> CM-P <sub>5</sub> PEPTIDE.....	50
FIGURE 28: CYS <sub>2</sub> CYS <sub>2</sub> CM-P <sub>5</sub> PEPTIDE DIMERS STRUCTURE AND RP-HPLC OF THE PURIFIED PRODUCTS (LEFT: PARALLEL, RIGHT: ANTIPARALLEL) FORMED BY TWO INTERMOLECULAR DISULFIDE BRIDGES.....	51
FIGURE 29: CHROMATOGRAPHIC EVOLUTION OF CYCLIZATION OF CYS <sub>2</sub> CYS <sub>2</sub> CM-P <sub>5</sub> PEPTIDE AT 0.1 mM.....	51
FIGURE 30: RP-HPLC (CRUDE AT LEFT UPPER PANEL) (PURE AT RIGHT UPPER PANEL) AND ESI-HRMS (LOWER PANEL) OF CYCLIZATION OF CYS <sub>2</sub> CYS <sub>2</sub> CM-P <sub>5</sub> PEPTIDE AT 0.03 mM AFTER 24 H.....	51
FIGURE 31: RP-HPLC (UPPER PANEL) AND ESI-HRMS (LOWER PANEL) OF ACYCLIC PEPTIDE CYS <sub>2</sub> CYS <sub>2</sub> (ACM)-CM-P <sub>5</sub> (CRUDE).....	52
FIGURE 32: RP-HPLC EVOLUTION (UPPER PANELS) AND ESI-HRMS (LOWER PANEL) OF DIMERIZATION OF CYS <sub>2</sub> CYS <sub>2</sub> (ACM)CM-P <sub>5</sub> (CRUDE) PEPTIDE AT 5 mM AFTER 72 H.....	52
FIGURE 33: RP-HPLC (UPPER PANEL) AND ESI-HRMS (LOWERPANEL) OF CYCLIZATION OF CYS <sub>2</sub> CYS <sub>2</sub> (ACM)-CM-P <sub>5</sub> PARALLEL DIMER AT 0,3 mM AFTER 30 MIN WITH I <sub>2</sub> .....	53
FIGURE 34: RP-HPLC (UPPER PANEL) AND ESI-HRMS (LOWERPANEL) OF ACYCLIC HCY <sub>2</sub> CYS <sub>2</sub> CM-P <sub>5</sub> PEPTIDE.....	54
FIGURE 35: RP-HPLC EVOLUTION (UPPER PANELS) AND ESI-HRMS (LOWER PANEL) OF CYCLIZATION OF STRUCTURALLY RESTRICTED PEPTIDE HCY <sub>2</sub> CYS <sub>2</sub> CM-P <sub>5</sub> AT 0.5 mM.....	54
FIGURE 36: RP-HPLC (LEFT PANEL) AT HIGH RESOLUTION (LESS GRADIENT SLOPE, RIGHT PANEL) AND ESI-HRMS (LOWER PANELS) OF CYCLIC AND DIMERS OF HCY <sub>2</sub> CYS <sub>2</sub> CM-P <sub>5</sub> PEPTIDE.....	55
FIGURE 37: HCY <sub>2</sub> CYS <sub>2</sub> CM-P <sub>5</sub> PEPTIDE DIMERS (LEFT: PARALLEL, RIGHT: ANTIPARALLEL) FORMED BY TWO INTERMOLECULAR DISULFIDE BRIDGES.....	55
FIGURE 38: RP-HPLC (UPPER PANEL) AND ESI-HRMS (LOWERPANEL) OF ACYCLIC PEPTIDE HCY <sub>2</sub> HCY <sub>2</sub> CM-P <sub>5</sub> ....	56
FIGURE 39: RP-HPLC (UPPER PANEL) AFTER 6H OF CYCLIZATION (CRUDE), AT HIGH RESOLUTION (LESS SLOPE OF GRADIENT) AND THE PURIFIED PRODUCT (LEFT LOWER PANEL), ESI-HRMS (RIGHT LOWER PANEL) OF CYCLIC HCY <sub>2</sub> HCY <sub>2</sub> CM-P <sub>5</sub> PEPTIDE.....	56
FIGURE 40: EXAMPLES OF THE <i>BACILLUS</i> LIPOPEPTIDE FAMILY, A) SURFACTIN, B) ITURIN, C) FENGYCIN.....	61
FIGURE 41: BIOLOGICALLY ACTIVE LIPOPEPTIDES, A) HISTATIN, B) SPIROIDESIN, C) DAPTOMYCIN.....	62

FIGURE 42: LIPIDATION OF PEPTIDES AT THE <i>N</i> AND <i>C</i> ENDS AND IN INTERMEDIATE POSITIONS. ....	63
FIGURE 43: A) REPRESENTATION OF <i>S-CIS/S-TRANS</i> ISOMERS OF A SECONDARY AMIDE BOND. B) ALTERNATIVE TRANSITION STATE CONFIGURATIONS FOR PEPTIDE BOND ROTATION. C) CANONICAL STRUCTURES OF THE AMIDE GROUP STRUCTURE.....	66
FIGURE 44: A) MONOMER OF MELITTIN, CUT FROM THE TETRAMERIC CRYSTAL STRUCTURE. POLAR AMINOACIDS ARE SHOWN IN GREEN, ALIPHATIC IN WHITE AND BASIC IN BLUE. B) WHEEL PROJECTION OF THE TWO INDEPENDENT HELICES (HELIX 1 AND 2) AND A POSSIBLE TOTAL HELIX OF MELITTIN. ....	69
FIGURE 45: A) MODEL OF THE BINDING OF THE <i>N</i> -TERMINAL DOMAIN OF HISTONE H1E TO THE NUCLEOSOME. REPRESENTATION OF THE <i>N</i> -TERMINAL DOMAIN BOUND TO CHROMATOSOMAL AND LINKER DNA. THE CHROMATOSOMAL DNA IS IN GREEN, THE LINKER DNA IS IN RED, THE HISTONE H1E <i>N</i> -TERMINAL DOMAIN IS IN BLUE, AND THE GLOBULAR DOMAIN IS IN GREEN. THE GLOBULAR DOMAIN IS LOCATED ACCORDING TO THE MODEL OF ZHOU ET AL. (1998). B) WHEEL PROJECTIONS OF THE TWO INDEPENDENT HELICES (DISTAL AND 2) AND A POSSIBLE TOTAL HELIX OF HISTONE H1E. ....	69
FIGURE 46: LIPIDATED ANALOGUES OF CM-P5. ....	72
FIGURE 47: STRUCTURAL COMPARISON OF ALA, GLY, PRO, SAR AND THE PRODUCTS OF UGI RESIDUES.....	73
FIGURE 48: SIMILARITY IN THE LIPID CHAIN LENGTH OF C10-CM-P5 AND C15-CM-P5 LIPOPEPTIDES SYNTHESIZED BY PEPTIDE COUPLING AND FMV0451 SYNTHESIZED BY UGI-4CR. ....	75
FIGURE 49: RP-HPLC (UPPER PANEL) AND ESI-HRMS (LOWER PANEL) OF C10-CM-P5. ....	75
FIGURE 50: RP-HPLC (UPPER PANEL) AND ESI-HRMS (LOWER PANEL) OF C15-CM-P5. ....	76
FIGURE 51: LIPIDATED ANALOGUES OF CM-P5 CONTAINING ALA, GLY OR PRO. ....	77
FIGURE 52: RP-HPLC (UPPER PANEL) AND ESI-HRMS (LOWER PANEL) OF C10G-CM-P5. ....	78
FIGURE 53: RP-HPLC (UPPER PANEL) AND ESI-HRMS (LOWER PANEL) OF C10A-CM-P5. ....	78
FIGURE 54: RP-HPLC (UPPER PANEL) AND ESI-HRMS (LOWER PANEL) OF C10P-CM-P5.....	79
FIGURE 55: NEWMAN PROJECTION ABOUT THE ALPHA CARBON OF C10A-CM-P5, C10G-CM-P5 AND C10P-CM-P5. .....	80
FIGURE 56: STRUCTURES OF THE ACYCLIC C10A-CYS-CYS-CM-P5, C10G-CYS-CYS-CM-P5 AND C10P-CYS-CYS-CM- P5 PEPTIDES. ....	81
FIGURE 57: RP-HPLC (UPPER PANEL) AND ESI-HRMS (LOWER PANEL) OF C10A-CYS-CYS-CM-P5 PEPTIDE. ....	82
FIGURE 58: RP-HPLC (UPPER PANEL) AND ESI-HRMS (LOWER PANEL) OF C10G-CYS-CYS-CM-P5 PEPTIDE. ....	82
FIGURE 59: RP-HPLC (UPPER PANEL) AND ESI-HRMS (LOWER PANEL) OF C10P-CYS-CYS-CM-P5 PEPTIDE. ....	83
FIGURE 60: RP-HPLC EVOLUTION DURING OXIDATION OF C10A-CYS-CYS-CM-P5 PEPTIDE AT 0.3 mM AFTER 4H (UPPER PANEL) AND 8H (LOWER PANEL) AND STRUCTURE OF THE DIMERS AND CYCLIC MONOMER FORMED. ....	84
FIGURE 61: RP-HPLC EVOLUTION DURING OXIDATION OF C10G-CYS-CYS-CM-P5 PEPTIDE AT 0.3 mM AFTER 3H (UPPER PANEL) AND 6H (LOWER PANEL) AND STRUCTURE OF THE DIMER AND CYCLIC MONOMER FORMED. ....	84
FIGURE 62: RP-HPLC EVOLUTION DURING OXIDATION OF C10P-CYS-CYS-CM-P5 PEPTIDE AT 0.3 mM AFTER 5H AND STRUCTURE OF THE DIMER AND CYCLIC MONOMER FORMED. ....	85
FIGURE 63: FT-IR SPECTRUM OF THE N-DODECYLISONITRILE. ....	87
FIGURE 64: <sup>1</sup> H-NMR SPECTRA OF THE N-DODECYLISONITRILE.....	88
FIGURE 65: <sup>13</sup> C-NMR SPECTRA OF THE N-DODECYLISONITRILE.....	88

FIGURE 66: RP-HPLC (UPPER PANEL), ESI-HRMS (LOWER PANEL) AND STRUCTURE OF C12UGIAC-CYSCYSCM-P5 PEPTIDE.....	90
FIGURE 67: RP-HPLC EVOLUTION DURING OXIDATION OF C12UGIAC-CYSCYSCM-P5 PEPTIDE AT 0.3 mM AFTER 3H AND STRUCTURE OF THE DIMERS AND CYCLIC MONOMER FORMED. ....	90
FIGURE 68: ESI-HRMS OF THE COMPOUNDS (ORDERED BY RETENTION TIME) FORMED DURING CYCLIZATION OF C10A-CYSCYSCM-P5 PEPTIDE.....	94
FIGURE 69: ESI-HRMS OF THE COMPOUNDS (ORDERED BY RETENTION TIME) FORMED DURING CYCLIZATION OF C10G-CYSCYSCM-P5 PEPTIDE.....	95
FIGURE 70: ESI-HRMS OF THE COMPOUNDS (ORDERED BY RETENTION TIME) FORMED DURING CYCLIZATION OF C10P-CYSCYSCM-P5 PEPTIDE. ....	96
FIGURE 71: ESI-HRMS OF THE COMPOUNDS (ORDERED BY RETENTION TIME) FORMED DURING CYCLIZATION OF C12UGIAC-CYSCYSCM-P5 PEPTIDE. ....	98
FIGURE 72: NATURAL EPOXYPEPTIDES INHIBITORS OF PROTEASOME AS ANTICANCER AGENTS. ....	102
FIGURE 73: BORTEZOMIB, YU-101 AND CARFILZOMIB PROTEASOME INHIBITORS.....	102
FIGURE 74: GENERAL TYPES OF CLEAVABLE LINKERS. ....	106
FIGURE 75: MALEIMIDE CONTAINING LINKERS AND LOW PLASMA STABILITY TEST. ....	107
FIGURE 76: APPROVED ANTICANCER TREATMENT: BRENTUXIMAB VEDOTIN (TRADE NAME ADCETRIS).....	108
FIGURE 77: MECHANISM OF TARGET AND INTRACELULAR RELEASE OF THE ANTICANCER BIOCONJUGATE PHLIP-AMANITIN (SPDP: MALEIMIDO DISULFIDE LINKER). ....	109
FIGURE 78: PET IMAGING OF EXTRACELLULAR pH WITH <sup>64</sup> Cu LABELED PHLIP-VARIANT3.....	110
FIGURE 79: ESI-HRMS OF THE LEFT-HAND FRAGMENT OF CARFILZOMIB.....	114
FIGURE 80: <sup>1</sup> H NMR SPECTRA OF THE BOC-PROTECTED LEU 9, 10 AND 11A (CDCL <sub>3</sub> , 400 MHZ). ....	116
FIGURE 81: <sup>1</sup> H NMR OF CARFILZOMIB IN CDCL <sub>3</sub> , 400 MHZ. ....	117
FIGURE 82: <sup>1</sup> H-NMR OF THE LINKER-OH IN DMSO-D <sub>6</sub> . ....	119
FIGURE 83: ESI-MS OF THE CRUDE LINKER-OH. ....	119
FIGURE 84: ESI-MS OF THE LINKER-OTs.....	120
FIGURE 85: <sup>1</sup> H-NMR OF THE LINKER-I IN DMF-D <sub>7</sub> , 400 MHZ. ....	121
FIGURE 86: ESI-MS OF THE LINKER-I. ....	121
FIGURE 87: ESI-HRMS OF THE LINKER-I. ....	121
FIGURE 88: ESI-HRMS (UPPER PANEL) AND MALDI (LOWER PANEL) SPECTRA OF THE PHLIP PEPTIDE CONTAINING CYS AT C-TERMINAL (AADDQNPWRAYLDLLFPTDTLLLDLCW). ....	123
FIGURE 89: ESI-HRMS (UPPER PANEL) AND MALDI (LOWER PANEL) SPECTRA OF THE PHLIP PEPTIDE CONTAINING CYS AT N-TERMINAL (ACDDQNPWRAYLDLLFPTDTLLLDLLW). ....	123
FIGURE 90: ESI-MS OF THE LINKER-CARFILZOMIB SALT IN PRECENSE OF HCOOH (UPPER PANEL) OR WITHOUT HCOOH (LOWER PANEL). ....	125
FIGURE 91: RP-HPLC OF THE BIOCONJUGATION OF LINKER-CFZ SALT WITH PHLIP-VARIANT3 CONTAINING CYS AT THE N-TERMINAL.....	125
FIGURE 92: ESI-HRMS OF THE BIOCONJUGATE PHLIP-VARIANT3-LINKER-CFZ. ....	126

FIGURE 93: <sup>1</sup> H NMR OF THE LEFT HAND FRAGMENT OF CARFILZOMIB IN CDCl <sub>3</sub> , 400 MHZ.....	131
FIGURE 94: <sup>13</sup> C NMR OF THE LEFT HAND FRAGMENT OF CARFILZOMIB IN CDCl <sub>3</sub> , 100 MHZ. ....	131
FIGURE 95: <sup>1</sup> H NMR OF BOC-LEU-WEINREB AMIDE DERIVATIVE IN CDCl <sub>3</sub> , 400 MHZ. ....	132
FIGURE 96: <sup>13</sup> C NMR OF BOC-LEU-WEINREB AMIDE DERIVATIVE IN CDCl <sub>3</sub> , 100 MHZ. ....	133
FIGURE 97: <sup>1</sup> H NMR OF BOC-LEU-ALKENE IN CDCl <sub>3</sub> , 400 MHZ. ....	134
FIGURE 98: <sup>13</sup> C NMR OF BOC-LEU-ALKENE IN CDCl <sub>3</sub> , 100 MHZ. ....	134
FIGURE 99: <sup>1</sup> H NMR OF THE CRUDE MIXTURE OF DIASTEREOMERIC BOC-LEU-EPOXIDES IN CDCl <sub>3</sub> , 400 MHZ..	136
FIGURE 100: <sup>1</sup> H NMR OF BOC-LEU-EPOXIDE-A IN CDCl <sub>3</sub> , 400 MHZ. ....	136
FIGURE 101: <sup>13</sup> C NMR OF BOC-LEU-EPOXIDE-A IN CDCl <sub>3</sub> , 100 MHZ. ....	137
FIGURE 102: <sup>1</sup> H-NMR OF BOC-LEU-EPOXIDE-B (IMPURE) IN CDCl <sub>3</sub> , 400 MHZ. R <sub>F</sub> = 0.37 (HEXANE/ETOAC 9:1). .....	137
FIGURE 103: <sup>1</sup> H NMR OF TRIFLUORACETATE SALT OF LEU-EPOXIDE-A IN CDCl <sub>3</sub> , 400 MHZ. ....	138
FIGURE 104: <sup>13</sup> C NMR OF TRIFLUORACETATE SALT OF LEU-EPOXIDE-A IN CDCl <sub>3</sub> , 100 MHZ. ....	139
FIGURE 105: RP-HPLC OF CARFILOMIB.....	140
FIGURE 106: ESI-HRMS OF CARFILOMIB.....	140
FIGURE 107: <sup>13</sup> C NMR OF CARFILZOMIB IN CDCl <sub>3</sub> , 100 MHZ. ....	141
FIGURE 108: <sup>1</sup> H NMR OF FMOC-CIT-PABOH IN DMSO-D6, 400 MHZ. ....	142
FIGURE 109: <sup>13</sup> C NMR OF LINKER-OH IN DMSO-D6, 100 MHZ. ....	143
FIGURE 110: ESI-MS OF THE PURE LINKER-OH. ....	144
FIGURE 111: <sup>13</sup> C NMR OF THE LINKER-I IN DMF-D7, 100 MHZ. ....	145
FIGURE 112: RP-HPLC OF PHLIP-VARIANT3 CONTAINING CYS AT <i>N</i> -TERMINAL (UPPER PANEL) OR <i>C</i> -TERMINAL (LOWER PANEL).....	146

## List of Schemes

SCHEME 1: PEPTIDE COUPLING WITH CARBODIIMIDES AND RACEMIZATION INHIBITOR.....	9
SCHEME 2: RACEMIZATION MECHANISMS. ACT: ACTIVATING.....	9
SCHEME 3: PROPOSED MECHANISM FOR THE REACTION OF PRIMARY AMINES WITH NINHYDRIN IN SOLID PHASE....	11
SCHEME 4: SYNTHESIS OF DISULFIDE BRIDGED ANALOGUES OF CM-P5. ....	26
SCHEME 5: SYNTHESIS OF CysCysCM-P5 PARALLEL DIMER USING ACM AND TRT PROTECTING GROUPS. ....	26
SCHEME 6: UGI-4C (RIGHT DOWN) AND DANISHEFSKY (RIGHT UP) REACTION MECHANISM. ....	64
SCHEME 7: EXAMPLES OF UGI-4CRS PERFORMED IN SOLID PHASE.....	65
SCHEME 8: SYNTHESIS OF <i>N</i> -SUBSTITUTED PEPTIDES BY UGI-4CR IN SOLID PHASE.....	65
SCHEME 9: SCHEMATIC REPRESENTATION OF TRIPLET-TRIPLET ENERGY TRANSFER MEASUREMENT IN UNFOLDED POLYPEPTIDE CHAIN. A) LOOP SEQUENCE, X, BETWEEN THE LABELS FOR TTET IN PEPTIDES OF THE CANONICAL SEQUENCE XAN-X-NALA-SER-GLY. ....	67
SCHEME 10: SEQUENTIAL SYNTHESIS OF THE <i>N</i> -DODECYLISONITRILE. ....	87
SCHEME 11: MECHANISM FOR THE FORMATION OF A MORPHOLINO ADDUCT FROM EPOXYPEPTIDES. ....	103
SCHEME 12: CONVERGENT SYNTHESIS OF CARFILZOMIB BY EARLY EPOXIDATION. ....	104
SCHEME 13: CONVERGENT SYNTHESIS OF CARFILZOMIB BY LATE-STAGE EPOXIDATION. ....	105
SCHEME 14: MORE USED ENZYMATICALLY CLEAVABLE LINKERS CONTAINING PAB. TRACELESS MECHANISM OF PAB RELEASE. ....	107
SCHEME 15: IRREVERSIBLE CYS SELECTIVE BIOCONJUGATION USING SIMPLE CARBONYLACRYLIC REAGENTS....	108
SCHEME 16: MALEIMIDE-CAPROIL-VAL-CIT-PAB-CL LINKER FOR THE TRACELESS RELEASE OF TERTIARY AND HETEROARYL AMINES FROM ADCs. ....	108
SCHEME 17: REPORTED MALEIMIDO-CAPROIC-VAL-CIT LINKER SYNTHESIS. ....	109
SCHEME 18: SYNTHESIS OF THE LEFT-HAND FRAGMENT OF CARFILZOMIB. ....	114
SCHEME 19: SYNTHESIS OF THE RIGH-HAND FRAGMENT OF CARFILZOMIB.....	115
SCHEME 20: FINAL COUPLING OF THE LEFT AND RIGHT HAND FRAGMENTS OF CARFILZOMIB.....	116
SCHEME 21: SOLID PHASE SYNTHESIS OF THE LINKER-OH USING DHP-RESIN. ....	118
SCHEME 22: COUPLING OF THE LINKER-I TO CARFILZOMIB.....	124
SCHEME 23: FINAL CONJUGATION OF LINKER-CFZ SALT TO PHLIP-VARIANT3 PEPTIDE CONTAINING CYS AT THE <i>N</i> -TERMINAL. NAPI SHOULD CAUSE THE INTERCHANGE OF IODO BY DIHYDROGENPHOSPHATE. ....	126

## Resumo

“MODIFICAÇÃO COVALENTE DE PEPTÍDEOS ANTIMICROBIANOS E ANTICANCERÍGENOS PARA A MELHORIA DE SUAS PROPRIEDADES FARMACOLÓGICAS.”

Seguindo a informação obtida por um estudo de concepção racional, sintetizaram-se análogos estabilizados helicoidais cíclicos, diméricos e lipidados do péptido Cm-p5. O monômero cíclico apresentou atividade aumentada *in vitro* contra *Candida albicans* e *Candida parapsilosis*, em comparação com Cm-p5. Inicialmente, 14 mutantes de Cm-p5 foram sintetizados seguindo um racional de sinal para melhorar a atividade antifúngica e as propriedades farmacológicas. Testes antimicrobianos mostraram que a atividade foi perdida em cada um dos 14 análogos, sugerindo como uma conclusão principal, que uma ponte de sal Glu-His poderia estabilizar a conformação helicoidal de Cm-p5 durante a interação com a membrana plasmática. Um derivado, obtido por substituição de Glu e His por Cys, foi sintetizado e oxidado com a geração de um monômero cíclico com atividade antifúngica melhorada. Além disso, dois dímeros foram gerados durante o procedimento de oxidação. Os dímeros mostraram uma estrutura secundária helicoidal em água, enquanto o monômero cíclico mostrou apenas esta conformação em SDS. Além disso, o dímero antiparalelo apresentou moderada atividade contra *Pseudomonas aeruginosa* e atividade significativa contra *Listeria monocytogenes*. Nem o monômero cíclico nem os dímeros eram tóxicos contra macrófagos ou células humanas THP-1.

Continuando com as modificações covalentes da estrutura do Cm-p5, no capítulo 2 se descreve o desenho, síntese e caracterização de 15 análogos lipídicos e cíclicos/lipidados do Cm-p5. Estudos anteriores mostram que a *N*-lipidação do Cm-p5 pela reação de Ugi-4C aumenta notavelmente a atividade antifúngica. Nosso teste biológico inicial mostra que a lipidação com ácido decanóico não mostrou nenhum efeito na atividade do Cm-p5, enquanto o ácido pentadecanóico o diminuiu. Esse resultado não está de acordo com o aumento da atividade no caso do análogo lipidado da reação de Ugi-4C. A reação de Ugi-4C não apenas introduz uma cadeia lipídica, também produz uma *N*-substituição que pode alterar o comportamento conformacional da cadeia lipídica. Para determinar a influência da *N*-substituição, três análogos contendo Ala, Gly ou Pro entre a cadeia lipídica e a sequência normal de Cm-p5 foram sintetizados. Gly e Pro estão implicados em várias mudanças conformacionais em proteínas ou peptídeos. Gly possui alta flexibilidade enquanto a Pro é o único aminoácido *N*-alquilado e participa na formação de giros ou estruturas rígidas. Adicionalmente, seguindo o esperado aumento de atividade por formação de ponte dissulfeto, foram preparadas variantes

semelhantes possuindo Ala (introduzida como comparação), Gly ou Pro entre a cadeia de decanoilo e o peptídeo CysCysCm-p5 cíclico/dimérico. Finalmente, a lipidação por reação Ugi-4C com n-dodecilisonitrila e posterior ciclização entre Cys produzem versões cíclicas e diméricas de ciclopeptídeos Ugi lipidados. Todos os compostos estão sob avaliação biológica que permitirá obter uma conclusão sobre o motivo estrutural necessário para produzir o análogo cíclico e lipidado do Cm-p5 mais antifúngico.

No capítulo 3, usamos a combinação de métodos de fase sólida e fase líquida para a síntese da droga anticâncer, carfilzomib (CFZ). A via convergente compreende a construção de tetrapéptidos em fase sólida seguida de acoplamento do epóxido preparado previamente. Os efeitos colaterais da CFZ incluem a insuficiência cardíaca e a falta de ar, de modo que o desenvolvimento da bioconjugação ou da entrega direcionada é realmente desejado. Com este objetivo, nós preparamos um ligante que não deixa resíduos, carbonilacrílico-Val-Cit-PABna forma de álcool em fase sólida usando a resina especial DHP em alto rendimento. Este ligante na forma de álcool foi tosilado e iodado com o objetivo de melhorar os rendimentos da reação de substituição com CFZ. Os peptídeos de inserção a pH baixo (pHLIPs) visam a acidez nas superfícies das células cancerígenas e apresentam utilidade numa vasta gama de aplicações, incluindo imagiologia de tumores e distribuição intracelular de agentes terapêuticos. Neste trabalho, pretendemos fundir a capacidade de seletividade de células tumorais do peptídeo pHLIP com a libertação sem resíduos, estabilidade e seletividade do novo ligante carbonilacrílico. Finalmente, a bioconjugação de CFZ com o peptídeo pHLIP através do ligante carbonilacrílico-Val-Cit-PAB, para a libertação sem resíduos e distribuição direcionada para tumores poderia melhorar significativamente a efetividade deste fármaco no tratamento do câncer.

## Abstract

“COVALENT MODIFICATION OF ANTIMICROBIAL AND ANTICANCER PEPTIDES FOR THE IMPROVEMENT OF THEIR FARMACOLOGICAL PROPERTIES.”

Following the information obtained by a rational design study, cyclic and dimeric helical stabilized analogues of the peptide Cm-p5 were synthesized. The cyclic monomer showed an increased activity in vitro against *Candida albicans* and *Candida parapsilosis*, compared to Cm-p5. Initially, fourteen mutants of Cm-p5 were synthesized following a rational design to improve the antifungal activity and pharmacological properties. Antimicrobial testing showed that the activity was lost in every of these fourteen analogues, suggesting as a main conclusion, that a Glu-His salt bridge could stabilize Cm-p5 helical conformation during the interaction with the plasma membrane. A derivative, obtained by substitution of Glu and His for Cys, was synthesized and oxidized with the generation of a cyclic monomer with improved antifungal activity. In addition, two dimers were generated during the oxidation procedure, a parallel and anti-parallel one. The dimers showed a helical secondary structure in water, whereas the cyclic monomer only showed this conformation in SDS. In addition, the antiparallel dimer showed a moderate activity against *Pseudomonas aeruginosa* and a significant activity against *Listeria monocytogenes*. Nor the cyclic monomer nor the dimers were toxic against macrophages or THP-1 human cells.

Continuing with the covalent modifications of the Cm-p5 structure, in chapter 2 is described the design, synthesis and characterization of 15 lipidated and cyclo-lipidated analogues of Cm-p5. Previous studies showed that *N*-lipidation of Cm-p5 by Ugi-4CR increase notably the antifungal activity. Our initial biological test showed that lipidation with decanoic acid did not display any effect in the activity of Cm-p5, while pentadecanoic acid decreased it. These results are not in accord with the increased activity in case of the Ugi lipidated analogue. The Ugi-4CR do not only introduces a lipid chain, also produce *N*-substitution that can alter the conformational behavior of the lipid chain. To determine the influence of *N*-substitution, three analogues containing Ala, Gly or Pro between the lipid chain and the normal sequence of Cm-p5 were synthesized. Gly and Pro are implied in several conformational changes in proteins or peptides. Gly possesses high flexibility while Pro is the only *N*-alkylated amino acid and participate in loop or rigid structure formation. In addition, following the expected increase of activity by disulfide bridge formation, similar variants possessing Ala (introduced as a comparison), Gly or Pro between a dodecyl chain and cyclic/dimeric CysCysCm-p5 were



prepared. Finally, lipidation by Ugi-4CR with n-dodecylisocyanide and subsequent cyclization between Cys produce cyclic and dimeric versions of Ugi lipidated cyclopeptides. All compounds are under biological evaluation that will permit to gain conclusion about the structural motif needed to produce the more antifungal cyclic and lipidated analogue of Cm-p5. In chapter 3, we used the combination of solid phase and liquid phase methods for the synthesis of the anticancer drug, carfilzomib (CFZ). The convergent route comprises the tetrapeptide construction in solid phase followed by coupling with the previously prepared Leu-epoxide. Side effects of CFZ include the heart failure and shortness of breath so that the development of bioconjugation for targeted delivery is desired. With this aim, we prepared a traceless carbonylacrylic-Val-Cit-PAB linker as an alcohol in solid phase using the special DHP resin in high yield. This alcohol linker was tosylated and iodinated with the aim of improve the yields of the substitution reaction with CFZ (substitution of tosylate need heating). The pH (low) insertion peptides (pHLIPs) target acidity at the surfaces of cancer cells and show utility in a wide range of applications, including tumor imaging and intracellular delivery of therapeutic agents. We pretend to merge the capacity of tumor cell selectivity of pHLIP peptide with the traceless, stability and selective delivery of the new carbonylacrylic linker. Finally, the bioconjugation of CFZ to pHLIP peptide through the carbonylacrylic-Val-Cit-PAB linker, for the traceless release and targeted delivery to tumors could significantly improve the effectiveness of this drug in cancer treatment.

## Summary

ACKNOWLEDGEMENTS .....	4
LIST OF ABBREVIATIONS.....	V
LIST OF TABLES .....	VII
LIST OF CHARTS .....	VII
LIST OF FIGURES.....	VIII
RESUMO.....	XIV
ABSTRACT.....	XVI
<b>CHAPTER 1 .....</b>	<b>1</b>
<b>1 INTRODUCTION. CHAPTER 1 .....</b>	<b>2</b>
1.1 OBJECTIVES OF OUR WORK. ....	3
<b>2 BIBLIOGRAPHIC REVISION. CHAPTER 1.....</b>	<b>4</b>
2.1 PEPTIDES AS DRUGS.....	4
2.2 ANTIMICROBIAL PEPTIDES. CHARACTERISTICS AND BIOLOGICAL IMPORTANCE. ....	5
2.3 RESISTANCE TO ANTIBIOTICS. ANTIFUNGALS AMPs AND CM-P5. COMMERCIALIZATION OF ANTIFUNGAL PEPTIDES. ....	6
2.4 PEPTIDE SYNTHETIC METHODS .....	7
2.5 SOLID PHASE PEPTIDE SYNTHESIS. POLYMERIC SUPPORTS.....	10
2.5.1 <i>Boc/Bzl Chemistry</i> .....	12
2.5.2 <i>Fmoc/tBu Chemistry</i> .....	13
2.6 PEPTIDE CHARACTERIZATION .....	13
2.7 SALT BRIDGE STABILIZATION OF SECONDARY STRUCTURES OF PEPTIDES AND PROTEINS .....	14
2.8 COVALENT MODIFICATIONS OF PEPTIDES.....	15
2.8.1 <i>Structural constraints by cyclization</i> .....	16
2.8.2 <i>Formation of disulfide bridges</i> .....	16
<b>3 RESULTS AND DISCUSSION. CHAPTER 1.....</b>	<b>18</b>
3.1 DESIGN OF CM-P5 MUTANTS .....	18
3.2 RESULTS AND DISCUSSION REGARDING CM-P5 PEPTIDE MUTANTS. ....	21
3.3 SALT BRIDGE AND HELICAL STABILIZATION. ....	24
3.4 RESULTS AND DISCUSSION REGARDING SALT BRIDGE AND HELICAL STABILIZATION .....	26
3.5 CIRCULAR DICHROISM ANALYSIS .....	28
3.6 <i>IN-VITRO</i> ANTICANDIDAL AND ANTIBACTERIAL ACTIVITY OF CM-P5 AND DERIVATIVES. ....	29
3.7 <i>IN-VITRO</i> TOXICITY OF CM-P5 ANALOGUES AGAINST HUMAN CELLS .....	30
3.8 DISCUSSION REGARDING BIOLOGICAL ACTIVITY.....	30
CONCLUSIONS. CHAPTER 1.....	33
FUTURE WORKS. CHAPTER 1.....	35

<b>4</b>	<b>EXPERIMENTAL SECTION. CHAPTER 1.....</b>	<b>36</b>
4.1	GENERAL REMARKS.....	36
4.1.1	<i>Materials</i> .....	36
4.1.2	<i>Peptide synthesis</i> .....	36
4.1.3	<i>Peptide Cleavage</i> .....	37
4.1.4	<i>Peptide Cyclization and Dimerization</i> .....	37
4.1.5	<i>Cyclization of the parallel dimer using Cys(Acm)</i> .....	37
4.1.6	<i>Analytical RP-HPLC</i> .....	38
4.1.7	<i>ESI-HRMS</i> .....	38
4.1.8	<i>Semipreparative RP-HPLC</i> .....	38
4.1.9	<i>CD spectroscopy</i> .....	38
4.1.10	<i>Microorganism strains and growth conditions</i> .....	39
4.1.11	<i>In vitro antimicrobial testing</i> .....	39
4.1.12	<i>Human cells and culture conditions:</i> .....	40
4.1.13	<i>Toxicity assay:</i> .....	40
4.2	ADDITIONAL FIGURES AND TABLES.....	41
4.3	GENERAL PROTOCOL FOR SOLID-PHASE PEPTIDE SYNTHESIS.....	41
4.3.1	<i>Solid phase synthesis of the antifungal peptide Cm-p5:</i> .....	42
4.3.2	<i>Solid phase synthesis of SRSELIVHQRFLF-NH<sub>2</sub> analogue (peptide 1):</i> .....	43
4.3.3	<i>Solid phase synthesis of SRSDLIVHQRFLF-NH<sub>2</sub> analogue (peptide 2):</i> .....	43
4.3.4	<i>Solid phase synthesis of SRSQIVHQRFLF-NH<sub>2</sub> analogue (peptide 3):</i> .....	44
4.3.5	<i>Solid phase synthesis of SRSALIVHQRFLF-NH<sub>2</sub> analogue (peptide 4):</i> .....	44
4.3.6	<i>Solid phase synthesis of SRSβALIVHQRFLF-NH<sub>2</sub> analogue (peptide 5):</i> .....	45
4.3.7	<i>Solid phase synthesis of SRSELKIVHQRFLF-NH<sub>2</sub> analogue (peptide 6):</i> .....	45
4.3.8	<i>Solid phase synthesis of SRSEKIVHQRFLF-NH<sub>2</sub> analogue (peptide 7):</i> .....	46
4.3.9	<i>Solid phase synthesis of SRSE--IVHQRFLF-NH<sub>2</sub> analogue (peptide 8):</i> .....	46
4.3.10	<i>Solid phase synthesis of SRSEKIVHQRFLF-NH<sub>2</sub> analogue (peptide 9):</i> .....	47
4.3.11	<i>Solid phase synthesis of SRSEKIVHQRFLF-NH<sub>2</sub> analogue (peptide 10):</i> .....	47
4.3.12	<i>Solid phase synthesis of RS--LIVHQRFLF-NH<sub>2</sub> analogue (peptide 11):</i> .....	48
4.3.13	<i>Solid phase synthesis of SRSE-IV--QRFLF-NH<sub>2</sub> analogue (peptide 12):</i> .....	48
4.3.14	<i>Solid phase synthesis of Ac-SRSELIVHQRFLF-NH<sub>2</sub> analogue (peptide 13):</i> .....	49
4.3.15	<i>Solid phase synthesis of (SRSELIVHQRFLF)<sub>2</sub>-K-NH<sub>2</sub> (peptide 14):</i> .....	49
4.3.16	<i>Synthesis of Structurally Restricted (Cyclic) Peptide (CysCysCm-p5):</i> .....	50
4.3.17	<i>Synthesis of Structurally Restricted Peptide (CysCysCm-p5)<sub>2</sub> (Parallel Dimer) using Cys(Acm) as mutant of His of Cm-p5:</i> .....	52
4.3.18	<i>Synthesis of Structurally Restricted (Cyclic) Peptide (HcyCysCm-p5):</i> .....	53
4.3.19	<i>Synthesis of Structurally Restricted (Cyclic) Peptide (HcyHcyCm-p5):</i> .....	56

4.4	MATERIALS AND METHODS. MOLECULAR DYNAMICS SIMULATIONS.....	57
<b>CHAPTER 2</b>		<b>58</b>
<b>1</b>	<b>INTRODUCTION. CHAPTER 2</b> .....	<b>59</b>
1.1	OBJECTIVES OF OUR WORK. ....	59
<b>2</b>	<b>BIBLIOGRAPHIC REVISION. CHAPTER 2</b> .....	<b>61</b>
2.1	LIPOPEPTIDES. IMPORTANCE AND CHARACTERISTICS.....	61
2.2	STRUCTURAL ACTIVITY RELATIONSHIP IN BIOLOGICALLY ACTIVE LIPOPEPTIDES. ....	62
2.3	LIPIDATION OF PEPTIDES.....	63
2.3.1	<i>Multicomponent Reaction. Peptide lipidation by Ugi-4CR.</i> .....	64
2.3.2	<i>Organocatalysis and Ugi reactions in solid phase.</i> .....	65
2.4	AMIDE BONDS AND TURN MOTIFS IN PROTEINS. IMPORTANCE OF GLY AND PRO RESIDUES. ....	66
2.4.1	<i>Melittin, the honeybee venom peptide. Secondary structure.</i> .....	68
2.4.2	<i>The helix-Gly-Gly-helix motif in the N-terminal domain of histone H1e.</i> .....	69
<b>3</b>	<b>RESULTS AND DISCUSSION. CHAPTER 2</b> .....	<b>71</b>
3.1	ANTIFUNGAL ACTIVITY OF PRELIMINARY LIPIDATED ANALOGUES OF CM-P5. WORK METHODOLOGY.....	71
3.2	SYNTHESIS OF LIPOPEPTIDES ANALOGUES OF CM-P5 BY COUPLING OF FATTY ACIDS.....	74
3.3	SYNTHESIS OF LIPOPEPTIDES ANALOGUES OF CM-P5 BY COUPLING OF DECAHOIC ACID AFTER ALA, GLY OR PRO. ....	77
3.4	SYNTHESIS OF LIPOPEPTIDES STRUCTURALLY RESTRICTED BY DISULFIDE BRIDGE FORMATION. ....	80
3.5	SYNTHESIS AND CHARACTERIZATION OF THE N-DODECYLISONITRILE. ....	86
3.6	LIPOPEPTIDES SYNTHESIS BY UGI-4CR IN SOLID PHASE. ....	88
	CONCLUSIONS. CHAPTER 2.....	91
	FUTURE WORKS. CHAPTER 2.....	92
<b>4</b>	<b>EXPERIMENTAL SECTION. CHAPTER 2</b> .....	<b>93</b>
4.1	GENERAL REMARKS.....	93
4.1.1	<i>Materials</i> .....	93
4.1.2	<i>Registration conditions of NMR spectra</i> .....	93
4.2	SYNTHESIS OF STRUCTURALLY RESTRICTED (CYCLIC) PEPTIDE (C10X-CYS-CYS-CM-P5): .....	93
4.3	SYNTHESIS OF N-DODECYLISONITRILE BY FORMYLATION AND DEHYDRATATION OF N-DODECYLAMINE.....	96
4.4	LIPOPEPTIDES SYNTHESIS BY UGI-4CR IN SOLID PHASE. ....	97
<b>CHAPTER 3</b>		<b>99</b>
<b>1</b>	<b>INTRODUCTION. CHAPTER 3</b> .....	<b>100</b>
1.1	PEPTIDE DRUGS CONJUGATES. CANCER TREATMENTS WITH CARFILZOMIB AND GENERAL OBJECTIVE OF OUR WORK.....	100
<b>2</b>	<b>BIBLIOGRAPHIC REVISION. CHAPTER 3</b> .....	<b>102</b>

2.1	$\alpha',\beta'$ -EPOXYKETONE PEPTIDES AS PROTEASOME INHIBITORS.....	102
2.2	TOTAL SYNTHESIS OF CARFILZOMIB.....	103
2.3	ANTIBODY DRUG CONJUGATES (ADCs). LINKER TECHNOLOGIES, MALEIMIDO LINKERS AND CARBONYLACRYLIC ACID APPROACH.....	105
2.3.1	<i>Enzymatically cleavable linkers: Peptide linkers. Traceless linkers.....</i>	106
2.3.2	<i>Maleimide containing linkers.....</i>	107
2.4	PHLIP PEPTIDES AND RELATED PHLIP-DRUG CONJUGATES.....	109
<b>3</b>	<b>RESULTS AND DISCUSSION. CHAPTER 3.....</b>	<b>111</b>
3.1	OUR PROPOSAL FOR THE PEPTIDE CONJUGATION OF CARFILZOMIB.....	111
3.2	CARFILZOMIB SYNTHESIS.....	113
3.2.1	<i>Solid-phase synthesis of the left-hand fragment of Carfilzomib.....</i>	113
3.2.2	<i>Synthesis of the right-hand fragment of carfilzomib and coupling to the left-hand fragment... 115</i>	115
3.3	CARBONYLACRYLIC-CAPROIC-VAL-CIT-PABOH LINKER PREPARATION IN SOLID PHASE.....	117
3.4	PHLIP-VARIANT3 SYNTHESIS CONTAINING CYS AT N OR C-TERMINALS.....	122
3.5	CARFILZOMIB COUPLING TO LINKER-I.....	124
3.6	FINAL COUPLING OF PHLIP TO LINKER-CARFILZOMIB BY THIOL-MICHAEL ADDITION.....	125
	CONCLUSIONS. CHAPTER 3.....	127
	FUTURE WORKS. CHAPTER 3.....	128
<b>4</b>	<b>EXPERIMENTAL SECTION. CHAPTER 3.....</b>	<b>129</b>
4.1	GENERAL REMARKS.....	129
4.1.1	<i>Materials.....</i>	129
4.1.2	<i>MALDI-TOF.....</i>	129
4.1.3	<i>ESI-MS.....</i>	129
4.2	SYNTHESIS OF THE LEFT-HAND FRAGMENT OF CARFILZOMIB: MORF-AC-HPH-LEU-PHE-OH.....	130
4.2.1	<i>Loading of Fmoc-Phe-OH to Cl-Trt Chloride resin (1.47 mmol/g).....</i>	130
4.2.2	<i>Cleavage of Morf-Ac-Hph-Leu-Phe-OH with TFA/DCM.....</i>	130
4.3	SYNTHESIS OF THE LEFT-HAND FRAGMENT OF CARFILZOMIB.....	131
4.3.1	<i>Synthesis of Boc-Leu-derived Weinreb amide.....</i>	131
4.3.2	<i>Synthesis of Boc-Leu-derived iso-propenyl ketone.....</i>	133
4.3.3	<i>Epoxidation of Boc-Leu-derived iso-propenyl ketone.....</i>	135
4.3.4	<i>Deprotection of Boc-Leu-Epoxy ketone.....</i>	138
4.3.5	<i>Coupling of the left- and right-hand fragments of Carfilzomib.....</i>	139
4.4	CARBONYLACRYLIC-CAPROIC-VAL-CIT-PABOH LINKER PREPARATION IN SOLID PHASE.....	141
4.4.1	<i>Synthesis of Fmoc-Cit-PABOH.....</i>	141
4.4.2	<i>Loading of Fmoc-Cit-PABOH to DHP Polystyrene resin and Linker-OH synthesis.....</i>	142
4.4.3	<i>General conditions for cleaving the Linker-OH from the DHP Polystyrene Resin.....</i>	142

4.4.4	<i>Tosylation of Linker-OH</i> .....	144
4.4.5	<i>Iodination of Linker-OTs</i> .....	144
4.5	SYNTHESIS OF PHLIP-VARIANT3 PEPTIDE CONTAINING CYS AT C AND N TERMINAL .....	145
4.5.1	<i>Loading of the first aminoacid to Wang-Resin (Steglich sterification)</i> .....	145
4.6	COUPLING OF THE LINKER-I TO CARFILZOMIB .....	146
4.7	CONJUGATION OF PHLIP-VARIANT3 TO LINKER-CARFILZOMIB-I .....	146
	ANNEXES .....	161
	ANNEX 1: STRUCTURE, NAME AND THREE AND ONE LETTER CODE OF THE 22 ESSENTIAL AMINOACIDS. ....	161
	ANNEX 2: RELATIVE SWELLING CAPACITY OF SOME SOLVENTS RELATED TO POLIESTIRENE RESINS.....	161
	ANNEX 3: <sup>1</sup> H-NMR OF PEPTIDES 6 (UPPER PANEL, FMV025) AND 8 (LOWER PANEL, FMV034) IN DMSO-D <sub>6</sub> .....	162



# Chapter 1

## 1 Introduction. Chapter 1

The global levels of fungal infections continue in rise,<sup>1</sup> but treatment options that can be used to treat these pathologies remain limited to only three classes of antifungal drugs: polyenes, azoles and echinocandins. The high toxicity of the existent antimycotics in the market and the increase of the resistance of these pathogenic microorganisms are the fundamental factors that motivate the need for development of new types of drugs, to be employed as internal, oral and less toxic antifungals.<sup>2</sup>

The AMPs (antimicrobials peptides) may have fungicidal or fungistatic activity, and may or may not have antibacterial activity at the same time that they exert their action against fungi. Isolated or synthetic antifungal peptides may be effective candidates in the treatment of systemic or superficial mycosis. There are different types of classifications for them that include defensins,  $\beta$ -barrelins, thionines, among others antifungal peptides and have activity against a variety of fungi such as *Candida albicans*, *Candida kefyr*, *Candida tropicalis* and *Saccharomyces cerevisiae*, responsible for recurrent diseases in plants and animals.<sup>3</sup>

Cm-p5 (SRSELIVHQRLF-NH<sub>2</sub>) is a peptide derived from the coastal tropical snail *Cenchritis muricatus* (*Gastropoda: Littorinidae*) that showed antifungal activity against the human pathogens *Candida albicans*, *Candida parapsilosis*, *Cryptococcus neoformans*, *Trichophyton mentagrophytes* and *Trichophyton rubrum*. This peptide did not exhibit any toxicity against the mammalian cell line *in vitro*. It was structurally characterized by CD Polarimetry and NMR Spectroscopy,<sup>4</sup> revealing an  $\alpha$ -helical structure under membranolytic conditions, and a tendency to a random structure in aqueous solution.<sup>5</sup>

Cm-p5 is not a suitable therapeutic agent due to its easy proteolytic degradation. The presence of two Arg residues in the structure probably facilitates trypsin degradation and free *N*-terminal can be targeted by aminopeptidases. The covalent modification of this peptide could improve the metabolic stability, once determined the significance of each amino acid for the biological activity.

Cm-p5 showed a fungistatic action in the 10-40  $\mu\text{g/mL}$  (6,7-26,9  $\mu\text{mol/L}$ ) range against *Candida albicans*, in a similar fashion observed by the conventional antifungal fluconazole (MIC= 8-16  $\mu\text{g/mL}$  (16-32  $\mu\text{mol/L}$ ), against *Candida albicans*) but different of the amphotericin B, which exhibited a fungicidal character eliminating the microbial population in 24 h.<sup>6</sup> Due to the low hemolytic<sup>6</sup> and cytotoxic activity of Cm-p5, the simplicity of its synthesis



and covalent modification and the similar antifungal activity compared to conventional fungistatics like fluconazole, we selected Cm-p5 for our investigation.<sup>7</sup>

The biological action mechanism of Cm-p5 is currently unknown. However, this molecule interacts preferentially with fungal phospholipids, does not interact with ergosterol (unlike amphotericin B)<sup>8</sup> and, to our knowledge, there is no information regarding whether is possible or not penetration in to cytoplasm. Based on the previous aspects four action mechanisms can be hypothesized: *i.* destabilization of cellular membrane,<sup>9</sup>*ii.* inhibition of cell wall synthesis (like echinocandins),<sup>10</sup> *iii.* inhibition of ergosterol synthesis<sup>11</sup> (like clotrimazole and fluconazole) or *iv.* intracellular enzymatic inhibition.<sup>12</sup> In any case, helical stabilization of Cm-p5 should play an essential role in the biological activity because permit the adoption of an amphipatic structure posing the positively charged Arg residues toward one face and hydrophobic residues opposed in the other face.

### **1.1 Objectives of our work.**

This chapter focuses on the development of better pharmacological active versions of the antifungal peptide Cm-p5, in an attempt to demonstrate the potential of the concept of secondary structure stabilization by disulfide bridges in AMPs of  $\alpha$ -helical acyclic conformation. Cm-p5 is prone to proteolytic degradation *in-vivo* and by determining the importance of all aminoacids in the sequence would be possible to know the structural features needed for the adoption of an  $\alpha$ -helix at contact with membranes and for the exertion of biological activity. For this aim, we present a general study of the relevance of several aminoacids in the biological activity of Cm-p5. The conclusions of this rational design of the Cm-p5 structure will permit to change the correct residues by Cys and produce the corresponding cyclic and helical stabilized analogue.

## 2 Bibliographic Revision. Chapter 1

### 2.1 Peptides as drugs

In recent years, peptides have received an increasing attention as potential pharmaceuticals, despite their intrinsic drawbacks in terms of pharmacological properties. The attractiveness of peptides as drugs is mainly due to their high degree of specificity in comparison with conventional drugs. Furthermore, massive peptide synthesis can be performed in a cost-benefit manner and more effective ADME (administration, distribution, metabolism and excretion) parameters can be obtained with rationally designed peptide derivatives.<sup>13</sup> At present, more than 20% of the current drugs are of peptide structure thanks to the development of combinatorial chemistry, the obtention of libraries in filamentous phages, the techniques of controlled release, the isolation of natural peptides,<sup>14</sup> the use of recombinant methods and the strategies for the introduction of covalent modifications.<sup>15</sup>

Solid phase and solution peptide synthesis technologies have advanced significantly, thus improving the availability of therapeutic peptides from an economic perspective. Previously, there were negative perceptions about the quality and scale achievable by the synthetic methodologies for the development of therapeutic peptide candidates. The production of tons of the peptide Fuseon (Enfuvirtide, 36 aminoacids), inhibitor of the human immunodeficiency virus (HIV), revolutionized the SPPS and turned it into the standard technology for obtaining these compounds in research and production stages.<sup>16</sup>

Peptides are used in the treatment of diabetes, malaria, arthritis, cancer, allergies, obesity and cardiovascular diseases.<sup>17</sup> They have great advantages as therapeutic and prophylactic agents due to their low drug-drug interaction and poor cytotoxicity.<sup>15</sup> Peptide drugs are quite common nowadays,<sup>18</sup> however, their usage is limited due to their low metabolic stability, low oral absorption, rapid excretion through the kidney and liver, low immunogenicity and high hemolytic activity.<sup>19</sup>

Peptides have a low half-life *in-vivo* because they are usually degraded by proteases.<sup>20</sup> Proteases are specific for L-aminoacids and are classified in endopeptidases and exopeptidases (amino or carboxypeptidases). The formers produce the hydrolysis of non terminal peptide bonds and the latter hydrolyze the residues of the *N* and *C* ends. Endopeptidases such as chymotrypsin rapidly degrade amide bonds where Phe, Trp or Tyr (slowly to His) participates and trypsin affects Arg and Lys. Aminopeptidases and carboxypeptidases are nonspecific in their action.<sup>21</sup>

To overcome these drawbacks, current research on peptides is aimed primarily at improving the pharmaceutical formulation to promote the release process, and the design of new methodologies for covalent modifications that enhance their properties.

## **2.2 Antimicrobial peptides. Characteristics and biological importance.**

AMPs (Antimicrobial Peptides) are a widely distributed defense mechanism in plants, insects, vertebrates, unicellular organisms and even mammals.<sup>22</sup> They present a broad spectrum of activity against fungi, bacteria, viruses and protozoa,<sup>23</sup> so they have an important protective action in organisms that lack an immune system while in vertebrates they are part of the innate immunity.<sup>22b</sup> In addition, they are not affected by mutations that cause resistance to classical antibiotics.<sup>24</sup>

The AMPs were discovered more than 90 years ago, with gramicidin being one of the first reported, since its discovery occurred in 1939 and its effectiveness in protecting against pneumococcal infection was demonstrated. In 1941, another AMP, tirocidine, was discovered and found to have activity against gram-positive and gram-negative bacteria. In the same year, it was also isolated from the plant *Triticuma estivum*, the AMP purotionina, which was effective against fungi and pathogenic bacteria.<sup>25</sup>

Although the first AMPs were discovered several years ago, research on this topic did not become relevant until 1980 when cecropins and magainins were found, mainly due to difficulties in the large-scale production. Since then, more than 5000 AMPs have been isolated from various natural sources and others have been synthesized by chemical methods.<sup>25</sup>

They are generally hydrophobic and amphipathic at physiological pH,<sup>26</sup> characteristics that favor their interaction with lipid bilayers, mainly those that form the membranes of pathogens.<sup>22a</sup> The structure of the AMPs is diverse, so numerous classifications have been published taking into account the organism producer, cell type, mechanism of action, etc. One of the more used criteria is based on the secondary structure, by which the AMPs have been divided into 4 groups:  $\alpha$ -helix,  $\beta$ -sheet stabilized by two or three disulfide bridges, extended structures with one or more predominant residues (such as Trp and Pro) and in the form of a loop due to the presence of disulfide bridges.<sup>26</sup>

AMPs have been found in a wide range of organisms. They can act as part of the innate defense system of plants, vertebrates and invertebrates, against infections.<sup>27</sup> In general, they have the ability to directly kill microbes. However, in recent years, the concept for this heterogeneous group has been extended to host defense peptides. This is due to their abilities to disturb growth and also to modulate the immune system.<sup>28</sup> Immunomodulation and, in some cases, “beneficial

immunogenicity” are extraordinary features which are not reachable by traditional antibiotics, because their chemical nature is functionally incompatible with the immune system.

AMPs can be used in the treatment of infectious diseases and/or complement the therapy with conventional antibiotics, since they show synergism.<sup>29</sup> In studies conducted by Nuding and others<sup>30</sup> it was demonstrated that the peptides HBD1, HBD3, HNP1, HD5, and LL-37 when combined with the antibiotics tigecycline, moxifloxacin and meropen have synergistic effect, which favors the antimicrobial activity against toxigenic and non-toxigenic strains of *Clostridium difficile*. Bacitracin has also shown this behavior in combination with topical antibiotics such as neomycin and polymyxin B.<sup>31</sup>

It has recently been shown that the peptide Ib-AMP-4 (derived from the plant *Impatiens balsamina*) has a potent activity against different gram-positive and gram-negative bacteria. In studies conducted by Fan and others,<sup>32</sup> it was shown that when combined with vancomycin, it inhibits the growth of Vancomycin-resistant *Enterococcus faecalis* (VRE). The effectiveness of other AMPs such as LZ1 has also been demonstrated. This peptide inhibits the growth of *Propionibacterium acnes* as well as *Staphylococcus epidermidis* and *Staphylococcus aureus*. In addition, it has been shown to inhibit the secretion of proinflammatory cytokines such as interleukin 1- $\beta$  (IL 1- $\beta$ ).<sup>33</sup>

Notably most AMPs are very hemolytic and toxic to mammalian cells (mellitin,<sup>34</sup> guavanin 2,<sup>35</sup> etc.) avoiding their use orally, therefore, only topical formulation is possible in the majority of cases (commercial triple antibiotics).<sup>36</sup>

### **2.3 Resistance to antibiotics. Antifungals AMPs and Cm-p5. Commercialization of antifungal peptides.**

Giving the lack of new classes of conventional antibiotics is necessary the development of new therapeutic principles and/or complements for infectious diseases.<sup>37</sup> Bacterial and fungal resistance to antibiotics is a great issue for medicine nowadays, not only due to the expected consequences of microbial resistant strains,<sup>38</sup> but also because of the unexpected effects in brain, neurons<sup>39</sup> (Alzheimer, ME or ALS conditions),<sup>40</sup> and biofilm formation in ear canal and teeth.<sup>41</sup>

In addition, abuse in the usage of antibiotics has been proposed as a drawback for natural microbiota, causing many and unexpected immunological, gastric, neurological, and opportunist microorganism disorders. In the same sense, antifungal or antibacterial drugs for systemic treatment are always accompanied by many side effects, making necessary the hospitable monitoring.<sup>42</sup>

Since 2000, 20 new antibiotics have been launched on the market and approximately 40 compounds are in clinical trials.<sup>43</sup> Of these, at least 15 are AMPs or mimetics that act directly as antimicrobial or immunomodulatory agents.

At the same time, the speed in the approval of new antimicrobial drugs remains in continuous decline,<sup>44</sup> with regulatory control criteria much more demanding than those that are necessary for any new drug to be licensed for human use.<sup>45</sup>

For example, peptide hLF1-11 (composed of the last 11 aminoacids of the *N*-terminus of human lactoferrin) is in phase I/II clinical trials. This peptide acts indirectly on infections through a mechanism of immunopotentialization of the host response against *Candida* and other non-fungal pathogens,<sup>46</sup> and it was found to be safe and tolerable when administered intravenously.<sup>47</sup> On the other hand, PAC-113 is one of the most advanced peptides, currently developed for the treatment of oral candidiasis and for vaginal, dermatological and ophthalmological applications.<sup>45</sup>

## 2.4 Peptide Synthetic Methods

Peptides can be obtained by chemical synthesis, recombinant deoxyribonucleic acid technology, transgenesis and enzymatic synthesis.<sup>48</sup> There is great interest in obtaining peptide structures either by extraction from natural sources or by chemical synthesis. In living organisms, peptides appear in minimal quantities and the extraction is costly and complicated. In addition, the modification of natural structures is a complex process (possibility of chemical modifications). Synthetic molecules are more robust, easy to transport and store, and their production is more economical and flexible.<sup>49</sup>

Pharmacologically active peptides such as oxytocin (hormone produced by the pituitary and which determines the contraction of the uterus and accelerates labor in mammals), corticotropin and secretin, have been synthesized since the 50s of the last century with optimization and automation improving year after year.<sup>50</sup>

To synthesize a peptide, two synthetic procedures are considered: synthesis in solution and synthesis in solid phase (SPPS).<sup>51</sup> Synthesis in solution is cheaper if it is used to obtain small peptides; but the mandatory purification of the obtained intermediates is a tedious and slow process that requires high specialization, a disadvantage with respect to the SPPS in the case of larger sequences.<sup>52</sup> SPPS requires a shorter reaction time, peptides are obtained with a high degree of peptidic purity and do not produce mechanical losses.<sup>50</sup>

There are two strategies of peptide synthesis: linear or steps synthesis in which each aminoacid is sequentially coupled<sup>53</sup> and it is used for small oligopeptides; and the convergent synthesis,

where short fragments are grown separately, which are then purified and assembled with high yields, more useful in the synthesis of large peptides and proteins.<sup>54</sup>

For the formation of the amide bonds by aminoacid binding, it is necessary to activate the carboxylate and selectively protect, temporarily and orthogonally, the functional groups outside to the coupling. The activation must guarantee high yields and low levels of racemization of the C $\alpha$  and is done by introducing an electroceptor group by means of: a) activation in situ (carbodiimides, uronium salts and phosphonium salts) or b) preparation and previous isolation of the active species (acyl chlorides, acylazides, anhydrides, active esters).<sup>49b</sup> The *in-situ* activation methods with carbodiimides (DIC, DCC, EDC) are more used due to their lower cost, although, the salts of uronium (HATU) and phosphonium (PyBOP) are more efficient and less toxic (Figure 1).

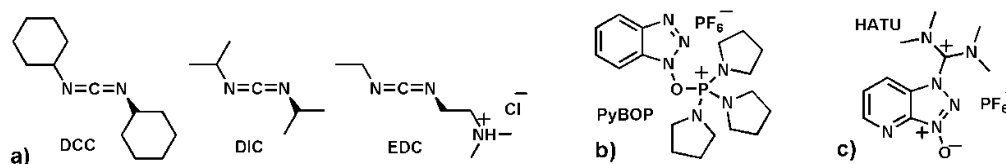
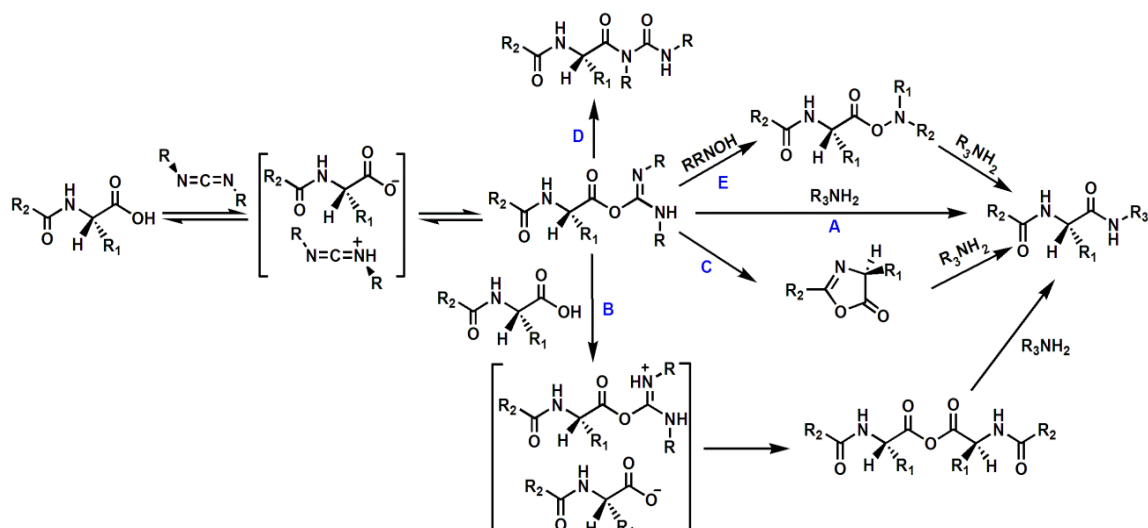


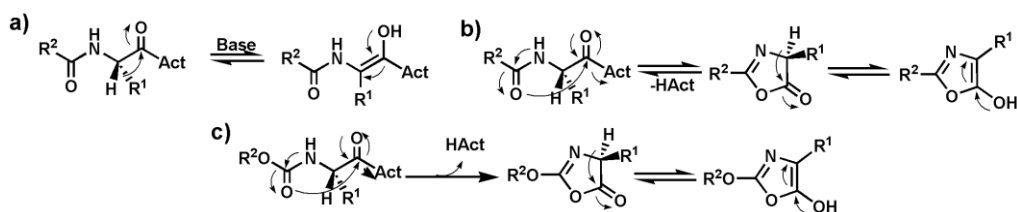
Figure 1: Common coupling reagents for peptides, a) carbodiimides, b) phosphonium salts and c) uronium salts.

During activation with carbodiimides (Scheme 1),<sup>55</sup> the protonation and the formation of an ion pair with the carboxylate (slower process in the presence of bases) generates *O*-acylureas which are potent acylating agents, not only of the amine (Scheme 1A), but of another carboxylate (Scheme 1B) and can cyclize to form the oxazolones (Scheme 1C). The formation of *N*-acylureas (Scheme 1D) is a frequent cause of diminution of yields, but can be avoided maintaining a low temperature or using apolar solvents. All postulated intermediaries are attacked by nucleophiles with decreasing reactivity in the *O*-acylurea series (Scheme 1A), 2-alkoxy-5(4H)-oxazolones (Scheme 1C) and symmetrical anhydrides (Scheme 1B). Which of the three is involved in the formation of the peptide bond depends on the presence, availability and reactivity of the amino component. The apolar solvents (DCM) and to a lesser extent the aprotic polar (DMF) favor the formation of *O*-acylureas.



Scheme 1: Peptide coupling with carbodiimides and racemization inhibitor.

The *O*-acylureas, the anhydrides and the 5(4*H*)-oxazolones in the presence of strong bases can cause the enolization of the C $\alpha$  of the amino acid following three mechanisms (Scheme 2): a) basic enolization, b) oxazolone formation in dipeptides (it causes that peptides should be always grown from the *C*-terminus to the *N*) and c) oxazolone formation in amino acids protected as carbamates (less important due to the lower basicity of *NH*).<sup>55</sup>



Scheme 2: Racemization mechanisms. Act: activating.

The use of the nucleophiles HOBt, HOAt, HOSu, HOObt, Oxyma Pure and OxymaK (Figure 2) diminishes the occurrence of collateral reactions (Scheme 1, B, C, D) during coupling and especially racemization. These substances are *N*-substituted oximes with electroacceptor groups that reinforce the alpha effect present between the *N* and the *OH*, turning them into excellent nucleophiles (HOMO of greater energy) and at the same time very good leaving groups. These compounds react quickly with the *O*-acylureas forming the corresponding activated esters (Scheme 1E), which are less reactive and more stable in presence of the bases.<sup>55</sup> Inconveniently benzotriazols as HOBt, HOAt and HOObt are explosives and especially Oxyma Pure have been developed to substitute them, showing inclusive more efficiency in terms of coupling times and diminutions of racemization. On the other hand, OxymaK increase the yield when Cl-Trt-

Chloride resin is used by avoiding early cleavage of the peptide due to acidity of the Fmoc-Aa-OH (pKa= 2-3) and any other racemization inhibitor (pKa= 4-5).

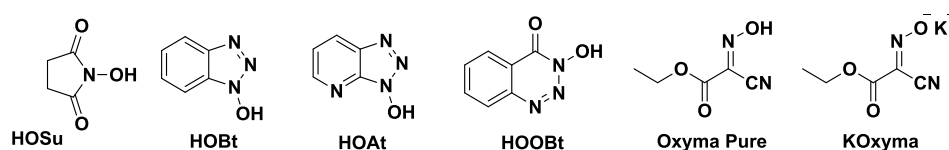


Figure 2: Most common racemization inhibitors.

To protect selectively, orthogonally and temporarily the functional groups other than the coupling, different protective groups and different protection schemes have been developed. After each coupling, the *N*-terminus which will participate in the formation of the following peptide bond is deprotected, so that orthogonal protective groups are used, meaning that they can be selectively eliminated in the presence of others, according to the reaction conditions.<sup>55</sup>

The amines are mostly protected in the form of carbamates, the most common being Fmoc, Boc, Cbz or Alloc and the carboxylic acids are commonly protected in the form of methyl, tertbutyl or benzyl esters (Figure 3). The Fmoc, MeO and BzlO groups are sensitive to basic conditions, Boc and tBuO to moderately acidic conditions, Cbz and BzlO to strongly acidic conditions or hydrogenolysis and Alloc is eliminated with Pd<sup>(0)</sup> catalyst.<sup>50</sup> The protection schemes are classified according to the difference of conditions to eliminate the *N*-end protective groups with respect to those of the side chains, the most used are the Boc/Bzl<sup>56</sup> and the Fmoc/tBu.<sup>57</sup>

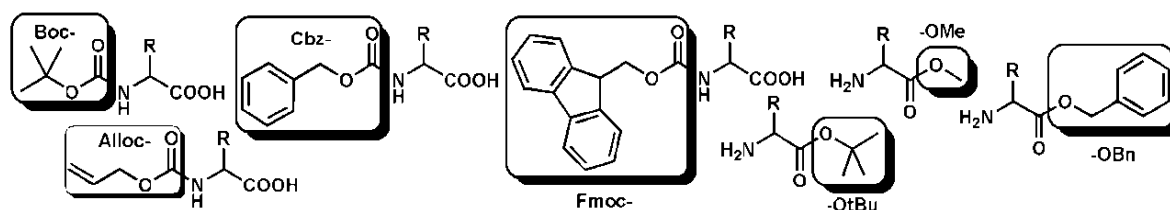


Figure 3: Some amino and carboxylate protecting groups.

## 2.5 Solid Phase Peptide Synthesis. Polymeric Supports.

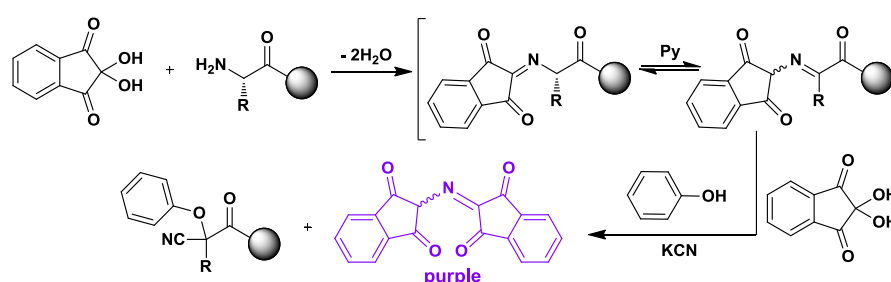
SPPS was developed by Merrifield in 1963 (Boc/Bzl methodology) and its name is due to the fact that the peptide sequence grows anchored to a polymeric support insoluble in any of the solvents used.<sup>58</sup> Among its main advantages is the ease of purification of the final product, the possibility of reusing the polymer matrix and the stability of these polymers at different conditions. In 1978 Sheppard incorporated the Fmoc/tBu protection scheme that has practically replaced the original Boc/Bzl methodology.<sup>49b</sup>



The SPPS is carried out by the covalent assembly of the selected amino acid (*C*-terminal deprotected) to an insoluble support. Consecutive steps of deprotection of the *N*-terminus and coupling of the desired amino acids, after activation, allow the peptide anchored to the support to grow by means of a linear synthesis strategy.<sup>50</sup>

In each coupling a complete and rapid conversion is necessary, which is achieved with an efficient reaction based on the combination of a carboxylic acid activator, an inhibitor of racemization and the use of an excess of reagents, which are eliminated with washed and vacuum filtration.

The completion of each coupling step is checked by the ninhydrin test, a sensitive and efficient colorimetric method that allows the detection, even in small amounts, of primary amines. The pale yellow ninhydrin reacts at 100°C in the presence of Py, phenol and KCN causing an *O*-phenylcyanohydrin and a purple complex, indicative of the presence of primary amines (Scheme 3, Reverse Strecker reaction).<sup>59</sup>



Scheme 3: Proposed mechanism for the reaction of primary amines with ninhydrin in solid phase.

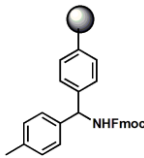
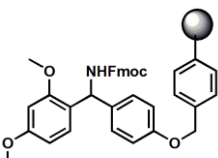
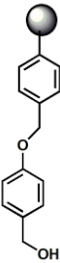
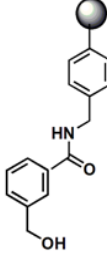
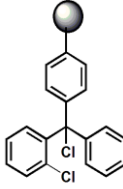
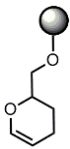
The anchoring to the resin is achieved with bifunctional molecules, which are permanently linked to the resin at one end, and on the other, they temporarily bind to the amino acid that will start the peptide to be synthesized. These molecules are called linkers and have a functional group capable of reacting orthogonally during the final step of cleavage, in conditions that may or may not affect the protective groups of the side chains of the amino acids, and which are responsible for selectively breaking the temporal link with the peptide (Table 1).<sup>60</sup>

A suitable synthetic strategy allows the preparation of diverse peptide structures and even introducing covalent modifications by combining the principle of orthogonality between the protective groups of the side chains, the  $\alpha$ -amino protector and the linker.<sup>61</sup>

The first solid supports were based on polystyrene (first generation resins) and are still the type of polymeric support most used in SPPS. This support is highly stable in the working pH range, is mechanically stable under vacuum filtration conditions, swells with solvents such as DMF, DCM and THF, and can be obtained with a substitution level of 0.3 to 1.2 mmol/g of

resin. Polyamide or second generation resins swell better in polar solvents and are more flexible than polystyrene resins.<sup>54</sup> PEG (third generation) resins can be of two types: with embedded PEG, which were developed to obtain more stable resins, swell in polar and non-polar solvents and present substitution of 0.15 to 0.5 mmol/g. The resins composed of a PEG/PPG network; which are compatible with polar and non-polar solvents, prevent the peptides from aggregation and favor the speed of the coupling reactions.<sup>54</sup>

Table 1: Some characteristics of the most used polymer supports.

Resin	MBHA	Rink or Am	Wang	HMBA	Trt	DHP
Methodology	Boc/ Bzl	Fmoc/tBu	Fmoc/tBu	Fmoc and Boc	Fmoc/tBu	Fmoc/tBu
Linker Structure						
Extreme C	Amide	Amide	Acid	Acid	Acid	Alcohol
Cleavage	HF	95% TFA	95%TFA	NaOH (1M)	1% TFA	PPTS
Lateral Chain	Unprotected			Protected		

### 2.5.1 Boc/Bzl Chemistry

The Boc/Bzl protection scheme presented by Merrifield upon introduction of the SPPS is based on the use of the Boc group as temporary protector of the  $\alpha$ -amino and benzyl groups (Bzl and Cbz, orthogonal to Boc) as protective groups of the side chains.<sup>62</sup> Glu(OBzl), Asp(OBzl), Lys(Cbz(2-Cl)) and Arg(Tos), His(Cbz), Cys(Acm), Ser(Bzl), Thr(Bzl), Trp(6-Dcb) and Trp(Cbz(2-Br)); that resist the deprotection conditions of Boc (TFA 40% in DCM). The treatment of Boc-Aa-Resin with TFA liberates isobutylene, CO<sub>2</sub> (causes an increase in the entropy that favors the reaction) and the amine remains protonated, so it must be neutralized before the next coupling. These groups are labile in acidic conditions (95% TFA) but can be selectively eliminated if necessary. For example, Cbz and OBzl are removed by hydrogenation or alkaline hydrolysis and the Acm is released with I<sub>2</sub>. In this protection scheme, the MBHA resin (Table 2) is used, whose connector is sensitive only to extremely acidic conditions, achieving the de-anchoring and the elimination of all the protective groups of the side chains by treatment with HF.<sup>53</sup>

## 2.5.2 Fmoc/tBu Chemistry

Many peptides are not stable to the vigorous cleavage conditions (HF) used in the Boc/Bzl methodology. Most suitable conditions to carry out the SPPS were accessible in 1978, when Sheppard developed the chemistry Fmoc/tBu.<sup>49b</sup>

The Fmoc/tBu protection scheme is based on the use of the Fmoc group as temporary protector of  $\alpha$ -amino and of tertbutyl and benzyl groups (tBu, Boc, Bzl) as protective groups of the side chains.<sup>62</sup> Glu(OtBu, OBzl), Asn(OtBu, OBzl), Lys(Boc), Arg(Pbf), His(Boc), Cys(Trt), Ser(tBu), Thr(tBu), Trp(Boc) are used; also Tyr(tBu), that resists the conditions of deprotection of the Fmoc (Pip 20% in DMF). These groups are labile under strongly acidic conditions (95% TFA), but they can be selectively eliminated if necessary. For example, Bzl is removed with hydrogenolysis and Trt is released with 1% TFA. Rink resin (Table 2) is used for this methodology; its connector is sensitive to acidic conditions, achieving the de-anchoring of the peptide by treatment with 95% TFA, which at the same time eliminates all the protective groups of the side chains.<sup>53</sup>

## 2.6 Peptide characterization

In the state of art, synthetic peptide characterization is a constituted science and it is not necessary a dept characterization in investigation stages. Peptide synthesis at the CIGB is relized under high quality control conditions due to the regulatory agencies controls that permit the use of these molecules in medical application. The synthetic proces is sequential (you have a register with the order of each aminoacid in the sequence) and include a previous checking of the enantiomeric purity and quality of all the commercial reagents, spetially the aminoacids. The stages of synthesis are register manually in time of coupling reaction, batch, quantity and type of regents, laboratory temperature, etc, a notably different approach when compared with isolated peptides from natural products. This permit to analice and correct instaintainly any problem that could be occur during the manufacturing proceses.

That quality control guaraticees the necessary reproducibility, reliability and exactitude in peptide characterization during investigation stage that could be realized only knowing the purity by RP-HPLC, the molecular mass by ESI-HRMS and if necessary, the secondary structure by CD. In investigation stages, biopharmaceutical industries need a rapid characterization methods for many peptidic analogues or covalent modifications of a drug candidate, validated with the experience and science and only the more active versions are charactericed depper because should pass to production stages.

Peptide characterization during production stage are realized knowing the purity by RP-HPLC, the yield of each batch (only a control of reproducibility because the purity is more important in solid phase synthesis), the molecular mass by ESI-HRMS, the sequence by ESI-HRMS-MS (only for the three first batch), the total structure and conformation by NMR (only for validation and registry, first batch).

Peptide sequenciation by ESI-HRMS-MS is more accurately for acyclic peptides, with the *N*-terminal deprotected and normaly only discret sectors of the sequence are sequenced. Many times, peptide sequenciation or NMR is not sufficient for the total structure elucidation and the use of many complementary techniques is desired.

An important aspect in the analysis of peptides with ESI ionization source is the tendency to produce multi-charged ions, which benefits the accuracy of measurements of high molecular masses such as those of peptides and proteins and, on the other hand, originates spectra of complicated masses. For peptides and proteins, the spectrum actually consists in series of quasimolecular ions that have multiple charge  $(M+nH)^{n+}$ , appearing in the spectra double (A2) and triple (A3) charged peaks, from which we can determine the molecular mass of the synthesized compound. This is a technique that is characterized by a high accuracy, which is due to the redundant *m/z* information that originates, corresponding to the different states with multiple charge of each species.<sup>63</sup>

The ESI-HRMS equipment at the CIGB have a QTOF-2 analyzer that only have exactitude in the second digit. On the other hand the resolution of the equipment is independent of the exactitude and QTOF-2 permit determine differences of masses between 0-1 Da, enabling the determination of the isotopic distribution and the corresponding multiple charge  $(M+nH)^{n+}$  peaks. The error in the second digit is not resolution of the equipment, is exactitude. For determine a major exactitude with the QTOF-2 analyzer is necessary to use an internal standar for the calibration. In investigation stages or quality controls, normaly is not used the internal standar.

## **2.7 Salt bridge stabilization of secondary structures of peptides and proteins**

In the stabilization of secondary structures of peptides and proteins, are involved factors such as hydrophobicity, van der Waals forces, hydrogen bonds, dipole-dipole and ion pairs interactions.<sup>64</sup> The ion pairs are formed between residues with charged side chain, as is the case of the oxygens of the carboxyl groups present in residues D or E, and the nitrogen atoms of the residues of Arg, Lys or His, when they are present at a distance less than 4Å.<sup>65</sup> Negative residues Asp and Glu favor the  $\alpha$ -helix when they are located near the *N*-terminal and in the

first turn. On the contrary, positively charged residues, Lys and His, stabilize the  $\alpha$ -helix when they are in positions near to the C-terminal.<sup>65</sup>

Several types of electrostatic forces favor the enthalpy component of the overall energy and balance the loss of conformational entropy by formation of an  $\alpha$ -helix.<sup>66</sup> These include the hydrogen bonds formed between  $\text{CO}_i \cdots \text{NH}(i+4)$  and the interactions between the side chains spaced at  $i$ ,  $i+3$  and  $i$ ,  $i+4$  and with the ends of the  $\alpha$ -helix (Figure 4).<sup>64b</sup>

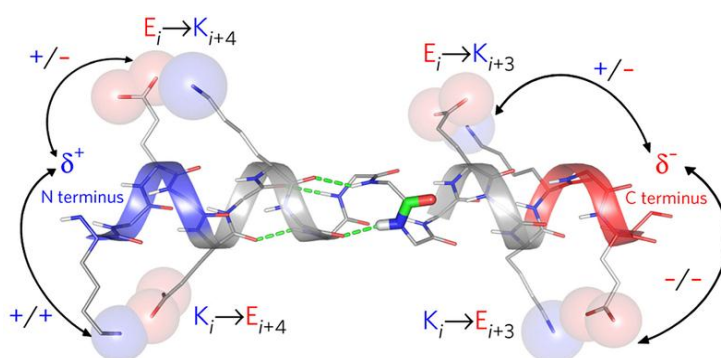


Figure 4: Stabilization of the  $\alpha$ -helix of a peptide by salt bridge interactions of the residues Glu(E) red and Lys(K) blue of the side chain spaced at  $i$ ,  $i+3$  and  $i$ ,  $i+4$  and by hydrogen bonds formed between  $\text{CO}_i \cdots \text{NH}(i+4)$  (green).<sup>64b</sup>

However, peptides, unlike proteins, are normally small molecules that do not have a secondary structure well defined in solution, and it is only by interaction with the active site or with a membrane (intermolecular interactions) that a defined conformation is induced. To achieve that a peptide sequence adopts a defined conformation or at least a 3D energy closer to that present in the parent protein, it is often necessary to form disulfide or lactam bridges that generate a certain conformational constraint.<sup>67</sup>

The introduction of a structural constraint by cyclization, although does not make the peptide adopt a defined secondary structure in solution, can decrease the degrees of freedom (accessible microstates, entropy of the system), making easier the interaction with the active site.<sup>67</sup>

## 2.8 Covalent modifications of peptides

The covalent modification of peptides by cyclization, polymerization, conjugation to carrier proteins,<sup>68</sup> introduction of *N*-substitutions or peptoid residues, variation of the *N* and *C* terminals,<sup>69</sup> pegylation,<sup>70</sup> change of aminoacids in the sequence, phosphorylation, glycosylation, lipidation<sup>71</sup> or the synthesis of peptide-steroidal hybrids<sup>72</sup> have been important ways in obtaining drugs within the fields of combinatorial chemistry and biotechnology. These changes give to the peptides a greater selectivity and resistance to proteases, and increase conformational rigidity or immunogenicity, each case accordingly.

### 2.8.1 Structural constraints by cyclization

The introduction of structural constraints into a synthetic peptide is one of the modifications that have been used to improve the therapeutic properties<sup>67</sup> or to mimic the secondary structure they present in a native protein.<sup>73</sup>

Cyclization can decrease the conformational flexibility of the linear peptide, improve membrane permeability and thermodynamic stability and metabolic stability,<sup>74</sup> besides increasing the stability to proteolysis by endo and exopeptidases.<sup>75</sup> This translates into an improved resistance of the peptide to extreme environments such as high temperatures, media with low or high pH values and high concentration of organic solvents. Cyclization can be achieved by formation of disulfide bonds, cyclic amide (lactam), ester, hydrazine, among others.<sup>76</sup>

The most accepted method to achieve specificity in the formation of intramolecular bridges is the use of an orthogonal protection system for the aminoacids that form the cycles.<sup>77</sup> Different protective groups have been developed to selectively obtain disulfide bridges by combining the cyclization reaction in solid phase and in solution.<sup>78</sup> The synthesis of peptides with one or more intramolecular bridges containing up to three disulfide bonds has been described.<sup>79</sup> The synthesis of four disulfide bonds is rarely reported.<sup>80</sup> However, Fangzhou Wu et al. reported recently the sequential synthesis of four disulfide bonds in insulin analogues with the use of six different protective groups of Cys.<sup>74</sup>

### 2.8.2 Formation of disulfide bridges

The formation of a single disulfide bond in peptides is generally carried out from the free thiol groups present in the aminoacid residues. It can also be carried out by the deprotection/oxidation method from the peptide with the protected thiol groups.<sup>81</sup>

The formation of several disulfide bridges can be achieved by the method of randomization of disulfide bridges in solution,<sup>82</sup> by a regioselective formation<sup>83</sup> or by the combination of both.<sup>84</sup> With the use of the method of randomization of disulfide bridges multiple products are obtained and those thermodynamically more stable prevail.<sup>74</sup> For the regioselective formation of several disulfide bridges, different groups are used to protect the pairs of cysteines that will be linked together.<sup>74, 85</sup> This is the method of choice to ensure the desired formation of the bonds, since an analytical control of the oxidation of the cysteines can be carried out as the disulfide bridges gradually form.<sup>86</sup> The formation of the disulfide bridges can be carried out both in solution and in solid phase. When the cyclization is carried out in solid phase, resins with a low substitution

level must be used to favor the intramolecular reaction by the phenomenon known as "pseudo-dilution".<sup>81</sup>

The most common oxidation method of thiol groups present in free Cys is using oxygen from the air as oxidizing agent, in an aqueous solution, at basic pH. This method is very simple, but it can take several days.<sup>75</sup> Oxidation of Cys residues present in peptides can be mediated by substances with low molecular weight with disulfide bonds or two free thiol groups such as cystine, cystamine, dithiothreitol, dithiobis-2-nitrobenzoic acid, or by other electroceptor substances such as diiodide, dimethylsulfoxide (DMSO), diamide and potassium ferrocyanide.<sup>75</sup> The competition between the formation of intramolecular disulfide bonds (cyclization) or intermolecular (oligomers) is mainly governed by the concentrations of the Cys pairs. Thus, to obtain the intramolecular bridges diluted solutions are used and to obtain dimers or oligomers, oxidation is carried out in concentrated solutions.<sup>81</sup> The formation of disulfide bridges can be verified by the Ellman colorimetric test (for oxidation from free thiol groups),<sup>87</sup> by RP-HPLC<sup>88</sup> and by mass spectrometry.<sup>89</sup> Characterization by RP-HPLC is based on the change in the retention time of the oxidized species with respect to its precursor. However, the retention times of the cyclic and acyclic species often coincide, and in order to distinguish them, it is necessary to carry out the iodoacetamide test in which the free thiol groups are protected and their retention time is different from the disulfide bridged cyclic compound.

It has been observed that Cys residues can be desulfurized during cyclization in slightly basic medium (pH 8-9). This process occurs by extraction of the C $\alpha$  proton from the Cys and elimination of H<sub>2</sub>S by an E1-Cb mechanism, with the formation of dehydroalanine. Then an intramolecular Michael addition with the free thiol of another Cys generates a thioether bond with the C $\beta$  of the desulfurized residue, however, if the Cys residues are very close (*i*, *i*+2) or sterically hindered, the intramolecular addition does not happen and the peptide remains in the form of dehydroalanin.<sup>90</sup>

### 3 Results and discussion. Chapter 1

#### 3.1 Design of Cm-p5 mutants

Normally, an Ala scanning is conducted for estimating the relative importance of each aminoacid in the biological activity of peptides.<sup>91</sup> However, a simpler and faster approach is the rational change of aminoacids<sup>92</sup> according to the natural structures currently found in AMPs, like the presence of many Arg, Lys, Cys and Trp residues (His in case of histatins),<sup>93</sup> and alternated positive charges to form a facial amphiphilic  $\alpha$ -helix or  $\beta$ -sheet. This is a fundamental structural principle that works well in many cases. AMPs possess a shape in which cationic and hydrophobic aminoacids organize spatially in discreet sectors of the molecule, forming an amphipathic pattern.<sup>94</sup>

Tryptophan is frequently found in interaction with the interfacial region of the lipid membrane,<sup>95</sup> Arg and Lys, have positive charge at physiological pH permitting the selective interaction with microbial membranes and Cys, in certain conditions, stabilize secondary structures by formation of disulfide bridges.<sup>96</sup>

Based on a simple electrostatic interaction model between cationic AMPs and negatively charged bacterial/fungi membranes, are notable several structural features in the helix projection of Cm-p5. This peptide presents hydrophobic residues at the C-terminus, a free N-terminus (positively charged), and an amphipathic helical structure with positive charges concentrated towards one side of the helix, but less defined hydrophobic region.

By analyzing the Schiffer-Edmundson (wheel) projection of Cm-p5 (Figure 5d), it is possible to notice that the polar side of the helix contains an unexpected hydrophobic Ile residue. In addition, polar residues, such as Glu and His, are curiously present in the putative hydrophobic face.

Previous research,<sup>19</sup> have demonstrated that inserting Arg-Cys (forming Cm-p3) or Met-Lys (forming Cm-p4) in the C-terminus of the mollusk derived peptide Cm-p1 did not improve antimicrobial activity, however Leu-Phe (forming Cm-p5) insertion gives rise to high antifungal activity (Figure 5).

Using the online server <http://heliquest.ipmc.cnrs.fr/cgi-bin/ComputParams.py>, helical parameters<sup>97</sup> of helicoidal peptides were obtained. Hydrophobicity (H, intrinsic capability of a peptide to move from an aqueous into a hydrophobic phase), frequency of polar residues (Freq. Polar), relative hydrophobic moment ( $\mu$ Hrel, quantitative measure of peptide amphipathicity,<sup>98</sup> defined as the vector sum of the hydrophobicities of the individual aminoacids) and the angle



moment (angleM: angle in radians between the horizontal plane and direction of  $\mu_{Hrel}$ ) are listed in Table 2.<sup>99</sup>

These parameters do not indicate in any sense that these peptides have helicoidal behavior and is not our interest to demonstrate that they form helix. All calculations were realized supposing  $\alpha$ -helical structure and as an explanation of the loss of antifungal activity for all these analogues of Cm-p5.

Table 2: Helical parameters for non-amidated Cm-p1, Cm-p3, Cmp4 and Cm-p5

	<b>Helix</b>	<b>H</b>	<b><math>\mu_{Hrel}</math></b>	<b>z</b>	<b>FreqPolar</b>	<b>angleM</b>
Cm-p1	SRSELIVHQR	0.18900	0.05685	1	0.700	5.18806
Cm-p3	SRSELIVHQRRC	0.20167	0.21172	2	0.667	5.35967
Cm-p4	SRSELIVHQRMK	0.17750	0.09499	2	0.667	1.98272
Cm-p5	SRSELIVHQLRF	0.44833	0.19215	1	0.583	0.24380

H represents hydrophobicity,  $\mu_{Hrel}$ : relative dipole moment of hydrophobicity, z: total charge, FreqPolar: frequency of polar groups, angleM: angle in radians between the horizontal plane and direction of  $\mu_{Hrel}$

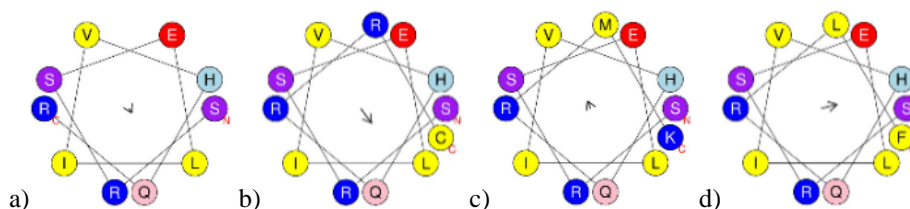


Figure 5: Schiffer-Edmundson projections of the antifungal peptides Cm-p1 (a), Cm-p3 (b), Cm-p4 (c) and Cm-p5 (d).

When analyzing in detail the effect of these C-terminal modifications in the Cm-p1 activity, it is observed that addition of Arg-Cys (forming Cm-p3) do not considerably change the frequency of polar groups, hydrophobicity or orientation (arrow in Figure 5b) of relative hydrophobic moment, but significantly alters the  $\mu_{Hrel}$  magnitude (Table 2). In contrast, the insertion of Met-Lys (forming Cm-p4) turn the direction of  $\mu_{Hrel}$  (arrow in Figure 5c), but poorly increases its magnitude (Table 2). Addition of Leu-Phe (forming Cm-p5), greatly modifies all the parameters, especially, H and  $\mu_{Hrel}$  (arrow in Figure 5d and Table 2). In this case, Phe is located in a  $i, i+4$  position respect to His, therefore there may occur a  $\pi$ - $\pi$ -interaction between the phenyl and imidazole groups of these residues, which could have some effect in helix stabilization. Based on a previous article,<sup>5</sup> Cm-p4 is a more active version of Cm-p1 than Cm-p3, which may indicate that the variation of the direction of  $\mu_{Hrel}$  is more relevant than the variation of its magnitude, particularly in Cm-p5, where  $\mu_{Hrel}$  is almost directed from the hydrophilic to the hydrophobic face (arrow in Figure 5d).

These previous results, apparently suggest that magnitudes of H,  $\mu_{Hrel}$  or its direction, are fundamental for activity, favoring sequences with elevated H (intrinsic capability of a peptide to move from an aqueous into a hydrophobic phase) or  $\mu_{Hrel}$  (quantitative measure of peptide

amphi-pathicity) and direction of  $\mu\text{Hrel}$  from hydrophobic phase to hydrophilic to promote membrane interaction.

Regarding these results, 14 analogues of Cm-p5 (Figure 6 and Table 3) were designed based on SAR. The experimental strategy of this work pretends, with a minimal use of resources, to gain an insight on how the antifungal activity of the Cm-p5 is affected by the change of aminoacids. Arg residues remained in almost all cases since positive charges in the polar face of the helix are essential for membrane interaction and biological activity.

The fundamental modifications introduced in the sequence of Cm-p5, based on aminoacids charge at physiological pH, were: *i.* change of the negative Glu residue, *ii.* introduction of another positive charge by mutation of Lys or Arg by Ile; *iii.* change of His by a positively charged Arg; *iv.* change of Leu5 by another positively charged residue (Lys) and *v.* truncated versions, where residues such as Leu, Arg, Ser, Glu or His were eliminated.

All the performed changes will assist in evaluating the contribution of each mutated residue to the helical stabilization and therefore, to the biological activity of the peptide. Glu was modified by the similar but neutral Gln (peptide 3 in Table 3), in the case of Asp (peptide 2 in Table 3), the negative charge was maintained but the length of the lateral chain was modified. The charge was also eliminated by mutation by Ala (peptide 4 in Table 3) and  $\beta$ -Ala (peptide 5 in Table 3), simulating the classical alanine scanning. Changing His for Arg (peptide 1 in Table 3), we will assess the role of the neutral His residue at physiological pH and the effect of a permanent positive charge. Further changes, such as Ile for Lys (peptide 7 in Table 3) or Arg (peptide 6 in Table 3) will introduce another positive charge within the hydrophilic face. Truncated analogues could indicate, for example, if the activity is influenced by the interaction of Glu and His in  $i+3$  (peptide 9 in Table 3) or Glu and Lys in  $i,i+2$  (peptide 10 in Table 3).

Dimeric MAP (Multi Antigenic Peptides) type peptide was synthesized, since, activity improvement in those cases was reported.<sup>100</sup> *N*-terminal acetylated Cm-p5 was produced to evaluate if the positively charged free *N*-terminus contributes to the antifungal activity.

Chemical synthesis is a valuable tool to obtain analogues of biologically active peptides found in natural sources. The experimental feasibility of SPPS allowed us to introduce rational changes to the peptide sequence, in order to generate several diverse structures. Fmoc/tBu chemistry is preferred and more useful if the peptide does not aggregate. Rink-MBHA-Resin is useful for the production of amidated and deprotected peptides and is a first generation polystyrene support, adequate for short sequences. The robust characterization of the produced peptides in this investigation step could be effected only by ESI-HRMS and RP-HPLC.

Monodimensional RMN determination is not sufficiently to differentiate simple aminoacid changes (Annex 3).

Table 3: Helical parameters of Cm-p5 analogues.

Peptide	Helix	H	$\mu$ Hrel	z	FreqPolar	angleM
Cm-p5	SRSELIVHQRLF	0.44833	0.19215	1	0.583	0.24380
Change of His						
1	SRSELIVRQRLF	0.35333	0.09818	2	0.583	0.14196
Change of Glu						
2	SRSDLIVHQRLF	0.43750	0.18479	1	0.583	0.20159
3	SRSQLIVHQRLF	0.48333	0.21791	2	0.583	0.35966
4	SRSALIVHQRLF	0.52750	0.25359	2	0.500	0.47042
5	SRS $\beta$ ALIVHQRLF	-	-	-	-	-
Change of Ile						
6	SRSELRVHQRLF	0.21417	0.41547	2	0.667	0.49375
7	SRSELKVHQRLF	0.21583	0.41384	2	0.667	0.49293
Change of Leu						
8	SRSEKIVHQRLF	0.22417	0.19104	2	0.667	1.49355
Truncated and change of Leu by Lys						
9	SRSE-IVHQRLF	0.33455	0.18199	1	0.636	2.44770
10	SRSEKIVHQ-LF	0.33636	0.46847	1	0.636	2.52341
11	-RS-LIVHQRLF	0.6060	0.33231	2	0.500	3.41529
12	SRSE-IV-QRLF	0.35500	0.42451	1	0.600	4.21201
Additional variants						
13	Ac-SRSELIVHQRLF	-	-	-	-	-
14	(SRSELIVHQRLF)2K	-	-	-	-	-

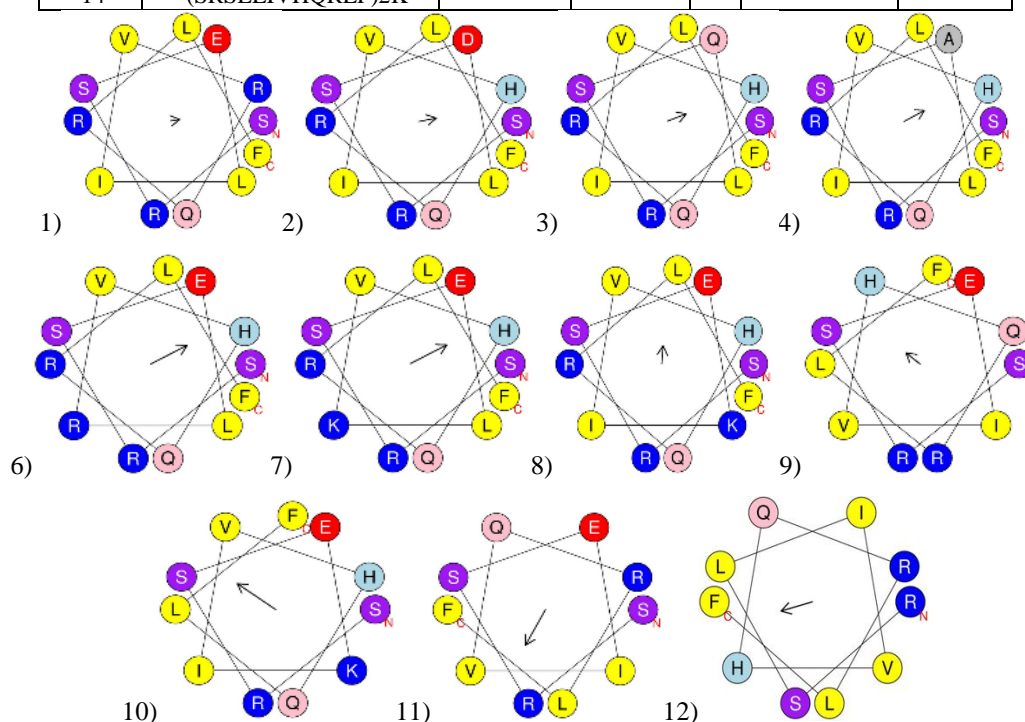


Figure 6: Schiffer-Edmundson projection of peptides analogues of Cm-p5.

### 3.2 Results and discussion regarding Cm-p5 peptide mutants.

Fourteen peptides were synthesized based on the previous design (Table 3). All the C-terminals of all the peptides were amidated (-NH<sub>2</sub>) since an Fmoc-Rink-MBHA resin was used. The Rink linker and the side-chain protecting groups were stables (orthogonals) functional groups toward

the Fmoc elimination treatment (Pip 20% in DMF) and coupling conditions. DIC/Oxyma combination (less than 1% of racemization)<sup>101</sup> was used for every manual coupling, showing an excellent efficiency due to simplicity of the synthesized sequences. Final cleavage and side chains deprotection, ether precipitation, centrifugation and lyophilization produced the crude product, ready for analytical mass determination and purification process. The functional screening of the designed peptides, based on antibacterial and antifungal activities, are listed in Table 4. Amphotericin B and Ampicillin were used as control for fungal and bacteria strains, respectively.

Table 4: Biological activity measured as Minimal Inhibitory Concentration (MIC) against different bacteria and fungi for each synthesized peptide. (NT: not tested)

	Peptide	MIC ( $\mu\text{g/mL}$ )				
		Sa	Ec	Ca	Cp	Tr
1	SRSELIVRQRLF-NH <sub>2</sub>	> 400	> 400	> 400	> 400	> 400
2	SRSDLIVHQRLF-NH <sub>2</sub>	> 400	> 400	> 400	> 400	> 400
3	SRSQLIVHQRLF-NH <sub>2</sub>	> 400	> 400	> 400	> 400	> 400
4	SRSALIVHQRLF-NH <sub>2</sub>	> 400	> 400	> 400	> 400	> 400
5	SRS $\beta$ ALIVHQRLF-NH <sub>2</sub>	> 400	> 400	> 400	> 400	> 400
6	SRSELRVHQRLF-NH <sub>2</sub>	NT	NT	> 400	> 400	NT
7	SRSELKVHQRLF-NH <sub>2</sub>	NT	NT	> 400	> 400	NT
8	SRSEKIVHQRLF-NH <sub>2</sub>	> 400	> 400	> 400	> 400	> 400
9	SRSE--IVHQRLF-NH <sub>2</sub>	> 400	> 400	> 400	> 400	> 400
10	SRSEKIVHQ--LF-NH <sub>2</sub>	> 400	> 400	> 400	> 400	> 400
11	--RS--LIVHQRLF-NH <sub>2</sub>	> 400	> 400	> 400	> 400	> 400
12	SRSE--IV--QRLF-NH <sub>2</sub>	> 400	> 400	> 400	> 400	> 400
13	Ac-SRSELIVHQRLF-NH <sub>2</sub>	NT	NT	10	10	10
14	(SRSELIVHQRLF)2K-NH <sub>2</sub>	NT	NT	> 400	> 400	NT
	Ampicillin	0,02	0,1953	NT	NT	NT
	Amphotericin B	NT	NT	0,25	0,25	0,125

Ca= *Candida albicans*, Cp= *Candida parapsilosis*, Tr= *Trichophyton rubrum*, Sa= *Staphylococcus aureus*, Ec= *Escherichia coli*

To our surprise, no aminoacid change, maintain or improve the antimicrobial activity of Cm-p5, indicating essential sequence characteristic needed to exert the biological activity. Substitution of His by Arg (peptide 1 in Table 3) involved a change in the protonation state of the aminoacid at position eight, increases the lateral chain length (reduces distance to the negative Glu), decreases  $\mu\text{Hrel}$  to half and its direction change slight with respect to Cm-p5 (Table 2, Figure 5). Decreasing  $\mu\text{Hrel}$ , changing the length of the lateral chain and/or the presence of permanent positive charge at the His position does not improve the antifungal activity. Similarly, modification of Glu residue by Gln, Ala,  $\beta$ Ala or Asp (peptides 2-5, Table 3), resulted in loses of antimicrobial activity. Apparently, the negative charge in the Glu residue (changing Glu by Gln) and the distance to this one (changing Glu by Asp) are essential for the activity; even more if we consider that magnitude of  $\mu\text{Hrel}$  and valor of H are practically the

same when Gln or Asp is present instead of Glu. Modification by Ala (peptide 4, Table 3), as expected, alter the H and magnitude of  $\mu\text{Hrel}$  but especially its direction, indicating some additional effects.  $\beta\text{Ala}$  (peptide 5, Table 3) has a similar behavior.

In order to increase the amphipathicity we added a positive residue (Arg or Lys) in the hydrophilic face, instead of Ile. In these cases, the change in direction of  $\mu\text{Hrel}$  is higher (increased angle between the horizontal plane and direction of  $\mu\text{Hrel}$ ), compared to any previous analogue, while H is half, but  $\mu\text{Hrel}$  duplicates (as expected, increase the amphipathicity). However, the original Arg apparently generates such repulsion with the additional Arg or Lys (peptides 6-7, Table 3) residues located in the same face that may destroy the helical conformation. Actually, this additional positive charge in the hydrophilic face originates several changes (repulsion, change in helical parameters) and a conclusion could not be established easily in order to explain the loss of activity.

Peptide eight in Table 3 was also inactive. The change of Leu5 by Lys produces a major increase in the angle between the horizontal plane and the  $\mu\text{Hrel}$  but its magnitude is maintained and H is the halved. In addition, unfavorable electrostatic interaction between Glu and Lys residues could be implicated in the inactivation of this analogue.

The behavior of truncated versions of Cm-p5 in terms of biological activity was mostly random and more difficult to understand, but remarkably all these peptides change dramatically the direction of  $\mu\text{Hrel}$  when compared with Cm-p5.

Direction of  $\mu\text{Hrel}$  can be more important for the correct interaction with the membranes that its magnitude (amphipathicity), taking into account that during Arg contact with negative phospholipid, only the vertical component of this vector, that split in half the helix from Arg to the opposed face (helix axis), is in cooperation with the dipole moment vector of the membrane. If the  $\mu\text{Hrel}$  direction have more horizontal component (perpendicular to the axis of the helix), its real magnitude is neglected and repulsive forces are implicated in an increased instability of the peptide bounded to membrane system even if positively charged residues, centered in one face, are present (Figure 9a in Experimental Section, Chapter 1).

Acetylated Cm-p5 maintains fungistatic properties (peptide 13 in Table 3), therefore, free *N*-terminal is not needed for activity, enabling the total protection of peptide toward aminopeptidase degradation in future research. The dimeric version (peptide 14 in Table 3), like MAP, did not show any activity. This may be due to steric hindrance between *C*-terminal joined chains, which would imply helix destruction.

In general, our results suggest four determinant structural factors in order to maintain the biological activity of Cm-p5. Glu and His residues must be in the  $i, i+4$  positions,  $\mu\text{Hrel}$  vector must be close to a parallel direction respect to the membrane pointing in the opposite direction of the hydrophilic face (Arg residues), and any repulsive interaction that could interfere in helicity should be diminished.

### 3.3 Salt bridge and helical stabilization.

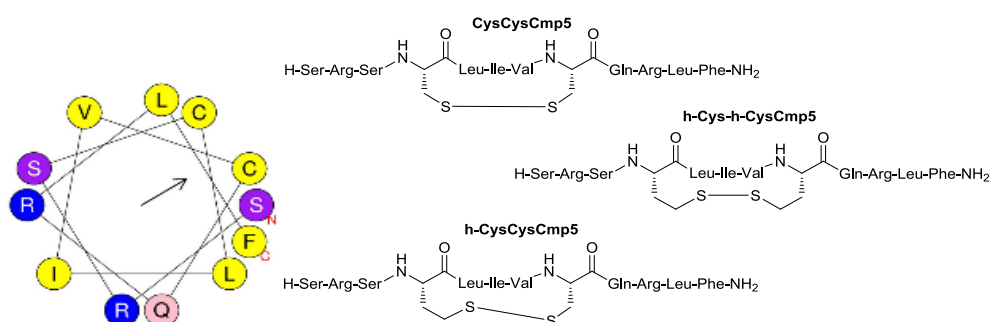
Based on the previous modifications (Table 3), we considered that the most remarkable finding was the relative position of His and Glu ( $\text{pK}_{\text{aR}} = 4.25$ ,  $\alpha$  (dissociation grade) = 99,97 %) (analytical calculation based in concentration of 10  $\mu\text{g/mL}$  of Cm-p5 and physiological pH) in Cm-p5. These residues could be participating in helical stabilization by forming salt bridge (defined as the combination of two non-covalent interactions: ion pair interaction and hydrogen bonding).<sup>102</sup> For Cm-p5, the modification of these residues (peptides 1-5 in Table 3), or the distance between them (peptide 9 in Table 3), involve the loss in biological activity. Recently, it has been revealed the role of salt bridge interaction in secondary structure stabilization of single  $\alpha$ -helix of peptides.<sup>64b</sup>

In proteins, such as T4 lysozyme, a salt bridge was identified between Asp ( $\text{pK}_{\text{aR}} = 3.65$ ,  $\alpha = 99,93$  %, supposing 10  $\mu\text{g/mL}$ ), at residue 70 and a His at 31. Although the imidazole ring of His31 is not protonated at physiological pH ( $\text{pK}_{\text{aR}} = 6.8$ ,  $\alpha = 79,85$ %, supposing 10  $\mu\text{g/mL}$ ), it has been demonstrated a shift of its  $\text{pK}_{\text{aR}}$  (protonated imidazole) to 9.05 ( $\alpha = 2.19$ % at 10  $\mu\text{g/mL}$ ), in the folded protein that simulate a protonated His at  $\text{pH} = 7.4$ , due to salt bridge formation.<sup>103</sup>

Cm-p5 changes to helical conformation only by interaction with membranes. In internal protein media or under membranolytic conditions, water content is low,<sup>104</sup> solvation of negative Asp or imidazole ring is not effective and the salt bridge can be spontaneously formed by negative enthalpy and entropy (hydrophobic effect). A possible mechanism in which this process could take place is the formation of a hydrogen bond between neutral imidazole ( $\text{pK}_{\text{aR}} = 13.1$ )<sup>105</sup> and negatively charged Asp residue. This donation of negative charge by Asp to the imidazole ring, increases the basicity, in consequence the  $\text{pK}_{\text{bR}}$  (from 7.2 to 4.95) ( $\text{pK}_{\text{aR}}$ : from 6.8 to 9.05) and its protonation grade from 20.25% to 97.81%.<sup>103</sup> In principle, the hydrolysis  $\text{pK}_{\text{hR}} = \text{pK}_{\text{bR}}$  of imidazole decreases ( $\text{pK}_{\text{aR}}$  increases) because of the effect of the negative charge of Asp at  $\text{pH} = 7.4$  (Figure 9b in Experimental Section, Chapter 1).

Weak acids anions as phosphate, water solvation or mono-positive cations ( $\text{Na}^+$  or  $\text{K}^+$ ) do not favor salt bridge formation (Figure 9b, Experimental Section, Chapter 1). On the other hand, di-positive cations ( $\text{Ca}^{2+}$  or  $\text{Mg}^{2+}$ , present as counter ions of phosphate in membranes) could reinforce the interaction (Figure 9c in Experimental Section, Chapter 1). This is the first time that a salt bridge between His and Glu in  $i, i+4$  position is proposed and further investigation is needed to confirm the implication in helical stabilization and, consequently, in the biological activity of Cm-p5.

If this salt bridge is essential for the antifungal activity of Cm-p5, in environments such as mucosa, skin or tumors, where pH is 5-6, the biological effect will be enhanced due to alteration in the dissociation degree of Glu (85% at pH= 5) or protonation degree of His (96.89 % at pH= 5). Also, the influence of the ionic strength or type of ions may alter this non-covalent interaction.<sup>93, 100</sup> We assume that covalent cyclization between these residues by substituting them with cysteine should stabilize the helical secondary structure, energetically favoring the action mechanism. A disulfide bridge (or any other covalent stabilization) should overcome all drawbacks related with the physiological behavior of this salt bridge and make peptides more resistant to proteolysis.



Peptide	H	$\mu\text{Hrel}$	z	F. Polar	angleM
CysCysCm-p5	0.74750	0.45805	2	0.417	0.56152
Cm-p5	0.44833	0.19215	1	0.583	0.24380

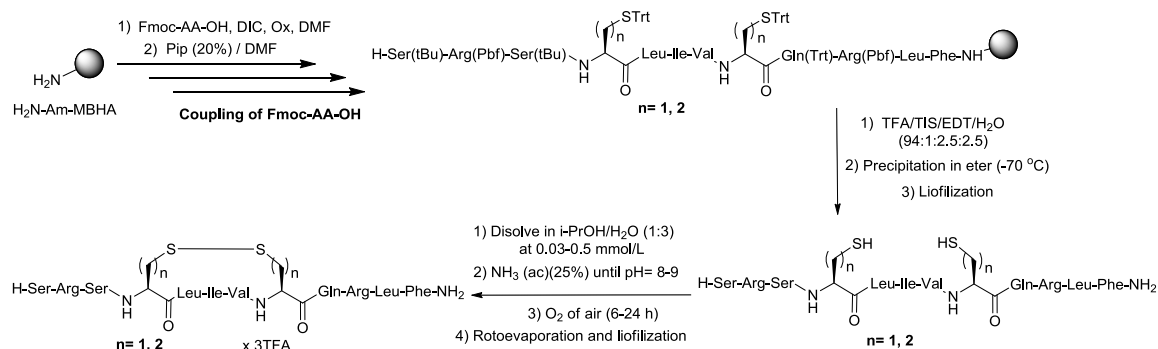
Figure 7: Designed cyclic analogues of Cm-p5. Helical wheel projection of CysCysCm-p5 and helicoidal parameters.

It is currently known that cyclization in  $i, i+3$  or  $i, i+4$  positions can stabilize an  $\alpha$ -helix.<sup>106</sup> In order to know whether Cys residue has the suitable length for maintaining a helical conformation without further deformation, we made a molecular dynamic study of mutated Cm-p5 (E4C and H8C) to estimate the covalent distance between thiol groups in  $i, i+4$  position. The analysis of distance between sulfur nuclei shows that they are located in the edge (2-10 Å) of the sulfur covalent radius (1.05 Å) necessary for a bond distance S-S of 2.10 Å (Chart 3,

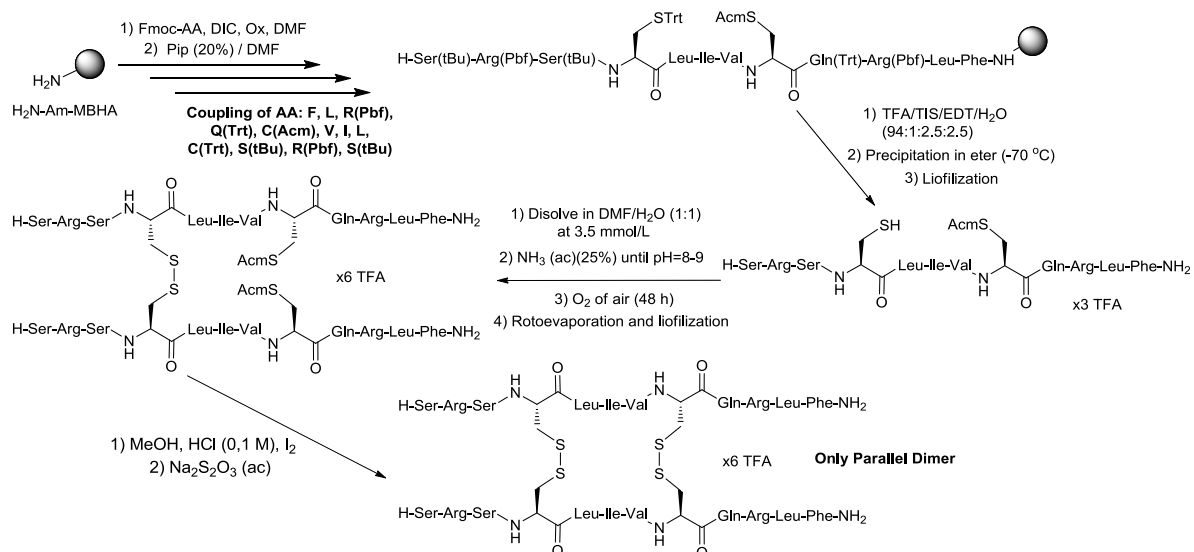
Experimental Section, Chapter 1). This result also points that using homo-cysteine residues (Hcy) or a combination of Cys and Hcy could improve the cyclization process and, consequently, helical stabilization. With these results in mind, we synthesized three new peptides, placing two Cys, two Hcy or one Cys and one Hcy instead of the Glu and His pair (Figure 7). It is important to note that, like in Cm-p5, these analogues have doubled the H valor as well as the  $\mu\text{Hrel}$  magnitudes. Also,  $\mu\text{Hrel}$  has the direction totally opposed to Arg residues, without any horizontal component that can repel the membrane relative dipole moment (Figure 9a, Experimental Section, Chapter 1).

### 3.4 Results and discussion regarding salt bridge and helical stabilization

The synthetic procedure for Cm-p5 cyclic analogues is presented in Scheme 4. Following the Fmoc/t-Bu peptide strategy, cleavage in presence of EDT, three new acyclic analogues were produced with high peptidic purity and yield.



Scheme 4: Synthesis of disulfide bridged analogues of Cm-p5.



Scheme 5: Synthesis of CysCysCm-p5 parallel dimer using Acm and Trt protecting groups.



The three dithiolated peptides were submitted to the cyclization process by oxidations with oxygen of air in water, showing some specificity for each compound. Usually, for other peptides under similar reactions, all acyclic starting material is consumed in 2-3 h. In the case of CysCysCm-p5 analogue, more time (6h) was needed for the consumption of all starting material and, coincidentally, acyclic and cyclic monomers have the same retention time, therefore, only mass analysis or Elman test can confirm the total conversion (Figure 25Figure 29 in Experimental Section, Chapter 1). In a first attempt, desulfured impeptidic purity was produced due to high pH (above 9). However, this problem was corrected by maintaining the pH strictly around 8-8.5. Surprisingly, in the standard cyclization conditions used for commercial peptides in our laboratory (0.5 mmol/L), CysCysCm-p5 analogue produced considerable quantities of dimeric byproducts (Figure 25Figure 29 in Experimental Section, Chapter 1), probably parallel and antiparallel dimers (Figure 8). Similar dimers were reported as impurities of CIGB-300 anticancer peptide, also produced in our lab.<sup>107</sup> Peak 4 (Figure 25Figure 29 in Experimental Section, Chapter 1) represents a conformer of peak 3, a dimer, as can be seen in the ESI-HRMS spectrum (Figure 25Figure 29 in Experimental Section, Chapter 1) and due to coalescence between peak 3 and 4 if the sample is previously stabilized for 2h at room temperature.

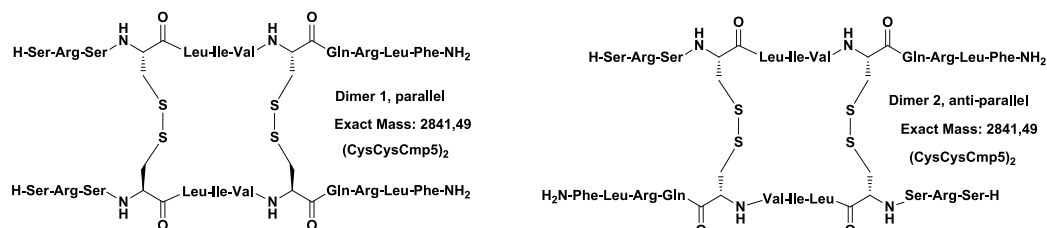


Figure 8: Parallel (left) and anti-parallel (right) dimeric CysCysCm-p5

Only at 0.03 mmol/L is guaranteed, the production of the cyclic monomer without formation of dimeric byproducts (Figure 25Figure 29in Experimental Section, Chapter 1). However, this concentration is not actually applicable to industrial processes and a better strategy would be to perform the cyclization on resin and to make the final cleavage of the cyclic monomer as a crude product.

In order to identify what peak in the RP-HPLC corresponds to the parallel or antiparallel dimer, we decided to change the orthogonality of Cys protection, using Cys(Acm) for the His mutation and Cys(Trt) for the Glu. With these new protecting groups, peptide cleavage from resin produced an acyclic monomer containing Cys(Acm) and free Cys residue. Dimerization of this compound at concentrated condition (1 mmol/L) (Figure 31 Figure 29in Experimental Section, Chapter 1), solvent evaporation, lyophilization, and finally the Acm deprotection with iodine and the concomitant cyclization guaranteed only the parallel dimer production. This

unequivocal parallel dimer has the same retention time compared to the first dimer produced in the CysCysCm-p5 peptide cyclization (Figure 25 in Experimental Section, Chapter 1), confirming the identification of the parallel dimer and its antiparallel counterpart.

As a comparison, cyclization of the peptide containing both Cys and Hcy has fewer tendencies to form both dimeric products in the same conditions (Figure 34Figure 36 in Experimental Section, Chapter 1). In the case of the analogue with two Hcy, only cyclic monomer is obtained at 0.5 mmol/L (Figure 38 in Experimental Section, Chapter 1).

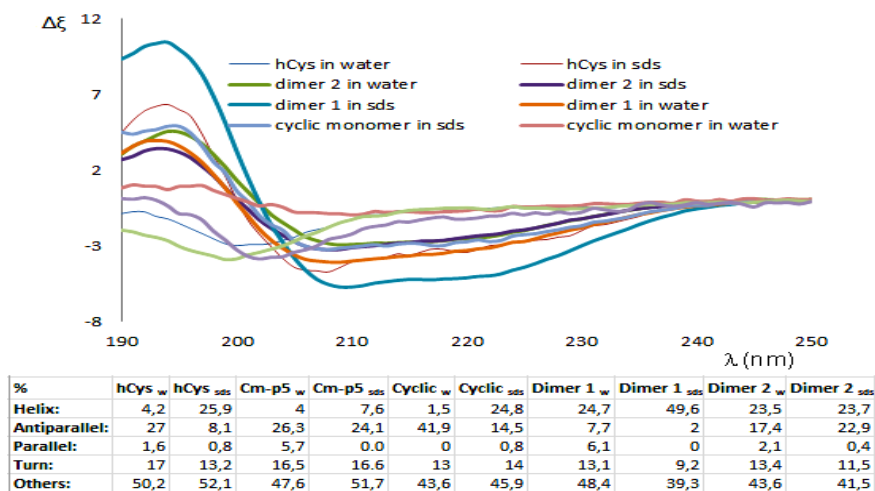
In conclusion, intra-chain disulfide bridge between  $i, i+4$  positions (residues 4 and 8) in Cm-p5 is more feasibly accessible when two Hcy or HcyCys combinations are introduced. On the contrary, inter-chain disulfide bridge when CysCys combination is introduced is clearly limited by steric hindrance. This type of inter-chain disulfide bridge is similar to the ones that are present in insulin and defensins. However, this is the first report, to our knowledge, of disulfide dimers between  $i, i+4$  position.

### 3.5 Circular dichroism analysis

The following peptides were submitted to CD analysis in water and 10% SDS-water mixture: Cm-p5, CysCysCm-p5 (cyclic monomer), HcyHcyCm-p5 (cyclic monomer) and the parallel and antiparallel dimers of CysCysCm-p5. It is evident that a better helical stabilization was obtained for the cyclic monomers in a 10% SDS solution when compared with Cm-p5. Interestingly, the CysCysCm-p5 cyclic monomer showed a major percent of antiparallel  $\beta$ -structure in water that in the case of HcyHcyCm-p5. It is important to note that dimer 1 (parallel) does not have much contribution of antiparallel  $\beta$ -strand to the structure under water or SDS conditions when compared with dimer 2 (antiparallel). Also, the latter have the same behavior in water or SDS, which may be an indication of the double of repulsion between free positive N-terminal (with hydrophilic forces) and hydrophobic Leu-Phe at C-terminus (with hydrophobic forces) for this antiparallel construction (acetylated version of CysCysCm-p5 could totally avoid this drawback). Based on the results shown in Chart 1, it is possible to conclude that, for the dimers, the inter-chain disulfide bridge is responsible for maintaining 25% of helical structure in water. Only in case of the parallel dimer (dimer 1) water molecules are excluded by SDS, and additionally, hydrophilic and hydrophobic forces at the *N* and *C* terminals contribute to considerably increase (up to 49%) the total segment of the helix (Chart 1). At 10% SDS (micellar critic concentration of SDS) and despite the difference in surface curvature, these types of micelles are similar or mimetize biological membrane of bacteria and fungus, and are also negatively charge. Remarkably, in the case of dimeric compounds, Chart

1, interaction with micelles is not needed for helicity induction; these compounds are predominantly  $\alpha$ -helices in water.

Chart 1: CD analysis in water and 10% SDS. Secondary structure content (in percentage) calculated with the online program Bestsel (<http://bestsel.elte.hu>).



Hcy: cyclicHcyHcyCm-p5, Cyclic: cyclic CysCysCm-p5, Dimer 1: parallel Dimer, Dimer 2: antiparallel Dimer

### 3.6 *In-vitro* anticandidal and antibacterial activity of Cm-p5 and derivatives.

Antifungal activity was evaluated for Cm-p5, Hcy, Cys cyclic monomers, (HcyHcyCm-p5 and CysCysCm-p5, respectively) and the two dimers (dimer 1 (parallel) and dimer 2 (antiparallel)) against three fungal and two bacterial species of clinical relevance (Table 5).

Table 5: Minimal Inhibitory Concentration (MIC) ( $\mu\text{g/mL}$ ) of Cm-p5 and derivatives against three *Candidas*, a Gram-positive and a Gram-negative bacterial species.

	Cm-p5	Cyclic CysCysCm-p5	Dimer 1	Dimer 2	Cyclic HcyHcyCm-p5
<b>Candida species</b>					
<i>C. auris</i>	11	27	30	31	NT
<i>C. parapsilosis</i>	32	14	39	>100	10
<i>C. albicans</i>	10	5	48	29	10
<b>Bacterial species</b>					
<i>Listeria monocytogenes</i>	> 100	100	50	12.5	NT
<i>Pseudomonas aeruginosa</i>	> 100	> 100	> 100	> 100	NT

Cyclic: cyclic CysCysCm-p5, Dimer 1: parallel dimer, Dimer 2: antiparallel dimer, Hcy: cyclic HcyHcyCm-p5

The antifungal Cm-p5 peptide kept the expected anticandidal activity against *C. albicans* and *C. parapsilosis*, as previously described.<sup>5</sup> Interestingly, a relevant activity was also observed in the case of *C. auris*, an emerging nosocomial pathogen. The Hcy cyclic monomer, only maintained the activity against *C. albicans*, but increased it against *C. parapsilosis*. The

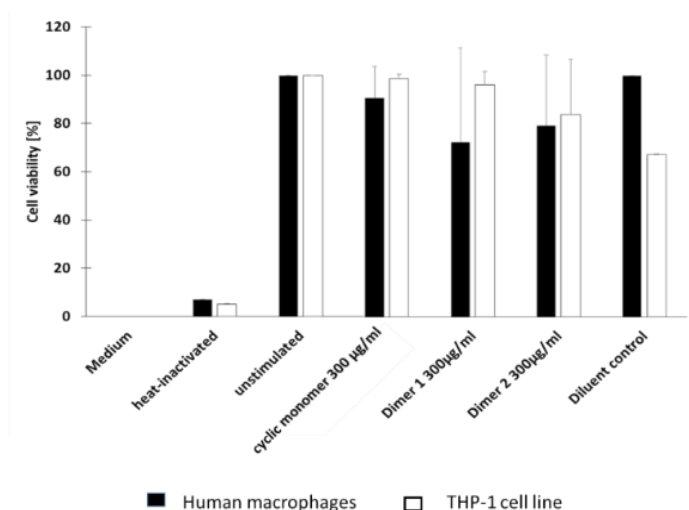
CysCysCm-p5 cyclic monomer even though it was not so effective against *C. auris*, has a minor MIC value against *Candida albicans*. The two dimers were the least effective against *Candida* species, showing MIC values around the 30 µg/mL or even higher (Table 5).

To assess if these antifungal peptides also exert antibacterial activity, Cm-p5, the Cys cyclic monomer and the two dimers were analyzed in an agar diffusion assay (Table 6 in Experimental Section, Chapter 1) and by determination of the minimal inhibitory concentration (MIC). Table 5 shows the antibacterial MIC of Cm-p5 and the derivatives against the Gram-positive species *Listeria monocytogenes* and the Gram-negative species *Pseudomonas aeruginosa* confirming the increased anti-bacterial activity of Cm-p5 dimers against *Listeria monocytogenes*. Cm-p5 exhibited a moderate antibacterial activity against *L. monocytogenes* at 1000 mg/L and 100mg/L, but had only minor effects against *P. aeruginosa* (Table 6) at 1000 mg/L. The cyclic monomer and especially the two dimers were more active than Cm-p5, which showed a significant activity at 20 mg/L (Table 6 in Experimental Section, Chapter 1).

### 3.7 *In-vitro* toxicity of Cm-p5 analogues against human cells

Cytotoxicity of the cyclic monomer and the two dimers of Cm-p5 against macrophages and THP-1 human cells were also tested. At 300 µg/mL of each compound (a higher concentration than the one used to determine MIC against fungal or bacterial species) no toxicity effects were observed in terms of percent cell viability (Chart 2).

Chart 2: *In vitro* cytotoxicity of CysCysCm-p5 cyclic monomer and dimers against macrophages and THP-1 human cells.



### 3.8 Discussion regarding biological activity

The cyclization by an intra-chain disulfide bond in cyclic CysCysCm-p5, improved the activity against *C. albicans* down to 5 µg/mL compared to the native Cm-p5 peptide (MIC= 10 µg/mL).<sup>5</sup>

A similar improvement was observed against *C. parapsilosis* (from 32 to 14  $\mu\text{g/mL}$ ) and a decreased activity was observed in the case of *C. auris* (from 11 to 27  $\mu\text{g/mL}$ ).

Possibly, the duplicated H value,  $\mu\text{Hrel}$  magnitudes and its direction totally opposed to Arg residues of the cyclic CysCysCm-p5 (Figure 3) together with the salt bridge substitution by a disulfide bond, favored the antifungal activity. In general, these results represent a significant improvement, taking in consideration that this derivative has a stable  $\alpha$ -helix structure, which is less dependent on a membrane mimetic environment, and consequently, a more effective approach to the fungal membrane. Also, this molecule is less dependent on physiological conditions and probably more proteolytically stable.

This peptide has the ability to change between  $\beta$ -sheet and a helical conformation (according to CD spectra Chart 1, therefore, it may have the chameleonic possibility to penetrate the membrane as a helix and/or interact with another membrane receptor as a  $\beta$ -sheet. Since the original Cm-p5 acts in a fungistatic manner against *Candida albicans*,<sup>6</sup> a possible complementary therapeutic approach could be conceived and implemented, similar to the combination of fluconazole and Amphotericin B,<sup>108</sup> taking in account that resistance to fluconazole increased dramatically in the last years.<sup>109</sup>

Antimicrobial peptides are prone to proteolytic degradation<sup>110</sup> and MIC determination in standard Mueller Hinton broth may not always lead to optimal results regarding the determination of their antimicrobial activity.<sup>111</sup> To assess the activity of Cm-p5 and the derivatives we used a modified agar overlay assay,<sup>112</sup> as well as standard MIC determinations (Table 5). In these experiments, we observed a notable increase in the antibacterial activity against Gram-positive as well as Gram-negative bacteria mostly for the antiparallel derivative.

While the strains included in this investigation (*L. monocytogenes* and *P. aeruginosa*) are not multidrug resistant microorganisms, it should be noted that *L. monocytogenes* is a major problem in food production, due to the ability to multiply at 4°C and tolerance of high salt concentrations. It can reproduce inside eukaryotic cells and it is one of the most serious foodborne pathogens. The 20-30% of listeriosis cases are produced by food and fatality for high-risk individuals is common.<sup>113</sup> On the other hand, *P. aeruginosa* is an opportunistic microorganism causing dangerous infections more often in immune compromised patients or patients with pre-existing diseases like severe burns. In these cases, severe infections and sepsis may frequently cause fatal outcomes.<sup>114</sup>

Other antibacterial peptides increase their activity when they are cyclic. Bactenecin is a natural antibacterial peptide from bovine neutrophils, which contains a disulfide bond due to Cys residues.<sup>115</sup> This peptide with such cyclic structure showed a relevant activity against the Gram-negative bacteria, *Escherichia coli*, *Pseudomonas aeruginosa*, and *Salmonella typhimurium*. When linear analogues are generated, the antibacterial (Gram negative) activity decreased substantially, whereas against Gram-positive microorganisms (*Staphylococcus epidermidis* and *Enterococcus faecalis*) such peptide versions displayed a positive interaction. Another example of cyclic peptides with antibacterial activity is Gramicidin S, a cationic cyclic decapeptide with primary structure cyclo-(Val-Orn-Leu-D-Phe-Pro)<sub>2</sub>, which is secreted by the bacterium *Bacillus brevis*, is a potent antimicrobial agent at  $\mu\text{M}$  concentrations, exhibiting high inhibitory activity against a broad spectrum of both Gram-positive and Gram-negative bacteria and pathogenic fungi.<sup>116</sup>

CysCysCm-p5 cyclic monomer and the two related dimers resulted nontoxic in terms of cell viability, as previously evaluated on human cells (Chart 2). Primary macrophages<sup>117</sup> and the cell lines THP-1<sup>118</sup> have been previously used as *in vitro* cellular models for testing the toxicity of antimicrobial peptides and they have been proved being sensitive enough to assess the availability of these molecules as potential anti-infection drugs in humans. Further experiments with fetal lung cells and determination of percent of cell vitality, certainly will improve this analysis, but, for now, is notable that even at the highest tested concentration, the new compounds are not cytotoxic for human cells. Besides, Cm-p5 resulted non-hemolytic for human and rabbit erythrocytes;<sup>6</sup> the absence of such activity for CysCysCm-p5 cyclic monomer and the two related dimers, in term of pharmacological and therapeutic standards for a possible anti-infective candidates, remains to be confirmed.

## Conclusions. Chapter 1

Fourteen mutants of Cm-p5 peptide were synthesized. The magnitudes of H,  $\mu$ Hrel or the direction if any other factor is not implied, are fundamental for activity, favoring sequences with elevated H or  $\mu$ Hrel and direction of  $\mu$ Hrel from hydrophobic phase to hydrophilic to promote membrane interaction. If other factors such as repulsion of positive charges or loss of non-covalent interaction are present, maintaining H,  $\mu$ Hrel or direction of  $\mu$ Hrel is not sufficient for maintaining biological activity. Notable examples constitute all the variants where either Glu4 or His8 were mutated, in which anti-fungal activity was lost. Substitution of these two residues with Cys permitted to synthesize a new cyclic analogue and two dimers that showed helix stabilization as indicated by CD analysis, suggesting the essential role of the Glu-His salt bridge. For the first time, to our knowledge, is proposed a salt bridge as a stabilizing factor for an anti-microbial peptide. CysCysCm-p5 and related dimers were not toxic for human macrophages. The cyclic monomer showed an increased activity *in vitro* against *C. albicans* and *C. parapsilosis* but not against *C. auris* compared to Cm-p5. In addition, the antiparallel dimer (dimer 2) showed a moderate antibacterial activity against *Pseudomonas aeruginosa* and a significant activity against *Listeria monocytogenes*.

It is important to note that helical stabilization is necessary for biological activity but not enough, since dimers (more helical character) have lower antifungal activity than Cm-p5 and the parallel version (the most helical stabilized compound) did not show any antibacterial activity against the tested microbes. The cyclic monomer changes between  $\beta$ -strand and helical conformation when submitted to membranolytic environment and antiparallel dimer (dimer 2) has an equal population of molecules as  $\beta$ -strand besides having a stabilized  $\alpha$ -helix (as judge by CD). Apparently, a constricted helix is not recommended and a  $\beta$ -strand/ $\alpha$ -helix equilibrium in cyclic monomers is needed for antifungal activity. This suggests that an induced-fit model of action mechanism could be better than the old key-lock model to explain the antifungal activity. These peptides may need several conformations to be active, because they have several stages in their mechanism of action: interact, penetrate and/or leave the membrane, and/or interact with the active site of several macromolecule targets.

Finally, the increased capacity of cyclic CysCysCm-p5 for fungal control compared to fluconazole<sup>7</sup> and low cytotoxicity, together with a stabilized  $\alpha$ -helix and disulfide bridges, that could advance the metabolic stability and *in-vivo* activity, improve the prospect of this new compound as potential antifungal systemic therapeutic candidate. Direct application of cyclic

CysCysCm-p5 or in synergy with amphotericin B, should diminish the doses of this fungicidal compound, highly toxic, but fundamental for the treatment of internal infections.



## Future works. Chapter 1

- ✓ Expand the conclusion and methodology of this study to other antimicrobial peptides that exists as  $\alpha$ -helices (melittin,<sup>34</sup> guavanin-2,<sup>35</sup> etc).
- ✓ Complete the structural characterization of the dimers and cyclic analogues of Cm-p5 using NMR techniques.
- ✓ Realize a deeper study of the salt bridge stabilization of Cm-p5 between the Glu and His residues.
- ✓ Determine the metabolic stability of the cyclic and dimers analogues of Cm-p5.
- ✓ Determine the hemolytic activity of the cyclic CysCysCm-p5 analogue.
- ✓ Determine the *in-vitro* antifungal activity of the cyclic CysCysCm-p5 analogue in the presence of sodium, calcium or phosphate salts.
- ✓ Determine the *in-vivo* antifungal activity of the cyclic CysCysCm-p5 analogue.
- ✓ Synthesize the *N*-acetylated versions of the cyclic and dimers analogues of Cm-p5.
- ✓ Evaluate the synergic effect of the cyclic CysCysCm-p5 in combination with fluconazole or amphotericin B.

## **4 Experimental Section. Chapter 1**

### **4.1 General Remarks**

#### **4.1.1 Materials**

All reagents and solvents were obtained from commercial suppliers and used without further purification. Fmoc-Rink-MBHA-Polystyrene and Fmoc-Rink-Chemmatrix resins were prepared by reaction of Fmoc-Rink-OH linker with commercial MBHA-Polystyrene or ChemMatrix resins following controlled acetylation after 0,53 mmol/g or 0.43 mmol/g substitution respectively. All the Fmoc-aminoacids, DIEA, I<sub>2</sub>, ascorbic acid, Ac<sub>2</sub>O and resins were purchased from Merck. Organic solvents (analytical grade) (DMF, DCM, MeOH, Et<sub>2</sub>O and ACN) were purchased from Merck. RP-HPLC quality ACN and ultrapure water quality were used for RP-HPLC analysis and purification.

#### **4.1.2 Peptide synthesis**

All reactions were carried in polypropylene syringes (10 mL) fitted with polypropylene frits at room temperature with mechanical shaking. Excess of solvent and reagent was eliminated by vacuum filtration. Side chain of aminoacids was protected with Pbf for Arg, Trt for Gln, Cys and His, tBu for Ser and Glu, and AcM for Cys in the synthesis of parallel dimer.

Solid-phase peptide synthesis was carried out using Fmoc/t-Bu chemistry on Rink amide resin based in polystyrene or PEG (ChemMatrix). The resin was washed with DMF (2×1 min), DCM (2×1 min), MeOH (2×1 min), DCM (2×1 min) and DMF (2×1 min). Fmoc removal was achieved with 20% piperidine in DMF (2×10 min), and the subsequent aminoacids were added using the following coupling conditions: Fmoc-Aa-OH/DIC/Oxyma (4 equiv. of each) in DMF, after negative ninhydrin test (approximately 30 min). Between the different steps, the resin was washed with DMF (4×1 min). Acetylation was achieved using the following condition: Ac<sub>2</sub>O/DIEA (8 equiv.) in DMF for 10 min. After the last coupling reaction, Fmoc is eliminated and peptide-resin is washed subsequently with DMF (4x1min), MeOH (4x1min) and Et<sub>2</sub>O (4x1min). Peptide-resin is dried in desiccator during three days and finally is frizzed at -20°C by 30 min before cleavage.

All peptides were obtained with more than 95% of peptidic purity as ascertained by analytical RP-HPLC. The molecular mass determined experimentally by ESI-HRMS corresponded with the theoretically calculated monoisotopic mass for each peptide.

### 4.1.3 Peptide Cleavage

Cleavage from the resin and global deprotection: (i) analogues 1-15: TFA/TIS/H<sub>2</sub>O (95:2.5:2.5, 5 mL/g of resin), (ii) thiolated analogues: TFA/TIS/EDT/H<sub>2</sub>O (94:1:2.5:2.5, 5 mL/g of resin) was added to the frizzing peptide-resin and left for 2h with shaking. Cleavage mixture was filtered and added over cold Et<sub>2</sub>O (50 mL, -70°C), mixed in vortex and centrifuged. The supernatant was discarded and the operation was repeated two more times. The solid residue was re-dissolved in H<sub>2</sub>O/ACN (7:3), frizzed at -70°C and lyophilized (LABCONCO, EUA). Approximately 70 % of crude peptide respect to the degree of the substitution of the resin is obtained. Working with 0.3 g of resin, at 0.53 mmol/g substitution for polystyrene resin, and taking in account approximately the range of molar mass of all peptide (1400-1500 g/mol), 70% (160 mg) of crude peptides was produce. In case of ChemMatrix dimer synthesis, we use 0.15 g of resin, yields of crude are only about 60% and given the double Cm-p5 molar mass of product, plus Lys residue (3092 g/mol), 119 mg of crude was produce.

### 4.1.4 Peptide Cyclization and Dimerization

Cyclization was conducted by dissolving the peptides crude (approx. 160 mg) in H<sub>2</sub>O (0.1% TFA)/ACN/*i*-PrOH (1:1:1) at 0,5 mmol/L guarantying e major cone of agitation and ball filled only halfway for guarantee a high contact air(O<sub>2</sub>)-solvent. Normally, 250 mL of solvent mixture was used in a necked flask of 1L. NH<sub>3</sub> (ac) (25%) was added until pH 8-9 and the reaction was stirred 4-12 h (after consumption of starring material, checked by RP-HPLC or ESI-HRMS) at room temperature. The pH is brought to 7 and the H<sub>2</sub>O/ACN/*i*-PrOH mixture was removed by rotary evaporator and residue was lyophilized (LABCONCO, EUA).

### 4.1.5 Cyclization of the parallel dimer using Cys(Acm)

Peptides (150 mg) containing Cys(Acm) and free Cys in the first or the second Cys residue were submitted to dimerization at high concentration in 30 mL DMF/H<sub>2</sub>O (1:1) during 72h (as follow by analytical RP-HPLC) in which the formation of white suspension is observed. Subsequently H<sub>2</sub>O (0.1% TFA)/MeOH (1:1) (V<sub>T</sub>= 250 mL) was added after (0.5 mM). Finally 1.5 equiv. of HCl (37%) (pH= 3,78) and 5 equiv. of I<sub>2</sub> (dissolved in MeOH) by Acm group are supplement and stirring is maintained over 3h or until no dimeric starring material was remaining by RP-HPLC. Iodine was removed by adding 1 M aqueous sodium thiosulfate drop-wise until the mixture is colorless or by treatment with activated charcoal and centrifugation. The pH is brought to 7 and the H<sub>2</sub>O/MeOH mixture was removed by rotary evaporator and residue was lyophilized (LABCONCO, EUA).

#### **4.1.6 Analytical RP-HPLC**

Analytical RP-HPLC was performed on an WellChrom HPLC (KNAUER, Germany) using the EZChrom-Elite® chromatography software ChromGate v3.1 from Agilent (USA) using a Zorbax RP-C18 (5  $\mu$ m, 4.6 $\times$ 150 mm) column, with flow rate of 0.8 mL/min and UV detection at 226 nm. Mobile phase with gradient of 5% to 60% B in 35 min, Solvent A: 0.1% TFA in H<sub>2</sub>O; solvent B: 0.1% TFA in ACN. Chromatograms were obtained at 226 nm and processed by the UNICORN 4.11 (GE Healthcare USA) software package.

#### **4.1.7 ESI-HRMS**

Low-energy ESI-HRMS spectra were obtained in the CIGB, La Habana, Cuba (Peptide characterization, page 13) by using a hybrid quadrupole time-of-flight QTOF-2™ instrument (Waters, Milford, MA, USA) fitted with a nanospray ion source in positive ion mode. Peptide solutions were collected from RP-HPLC, dissolved in 1 mL of 60% (v/v) ACN/water solution containing 0.2% formic acid and loaded into a metal-coated borosilicate capillary nanotip (Proxeon, Denmark), inserted into the Z-spray nanoflow electrospray ion source, and slightly pressured with nitrogen to guarantee their stable spray during measurement. The capillary and cone voltage were set to 900 to 1200 and 5 to 35 eV, respectively. Mass spectra were acquired in the m/z range of 400–2000 Th. A solution of NaI and CsI was used as reference for the calibration of the spectrometer. Electrospray ionization mass spectrometry spectra were processed using the MassLynx version 4.1 program (Micromass, England).

#### **4.1.8 Semipreparative RP-HPLC**

Crude peptides (directly cleaved or cyclized) (50 mg for run or 100 mg in case cyclized crude, because contain approximately 50% of NH<sub>4</sub>CF<sub>3</sub>COO) were dissolved in DMSO (3mL) and purified on a LaChrom (Merck Hitachi, Germany) HPLC system using a RP-C18 column (Vydac, 25 $\times$ 250 mm, 25  $\mu$ m). A linear gradient from 15%-60% over 55 min or 25%-60% of solvent B over 65 min and a flow rate of 5mL/min were used for linear peptides and cyclic and dimeric analogues respectively. Detection was accomplished at 226 nm. Solvent A: 0.1% (v/v) of TFA in water. Solvent B: 0.05% (v/v) of TFA in ACN. Fractions of high RP-HPLC homogeneity and with the expected mass were combined, lyophilized, and submitted to antimicrobial testing. All peptides synthesized was purified to >95% by RP-HPLC.

#### **4.1.9 CD spectroscopy**

The CD measurements were made on a J-1500 CD spectrometer (Jasco, Tokyo, Japan) at 24°C in a thermally controlled quartz cell with a 1 mm path length over 190 to 250 nm. The samples were prepared by dissolving the peptides in water and 10% SDS/water mixture. The final

peptide concentration for the CD measurements was ~35-70  $\mu\text{M}$  (100  $\mu\text{g}/\text{mL}$ ). Data were collected every 0.1 nm, the bandwidth was set at 1.0 nm, and the sensitivity was 10000 mdeg. Data integration time was 1 sec, and scanning speed was 100 nm/min. The number of accumulations was 18. Percent of secondary structure was calculate with the Bestsel online program which are available at the <http://bestsel.elte.hu> server.<sup>119</sup>

#### **4.1.10 Microorganism strains and growth conditions**

Three *Candida* species were used: *Candida albicans* (ATCC 24433) was obtained from the Institute of Medical Microbiology and Hygiene, University Clinic of Ulm, Germany. *Candida parapsilosis* (ATCC 22019) was obtained from the laboratory of Medical Mycology, “Pedro Kourí” Institute of Tropical Medicine, Havana Cuba; *Candida auris* (DSMZ-No. 21092, CBS 10913, JCM 15448)<sup>120</sup> was obtained from the Leibniz Institute DSMZ-German Collection of microorganisms and cell cultures. Yeast Extract–Peptone–Dextrose (YPD) medium (liquid) was used for pre-culture inoculum at 70 r.p.m agitated conditions at 37 °C for 24 h. *Trichophyton rubrum* (ATCC 28189) was obtained from American Type Culture Collection and was cultured in Potato dextrose agar and for inoculums in Roswell Park Memorial Institute (RPMI) 1640 Medium.Four bacteria genera were used: *Staphylococcus aureus* (ATCC 23235), *Escherichia coli* (ATCC 25922), *Listeria monocytogenes* (ATCC BAA-679/EGD-e) and *Pseudomonas aeruginosa* (ATCC 27853). Bacteria were cultured at 37 °C and 5% CO<sub>2</sub> overnight as pre-culture inoculum in culture media.

#### **4.1.11 *In vitro* antimicrobial testing**

For *Candida* species and *T. rubrum*: The minimal inhibitory concentration (MIC) of Cm-p5 derivatives (cyclic monomer and the two dimers) was determined according to the “Clinical and Laboratory Standards Institute” guidelines M27-A3 broth micro dilution assay<sup>121</sup> with modifications (turbidimetric detection). Based on cell density measurements, the MIC was derived from a Lambert-Pearson plot.<sup>122</sup> Flat- lowered sterile 96 well plates (SARSTEDT, AG & Co KG, Nümbrecht), RPMI 1640 without sodium bicarbonate, MOPS-buffered (Sigma-Aldrich-Merck, Darmstadt) were used for the test, and readings were performed at  $\lambda= 600$  nm with TECAN infinite M200 microplate reader (Tecan Group Ltd., Männedorf). For filamentous fungi the minimal inhibitory concentration was determined according to CLSI guidelines M38-A2.<sup>112</sup>

For bacteria genera: Agar overlay assay: Bacteria were cultured at 37°C and 5% CO<sub>2</sub> overnight, pelleted by centrifugation and washed in 10 mM sodium phosphate buffer. Following resuspension in 10 mM sodium phosphate buffer optical density was determined at 600 nm.

$2 \times 10^7$  bacteria were seeded into a petri dish in 1% agarose, 10 mM sodium phosphate buffer. After cooling at 4°C for 30 min, 3-5 mm holes were punched into the 1% agarose. Peptides adjusted to the desired concentration in 10 µl of buffer were filled into the agar-holes. Following and incubation at 37°C in ambient air for 3h plates were overlaid with 1% agarose, tryptic soy solved in 10mM phosphate buffer. Inhibition zones in mm were determined following 16-18 h incubation time at 37°C/5% CO<sub>2</sub>.<sup>112</sup>

Minimal inhibitory concentration (MIC) determination: MIC determinations were performed in Mueller Hinton broth according to CLSI reference method M7A9 with modifications for bacteria.<sup>113</sup> All tests were performed in triplicate.

#### **4.1.12 Human cells and culture conditions:**

hMDMs (human monocyte derived macrophages): Peripheral Blood Mononuclear Cells (PBMCs) were isolated from human buffy coat via high density gradient centrifugation (Ficoll-Paque Plus; GE Healthcare, Munich). Monocytes were then purified from the PBMCs through adherence. Following, the cells were stimulated with granulocyte macrophage colony-stimulating factor (GM-CSF), 10 ng/mL (MiltenyiBiotec, BergischGladbach) for 6 days at 37°C and 5% CO<sub>2</sub> in RPMI 1640 medium (GIBCO, Invitrogen, Munich) supplemented with L-glutamine, 2 mM (PAN Biotech, Aidenbach), HEPES 10 mM (Biochrom, GmbH, Berlin), penicillin/streptomycin (100 U/mL-100 µg/mL (Biochrom, GmbH, Berlin).

THP-1 cell line (ECACC, Porton Down, UK, 88081201): human monocytic cell line derived from an acute monocytic leukemia patient was differentiated to macrophage like cells in cell culture medium. Mercaptoethanol, 0.05 mM (Sigma, Merck KGaA, Darmstadt), 10% FCS (Biochrom, GmbH, Berlin) and Phorbol 12-Myristate 13-Acetate (PMA), 1 µg/mL (Sigma, Merck KGaA, Darmstadt) were used as supplemented, overnight at 36°C and 5% CO<sub>2</sub>.

#### **4.1.13 Toxicity assay:**

THP-1 cells,  $1 \times 10^5$  macrophages, per well were distributed into a microplate (Nunclon™ Delta 96-Well MicroWell™ Plates, Sterile, Thermo Scientific, Germany) in cell culture medium supplemented with 5% heat inactivated human serum (PAN Biotech, Aidenbach). Controls were media control, heat inactivated cells and diluent control, DMSO (Carl Roth, Karlsruhe). Cells were then stimulated with the Cm-p5 derivatives in different concentrations overnight. 20µl PrestoBlue Cell Viability Reagent (Thermo Fisher Scientific Life Technologies GmbH, Darmstadt) per well was added for 20 min at 37°C/5% CO<sub>2</sub>. The fluorescence was measure at an excitation wavelength of 560 nm and emission wavelength of 600 nm with the TECAN

infinite M200 microplate reader (Tecan Group Ltd., Männedorf). The optical density (OD) of the media control was then subtracted from other results. Unstimulated cells were set to 100% viability.

## 4.2 Additional Figures and Tables

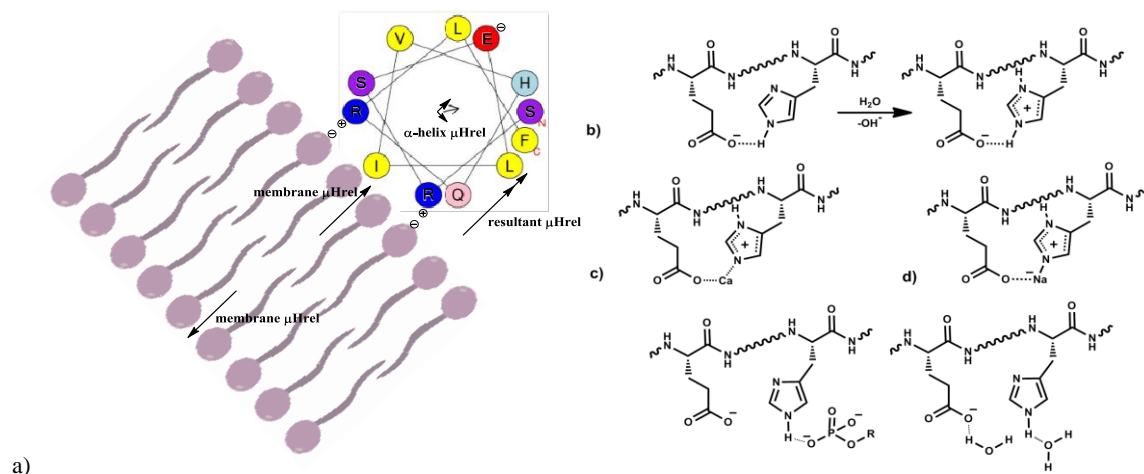


Figure 9: Proposed relative orientation of  $\mu$ Hrel with respect to the dipole moment of charged residues that maximize the resultant dipole moment vector needed for optimal interaction with antimicrobial membranes (a). Formation (b), stabilization (c) and destabilization (due to negatively charged sodium atom) (d) of salt bridges between His and Glu in  $i, i+4$  positions.

Table 6: Agar diffusion test (mm) of Cm-p5, CysCysCm-p5 cyclic monomer and dimers against Gram-positive and Gram-negative bacterial species.

Bacteria →	c(mg/L) ↓	<i>Listeria monocytogenes</i>	<i>Pseudomonasaer uginosa</i>
Cm-p5	1000	1.1	0.6
	100	0.4	-
	20	-	-
Cyclic	1000	0.9	0.8
	100	0.5	0.4
	20	-	-
Dimer 1	1000	1.2	1
	100	0.7	0.7
	20	0.3	0.3
Dimer 2	1000	1.2	1
	100	0.8	0.6
	20	0.3	0.3

## 4.3 General protocol for solid-phase peptide synthesis

Coupling reactions were performed manually on Rink-MBHA resin (0.3 g, 0.53 mmol/g) by a stepwise Fmoc/*t*Bu strategy. Aminoacids were coupled using DIC/Oxyma activation, and completion of the coupling reaction was monitored by the ninhydrin test. Fmoc-deprotection was carried out using 20% piperidine solution in DMF. All final product were cleaved from the resin with the cocktail TFA/TIS/water (95:2.5:2.5), or TFA/TIS/EDT/water (94:1:2.5:2.5) for

Cys containing peptides, precipitated from diethyl ether at  $-70^{\circ}\text{C}$ , then taken up in 1:2 ACN/water and lyophilized. All Cm-p5 analogues were analyzed by RP-HPLC, C18 column (Vydac,  $4.6 \times 150$  mm,  $5\mu\text{m}$ ) ( $\lambda = 226$  nm) (linear gradient of 5 to 60% of solvent B for 35 min, at 0.8 mL/min flow) (solvent A:  $\text{H}_2\text{O}$ , 0.1% TFA; solvent B: ACN, 0.05% TFA) to determine peptidic purity and ESI-HRMS characterization. To improve resolution in case of HcyCysCm-p5 and HcyHcyCm-p5 we use linear gradient of 5 to 60% of solvent B during 50 min, at 0.8 mL/min flow. In All cases, final products were dissolved in DMSO and purified by preparative RP-HPLC, C18 column (Vydac,  $25 \times 250$  mm,  $25\mu\text{m}$ ) ( $\lambda = 226$  nm) (with a linear gradient of 15 to 80% of B for 60 min, at 5 mL/min flow).

Note: Cyclic and dimeric peptides were purified with a different gradient due to the proximity in their retention times (linear gradient of 25% to 65% of solvent B for 60 min, at 5 mL/min flow)

#### 4.3.1 Solid phase synthesis of the antifungal peptide Cm-p5:

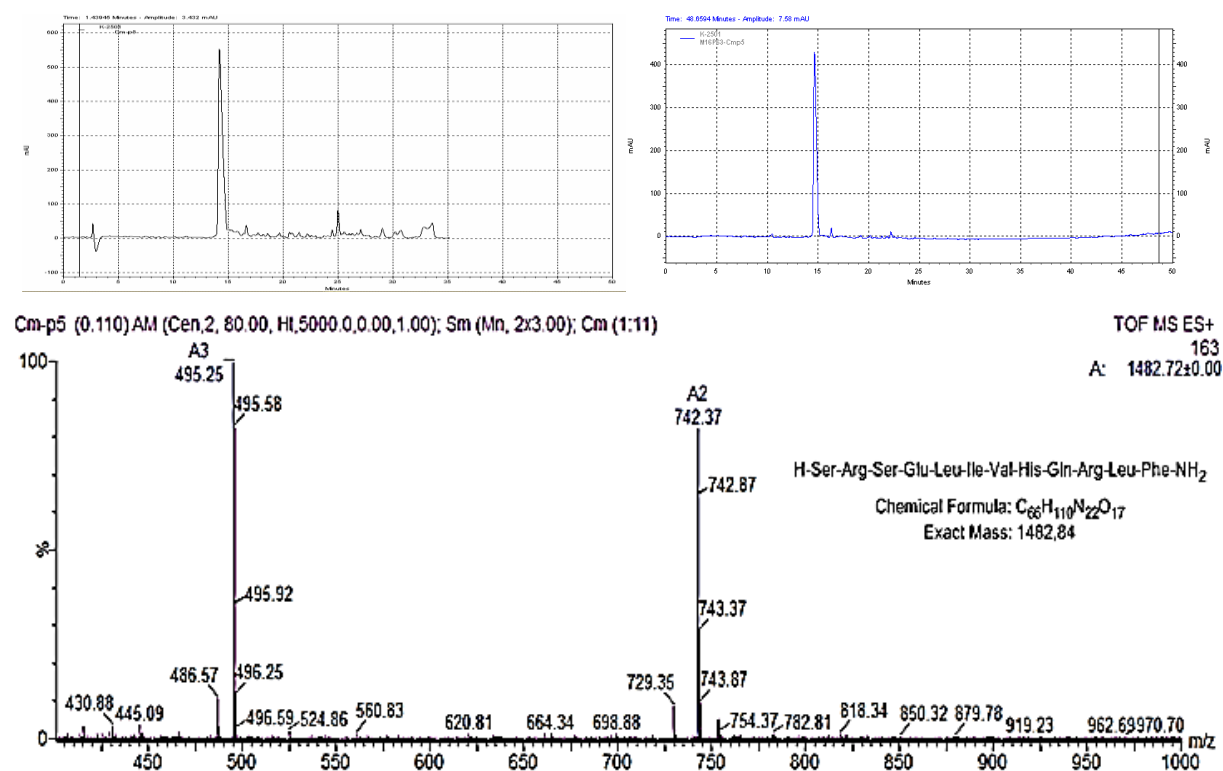


Figure 10: RP-HPLC (crude in the left upper panel) (pure in the right upper panel) and ESI-HRMS (lower panel) of Cm-p5 peptide.



### 4.3.2 Solid phase synthesis of SRSELIVRQRLF-NH<sub>2</sub> analogue (peptide 1):

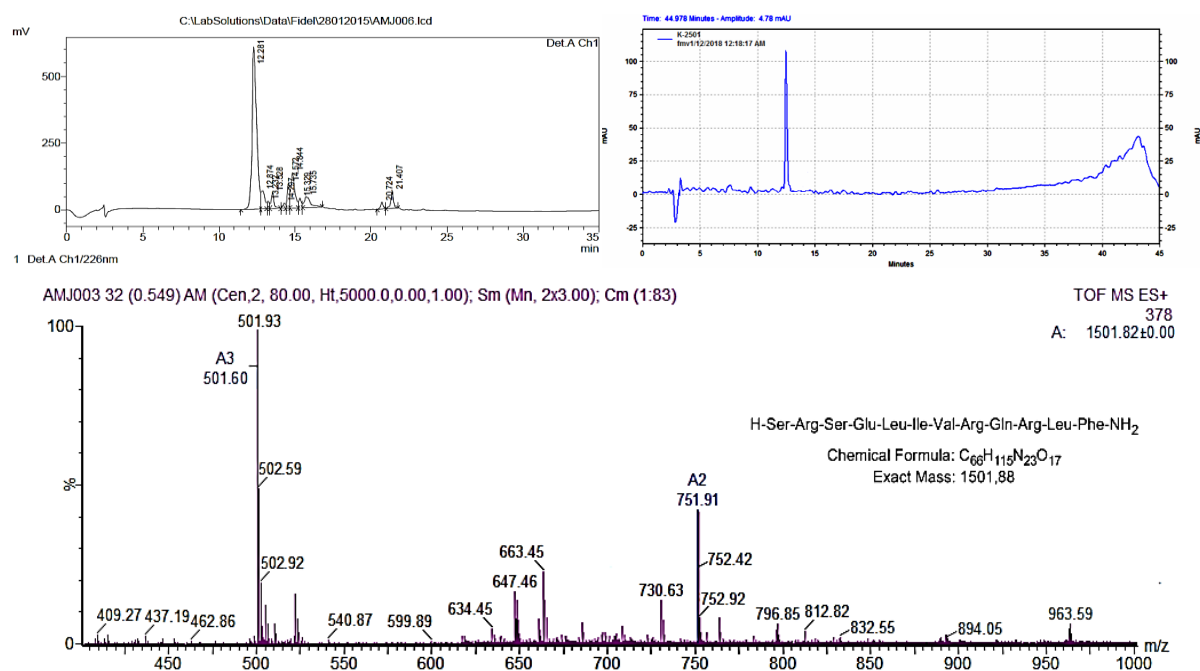


Figure 11: RP-HPLC (crude in the left upper panel) (pure in the right upper panel) and ESI-HRMS (lower panel) of peptide 1.

### 4.3.3 Solid phase synthesis of SRSDLIVHQRLF-NH<sub>2</sub> analogue (peptide 2):

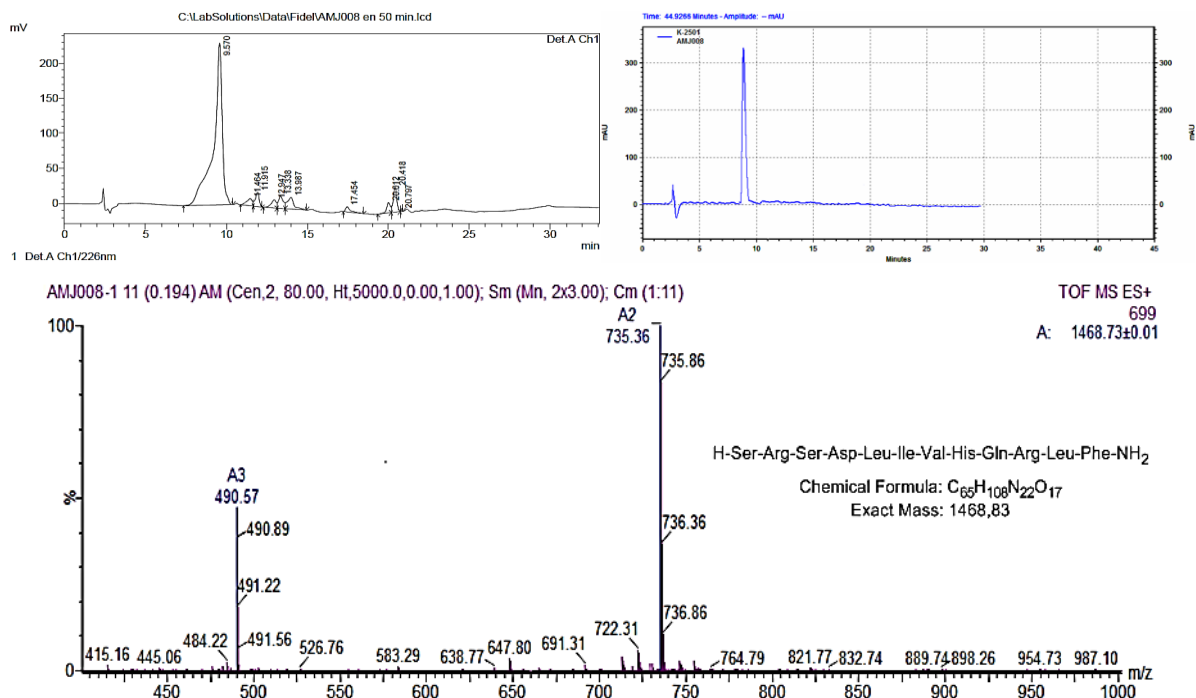


Figure 12: RP-HPLC (crude in the left upper panel) (pure in the right upper panel) and ESI-HRMS (lower panel) of peptide 2.

### 4.3.4 Solid phase synthesis of SRSQLIVHQRLF-NH<sub>2</sub> analogue (peptide 3):

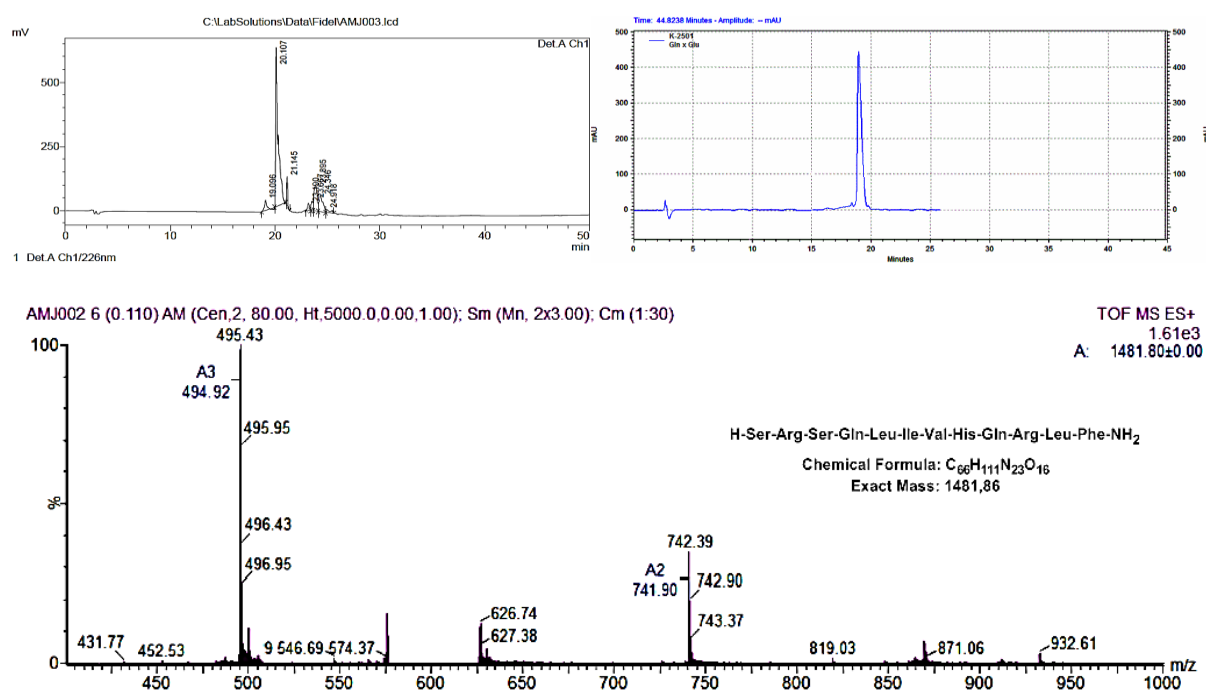


Figure 13: RP-HPLC (crude in the left upper panel) (pure in the right upper panel) and ESI-HRMS (lower panel) of peptide 3.

### 4.3.5 Solid phase synthesis of SRSALIVHQRLF-NH<sub>2</sub> analogue (peptide 4):

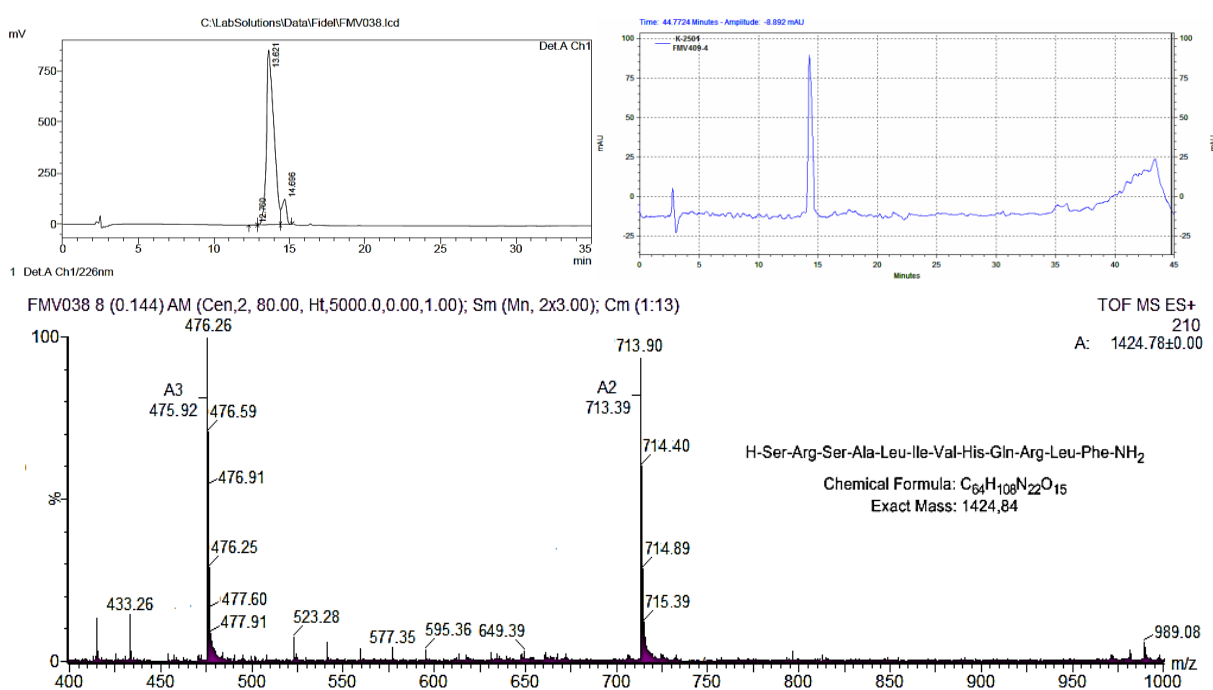


Figure 14: RP-HPLC (crude in the left upper panel) (pure in the right upper panel) and ESI-HRMS (lower panel) of peptide 4.

### 4.3.6 Solid phase synthesis of SRS $\beta$ ALIVHQRLF-NH<sub>2</sub> analogue (peptide 5):

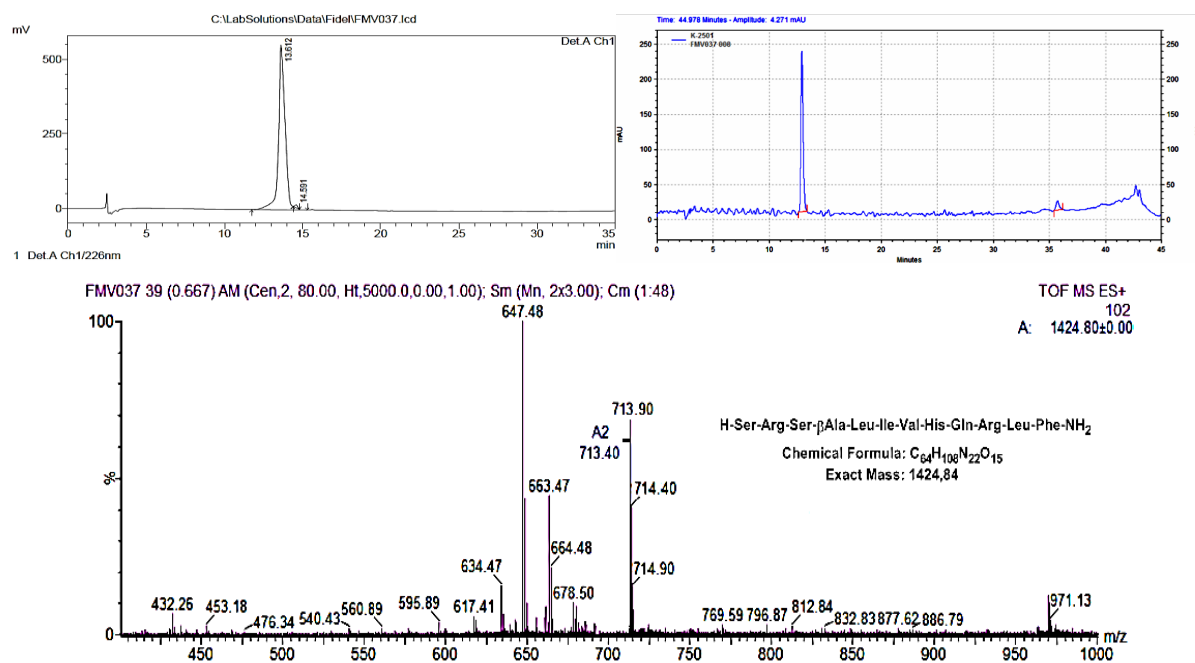


Figure 15: RP-HPLC (crude in the left upper panel) (pure in the right upper panel) and ESI-HRMS (lower panel) of peptide 5.

### 1.1.7 Solid phase synthesis of SRSELRVHQRLF-NH<sub>2</sub> analogue (peptide 6):

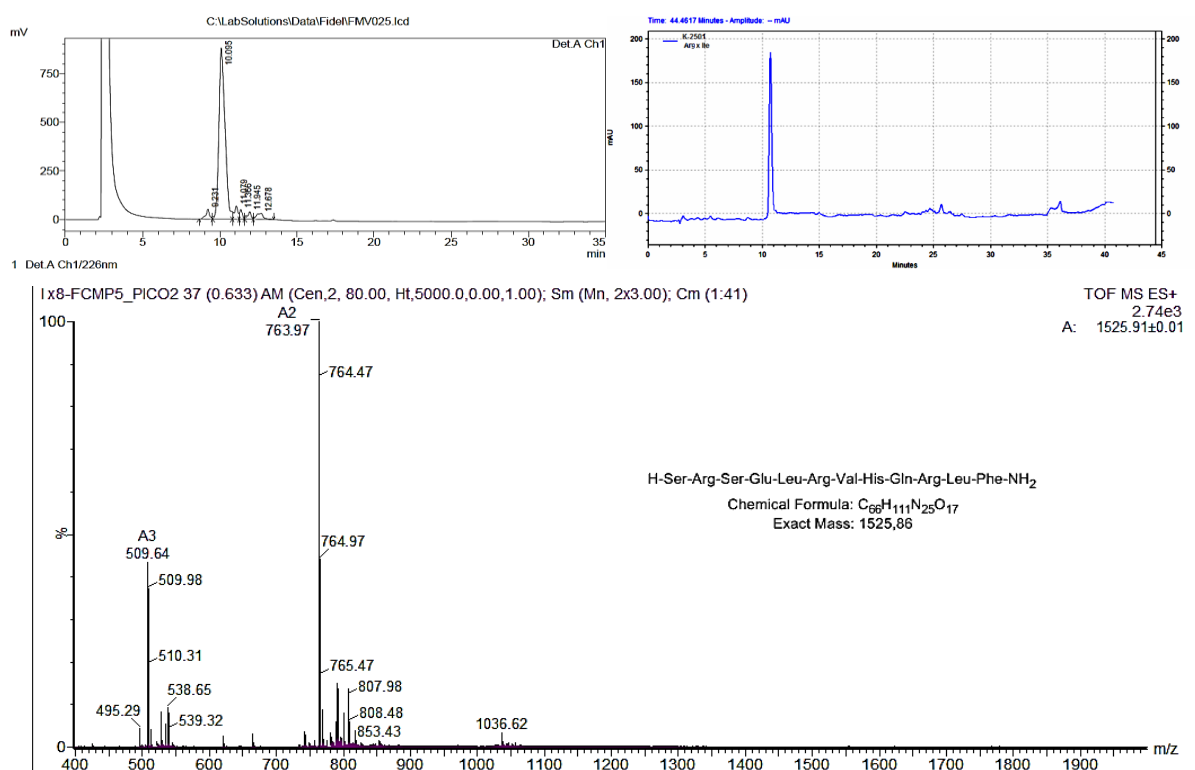


Figure 16: RP-HPLC (crude in the left upper panel) (pure in the right upper panel) and ESI-HRMS (lower panel) of peptide 6.

### 4.3.7 Solid phase synthesis of SRSELKVHQRLEF-NH<sub>2</sub> analogue (peptide 7):

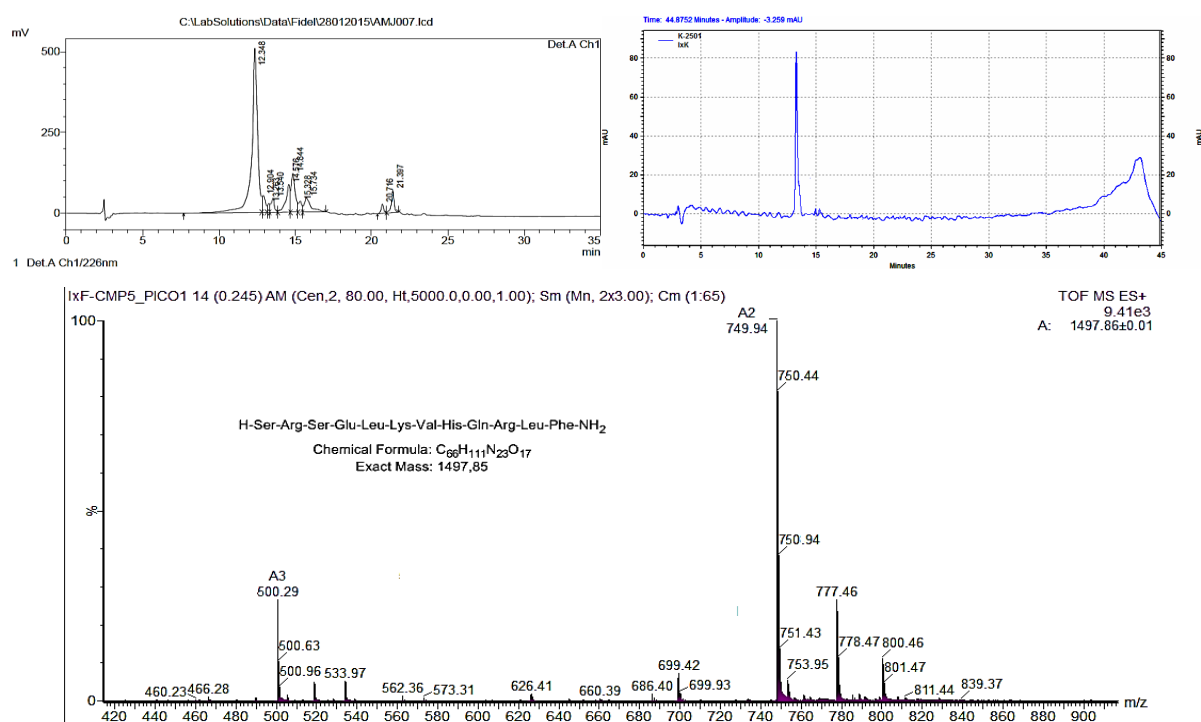


Figure 17: RP-HPLC (crude in the left upper panel) (pure in the right upper panel) and ESI-HRMS (lower panel) of peptide 7.

### 4.3.8 Solid phase synthesis of SRSEKIVHQRLEF-NH<sub>2</sub> analogue (peptide 8):

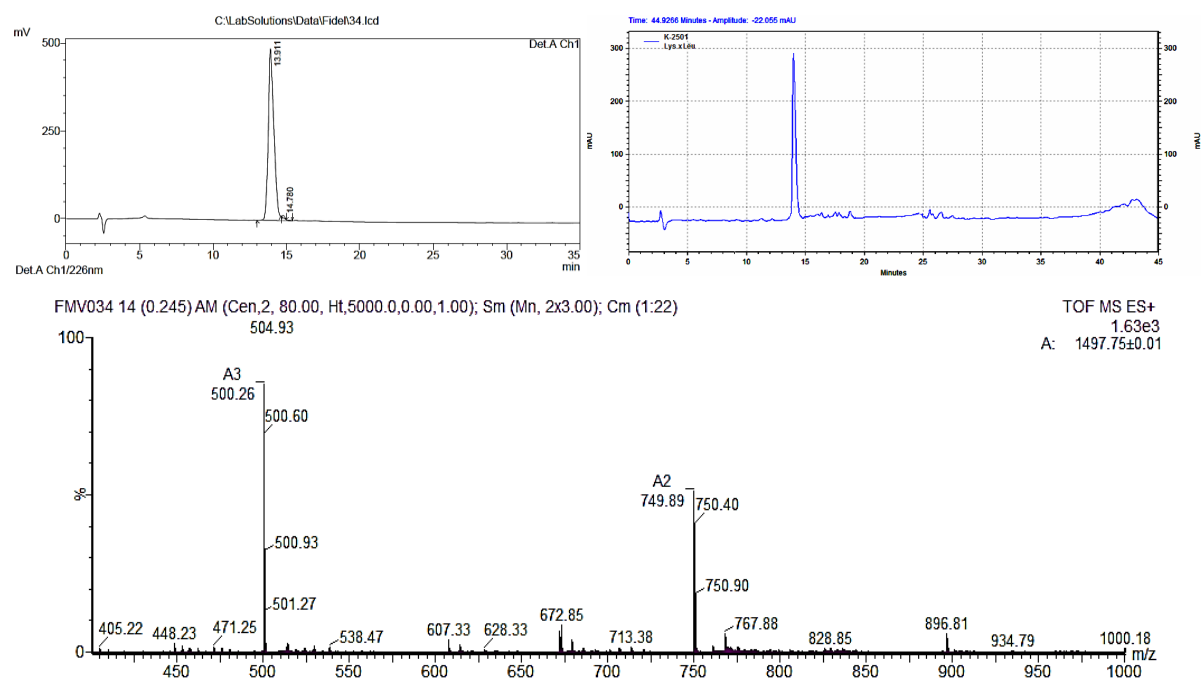


Figure 18: RP-HPLC (crude in the left upper panel) (pure in the right upper panel) and ESI-HRMS (lower panel) of peptide 8.

### 4.3.9 Solid phase synthesis of SRSE--IVHQRLF-NH<sub>2</sub> analogue (peptide 9):

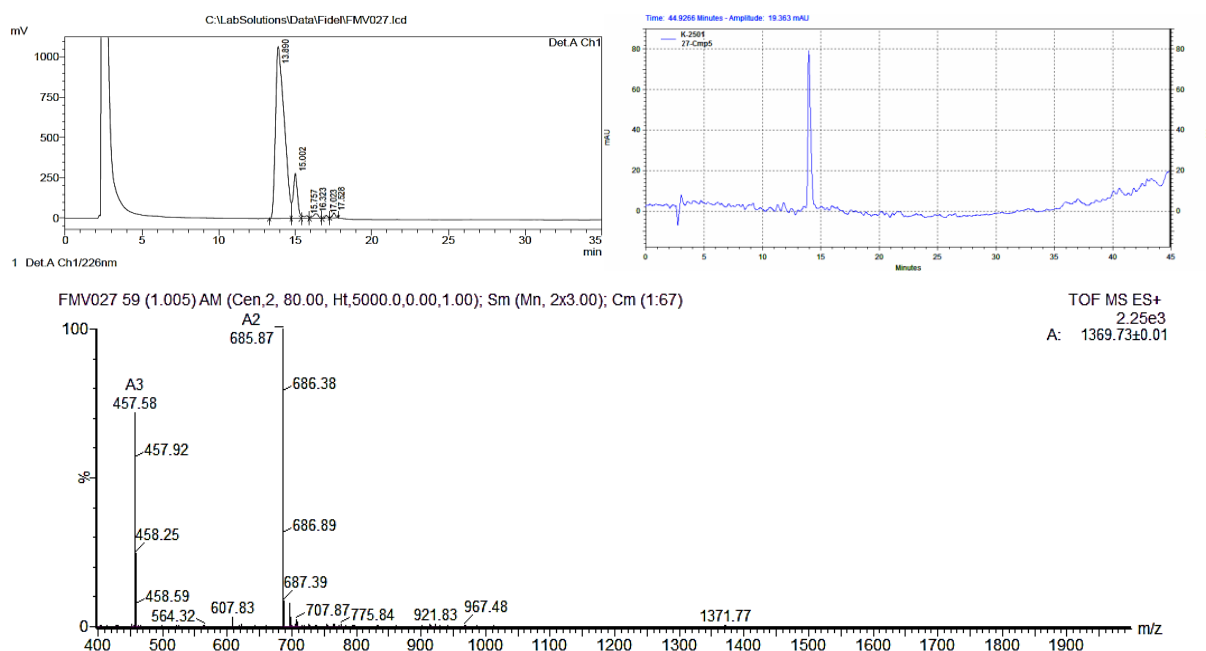


Figure 19: RP-HPLC (crude in the left upper panel) (pure in the right upper panel) and ESI-HRMS (lower panel) of peptide 9.

### 4.3.10 Solid phase synthesis of SRSEKIVHQ--LF-NH<sub>2</sub> analogue (peptide 10):

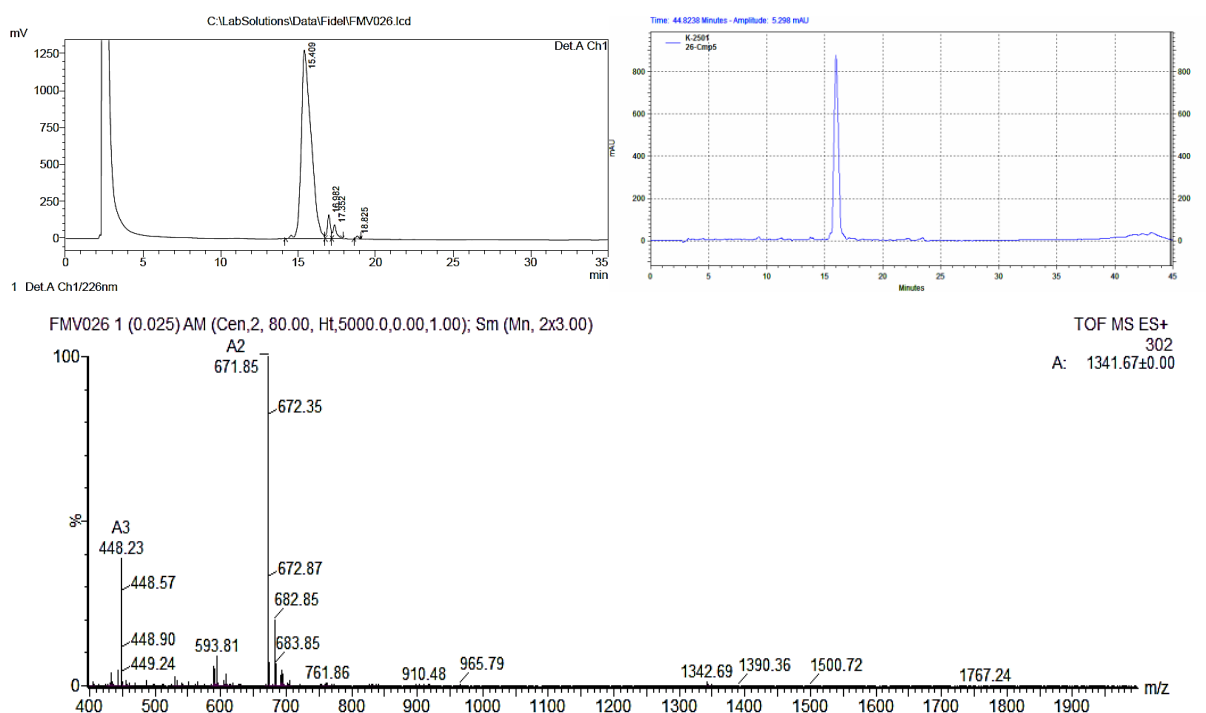


Figure 20: RP-HPLC (crude in the left upper panel) (pure in the right upper panel) and ESI-HRMS (lower panel) of peptide 10.

### 4.3.11 Solid phase synthesis of RS-LIVHQRFLF-NH<sub>2</sub> analogue (peptide 11):

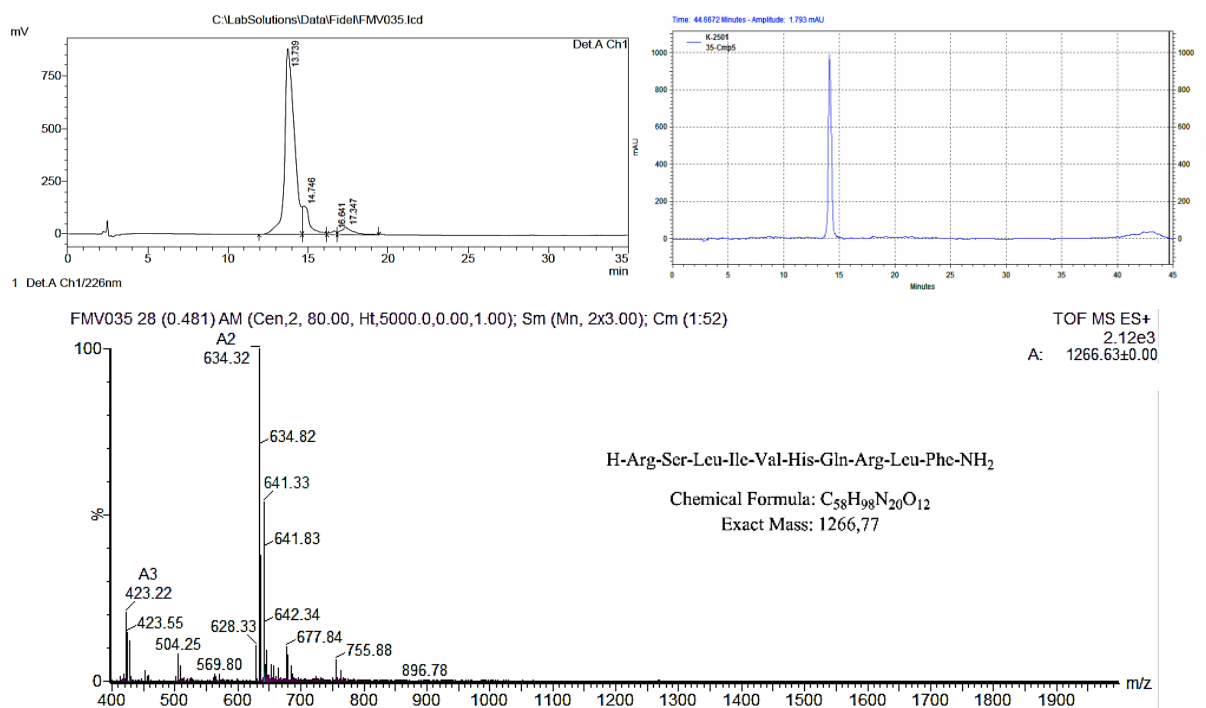


Figure 21: RP-HPLC (crude in the left upper panel) (pure in the right upper panel) and ESI-HRMS (lower panel) of the peptide 11.

### 4.3.12 Solid phase synthesis of SRSE-IV--QRLF-NH<sub>2</sub> analogue (peptide 12):

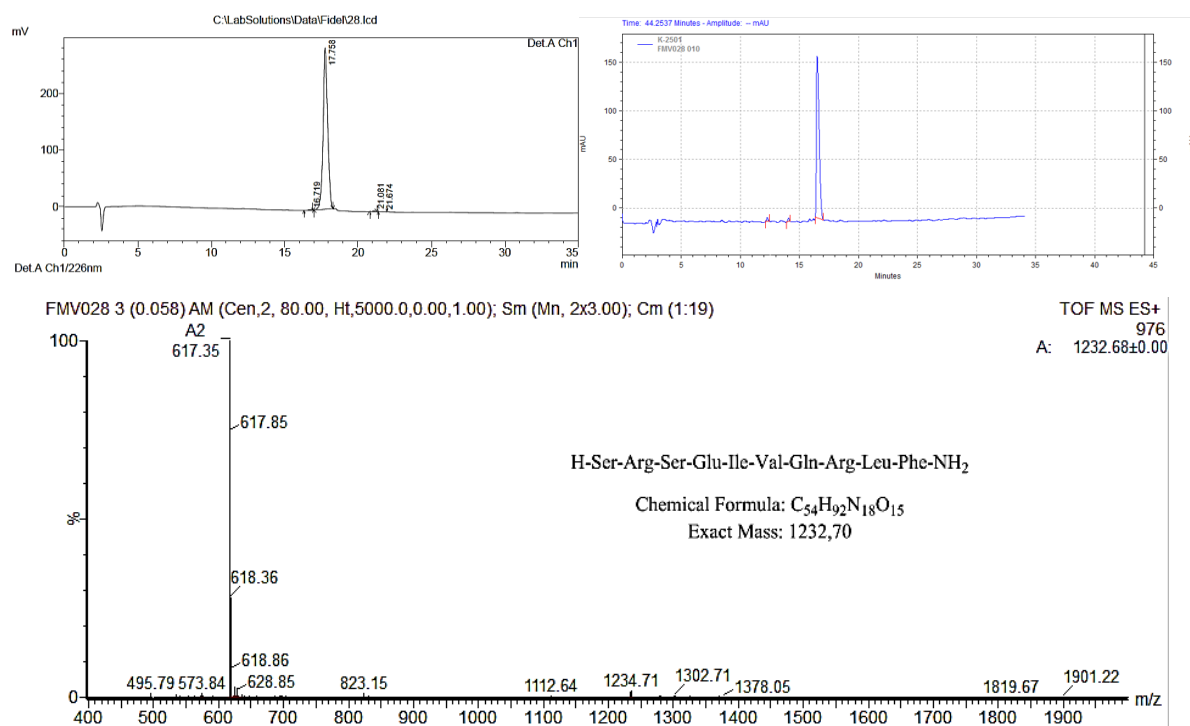


Figure 22: RP-HPLC (crude in the left upper panel) (pure in the right upper panel) and ESI-HRMS (lower panel) of peptide 12.

### 4.3.13 Solid phase synthesis of Ac-SRSELIVHQLRF-NH<sub>2</sub> analogue (peptide 13):

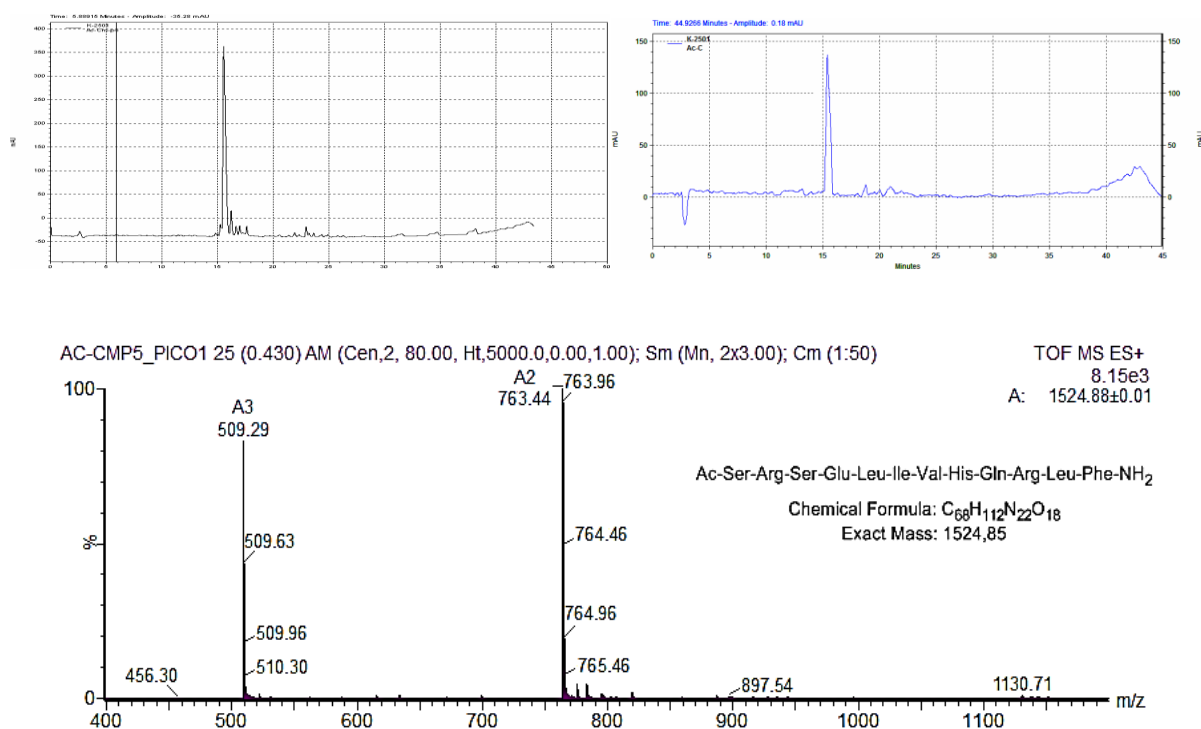


Figure 23: RP-HPLC (crude in the left upper panel) (pure in the right upper panel) and ESI-HRMS (lower panel) of peptide 13.

### 4.3.14 Solid phase synthesis of (SRSELIVHQLRF)<sub>2</sub>-K-NH<sub>2</sub> (peptide 14):

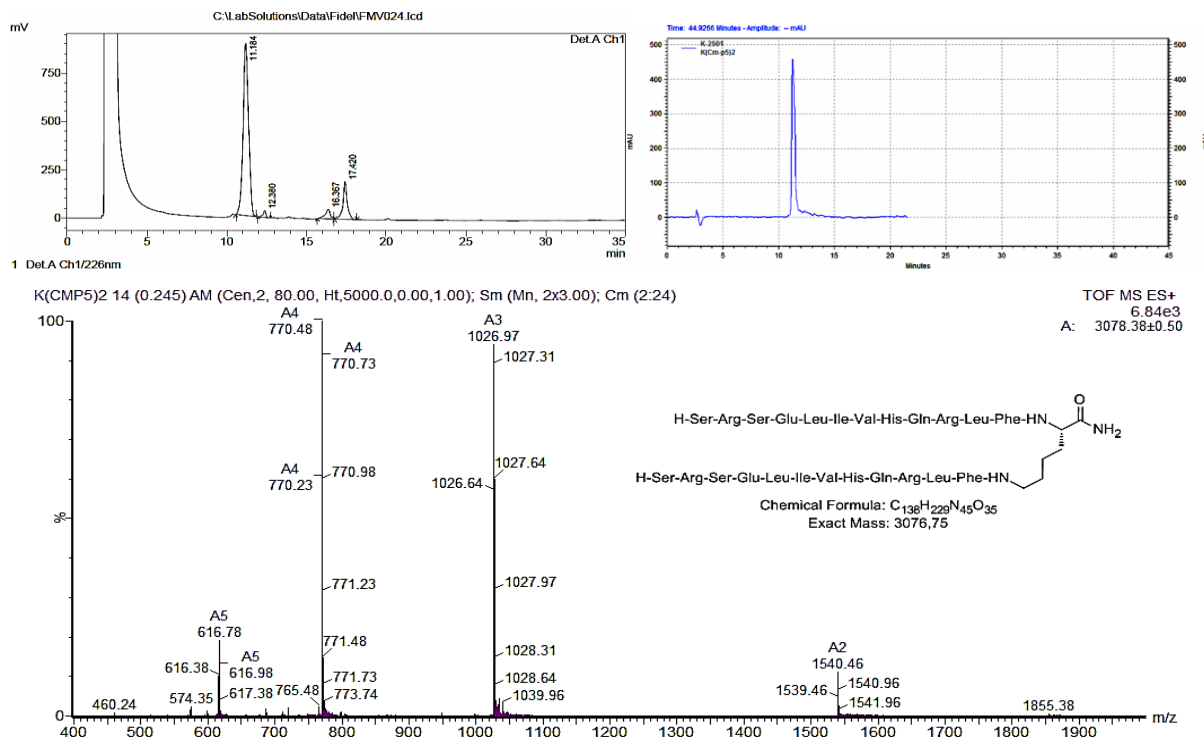


Figure 24: RP-HPLC (crude in the left upper panel) (pure in the right upper panel) and ESI-HRMS (lower panel) of peptide 14.





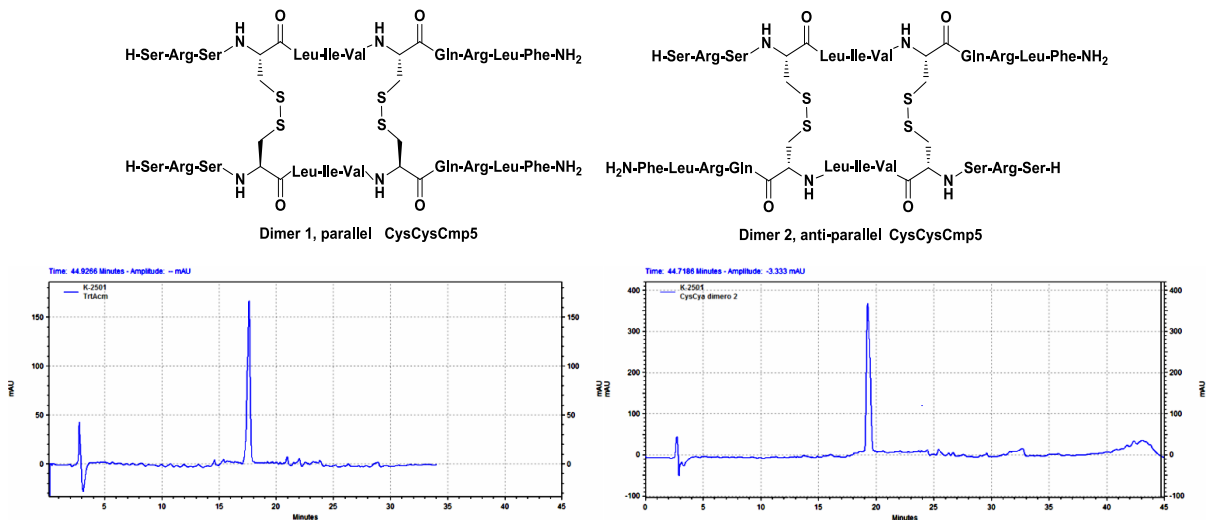


Figure 28: CysCysCm-p5 peptide dimers structure and RP-HPLC of the purified products (left: parallel, right: antiparallel) formed by two intermolecular disulfide bridges.

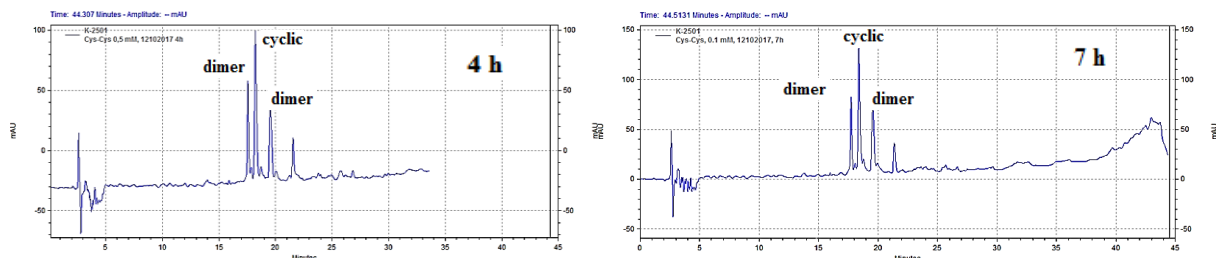


Figure 29: Chromatographic evolution of cyclization of CysCysCm-p5 peptide at 0.1 mM.

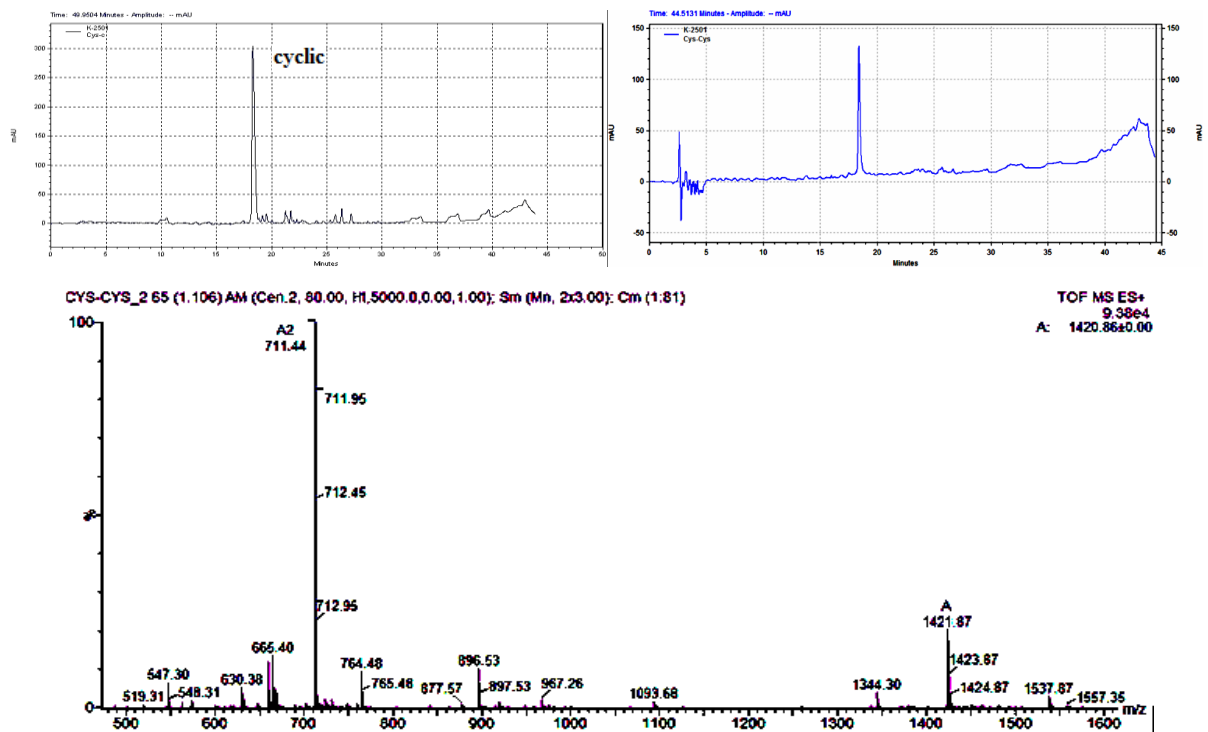


Figure 30: RP-HPLC (crude at left upper panel) (pure at right upper panel) and ESI-HRMS (lower panel) of cyclization of CysCysCm-p5 peptide at 0.03 mM after 24 h.

### 4.3.16 Synthesis of Structurally Restricted Peptide (CysCysCm-p5)<sub>2</sub> (Parallel Dimer) using Cys(Acm) as mutant of His of Cm-p5:

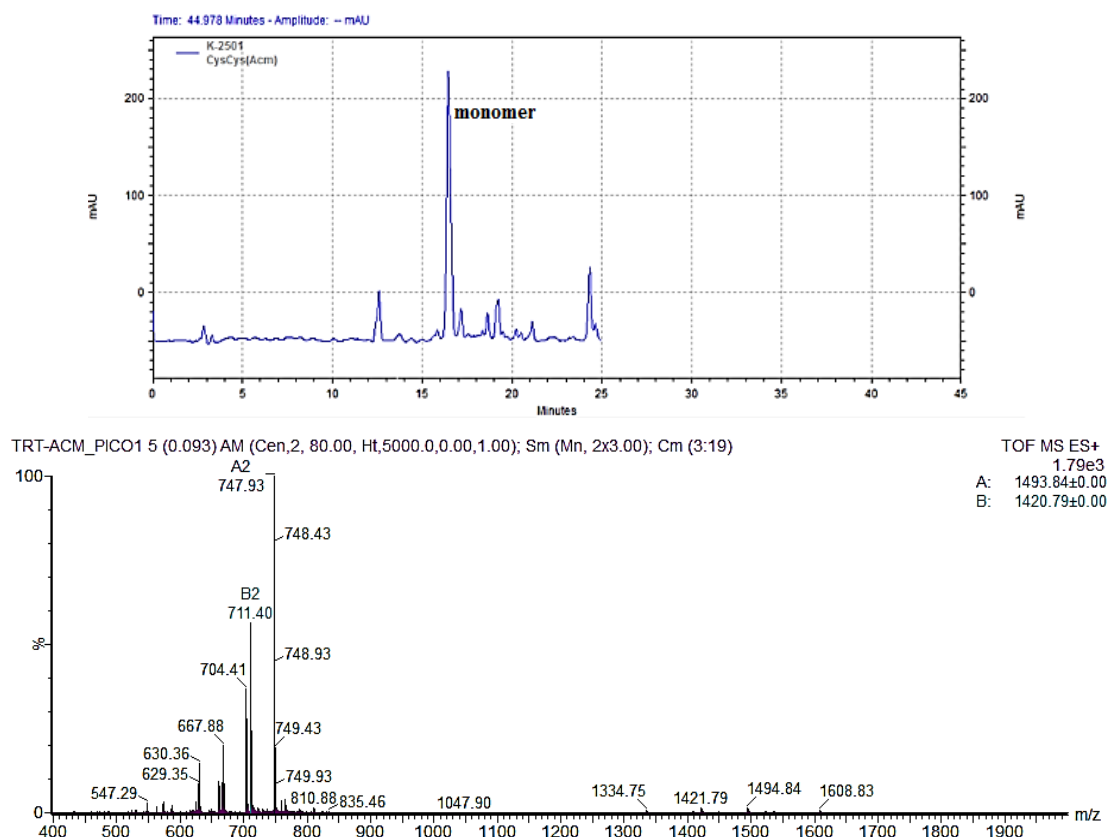


Figure 31: RP-HPLC (upper panel) and ESI-HRMS (lower panel) of acyclic peptide CysCys(Acm)-Cm-p5 (crude).

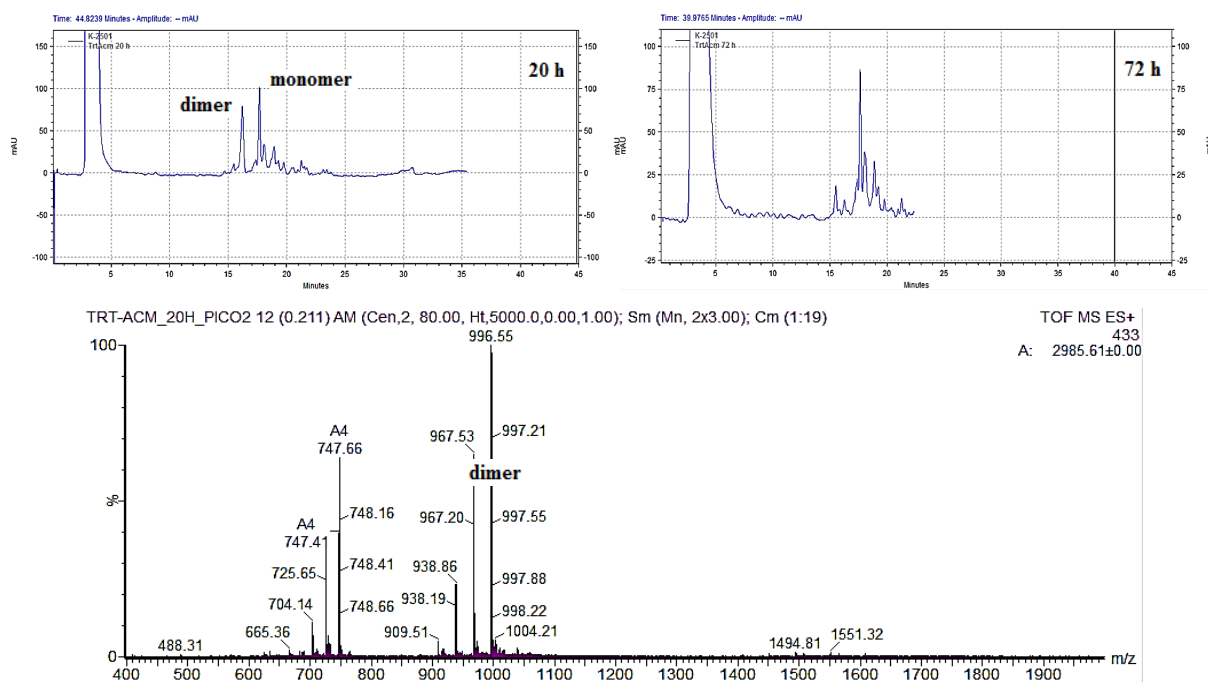


Figure 32: RP-HPLC evolution (upper panels) and ESI-HRMS (lower panel) of dimerization of CysCys(Acm)Cm-p5 (crude) peptide at 5 mM after 72 h.

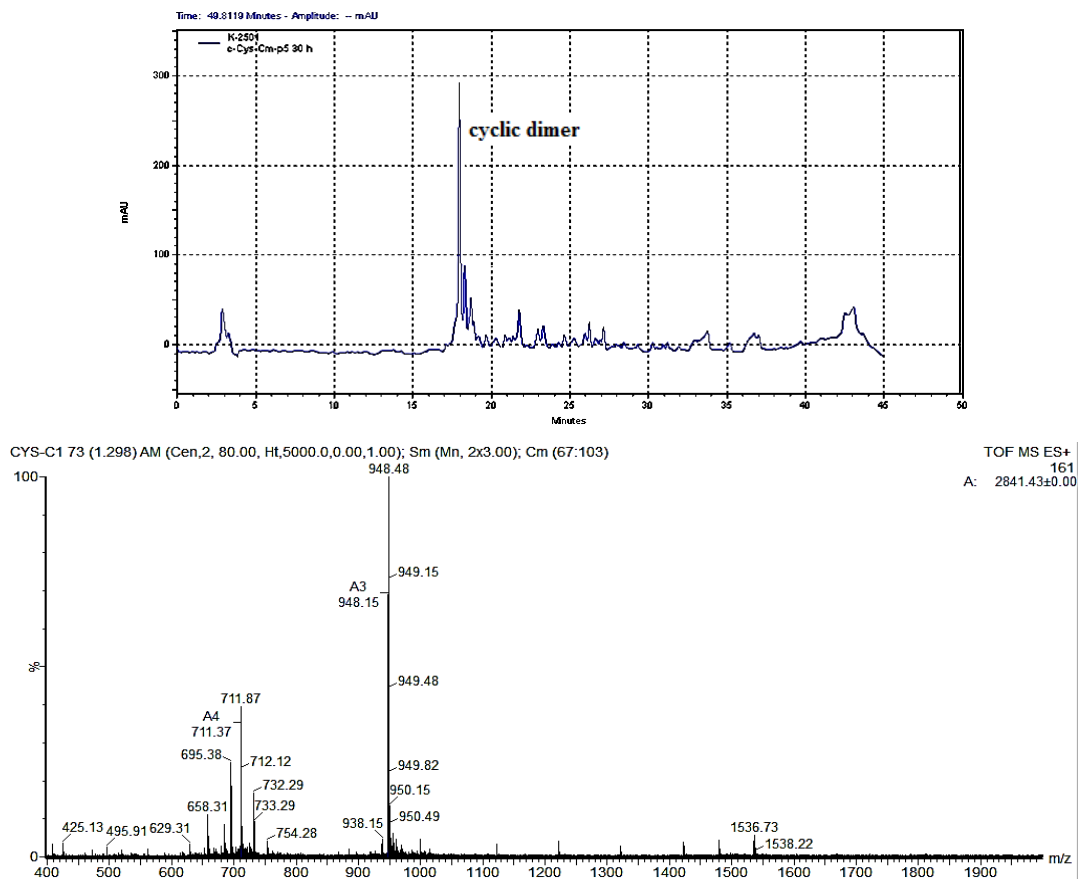
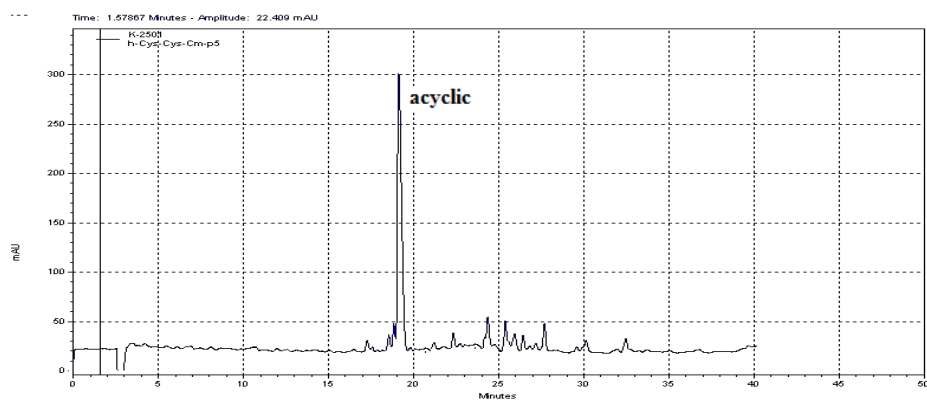


Figure 33: RP-HPLC (upper panel) and ESI-HRMS (lowerpanel) of cyclization of CysCys(Acm)-Cm-p5 parallel dimer at 0,3 mM after 30 min with I<sub>2</sub>.

#### 4.3.17 Synthesis of Structurally Restricted (Cyclic) Peptide (HcyCysCm-p5):



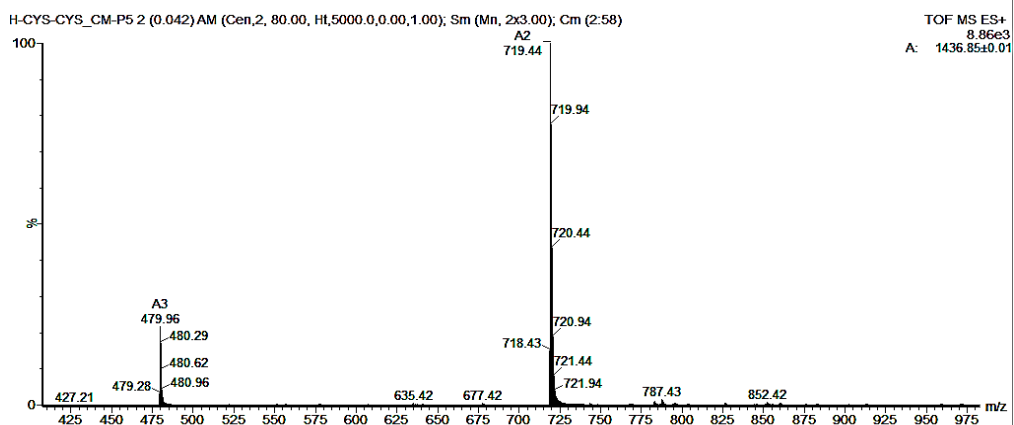


Figure 34: RP-HPLC (upper panel) and ESI-HRMS (lowerpanel) of acyclic HcyCysCm-p5 peptide.

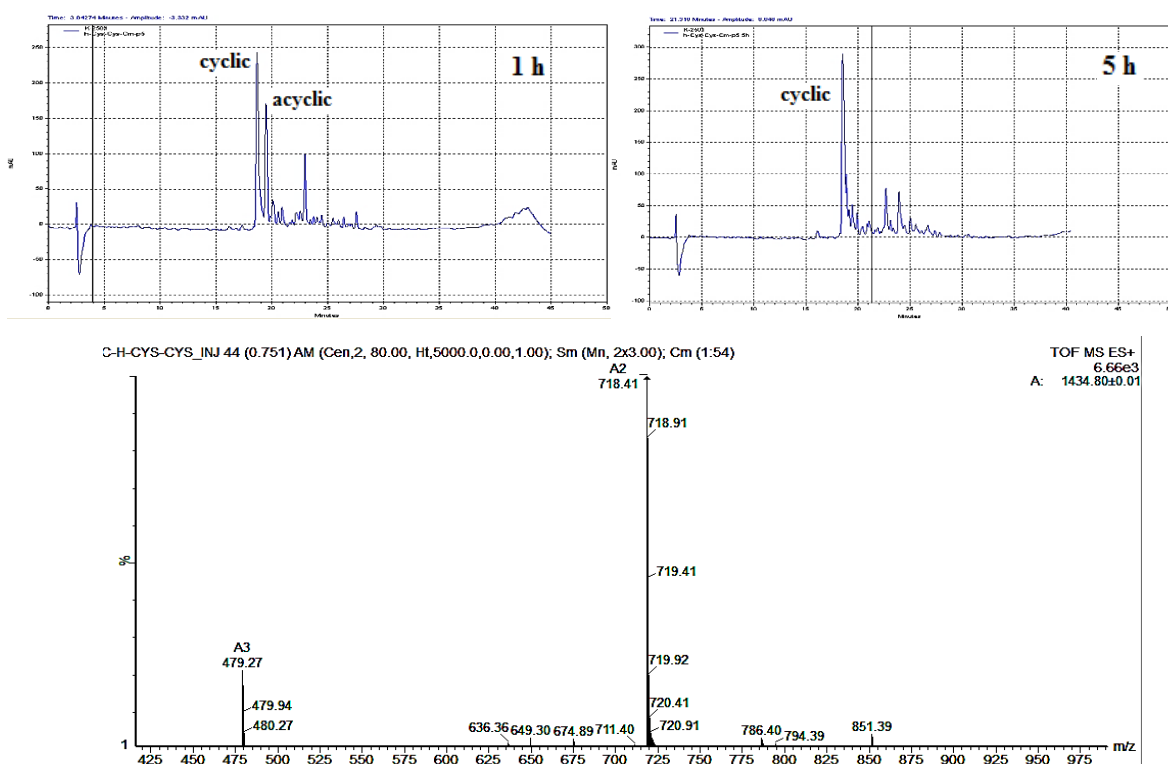
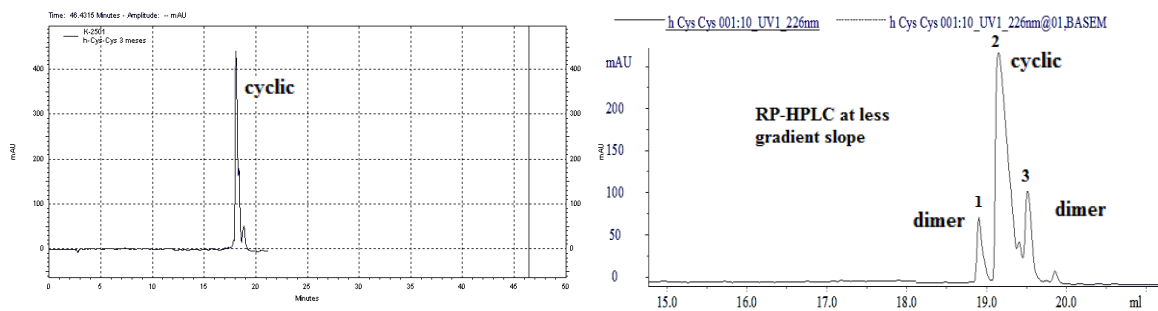


Figure 35: RP-HPLC evolution (upper panels) and ESI-HRMS (lower panel) of cyclization of structurally restricted peptide HcyCysCm-p5 at 0.5 mM.



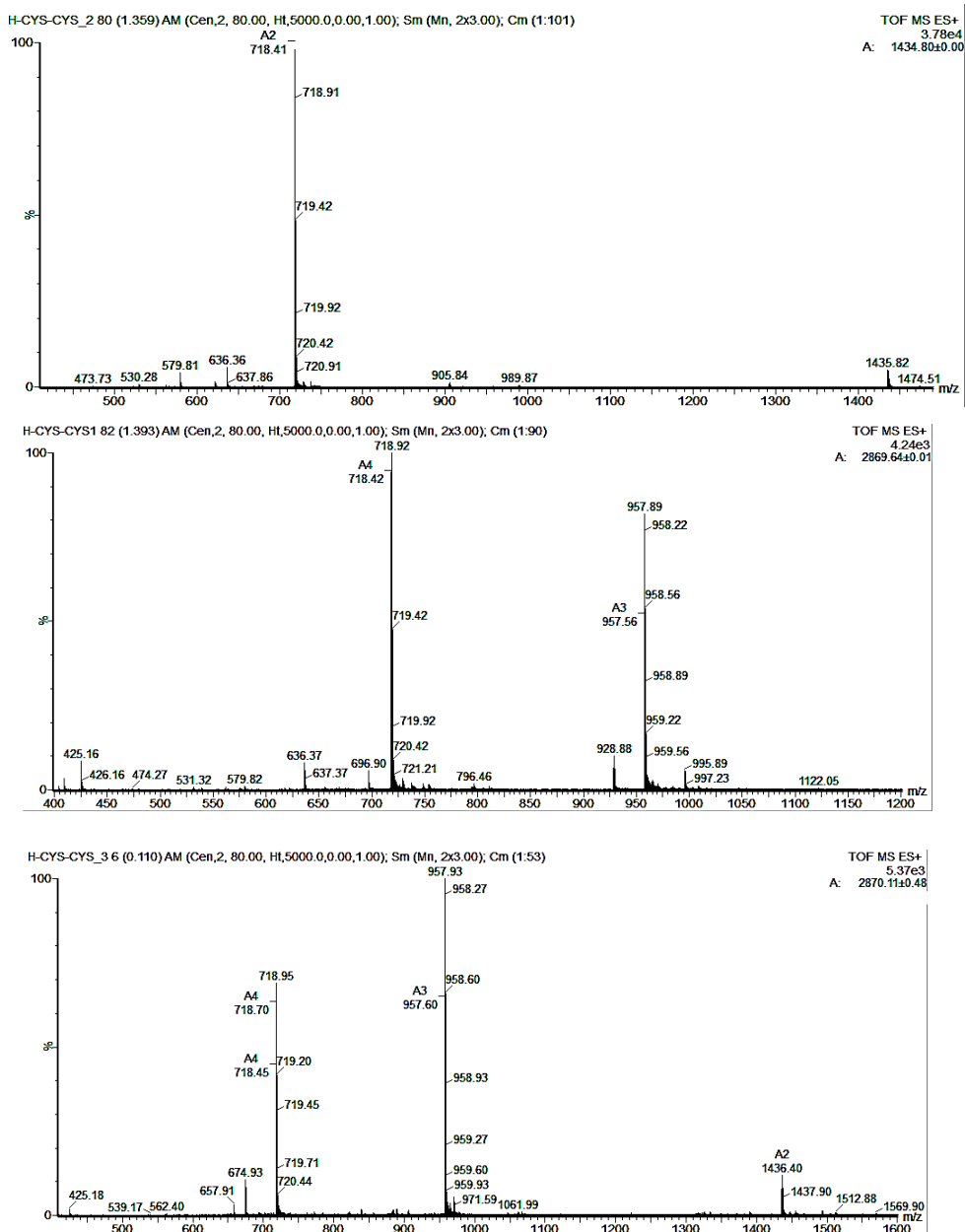


Figure 36: RP-HPLC (left panel) at high resolution (less gradient slope, right panel) and ESI-HRMS (lower panels) of cyclic and dimers of HcyCysCm-p5 peptide.

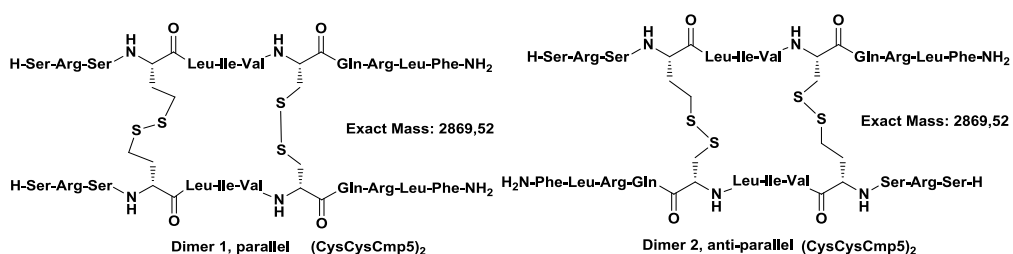


Figure 37: HcyCysCm-p5 peptide dimers (left: parallel, right: antiparallel) formed by two intermolecular disulfide bridges.

### 4.3.18 Synthesis of Structurally Restricted (Cyclic) Peptide (HcyHcyCm-p5):

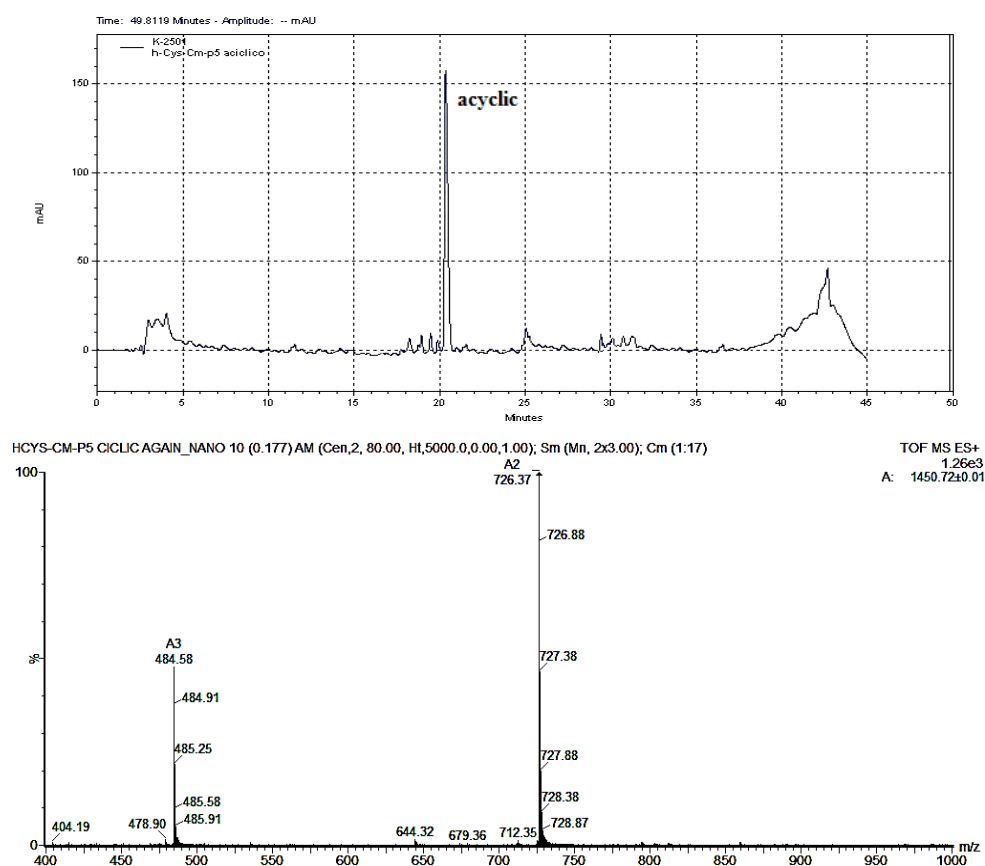


Figure 38: RP-HPLC (upper panel) and ESI-HRMS (lowerpanel) of acyclic peptide HcyHcyCm-p5.

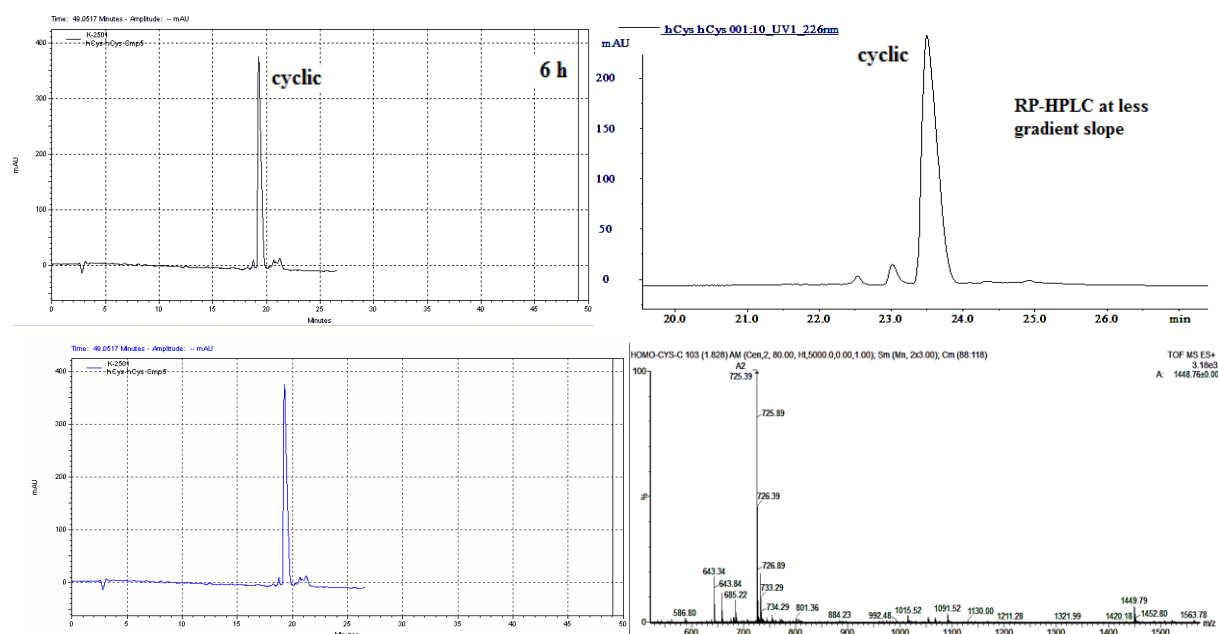
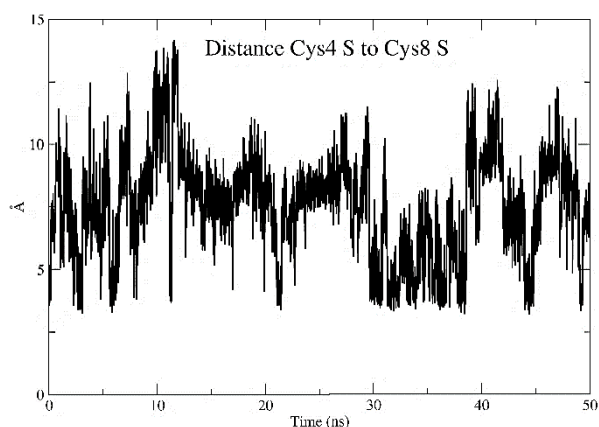


Figure 39: RP-HPLC (upper panel) after 6h of cyclization (crude), at high resolution (less slope of gradient) and the purified product (left lower panel), ESI-HRMS (right lower panel) of cyclic HcyHcyCm-p5 peptide..

#### 4.4 Materials and methods. Molecular dynamics simulations

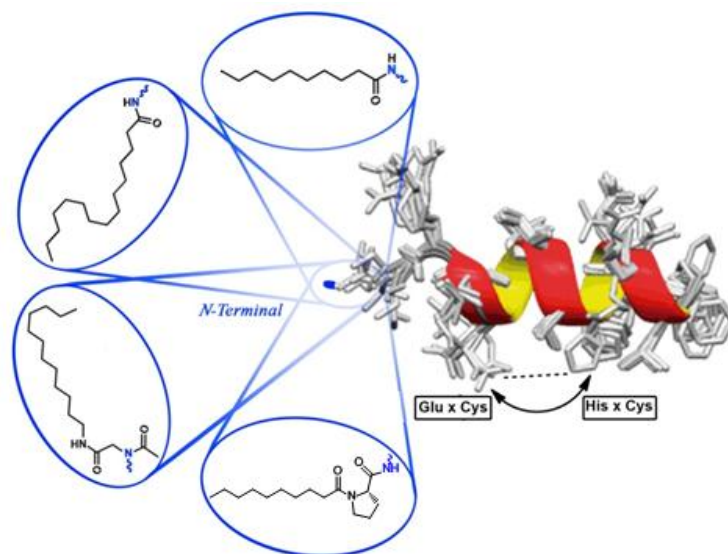
Peptide (SRSCLIVCQRLF) model was built with the acetylated *N*-terminal in order to avoid electrostatic effects of the terminal amine group. Model was fully solvated in an octahedral box of TIP3P water model with periodic boundary conditions. The MDS (molecular dynamic simulation) was performed using AMBER 11 and supposing an initial  $\alpha$ -helical peptide.<sup>123</sup> The model was prepared with a 3-steps protocol. First, 2000 steps were ran for side chains optimization, second, a 50000 steps of thermalization at 300 K with a Berendsen thermostat at constant volume, and third, a 50000 steps at the same temperature with constant pressure (isotropic position scaling) of 1 atm. Finally, 50 ns of MDS under the NPT ensemble condition were performed. This system remained stably structured along the whole MDS. Results of the distance between sulfur atoms are showed in Chart 3, supposing an initial helical structure of the acyclic peptide CysCysCm-p5.

Chart 3: Simulation by molecular dynamic of the distance between sulfur atoms in the  $\alpha$ -helix of acyclic peptide CysCysCm-p5.



# Chapter 2

"Synthesis of lipidated and cyclic analogues of Cm-p5 peptide, with stabilized  $\alpha$ -helix and containing different turn motif between the N-terminal and the lipid"





## Chapter 2

### 1 Introduction. Chapter 2

#### 1.1 Objectives of our work.

Previous studies have shown that the lipidation of Cm-p5 by Ugi-4CR in solid phase influence the antifungal activity of Cm-p5 in different degrees, depending on the position where the lipid is introduced. For example, the lipidation in intermediate position produces analogues with less antimicrobial activity, which should be related with the loss of helical character, due to the introduction of *N*-alkylation by Ugi-4CR. On the other hand, the *N*-lipidation in the *C*-terminal maintains the activity and in *N*-terminals produces the most active versions of Cm-p5 known until today.

For the lipidation by Ugi-4CR in solid phase is needed to produce an isocyanolipid, which is in disadvantage with the easy way of coupling fatty acids at the *N*-terminal of peptides. The increase of antimicrobial activity of peptides by fatty acids coupling at the *N*-terminal has been widely described.<sup>124</sup> At this stage of our investigation, the synthesis of *N*-lipidated analogues of Cm-p5 by simple coupling of fatty acids is desired and will allow determining the optimal size of the lipid chain for the antifungal activity.

The fundamental structural difference between an Ugi lipidated analogue and a simple coupling of lipid chain is the presence of *N*-substitution at the union point of the lipid. Pro residues in proteins have a similar influence that an *N*-substitution and are implicated in several conformational changes, indispensable for the biological activity. Gly residues are also important in those cases and together with Pro are normally present in loops and surfaces of proteins, conferring flexibility and conformational freedom.

In chapter 1, we demonstrated the effectiveness of the introduction of disulfide bridge construction in the stabilization of the  $\alpha$ -helical secondary structure of Cm-p5. This disulfide bridge, between the Glu and His position, produced a more active version of Cm-p5, which could be more stable metabolically. In addition, the implication of Glu and His in salt bridge interaction was indirectly demonstrated.

In a nutshell, the lipidation at the *N*-terminal and the cyclization by disulfide bridge produce the most active versions of Cm-p5 reported until today. Due to that, the synthesis of *N*-lipidated and cyclic analogues of Cm-p5 is desired for future investigation. With this aim, the objectives of this chapter are focused on:

✓ Synthesize *N*-lipidated analogues of Cm-p5 by fatty acids coupling of different chain length and evaluate the antimicrobial activity.

- ✓ Synthesize *N*-lipidated analogues of Cm-p5 by coupling of a fatty acid after the introduction of Ala, Gly or Pro at the *N*-terminal.
- ✓ Synthesize *N*-lipidated analogues of CysCysCm-p5 by coupling of a fatty acid after the introduction of Ala, Gly or Pro at the *N*-terminal.
- ✓ Produce the dimers and cyclic analogues of the last three lipopeptides by disulfide bridge formation in pseudo-diluted conditions.
- ✓ Synthesize n-dodecylisonitrile by formilation and deshydration of n-dodecylamine.
- ✓ Synthesize the *N*-lipidated analogue of CysCysCm-p5 by Ugi-4CR in solid phase with n-dodecylisonitrile, acetic acid and paraformaldehyde.
- ✓ Produce the dimers and cyclic analogues of the last lipopeptides by disulfide bridge formation in pseudo-diluted conditions.

## 2 Bibliographic Revision. Chapter 2

### 2.1 Lipopeptides. Importance and characteristics

The presence of a lipid group in a peptide modulates the hydrophobicity and secondary structure, while retaining the ability of binding to designated receptors. Lipidation improves metabolic stability, membrane permeability, bioavailability, and changes the pharmacokinetic and pharmacodynamic properties of peptides.<sup>125</sup>

Lipopeptides have been proven as powerful and versatile alternatives against a wide variety of pathogens.<sup>126</sup> Natural or synthetic lipopeptides may have surfactant, antibacterial and antifungal activity, and have been evaluated as transfer agents for the release of genes. They have amphiphilic character and are used as biosurfactants and antibiotics. Lipopeptides have been used in clinical applications, as well as in the preservation of foods and daily products.<sup>127</sup>

Bacteria members of the genus *Bacillus* are considered effective microbial sources for the production of these type of bioactive molecules.<sup>128</sup> There are three *Bacillus* lipopeptide families that have been studied for their antagonistic potency against several phytopathogens: Surfactin, Iturina and Fengycin (Figure 40).<sup>129</sup> Also in actinobacteria, species of the genus *Streptomyces* has been reported the production of various antimicrobial lipopeptides with application in the pharmaceutical industry.<sup>130</sup> These compounds are widely considered as potential alternatives for the growing problem of resistance to conventional antibiotics, fungal infections and other diseases that threaten life.<sup>127</sup>

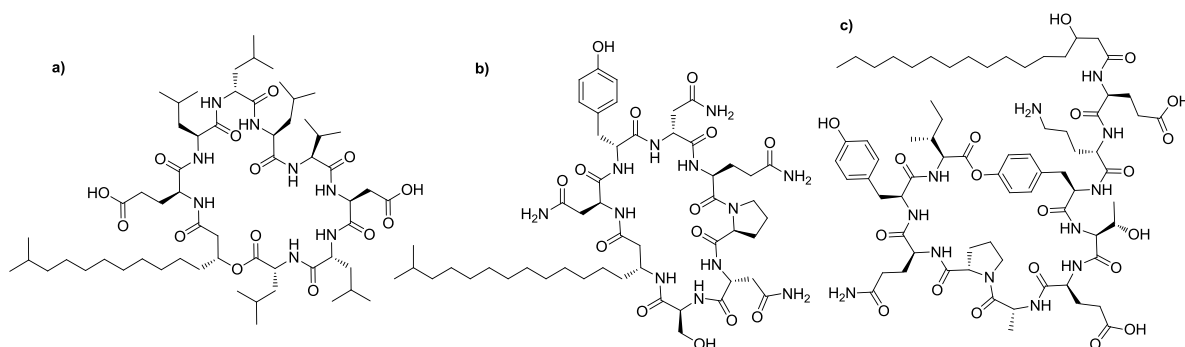


Figure 40: Examples of the *Bacillus* lipopeptide family, a) Surfactin, b) Iturin, c) Fengycin.

Lipopeptides such as Polymyxin B (one component of the commercial triple antibiotics) interact primarily with the lipopolysaccharide (LPS) component of the bacterial outer membrane by electrostatic interaction while the tail of *N*-terminal fatty acid exerts the bactericidal action because it inhibits the synthesis of the outer membrane.<sup>131</sup>

Many of these molecules also play an important role in the processes of induction of apoptosis<sup>132</sup> and are recognized by the TLRs, an essential components of the innate and adaptive

immune response, since they are responsible for the recognition of the different pathogens and trigger responses aimed at eliminating pathogens and developing immunological memory.<sup>133</sup> Linear lipopeptides (histatins) are applied as transfer agents for the efficient release of genes (Figure 41a),<sup>134</sup> in the inhibition of proteases and some of them have neurotoxic properties.<sup>71</sup> The growth of the toxic cyanobacterium *Microcystis aeruginosa* is controlled by the Spiroidesin (Figure 41b) synthesized by the cyanobacterium *Anabaena spiroides*.<sup>135</sup> The lipopeptide daptomycin (Figure 41c), known as Cubicin, is marketed and applied against infections caused by Gram-positive bacteria in USA since 2003.<sup>136</sup>

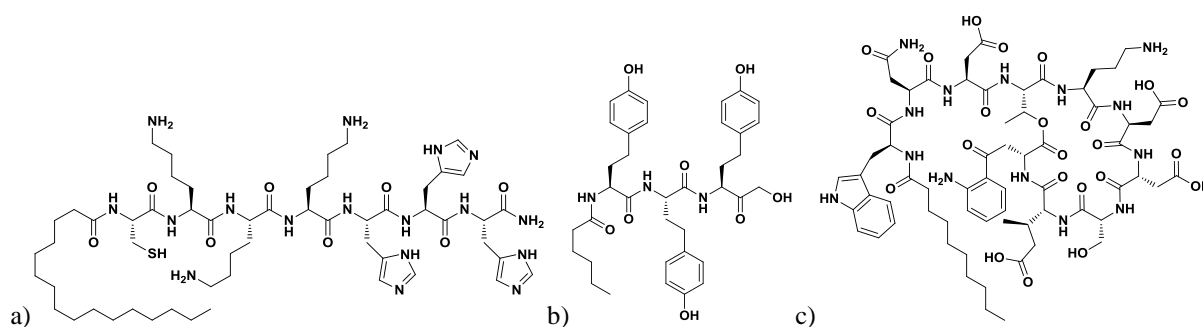


Figure 41: Biologically active lipopeptides, a) histatin, b) spiroidesin, c) daptomycin.

## 2.2 Structural activity relationship in biologically active lipopeptides.

Certain lipopeptides can have strong antimicrobial and hemolytic activities. It has been demonstrated that their activity is generally linked to interactions with the plasma membrane, playing the sterol components a major role in this interaction.<sup>127</sup> In general, adding a lipid of certain length (typically C10-C12) to a peptide will increase the bactericidal activity. Lipopeptides with a higher number of carbon atoms, for example 14 or 16, will typically have antibacterial activity in the lipid tail as well as antifungal activity.<sup>124</sup>

Lipopeptide detergents (LPDs) are composed of amphiphiles and two alkyl chains, which are located on the last part of the peptide backbone. They were designed to mimic the architecture of the native membranes in which two alkyl chains in a lipid molecule interact facially with the hydrophobic segment of AMPs.<sup>137</sup>

After the extraction in 1968 of the first biosurfactant lipopeptide surfactin, produced by the bacterium *Bacillus subtilis*, the extraction and synthesis methods of this type of molecules experienced a constant increase, and in 2005, 23 families of compounds were already known, of which 21 were cyclolipopeptides.<sup>138</sup>

## 2.3 Lipidation of peptides

The lipidation of peptides and intracellular proteins is carried out by incorporating fatty acids, isoprene and glycopospholipids. Such modifications change the flexibility in the position occupied by the lipid,<sup>139</sup> increase the hydrophobicity and they also contribute to the association with the cell membrane.<sup>140</sup> The incorporation of the lipid facilitates the interaction with the microbial surface, being this an aspect of a great importance because short peptides (less than 12 aminoacids), without conformational restrictions, do not possess strong antimicrobial actions under physiological conditions.<sup>141</sup>

The synthetic methods to achieve lipidation depend on the position where the introduction of the lipid is desired. At the *N*-terminus, it is usually carried out by coupling a fatty acid or a phospholipid<sup>142</sup> such as myristic and palmitic acids, among others (Figure 42a).<sup>132</sup> In intermediate positions, it is achieved by using aminoacids derivatized with lipids such as Lys, Asp, Glu, Ser, Trp, Orn, Thr and Cys<sup>138, 143</sup> (Figure 42b). Also, by reduction of Glu or Asp to aldehyde (via Weinreb amides) and subsequent reaction with alkyl bromides via Wittig reaction (Figure 42c), or by coupling bromoacetic acid followed by substitution ( $S_N2$ ) with lipidic amines (Figure 42d).<sup>144</sup> Lipidation at the *C*-terminus is less frequent because it must be performed after cleavage, in liquid phase or with the use of special linkers, which are very expensive (Figure 42e).<sup>145</sup> The use of side chains or the *N* and *C* ends to introduce these modifications is not possible in peptides where these sites are essential for activity. An alanine scanning must be performed in advance to know which residues are essential to maintain the biological activity.<sup>144</sup>

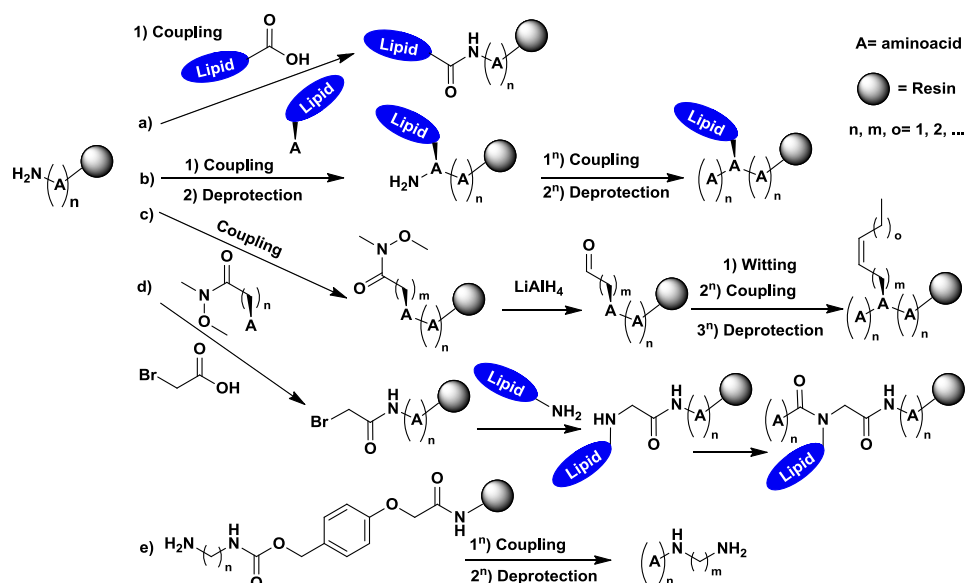
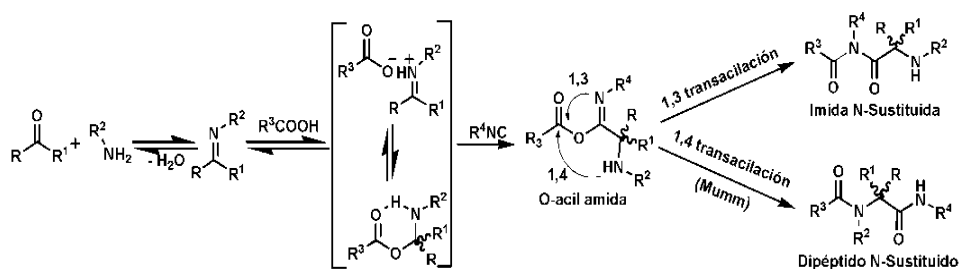


Figure 42: Lipidation of peptides at the *N* and *C* ends and in intermediate positions.

Recently Morales et al. reported a lipidation method of the *N* and *C*-terminus, as well as in intermediate positions of the peptide skeleton employing multicomponent reactions (Section 2.3.2, page 6565).<sup>146</sup>

### 2.3.1 Multicomponent Reaction. Peptide lipidation by Ugi-4CR.

In 1959 Ivar Ugi described the first four-component reaction, where an amine, a carbonyl compound (aldehyde or ketone), an isocyanide and a carboxylic acid gave rise to an *N*-substituted dipeptide and water as the only by-product. The general mechanism of the Ugi-4CR includes the initial formation of a Schiff base and the protonation by the carboxylic acid (activation by increased electrophilicity), which leads to the reversible double addition on the isocyanide. The obtained *O*-acylamine or  $\alpha$ -adduct is a powerful electrophile capable of irreversibly and intramolecularly acylating the *N* of the amine (Mumm rearrangement) or the *N* of the isonitrile (Scheme 6).<sup>147</sup> In excess of acid and at high temperatures the formation of *N*-substituted dipeptides is favored but when the isonitrile radical is bulky (eg.  $R^4 = t\text{-Bu}$ ) the imide can be obtained by Danishefsky reaction.<sup>148</sup>

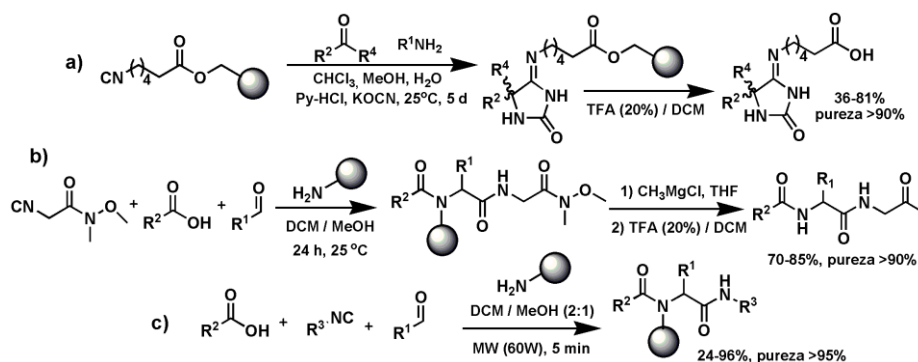


Scheme 6: Ugi-4C (right down) and Danishefsky (right up) reaction mechanism.

The variation of the acid and amino component that take part in the reaction gives access to great diversity of structures.<sup>149</sup> The following can be used as acid components:  $\text{HN}_3$ ,  $\text{RCOOH}$ ,  $\text{HNCO}$ ,  $\text{HSCN}$ ,  $\text{H}_2\text{O}$ ,  $\text{H}_2\text{S}$  and  $\text{H}_2\text{Se}$ , monocarboxylic acid and salts of secondary amines. On the other hand, the amino component could be:  $\text{NH}_3$ , primary or secondary amines, hydrazines, hydroxylamines and their derivatives.<sup>150</sup>

The Ugi-4CR is exothermic and is usually carried out at room or lower temperature, since the increase of that, can induce collateral reactions. High concentration of the reactants favors the speed. However, kinetics of Mumm rearrangement is of 1st order (intramolecular process, not influenced by concentration) and when there are substituents in the  $\text{C}\alpha$  of the acid and/or of the amine, reaction times close to 24 h or more are needed to achieve high yields. The previous obtention of the imine prevents the occurrence of collateral processes, such as the Passerini

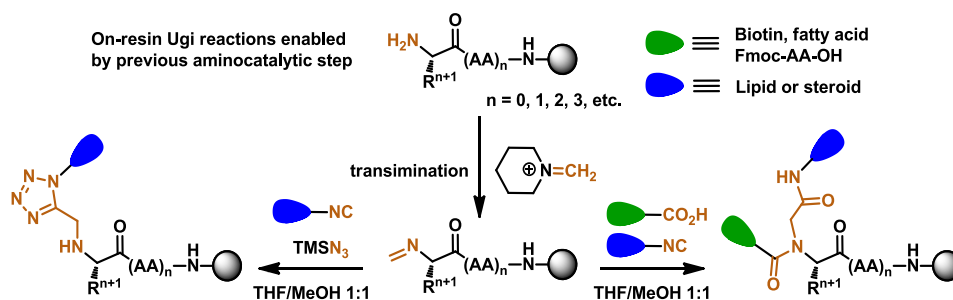
reaction. The Ugi-4CR should be carried out in protic polar solvents such as MeOH or  $\text{CF}_3\text{CH}_2\text{OH}$ , although it has also been reported in THF/MeOH and  $\text{CH}_2\text{Cl}_2/\text{MeOH}$ . This reaction can be catalyzed by Lewis acids such as  $\text{TiCl}_4$  and  $\text{ZnCl}_2$  and is not stereoselective.<sup>151</sup> The Ugi reaction has been implemented in solid phase with simple substrates, for which resins have been functionalized as isocyanide (Scheme 7a),<sup>152</sup> amino (Scheme 7b and 8c)<sup>153</sup> or as carboxylic acid.<sup>154</sup> The yield in most of these cases is good (80-90%) and hydantoin-4-imides (Scheme 7b), 1,4-benzodiazepines-2,5-diones, diketopiperazines, cetopiperazines and dihydroquinoxalinones have been obtained.<sup>155</sup> However, the solid phase Ugi-4CR takes 24 h or several days to complete. Nielsen et al. demonstrated that the speed of these reactions in solid phase can be increased by irradiation with microwaves during 5 min with 60W of power (Scheme 7c).<sup>156</sup>



Scheme 7: Examples of Ugi-4CRs performed in solid phase.

### 2.3.2 Organocatalysis and Ugi reactions in solid phase.

Organocatalysis is the use of small organic molecules as catalysts. This method makes synthesis processes much more efficient.<sup>157</sup> Recently, Morales et al. used an organocatalytic process of solid phase transimination between piperidine and paraformaldehyde to guarantee the previous formation of methylenimines in peptides anchored to resins with the unprotected amino terminal. The preformed imines reacted easily with carboxylic acids and isocyanides by the Ugi-4CR, forming the corresponding *N*-substituted peptides (Scheme 8).<sup>146</sup>



Scheme 8: Synthesis of *N*-substituted peptides by Ugi-4CR in solid phase.

## 2.4 Amide bonds and turn motifs in proteins. Importance of Gly and Pro residues.

Amide bonds have a significant delocalization of the lone pair of electrons on the nitrogen atom, which gives the group a partial double bond character. The partial double bond renders the amide group planar, occurring in either the *s-cis* or *s-trans* isomers. In the unfolded state of proteins, the peptide groups are free to isomerize and adopt both isomers; however, in the folded state, only a single isomer is adopted at each position (with rare exceptions). The *s-trans* form is overwhelmingly preferred in most peptide bonds (roughly 1000:1 ratio in *s-trans*:*s-cis* populations). However, X-Pro peptide groups tend to have a roughly 30:1 ratio, presumably because the symmetry between the C $\alpha$  and C $\delta$  atoms of Pro, makes the *s-cis* and *s-trans* isomers nearly equal in energy (Figure 43).<sup>158</sup>

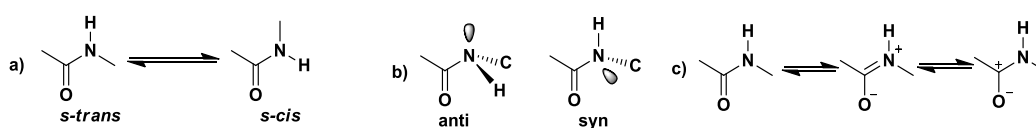


Figure 43: a) Representation of *s-cis*/*s-trans* isomers of a secondary amide bond. b) alternative transition state configurations for peptide bond rotation. c) canonical structures of the amide group structure.

Gly and Pro residues have a major influence on the kinetics of loop formation in proteins. Glycine and proline residues are frequently found in the turn, loop structures of proteins, and are believed to play an important role during early chain folding.

Krieger et al., with the aim of triplet-triplet energy transfer (TTET) from xanthone (Xan) to naphthylalanine (NAla), measured directly the kinetics of intrachain contact formation in polypeptide chains to demonstrate the importance of Gly and Pro residues in loop formation (Scheme 9). TTET from a triplet donor to a triplet acceptor group involves the transfer of two electrons (Dexter mechanism) and it requires van der Waals interactions between the two groups.<sup>159</sup>

In the Loops of varying length are used to assess the distance dependence of the effect exerted by a single Gly, *cis-Pro*, or *trans-Pro* residue. Loop formation is significantly slower around *trans-prolyl* peptide bonds and faster around Gly residues, compared to any other amino acid. Gly showed faster rate constants for contact formation than any other amino acid as expected from the increased backbone flexibility due to the lack of a C $\alpha$  lateral chain.<sup>159</sup>

Table 7 the rate constants for end-to-end contact formation are shown, measured by TTET from xanthone (Xan) to 1-naphthyl alanine (NAla) in host guest peptides of the sequence Xan-Ser-Xaa-Ser-NAla-Ser-Gly with varying guest amino acid (Xaa).

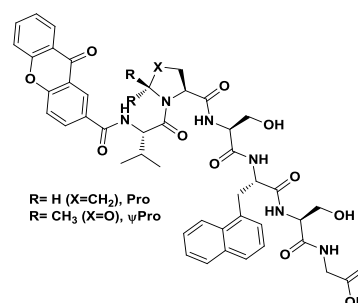
Loops of varying length are used to assess the distance dependence of the effect exerted by a single Gly, *cis-Pro*, or *trans-Pro* residue. Loop formation is significantly slower around *trans-*



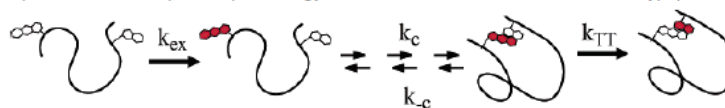
prolyl peptide bonds and faster around Gly residues, compared to any other amino acid. Gly showed faster rate constants for contact formation than any other amino acid as expected from the increased backbone flexibility due to the lack of a C $\alpha$  lateral chain.<sup>159</sup>

Table 7: Effect of different amino acids on local peptide dynamic

Xaa	$k_c$ ( $10^7$ s <sup>-1</sup> )	sequence	% <i>cis</i>
Gly	12 $\pm$ 1	SP	15 $\pm$ 1
Ala	8.0 $\pm$ 0.7	SPS	17 $\pm$ 2
Ser	6.7 $\pm$ 0.7	SSS	-
Glu	5.4 $\pm$ 0.2	SGS	-
Arg	5.5 $\pm$ 0.7	VPS	16 $\pm$ 2
His	4.9 $\pm$ 0.4	V( $\Psi$ P)S	72 $\pm$ 5
Ile	4.4 $\pm$ 0.3	SSPS	18 $\pm$ 4
<i>Trans</i> Pro	2.0 $\pm$ 0.3	SVPS	18 $\pm$ 2
<i>Cis</i> Pro	25 $\pm$ 5	SV( $\Psi$ P)S	78 $\pm$ 6



Scheme 1. Schematic Representation of Triplet-Triplet Energy Transfer Measurements in Unfolded Polypeptide Chains



Scheme 9: Schematic representation of Triplet-Triplet energy transfer measurement in unfolded polypeptide chain. a) Loop sequence, X, between the labels for TTET in peptides of the canonical sequence Xan-X-NAla-Ser-Gly.

The presence of a Pro residue leads to a more complex dynamic, with a slow and a very fast process of contact formation. The most interesting effect is observed for loop formation around *cis*-prolyl bonds ( $\psi$ Pro), which shows the fastest kinetics of all sequences despite an increased activation energy. Pseudo-proline ( $\psi$ Pro) is known to increase the *cis* content of a Val-Pro peptide bond to about 80% due to steric effects induced by the methyl groups in the *s-trans* conformation (Loops of varying length are used to assess the distance dependence of the effect exerted by a single Gly, *cis*-Pro, or *trans*-Pro residue. Loop formation is significantly slower around *trans*-prolyl peptide bonds and faster around Gly residues, compared to any other amino acid. Gly showed faster rate constants for contact formation than any other amino acid as expected from the increased backbone flexibility due to the lack of a C $\alpha$  lateral chain.<sup>159</sup>

Table 7). The fast loop formation around *cis*-prolyl isomers is due to the largely restricted conformational space and shorter end-to-end distances, compared to *trans* isomers, which results in a drastic increase of pre-exponential factor for loop formation. Further results showed that Gly and Pro residues only influence formation of short loops containing between 2 and 10 residues, the typical loop size in native proteins. The rate constants for formation of these loops during protein folding can be modulated by a factor of 10 by the presence of either Gly/*cis*-Pro or *trans*-Pro.<sup>159</sup>

Finally, in randomized Pro containing peptides, an equilibrium between *trans* and *cis*-prolyl conformation is normally present (Studies on model peptides showed that the *cis* content depends on the preceding aminoacid and varies between 7% and 38%, in contrast to about 0.15%-0.5% *cis* isomer at nonprolyl peptide bonds (Loops of varying length are used to assess the distance dependence of the effect exerted by a single Gly, *cis-Pro*, or *trans-Pro* residue. Loop formation is significantly slower around *trans-prolyl* peptide bonds and faster around Gly residues, compared to any other aminoacid. Gly showed faster rate constants for contact formation than any other aminoacid as expected from the increased backbone flexibility due to the lack of a C $\alpha$  lateral chain.<sup>159</sup>

Table 7).<sup>159</sup>

If *cis-Pro* has tendency to form loop quickly, the result is a displacement of the equilibrium to the formation of more *cis* conformer and this is the cause of loop, hairpin or any other twisted secondary structure induction in peptides and proteins by Pro.

#### 2.4.1 Melittin, the honeybee venom peptide. Secondary structure.

Melittin is the main component (40–60% of the dry weight) and the major pain producing substance of honeybee (*Apis mellifera*) venom. Melittin is a basic peptide consisting of 26 aminoacids, with no disulfide bridge.<sup>34</sup> The *N*-terminal part of the molecule is predominantly hydrophobic, while *C*-terminal part is hydrophilic and strongly basic (Table 8 and Figure 44b). In water, it exists in form of tetramer but monomers also can spontaneously auto-aggregate into cell membranes. The peptide is certainly helical, with a bend induced by a Pro residue (or GLP residues, Figure 44). This conformation is fundamental for the mechanism of membrane insertion as well as the conformation(s) involved in the process.<sup>160</sup>

As we can see in the wheel projection of melittin (and the independent parts of sequence that form  $\alpha$ -helix), this peptide does not have a common/perfect amphipathic helicity (Figure 44a). Helix 2 has two Arg and two Lys distributed over the wheel and helix 1 has only one positive charged Lys residue and is fundamentally hydrophobic. Residues KRKR in helix 2 are joined in the *C*-terminal, like in model penetrating peptides and the helix one could be responsible for the interaction with the phospholipid in the membrane.

Table 8: Helical parameters for two independent helices and a possible total helix of melittin.

<http://heliquest.ipmc.cnrs.fr/cgi-bin/ComputParams.py><sup>97</sup>

	Helix sequence	Hydrophobicity	Hyd.Moment	z	FreqNoPolar	Val_angleM
Helix 1	GIGAVLKVLTTGL	0.68000	0.48857	1	0.545	4.93691
Helix 2	PALISWIKRKRQQ	0.28167	0.35356	4	0.417	4.42248
Melittin	GIGAVLKVLTTGLPALISWIKRKRQQ	0.51077	0.39424	5	0.500	4.85721

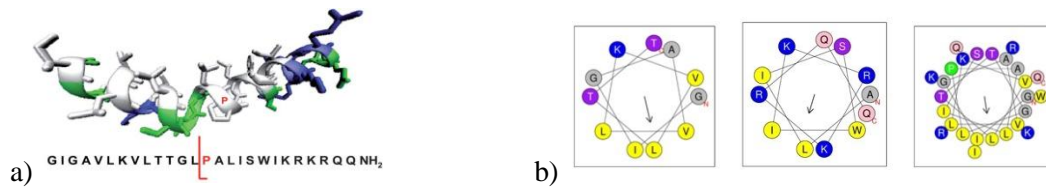


Figure 44: a) Monomer of melittin, cut from the tetrameric crystal structure. Polar aminoacids are shown in green, aliphatic in white and basic in blue. b) Wheel projection of the two independent helices (helix 1 and 2) and a possible total helix of melittin.

### 2.4.2 The helix-Gly-Gly-helix motif in the *N*-terminal domain of histone H1e.

The linker histone H1e has a central role in stabilizing both the nucleosome and chromatin higherorder structure. It has also been described as a general transcriptional repressor because it contributes to chromatin condensation, which limits the access of the transcriptional machinery to DNA. However, recent studies show that linker histones participate in complexes that can either activate or repress specific genes.<sup>161</sup>

H1e histones have a characteristic three-domain structure. The central globular domain consists of a three-helix bundle with a  $\beta$ -hairpin at the *C*-terminus (Figure 45a). The *N*-terminus and the *C*-terminus are highly basic. The terminal domains are, in general, unstructured in solution. The *N*-terminal domains of H1e histones have two distinct subregions. The distal part is rich in Ala and Pro and is highly hydrophobic, whereas the adjacent region to the globular domain is highly basic and may be involved in the location and anchoring of the globular domain (Table 9 and Figure 45b).<sup>162</sup>

Table 9: Helical parameters for two independent helices and a possible total helix of the *N*-terminal domain of histone H1e. <http://heliquest.ipmc.cnrs.fr/cgi-bin/ComputParams.py><sup>97</sup>

	helix	Hydrophobicity	Hyd.Moment	z	Freq. Polar	Val_angleM
Distal helix	EKTPVKKKARKAA	-0.26692	0.17970	5	0.615	5.68730
Adjacent helix	GGAKRKTSG	-0.27333	0.13588	3	0.889	2.48578
<i>N</i> -terminal	EKTPVKKKARKAAGGAKRKTSG	-0.26955	0.15145	8	0.727	5.43221

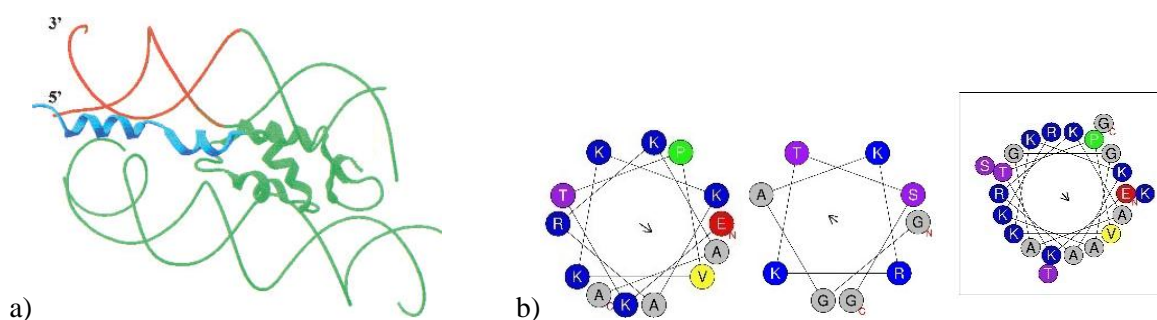


Figure 45: a) Model of the binding of the *N*-terminal domain of histone H1e to the nucleosome. Representation of the *N*-terminal domain bound to chromatosomal and linker DNA. The chromatosomal

DNA is in green, the linker DNA is in red, the histone H1e *N*-terminal domain is in blue, and the globular domain is in green. The globular domain is located according to the model of Zhou et al. (1998). b) Wheel projections of the two independent helices (distal and 2) and a possible total helix of histone H1e.

The conformational properties of the peptide NE-1 (Histone H1e *N*-terminal fragment, residues 15–36, positively charged region of the *N*-terminal domain)(Ac-EKTPVKKKARKAAGGAKRKTSG-NH<sub>2</sub>) have been studied by circular dichroism and <sup>1</sup>H-NMR. NE-1 is mainly unstructured in aqueous solution, but in the presence of the secondary-structure stabilizer TFE, it acquires two fragments of  $\alpha$ -helical structure that comprise almost all the peptide, namely, from Thr17 to Ala27 and from Gly29 to Thr34 (Table 9 and Figure 45b). Both helical regions are highly amphipathic, with the basic residues on one face of the helix and the apolar ones on the other. The two helical elements are separated by a Gly–Gly motif. Gly–Gly motifs at equivalent positions are found in many vertebrate H1e subtypes. Structure calculations show that the Gly–Gly motif behaves as a flexible linker between the helical regions (Table 9 and Figure 45b). The wide range of relative orientations of the helical axes allowed by the Gly–Gly motif may facilitate the tracking of the phosphate backbone by the helical elements or the simultaneous binding of two nonconsecutive DNA segments in chromatin.<sup>163</sup>

A Gly–Gly motif is also found in the porins of *Escherichia coli* and other bacterial species.<sup>164</sup> The motif confers flexibility to the third loop of the protein, which appears to have functional implications.<sup>165</sup> Another example of structural flexibility associated with a Gly sequence is calmodulin-related TCH<sub>2</sub> protein from *Arabidopsis*. The overall structure consists of two globular domains separated by a flexible linker region that contains a (Gly)<sub>4</sub> motif.<sup>166</sup>

### 3 Results and Discussion. Chapter 2

#### 3.1 Antifungal activity of preliminary lipidated analogues of Cm-p5. Work methodology.

It is known that the lipidation of AMPs slightly increases the biological activity and it is common to find natural antimicrobial peptides containing lipid chains (Polymyxin B, Actinonin, Surfactin). These natural peptides are usually cyclic and it is apparent the conformational restriction of the lipid chain in one side of the cyclic structure, which perhaps favors the interaction with biological membranes. In general, the presence of hydrophobic aminoacids and lipids in natural peptides has the fundamental objective of increasing the amphiphilicity and hydrophobicity, which allows either to penetrate cell membranes more easily or to interact with other biological targets of the same nature.<sup>167</sup>

Cm-p5 is a linear peptide, without any conformational restriction and perhaps capable of adopt several secondary structures during its action mechanism. However, the  $\alpha$ -helical structure could be responsible for the interaction with the negative membranes of fungus and is probable that any alteration of this rearrangement, also limits the biological activity. Without  $\alpha$ -helix, the linear peptide loses the preferred orientation of the lateral chain of aminoacids unless a  $\beta$ -turn or another secondary structure could support the activity.

In 2015, we synthesized five lipidated analogues of Cm-p5 applying a new methodology of Ugi-4CR in solid phase (Figure 46). The biological activity results of this analogues indicated that the introduction of *N*-substitutions with lipids at intermediate positions decreased the antifungal activity. However, by lipidation of the *N* or *C*-terminus using the Ugi-4CR, the activity was not affected (lipidation at *C*-terminal) or was improved (lipidation at *N*-terminal). The chemical derivatives FMV02421 and FMV0451 lipidated at the *N*-terminal of the Cm-p5 peptide showed MICs close to or lower than the parental peptide against different strains of the pathogenic yeast *Candida albicans*, which showed that the modifications have a positive effect on the antifungal activity of these peptides. The analogue FMV0451 (MIC= 1.83  $\mu\text{mol/L}$ ), more active than the Cm-p5 (MIC= 6.75  $\mu\text{mol/L}$ ) (Table 10), was obtained by lipidation at the *N*-terminal using acetic acid as acid component of the Ugi reaction, paraformaldehyde and *n*-dodecylisocyanide.<sup>168</sup>

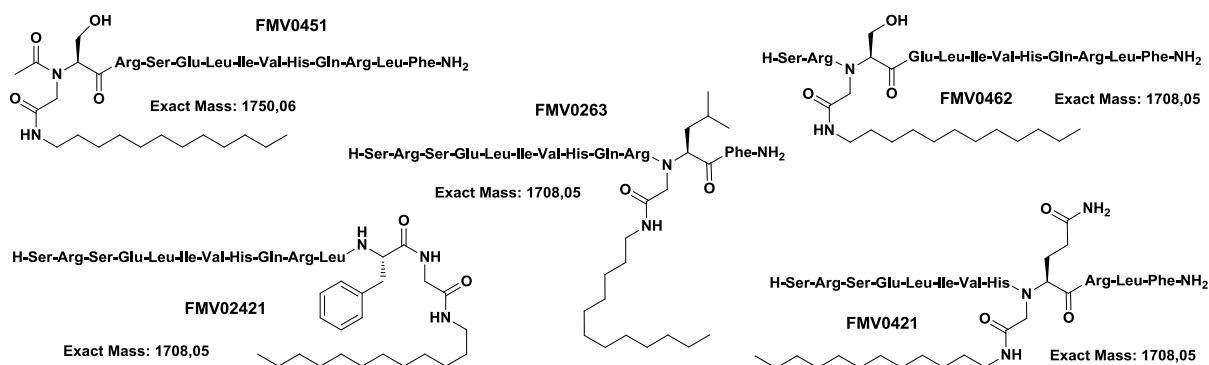


Figure 46: Lipitated analogues of Cm-p5.

Table 10: Antifungal activity of the lipitated analogues of Cm-p5.

	MIC ( $\mu\text{g/mL}$ )		
	<i>C. albicans</i>	<i>C. parapsilosis</i>	<i>T. reesei</i>
FMV02421	12,5	50	50
FMV0243	> 100	> 100	50
FMV0421	50	> 100	50
FMV0451	3,125	> 100	50
FMV0462	> 100	> 100	> 100
Anfo B	0,25	0,25	0,125

Sa: *Staphylococcus aureus*, Ec: *Escherichia coli*, Ca: *Candida albicans*, Cp: *Candida parapsilosis*, Tr: *Trichophyton rubrum*, NT: Non tested.

*N*-substitutions of amide bonds, similar to Pro residues, impose a restricted *s-cis* conformation around the amide bond. The intermediate *N*-alkylations interrupt the  $\alpha$ -helical backbone, favoring the *s-cis* conformation of the implicated amide bond and should be directly related with the loss of activity because the peptide loses the capacity of acquiring helicoidal character during the interaction with membranes. The losses of helicoidal character destroys the amphipathicity by dispersion of the polar or apolar residues, unless an amphipathic  $\beta$ -turn structure will be formed, which is not apparently the present case.

The Ugi-4CR allows generating *N*-substituted peptides in one-step, however, compared to the lipidation method by simple coupling of fatty acids, is experimentally more complex. For this reason, it is important to determine if coupling a fatty acid with similar chain size as the one obtained by *N*-terminal lipidation by Ugi-4CR with *n*-dodecylisonitrile produces the same biological effect. Furthermore, Cm-p5 interacts with the membrane of microorganisms either to destabilize it or to penetrate the cell. The increase in activity by lipid binding to the *N*-terminus may be due to a stronger interaction with membranes and is necessary to evaluate the effect of a larger carbon chain, more similar to the phospholipids present in membranes.

The Ugi motifs produced, when formaldehyde and acetic acid are used, have similar structure to sarcosine (*N*-methylglycine), the simplest peptoid monomer. Both cases lack the structural restrictions on backbone angles present in the cyclic Pro residue. Sarcosine scanning, similar to Ala scanning, is the usual method employed to determine the conformational influence of this residue in all the amino acid position of a biologically active peptide. On the other hand, Gly, Ala or Pro residues are in the extremes of amide bond possible conformations. Pro, for example, favors the formations of *s-cis* amide bond, Ala the *s-trans* and Gly does not have preference and, remarkably, has the largest conformational freedom due to the lack of a lateral chain (Figure 47).

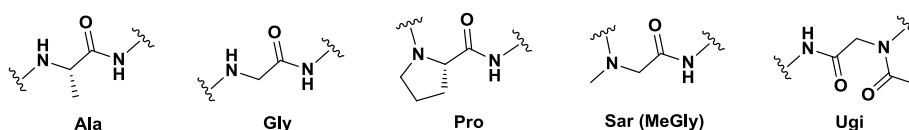


Figure 47: Structural comparison of Ala, Gly, Pro, Sar and the products of Ugi residues.

Considering that the lipid motif produced by coupling of fatty acids does not have the conformational behavior produced by the Ugi-4CR, we need to study the influence of the lipidic chain related conformation in the activity. With this aim, we pretend to compare the influence of Ala, Gly or Pro residues, positioned between the lipid and the *N*-terminal of Cm-p5, in the antifungal activity.

In chapter 1, it is shown that replacing the His and Glu residues of the Cm-p5 sequence, eliminates completely the antifungal activity. In contrast, substitution of Glu and His by Cys and subsequent cyclization produces an analogue that showed a notable increased antifungal activity. To produce a final pharmacological candidate of Cm-p5, is desired the combination of this covalent modification: the introduction of lipid at the *N*-terminal by Ugi reaction with the same study of the influence of Ala, Gly or Pro residues between the lipid and the terminal Ser. If the effects of disulfide bridge cyclization and lipidation by Ugi-4CR in fungistatic character are additive, a cyclic derivative, also lipidated by Ugi-4CR could be the most active version of Cm-p5 obtained until today.

The experimental design of this research has as objective to use a minimum number of variables that allow establishing generalizable conclusions about the influence of different ways of joining the lipids in the *N*-terminal of Cm-p5 or the cyclic versions in the biological activity. For the development of this research, it was necessary to divide the work in four fundamental parts:

- ✓ *N*-terminal lipidation of Cm-p5 with saturated fatty acids of different chain sizes to determine the optimal lipid chain for antifungal activity.
- ✓ The lipidation of Cm-p5 after coupling Ala, Gly or Pro at the *N*-terminal to evaluate the conformational effects of these aminoacids in the biological activity.
- ✓ The lipidation of CysCysCm-p5 after coupling Ala, Gly or Pro at the *N*-terminal and subsequent cyclization to evaluate the conformational effects of these aminoacids in the activity of helical stabilized and lipidated analogues of Cm-p5.
- ✓ The synthesis of n-dodecylisocyanide by formylation and dehydration of commercial n-dodecylamine for using it in the modification of CysCysCm-p5 by Ugi-4CR.
- ✓ The lipidation of CysCysCm-p5 by Ugi-4CR with n-dodecylisocyanide, paraformaldehyde and acetic acid and subsequent cyclization to evaluate the conformational effects of these aminoacids in helical stabilized and lipidated analogues of Cm-p5.

The results obtained in each stage of the experimental work are described below and follow the methodology of peptide characterization described in the section 3.1 of Chapter 1. The n-dodecylisocyanide was characterized by FT-IR and NMR. The molecules synthesized in solid phase were characterized by analytical RP-HPLC and ESI-HRMS and purified by preparative RP-HPLC.

### **3.2 Synthesis of lipopeptides analogues of Cm-p5 by coupling of fatty acids.**

The synthesis of Cm-p5 lipopeptides by coupling of fatty acids at the *N*-terminus was carried out in order to determine the importance of the size of the lipid carbonated chain and the structural binding motif in the biological activity (Figure 48). It is also important to determine if the coupling of a fatty acid with the same chain size as that obtained by lipidation of the *N*-terminal by Ugi with n-dodecylisocyanide gives the same biological effect with a simpler procedure.

The binding of a 15-carbon lipid chain (pentadecanoic acid) to the *N*-terminus, produce a similar analogue to the one obtained by Ugi-4CR using n-dodecylisocyanide. On the other hand, by union of capric acid to the *N*-terminal we could evaluate the biological effect of the insertion of this minor carbon chain, both in the antifungal action and in the hemolytic character of Cm-p5 (Figure 48).





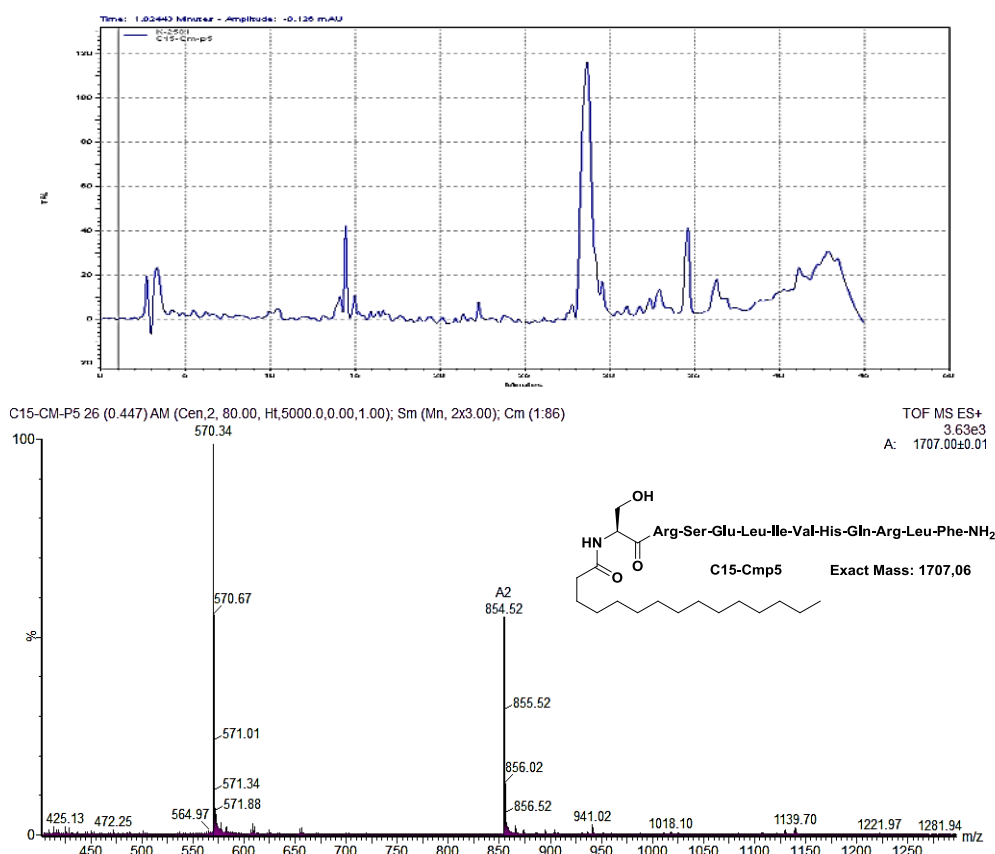


Figure 50: RP-HPLC (upper panel) and ESI-HRMS (lower panel) of C15-Cm-p5.

The antifungal activity of C10-Cm-p5 and C15-Cm-p5 was evaluated (Table 11). It was found that the introduction of a small lipid chain does not modify the activity of Cm-p5. On the other hand, the coupling of pentadecanoic acid decrease the activity; therefore, the size of the lipid chain is not the only determining factor in the activity, taking into account that FMV0451 and C15-Cm-p5 have the same size of the lipid chain.

Table 11: Antifungal activity of decanoil and pentadecanoil lipidated analogues of Cm-p5.

	MIC (ug/mL)		
	<i>C. albicans</i>	<i>C. parapsilosis</i>	<i>C. krusei</i>
<b>C10-Cm-p5</b>	10	10	10
<b>C15-Cm-p5</b>	> 20	> 20	> 20
<b>Anfo B</b>	0,5	0,5	> 16
<b>Cm-p5</b>	10	10	-

The fundamental difference between C15-Cm-p5 and FMV0451 is the structural motif that produces the Ugi-4CR, an *N*-substitution that can alter the conformational balance of the lipid chain attached to the *N*-terminus. It is possible that this *N*-substitution have a similar behavior that Pro or sarcosine in peptides, favoring a rigid *s-cis* conformation of the amide bond.

### 3.3 Synthesis of lipopeptides analogues of Cm-p5 by coupling of decanoic acid after Ala, Gly or Pro.

In natural lipidated AMPs, it is common to find a lipid anchored to cyclic rigid structures that restrict the conformational behavior. A similar effect of restricted conformation could be present in FMV0451 due to the *N*-substitution (that is not present in C15-Cm-p5).

A good approach to discover the influence of the lipid chain conformation in the activity of Cm-p5, using the tools of peptide chemistry, may be the synthesis of lipidated analogues containing Ala, Gly or Pro between the lipid chain and the peptide *N*-terminal (Figure 51). Pro should mimic the best the Ugi motif and Gly should permit total free rotation of lipid chain. Ala, on the other hand, is totally opposed to the Ugi motif, favoring rigid *s-trans* conformation and could be used as control.

Considering the new amino acid residue introduced, the use of decanoic acid reach only two carbon less than the Ugi product with *n*-dodecylisocyanide. Although it provides a smaller chain, we prefer to continue using decanoic acid to avoid the possibility of increased hemolysis, as it has been reported for many lipopeptides.<sup>169</sup>

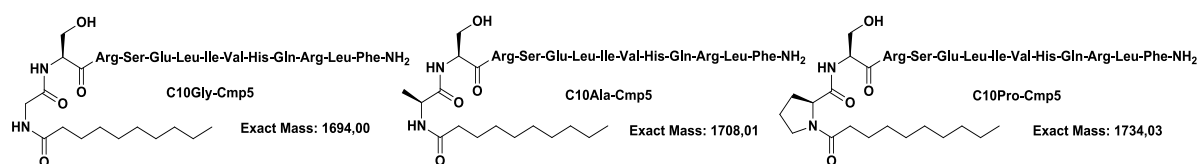


Figure 51: Lipidated analogues of Cm-p5 containing Ala, Gly or Pro.

To synthesize these compounds, the sequence of the dodecapeptide Cm-p5 is completed and Ala, Gly or Pro is finally coupled, on the MBHA derivatized resin with the linker Am (Rink). Subsequently, commercial decanoic acids are bound to the deprotected *N*-terminal using DIC/Oxyma (Section 4.1.2, Chapter 1). After the appropriate treatment, the lipopeptides are cleaved (Section 4.1.3, Chapter 1) and the analytical determination by RP-HPLC showed 72% peptidic purity,  $t_R = 21.5$  min for C10G-Cm-p5 (Figure 52), 75% peptidic purity,  $t_R = 26$  min for C10A-Cm-p5 (Figure 53) and 70% peptidic purity,  $t_R = 27$  min for C10P-Cm-p5 (Figure 54). The ESI-HRMS verifies the identity of the synthesized peptide after collection of the fraction corresponding to the aforementioned peak. These three new Cm-p5 analogues were purified and submitted to biological activity evaluation.

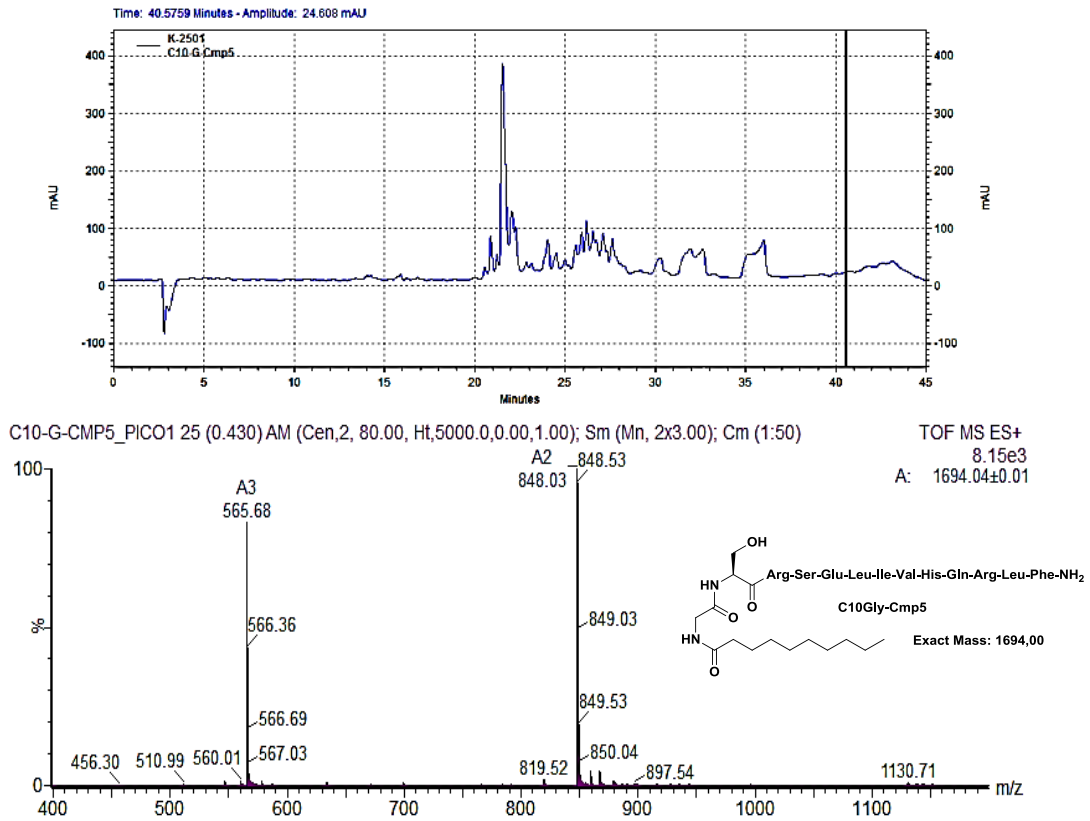


Figure 52: RP-HPLC (upper panel) and ESI-HRMS (lower panel) of C10G-Cm-p5.

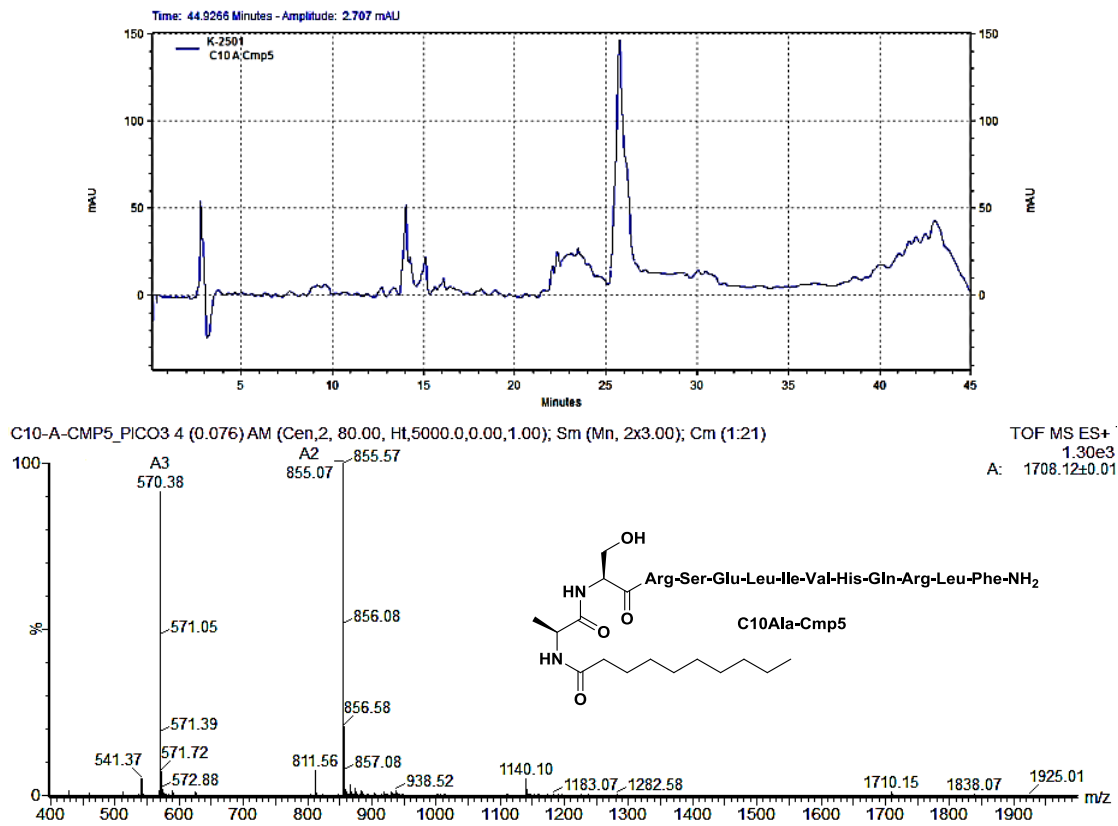


Figure 53: RP-HPLC (upper panel) and ESI-HRMS (lower panel) of C10A-Cm-p5.



The *s-cis* conformation is preferred in the C10P-Cm-p5 because the rotational barrier from *s-trans* to *s-cis* isomers is lower than in the case of C10A-Cm-p5 and the process is spontaneous. The *s-cis* conformer is favored thermodynamically and kinetically, reaching the equilibrium at a 29.9:1 ratio of *s-cis*:*s-trans*. This analogue is the most structurally similar to FMV0451 obtained by Ugi reaction and the lipid chain may have the same preference for the *s-cis* form. Rotation about the C $\alpha$  of Ala, Gly or Pro also could influence the lipid chain conformational behavior linked to *N*-terminal of Cm-p5. Newman projections considering only steric effect (nonelectrostatic, dipole moments or hydrogen bonding interactions were taken into account) and that Pro has favored *s-cis* conformation, both Ala *trans* conformation and Gly are showed in Figure 55. Also in that case, Pro orientate *s-cis* the lipid chain with respect to peptide backbone, Ala *s-trans* and Gly permit both conformations.

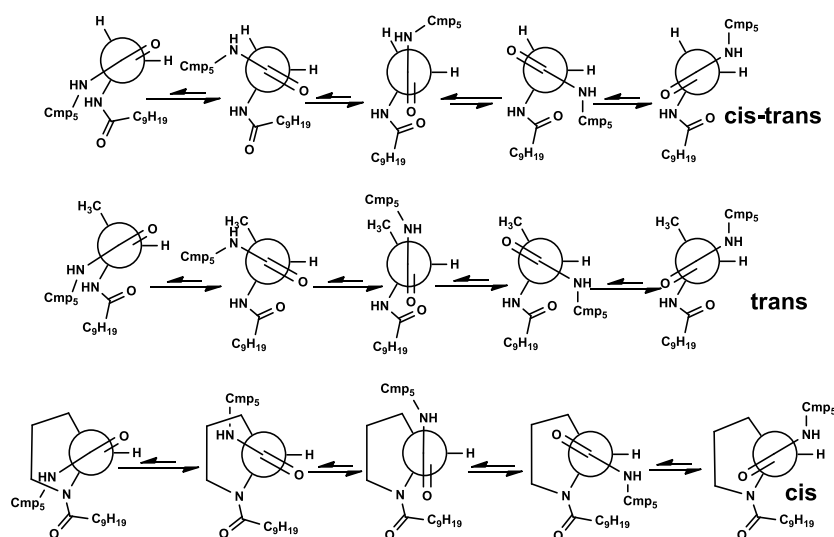


Figure 55: Newman projection about the alpha carbon of C10A-Cm-p5, C10G-Cm-p5 and C10P-Cm-p5.

### 3.4 Synthesis of lipopeptides structurally restricted by disulfide bridge formation.

Taking into account the results of chapter 1, the helical stabilized and cyclic analogue CysCysCm-p5 showed more activity against *Candida albicans*; thus lipidated and cyclic similar structures based on this analogue are desired. The same influence of the conformational effects of Ala, Gly and Pro could be accessed by the synthesis of C10A-CysCysCm-p5, C10G-CysCysCm-p5 and C10P-CysCysCm-p5 (Figure 56), followed by the cyclization and dimerization by disulfide bond. Since antiparallel dimer and cyclic monomer of CysCysCm-p5 were active and the simplest way to obtain both is during the cyclization reaction, we decided to oxidize the thiol groups of C10X-CysCysCm-p5 in similar conditions.



Figure 57: RP-HPLC (upper panel) and ESI-HRMS (lower panel) of C10A-CysCysCm-p5 peptide.

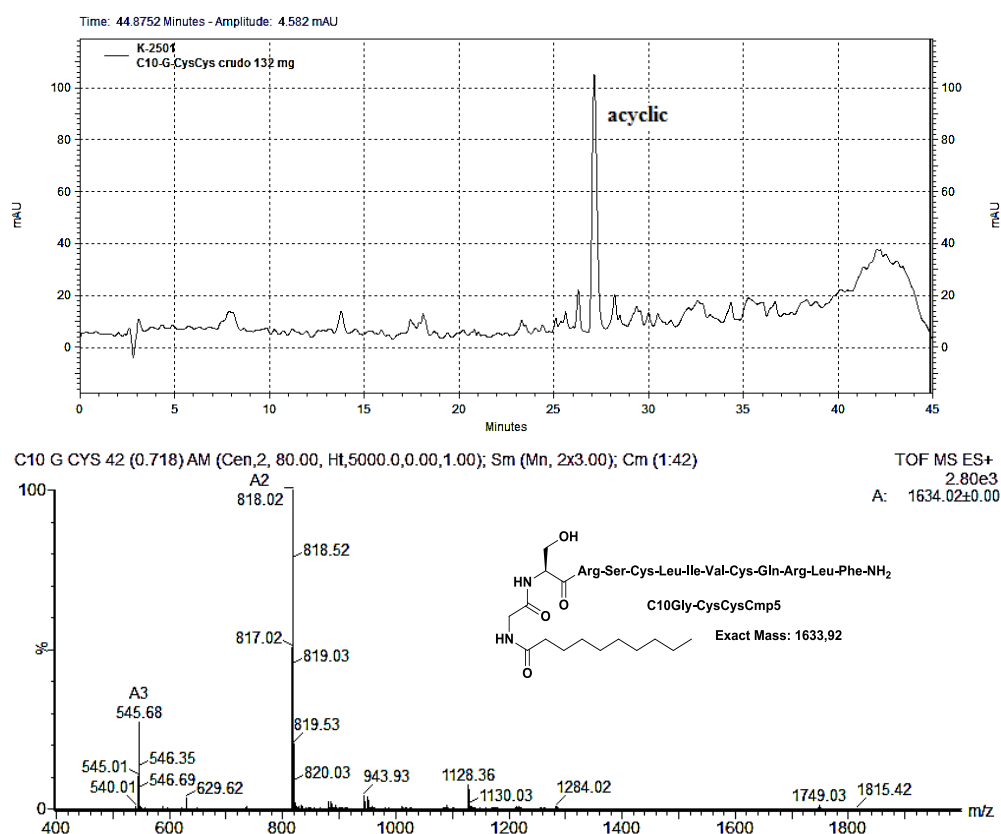


Figure 58: RP-HPLC (upper panel) and ESI-HRMS (lower panel) of C10G-CysCysCm-p5 peptide.

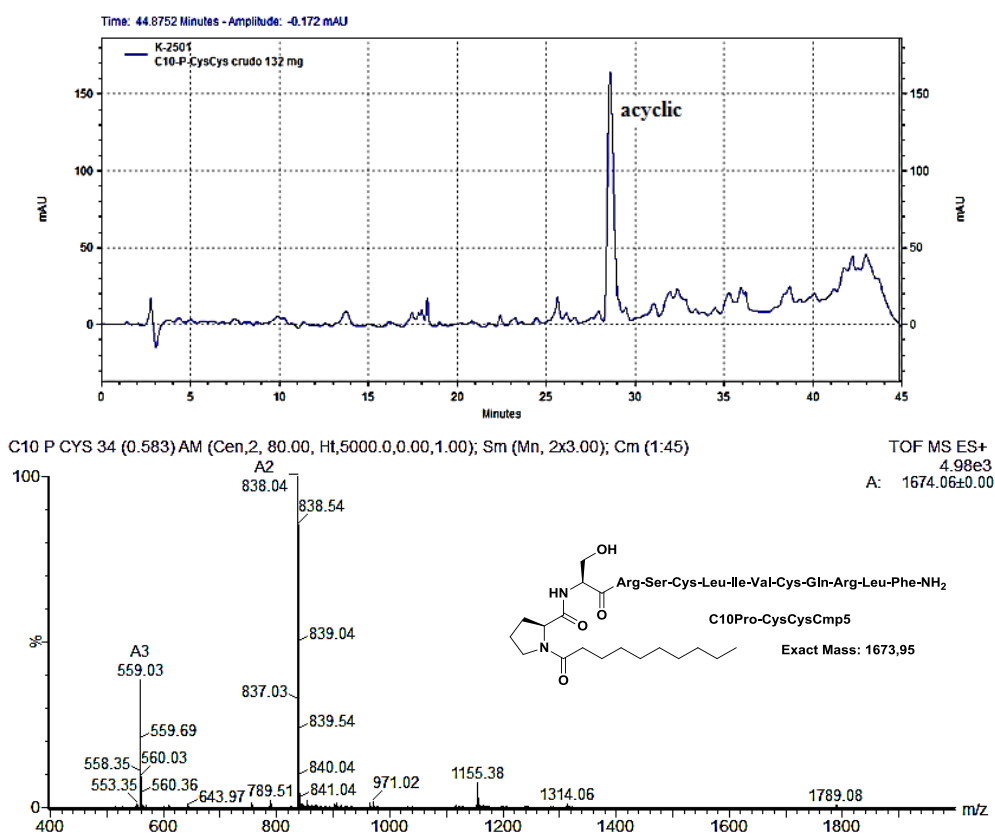
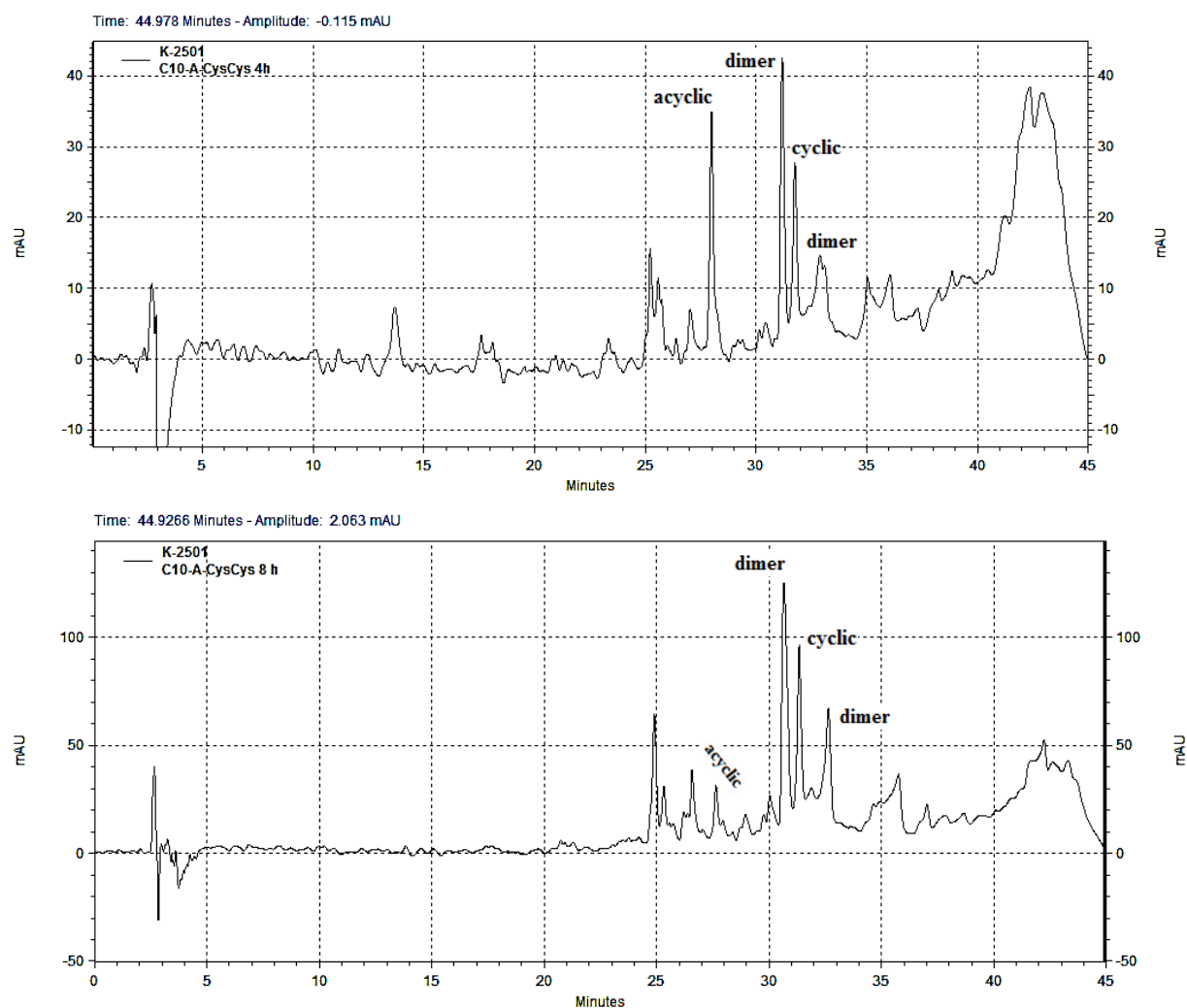




Figure 59: RP-HPLC (upper panel) and ESI-HRMS (lower panel) of C10P-CysCysCm-p5 peptide.

Next, cyclizations (Section 4.1.4, Chapter 1) were carried out in liquid phase and aqueous medium with dioxygen of the air as oxidizing agent in high dilution conditions (0.3 mmol/L). This simple method is sufficient for these molecules due to the simplicity of the process (small peptide chain, formation of a single intramolecular bridge, spatial closeness of the thiol groups to be cycled). The freeze-dried crude of the lipopeptides C10X-CysCysCm-p5 was attempted to dissolve in H<sub>2</sub>O (0.1% TFA)/ACN (3:1) at a concentration of 0.3 mM; however, it was necessary to add 30% of *i*Pr-OH to achieve total solubilization. Then, aqueous ammonia (25%) was added until pH reached 8. The mixture was stirred, while open to air. Completion of the reaction was checked by RP-HPLC until total disappearance of the starting material. The Figure 60, Figure 61, Figure 62 show the chromatographic evolution during 4-8 h of stirring. During this time, a complex mixture of products was formed and the three predominant peaks were analyzed by ESI-HRMS (Experimental Section, Chapter 2).





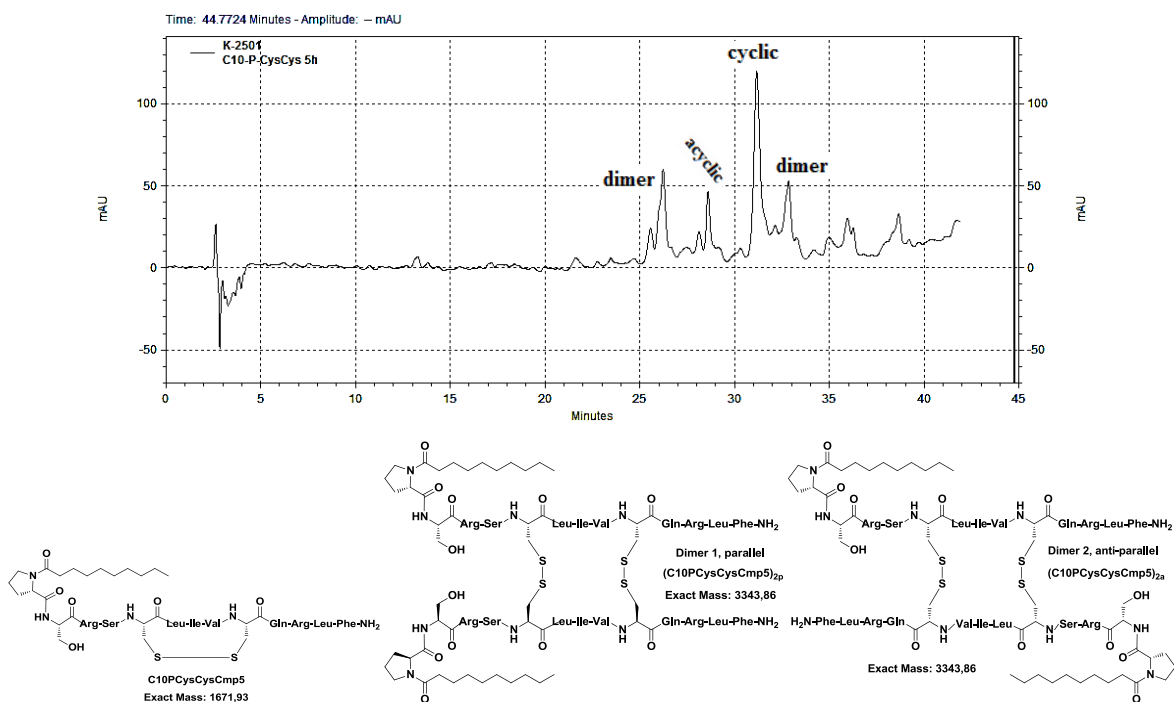


Figure 62: RP-HPLC evolution during oxidation of C10P-CysCysCm-p5 peptide at 0.3 mM after 5h and structure of the dimer and cyclic monomer formed.

The mass of peaks 1 and 3 doubled the mass of the cyclic peptide suggesting that they are dimers. Although it was not proven, like the dimers of CysCysCm-p5 described in chapter one, it is likely that peak 1 is the parallel dimer of the molecule which, being more symmetric, interacts less with the C18 chains of the stationary phase in RP-HPLC and therefore is less retained (smaller  $t_R$ ). Peak 3 should be the antiparallel dimer, but we must confirm these assumptions.

Chromatograms show different behavior for each oxidized analogue. In the case of C10A-CysCysCm-p5 (Figure 60), we can observe the consumption of the acyclic starting material after 8h of reaction and the formation of notable quantities of dimers besides the cyclic product, all of them with different time retention than starting material. For C10G-CysCysCm-p5 (Figure 61) and C10P-CysCysCm-p5 (Figure 62) the behavior was similar, but almost all the product was cyclic, with less amounts of dimeric analogues. As expected, Gly and Pro have similar orientation of the lipid chain, favoring a conformation in which the repulsion between lipids avoid the possibility of intermolecular reactions. On the contrary, Ala imposes conformations of the decanoil moiety opposed to the thiol group during cyclization, permitting the intermolecular contact.

For the preparative RP-HPLC, the peptides were dissolved in pure DMSO due to the high hydrophobicity that they present. Nine dimeric or cyclic lipidated analogues of Cm-p5 were obtained in more than 95% peptidic purity and will be submitted to biological evaluation.

### **3.5 Synthesis and characterization of the n-dodecylisonitrile.**

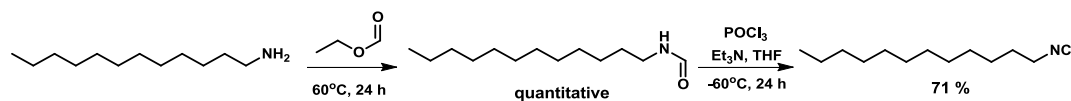
One of the objectives of this work is the synthesis of n-dodecylisonitrile for the subsequent incorporation into the peptide sequence of CysCysCm-p5 by Ugi-4CR in solid phase. The length of the carbon chain was chosen after a previous work, in which one analogue synthesized with this isonitrile showed a moderate increase in the antifungal activity. Although it is not common to find lipopeptides in the nature with very large lipid chains (usually only 8-16 carbon atoms) and it is expected that a very extensive carbon chain increases the hemolytic activity of Cm-p5, only experimental results would corroborate these hypotheses.

Isoyanides can be synthesized by different strategies but the most used is the sequential formylation/dehydration of amines (Scheme 10). The n-dodecylamine is commercial and it can be formulated in several ways. However, due to the high reactivity (nucleophilicity) and low steric hindrance of the amino group, the reflux with ethyl formate guarantees complete conversion to formamide, without using other stronger formylating agents such as mixed formic-acetic anhydride. Experimentally, the amine is dissolved in ethyl formate and heated at 60°C for 12 h. The reaction proceeds quantitatively, which is corroborated by TLC (n-hexane/EtOAc, 1:1). After evaporating the ethyl formate, the solid obtained is used in the next step without further purification.

Dehydration can be performed in several ways; a simple option is the use of POCl<sub>3</sub> in excess of bases. The dried formamide is dissolved in THF and dehydrated with POCl<sub>3</sub> and an excess of Et<sub>3</sub>N. The absence of other functional groups in the lipid chain (alcohols, amides, etc.), sensitive to the strongly dehydrating action of POCl<sub>3</sub>, allows it to be used in this procedure, although the process must be carried out under very mild conditions to avoid the occurrence of collateral reactions. With that purpose, an EtOH/N<sub>2</sub> (l) bath is used to keep the temperature below -60°C, inert N<sub>2</sub> atmosphere and slowly addition of POCl<sub>3</sub> (1M in THF) during 30 min.

The treatment of the reaction before the purification by column is determinant and somewhat cumbersome, but it is essential to do it in this way to obtain as much product as possible. The reaction mixture is concentrated to dryness. Unlike other reported techniques, to eliminate the POCl<sub>3</sub> excess and salts formed, H<sub>2</sub>O or saturated NaHCO<sub>3</sub> should never be added, because of the high capacity of the lipids to form stable emulsions that would prevent the separation of the phases during the following extractions. Instead, the dry reaction crude is extracted with small

portions of n-hexane, which are combined, then concentrated to dryness and finally purified by LCC (hexane/EtOAc, 10:1) yielding 71% of n-dodecylisocyanide.



Scheme 10: Sequential synthesis of the *n*-dodecylisocyanide.

The *n*-dodecylisocyanide was characterized by FT-IR, <sup>1</sup>H-NMR and <sup>13</sup>C-NMR spectroscopic techniques. The Figure 63 shows the FT-IR spectrum with signals on the 2911 and 2847 cm<sup>-1</sup> corresponding to valence vibrations  $\nu_{\text{Csp}^3\text{-H}}$  of methyl groups and methylenes. The signal at 1468 cm<sup>-1</sup> corresponds to the double vibration  $\delta_{\text{asCH}_3} + \delta_{\text{sCH}_2}$  that is associated with the doubling of scissors  $\delta_{\text{sCH}_2}$  and usually appears superimposed with the band  $\delta_{\text{asCH}_3}$  of the methyl group. The rocking band has some diagnostic utility; in this compound, it appears as a weak band at 720 cm<sup>-1</sup> since a carbon chain with 11 consecutive methylene groups occurs. On the other hand, in 2148 cm<sup>-1</sup> a band of average intensity, corresponding to the vibration of stretching of the isocyanide triple bond, that appears between 2100-2200 cm<sup>-1</sup>.<sup>63</sup>

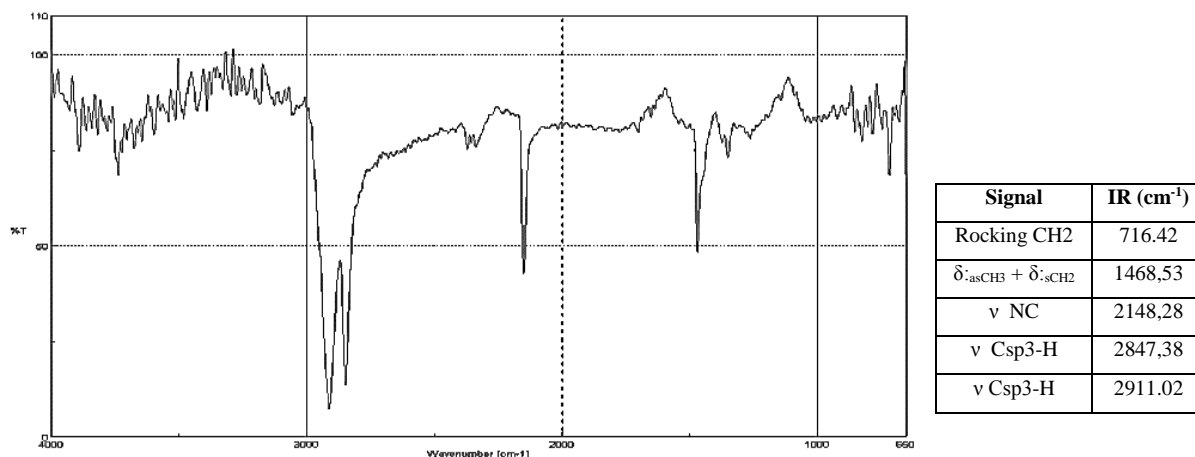


Figure 63: FT-IR spectrum of the *n*-dodecylisocyanide.

The Figure 64 shows the <sup>1</sup>H-NMR spectrum of *n*-dodecylisocyanide where are observed the classic signals of protons linked to sp<sup>3</sup> carbons corresponding to the lipid hydrocarbon chain. The signals of the protons are deshielded as the proximity to the isocyanide group increases, which gives a measure of how the electronegativity of the *N*-sp of the *NC* influences the proton displacements. Therefore, the signal of the methylene directly attached to the isocyanide group appears as a characteristic triplet at 3.37 ppm.

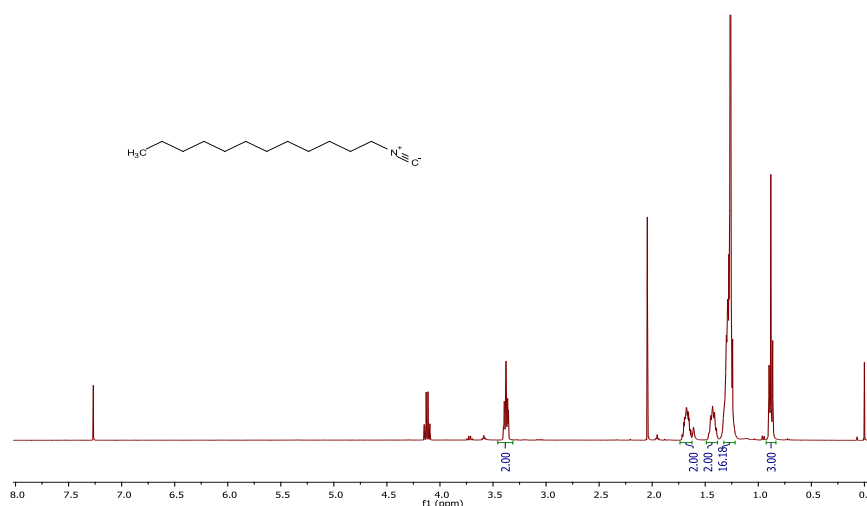


Figure 64:  $^1\text{H}$ -NMR spectra of the n-dodecylisonitrile.

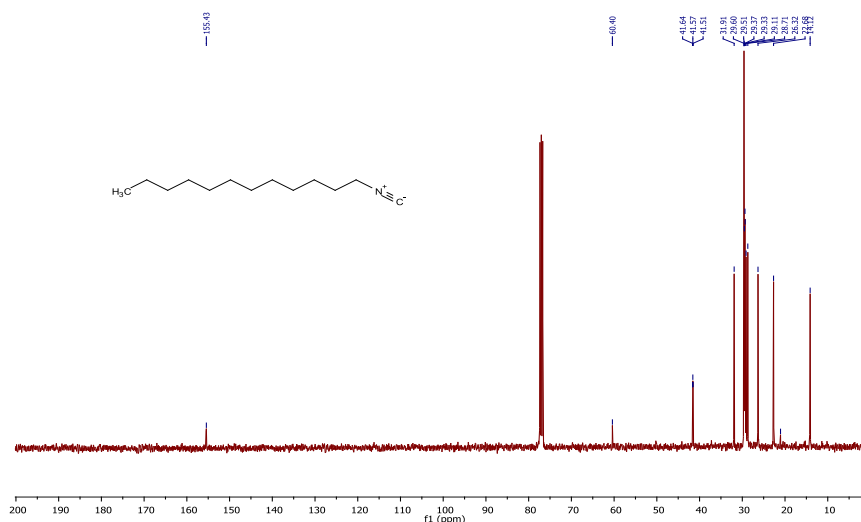


Figure 65:  $^{13}\text{C}$ -NMR spectra of the n-dodecylisonitrile.

The Figure 65, shows the  $^{13}\text{C}$ -NMR spectrum of n-dodecylisonitrile where we can see signals corresponding to the  $C\text{-}sp^3$  of the aliphatic chain, whose displacement is greater as they get closer to the  $\text{NC}$  group. As characteristic signal, the carbon of the highly deshielded isonitrile, is observed at 155 ppm due to the  $sp$  hybridization that presents.

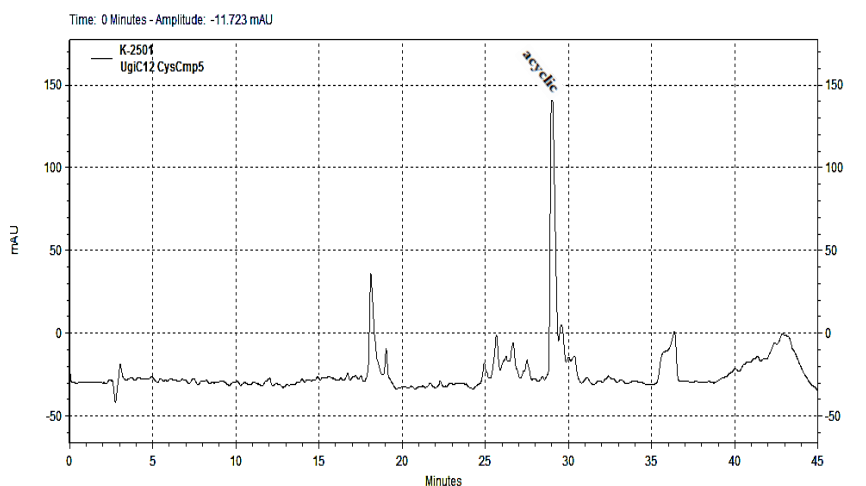
### 3.6 Lipopeptides synthesis by Ugi-4CR in solid phase.

Lipidation of the  $N$ -terminus of Cm-p5 by Ugi-4CR with n-dodecylisonitrile, increases the antifungal activity. Ugi reaction allows generating  $N$ -substituted dipeptides in a single step, however, compared to the lipidation method by simple coupling of fatty acids, this reaction is more complex experimentally and the reactants are more expensive.

The lipid with fifteen carbons did not maintain the activity of Cm-p5, which indicates that not only the size of the lipid chain is determinant. Another factor influences, perhaps similar to what occurs in natural lipopeptides because the main difference of the Ugi product with the pentadecylated analogue is the *N*-substitution that changes the conformational equilibrium of the lipid chain. It is finally necessary, taking into account the result of chapter 1, to test the combination of the covalent modification by cyclization and lipidation at the *N*-terminal by Ugi reaction.

To synthesize this compound the sequence of the dodecapeptide CysCysCm-p5 is completed by successive coupling of the aminoacids Phe, Leu, Arg, Gln, Cys, Val, Ile, Leu, Cys, Ser, Arg and Ser, on the MBHA resin derivatized with the linker Rink and with the use of the Fmoc/tBu methodology (Section 4.1.2, Chapter 1). The Ugi-4CR on the free *N*-terminal of the peptide is then carried out with paraformaldehyde, *n*-dodecylisocyanide and acetic acid, following the previously described procedure.<sup>150</sup>

After 36 h of reaction, the lipidated peptide is cleaved from the resin (Section 4.1.3, Chapter 1) and the analytical determination by RP-HPLC showed 65% peptidic purity and  $t_R = 29$  min. To verify the identity of the synthesized peptide, the fraction corresponding to the aforementioned peak is collected and ESI-HRMS is performed, showing coincidence between the mass observed and the expected mass (Figure 66).







## Conclusions. Chapter 2

- ✓ It is possible to covalently modify the Cm-p5 antifungal peptide by cyclization with disulfide bridges between Cys and *N*-terminal lipidation using multicomponent reactions or peptide coupling.
- ✓ The coupling of decanoic acid or pentadecanoic acid to the *N*-terminus of Cm-p5 made possible to obtain two lipidated analogues efficiently. This modification did not improve the biological activity of Cm-p5.
- ✓ The cyclization of lipidic analogues of CysCysCm-p5 produces more quantities of dimers when it has an alanine residue between the lipid and the peptide and shows a similar behavior for Gly, Pro or the Ugi lipidated versions.
- ✓ The formylation with ethyl formate and dehydration with POCl<sub>3</sub> of n-dodecylamine is an efficient method to obtain n-dodecylisocyanide.
- ✓ By Ugi-4CR using acetic acid, n-octadecylisocyanide and paraformaldehyde on the free *N*-terminus of the CysCysCm-p5 peptide anchored to the solid support, an *N*-substituted analogue and *N*-acetylated lipopeptide was obtained.

## **Future works. Chapter 2**

- ✓ Evaluate the antimicrobial activity of the 15 new analogues of Cm-p5.

## 4 Experimental Section. Chapter 2

### 4.1 General Remarks

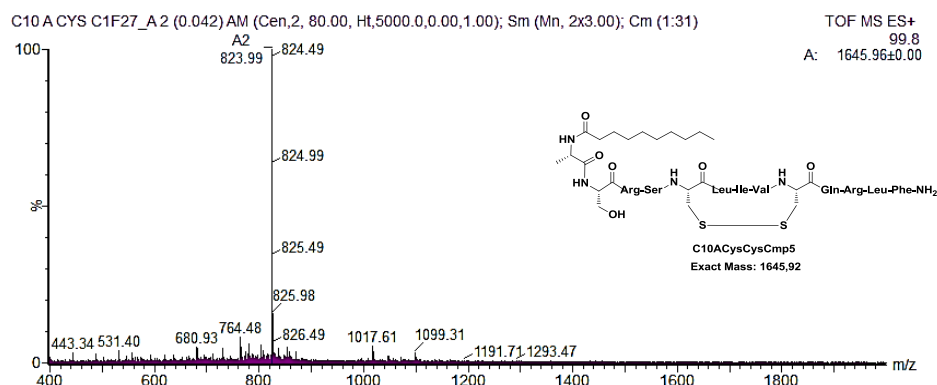
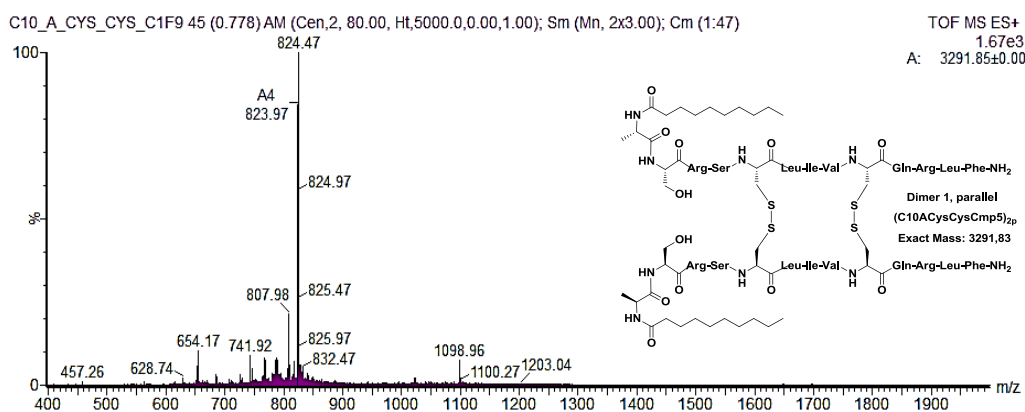
#### 4.1.1 Materials

In this section was used the same materials, method of peptide synthesis, peptide cleavage, peptide cyclization and dimerization, analytical RP-HPLC, ESI-HRMS and semipreparative RP-HPLC as described in sections 4.1.1-4.1.4 and 4.1.6-4.1.8 of Chapter 1.

#### 4.1.2 Registration conditions of NMR spectra

The  $^1\text{H-NMR}$  and  $^{13}\text{C-NMR}$  spectra were recorded at the UFSCar, São Paulo, Brasil on a Bruker spectrometer, with a resonance frequency of 400 MHz or 100 MHz respectively and using TMS as an internal reference. The chemical shifts ( $\delta$ ) are reported in ppm and the coupling constants (J) in Hz.

### 4.2 Synthesis of Structurally Restricted (Cyclic) Peptide (C10X-CysCysCm-p5):



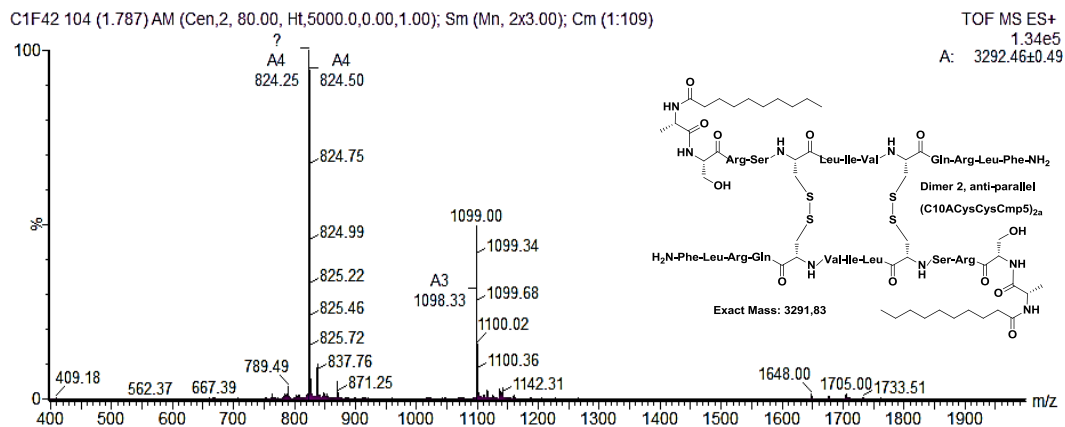
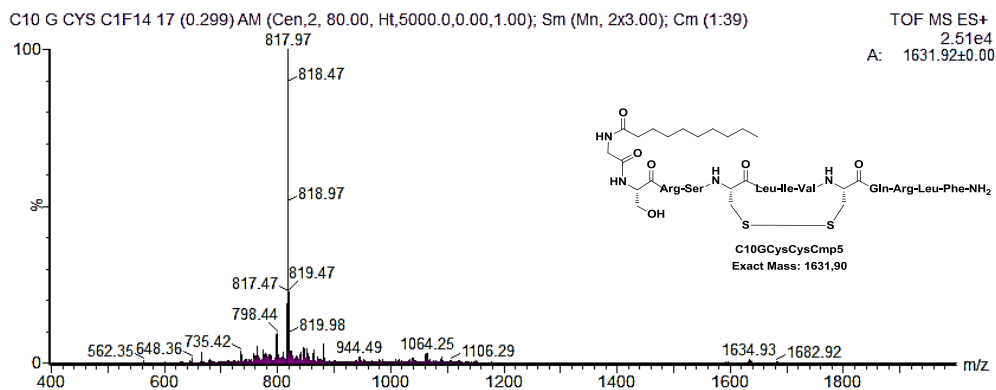
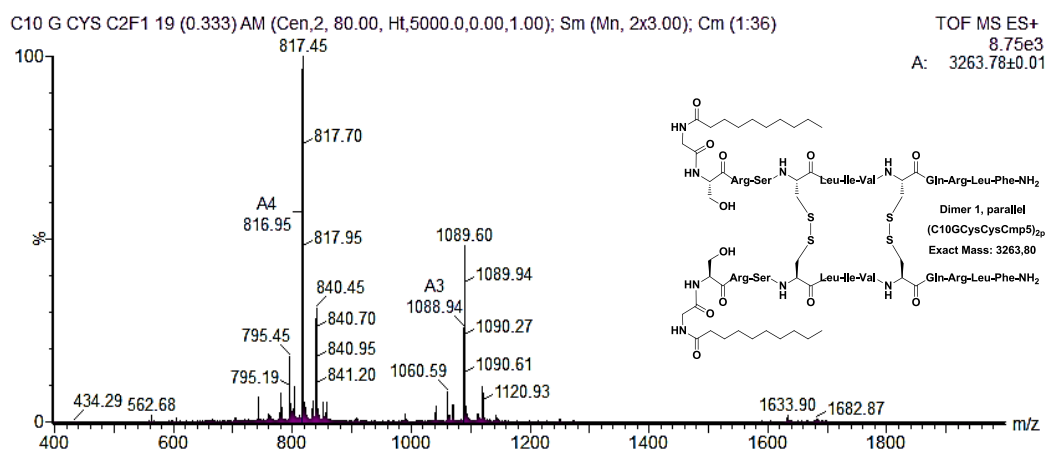


Figure 68: ESI-HRMS of the compounds (ordered by retention time) formed during cyclization of C10A-CysCysCm-p5 peptide.



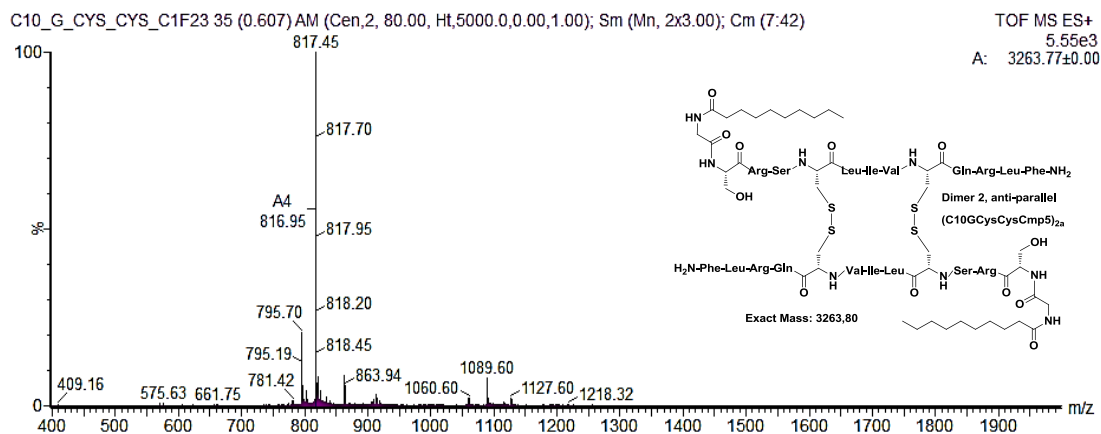
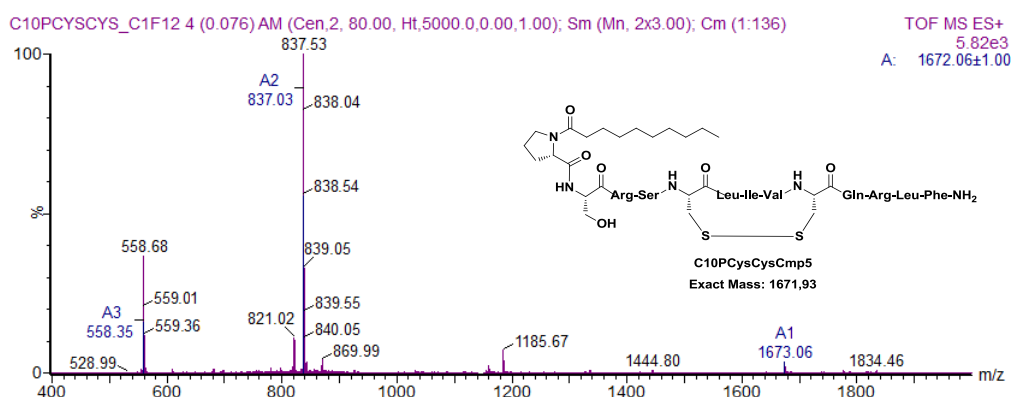
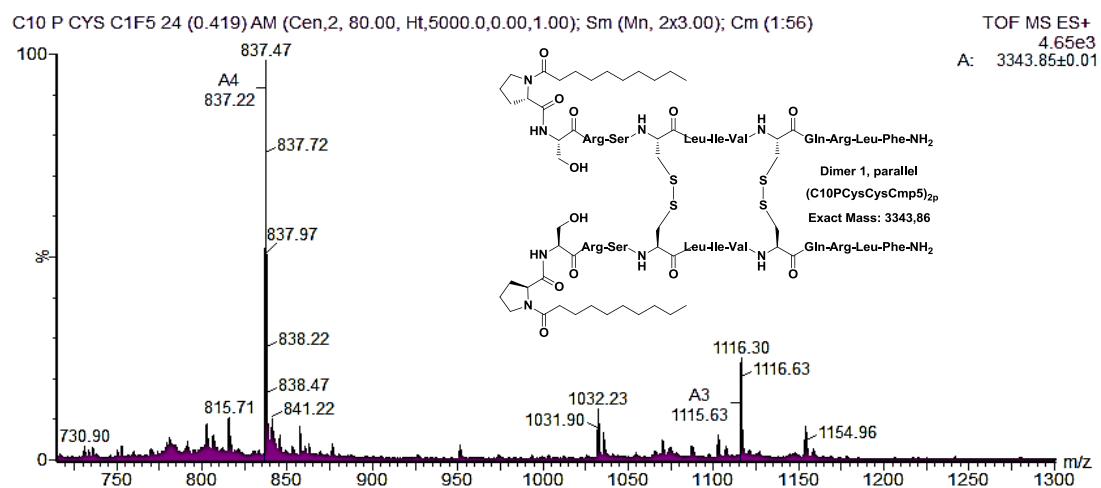


Figure 69: ESI-HRMS of the compounds (ordered by retention time) formed during cyclization of C10G-CysCysCm-p5 peptide.



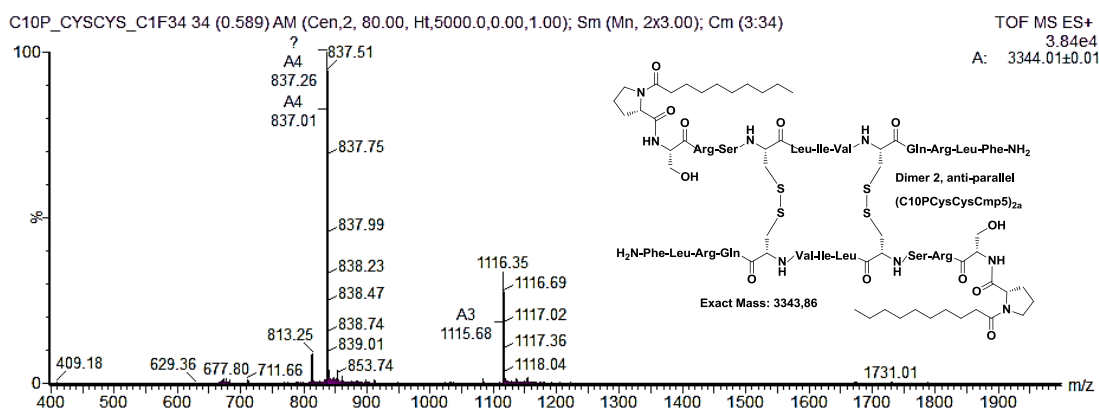


Figure 70: ESI-HRMS of the compounds (ordered by retention time) formed during cyclization of C10P-CysCysCm-p5 peptide.

### 4.3 Synthesis of *n*-dodecylisonitrile by formylation and dehydration of *n*-dodecylamine.

In a 50 mL flask, commercial *n*-dodecylamine (2.00 g, 10.8 mmol) is dissolved in HCOOEt (20 mL). The resulting solution is refluxed for 24 h at 60°C in a bath of sand and TLC (*n*-hexane/EtOAc, 1:1) checks the quantitative formation of formamide. The reaction crude is concentrated to dryness, dried by evaporation with toluene and keep in a vacuum desiccator for 24 h. Dry formamide (2.3 g, 10.8 mmol) is dissolved in 10 mL of dry THF, in a three-necked flask with a dropping funnel, 22.6 mL (162 mmol) of Et<sub>3</sub>N are added and the whole closed system is made inert with atmosphere of N<sub>2</sub> (g). The reaction medium is cooled with an EtOH/N<sub>2</sub> (1) bath (-60°C) and 3 mL (32.4 mmol) of POCl<sub>3</sub> dissolved in 15 mL of dry THF (approx. 2M) are dropped for 30 min. Then the reaction is allowed to reach room temperature for 24 h. After checking the formation of the desired product by TLC (*n*-hexane/EtOAc, 10:1) the mixture is concentrated to dryness. The obtained solid is extracted with *n*-hexane (5×25mL), decanted and all fractions are combined. The organic phase is concentrated under reduced pressure and the resulting crude is purified by column chromatography (*n*-hexane/EtOAc, 15:1) to obtain pure *n*-dodecylisonitrile as a light yellow oil (1.50 g, 71%).

**R<sub>f</sub>**= 0.83 (*n*-hexane/EtOAc, 10:1).

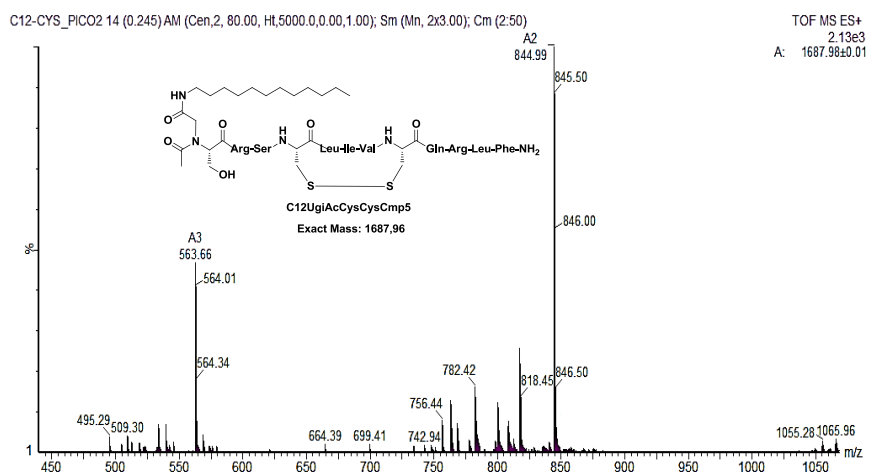
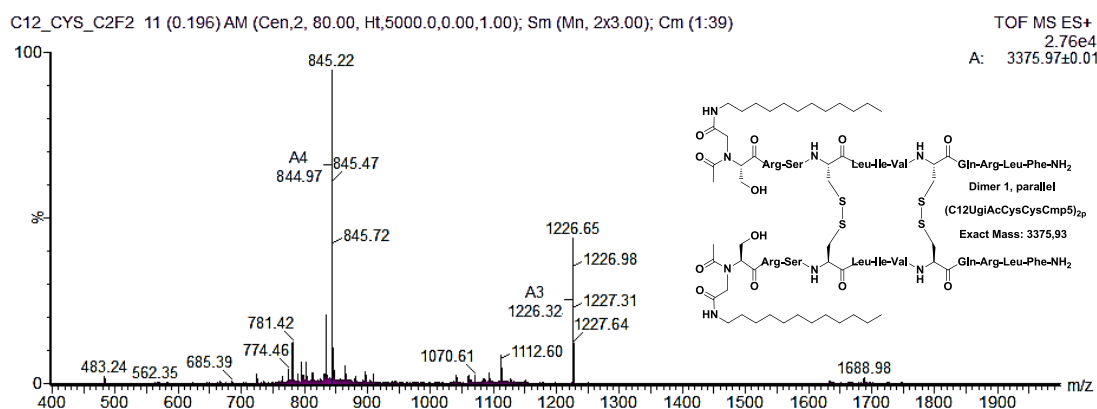
**FT-IR (KBr)**  $\nu_{\max}/\text{cm}^{-1}$ : 2927, 2857, 2148, 1460.

**<sup>1</sup>H NMR** (400 MHz, CDCl<sub>3</sub>)  $\delta$ : 3.41–3.35 (tt, 2H, *J* = 1.9/6.7 Hz, CH<sub>2</sub>NC), 1.73–1.63 (m, 2H), 1.44 (m, 2H), 1.33–1.22 (m, 16H), 0.88 (t, *J* = 6.9 Hz, 3H).

$^{13}\text{C}$  NMR (100 MHz,  $\text{CDCl}_3$ ) $\delta$ :155.56, 60.53, 41.70, 32.03, 29.73, 29.64, 29.50, 29.46, 29.24, 28.84, 26.45, 22.81, 14.25.

#### 4.4 Lipopeptides synthesis by Ugi-4CR in solid phase.

The Ugi-4CR in solid phase is carried out in a THF/MeOH (1:1) mixture and MeOH alone is not used, because it does not adequately swell the commonly used polystyrene resins. In contrast, THF is the solvent with the highest swelling power (Annex 2) and has been used in reactions of Ugi mixed with MeOH. As in previous works,<sup>146, 171</sup> the heterogeneous reaction process between the on-resin peptide as the amino component and paraformaldehyde is not efficient. It is necessary to perform the imine by organocatalysis using 4 equiv. of piperidine and 4 equiv. of (using  $\text{CH}_2\text{O}$ )<sub>n</sub> in dioxane/MeOH for 1 h (paraformaldehyde is partially soluble in dioxane). Then, piperidine is removed by washing with THF, the acetic acid (4 equiv.) and dodecylisocyanide (4 equiv.) components dissolved in THF/MeOH (1:1) are added, checking the occurrence of reaction by ninhydrin test after 1h. However, as it has already been shown, to complete the reaction, 36-72 h were needed due to slow Mumm rearrangement (Section 2.3.1).



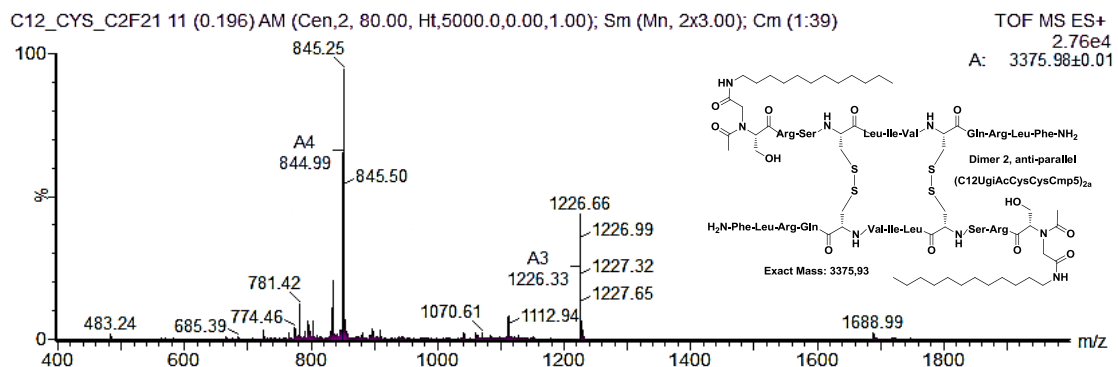
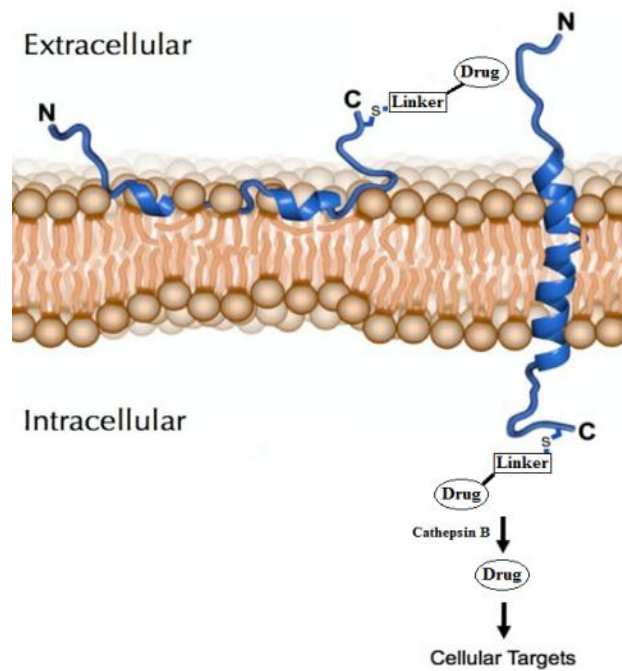


Figure 71: ESI-HRMS of the compounds (ordered by retention time) formed during cyclization of C12UgiAc-CysCysCm-p5 peptide.



# Chapter 3

"Merging peptides and small drugs for traceless release and targeted delivery to tumors"



## Chapter 3

### 1 Introduction. Chapter 3

#### 1.1 Peptide drugs conjugates. Cancer treatments with Carfilzomib and general objective of our work.

For decades, the targeting therapy with antibody-drug conjugates (ADCs) and peptide-drug conjugate (PDCs), usually composed of monoclonal antibodies or peptides, toxic payloads and cleavable/noncleavable linkers, has been extensively studied.<sup>172</sup> The conjugates enable the selective delivery of cytotoxic payloads to targeted cells, which results in improved efficacy, systemic toxicity reduced and better pharmacokinetics (PK)/pharmacodynamics (PD) compared with traditional chemotherapy.<sup>173</sup> PDCs and ADCs are based in a similar concept, but with vastly different structures and properties. Humanized antibodies introduce high specificity and prolonged half-life, while small peptides exhibit higher drug loading and enhanced the tissue penetration capacity. In addition, the flexible linear or cyclic peptides are also modified more easily.<sup>174</sup>

There are four ADCs approved by FDA and several under clinical trials. However, preclinical and clinical studies found that therapy strategies based on the targeting of specific proteins is significantly hampered by tumor heterogeneity, which can promote tumor evolution, leading to the loss of cell surface proteins and, eventually, to therapy resistance and disease progression. Moreover, targeted cancer biomarkers tend to be over expressed in a tumor-associated, not tumor-specific manner.

Peptide therapeutics has played a notable role in medical practice since the advent of insulin therapy in the 1920s. Thanks to the reduction of the main limitations that arose during their collection, synthesis and application, over 60 peptidic drugs are approved in the United States and other major markets. Peptides continue to enter in clinical development at a steady phase and the use of peptides or proteins as drugs has taken a sharp boom. Particularly, membrane penetrating peptides or those that can respond to different stimuli, such as pH, redox potential, temperature, light and enzymes, may offer controllable actions in specific targeted body locations.

Proteases encompass a broad range of hydrolytic enzymes that catalyze the cleavage of proteins and peptides. Deregulated proteolytic activities frequently have causative or exacerbated functions in pathological conditions, and therefore many proteases represent important therapeutic targets. The generation of small molecule drugs acting as protease inhibitors is a successful manner to fight several diseases. Successful examples of therapeutic intervention

using protease inhibitors include: angiotensin, converting enzyme inhibitors for the treatment of hypertension, HIV aspartyl protease inhibitors to prevent the development of AIDS and application of proteasome inhibitors in the treatment of myeloma. Proteasomes are proteases complexes which degrade unneeded or damaged proteins by proteolysis, a chemical reaction that breaks peptide bonds.<sup>175</sup>

The selective proteasome inhibitor Carfilzomib is a tetrapeptide epoxyketone and an analog of epoxomicin. It is an anti-cancer drug that inhibits covalently and irreversibly the chymotrypsin-like activity of the 20S region of proteasome and displays minimal interactions with non-proteasomal targets. The build-up of polyubiquitinated proteins resulted of the inhibition of proteasome-mediated proteolysis, may cause cell cycle arrest, apoptosis and inhibition of tumor growth.<sup>176</sup> This drug improve safety profiles over many cytotoxic drugs that can escape from the targeted cell and, in a process called "bystander killing", attacking neighboring cells.<sup>177</sup>

In phase II trials of carfilzomib, the most common adverse events were hematologic toxicity with thrombocytopenia, anemia, lymphopenia, neutropenia, pneumonia, fatigue and hyponatremia.<sup>178</sup> Furthermore, gastrointestinal disturbances, including diarrhea and nausea are non-hematologic side effects, commonly reported with proteasome inhibitors. Additionally, cardiovascular toxicity is an outcome of Carfilzomib treatment due to the effects on proteasomes in the myocardium.<sup>179</sup>

The development of targeted delivery strategies for Carfilzomib could eliminate the adverse effects, reduce doses and increase effectiveness. The characteristics as a highly selective and irreversible inhibitor of the proteasome should make it a special candidate for the bioconjugation with peptides sensitive to the acidic pH of the tumor cells.

## 2 Bibliographic Revision. Chapter 3

### 2.1 $\alpha,\beta'$ -epoxyketone peptides as proteasome inhibitors

The ubiquitin-proteasome pathway of cell-cycle progression is controlled by the multi-enzyme complex proteasome and is involved in the termination of signal transduction cascades and the removal of mutant, damaged and misfolded proteins. This protease is a promising therapeutic target, and a synthetic dipeptidyl peptide boronate, named Bortezomib (Velcade), is the first clinical FDA-approved drug that have proteasome inhibition as action mechanism.<sup>178</sup> Natural products like epoxomicin are microbial metabolites posing a epoxy-ketone integrated with a peptidic skeleton that exhibit anticancer activities as a result of proteasome inhibition (Figure 72).<sup>180</sup>

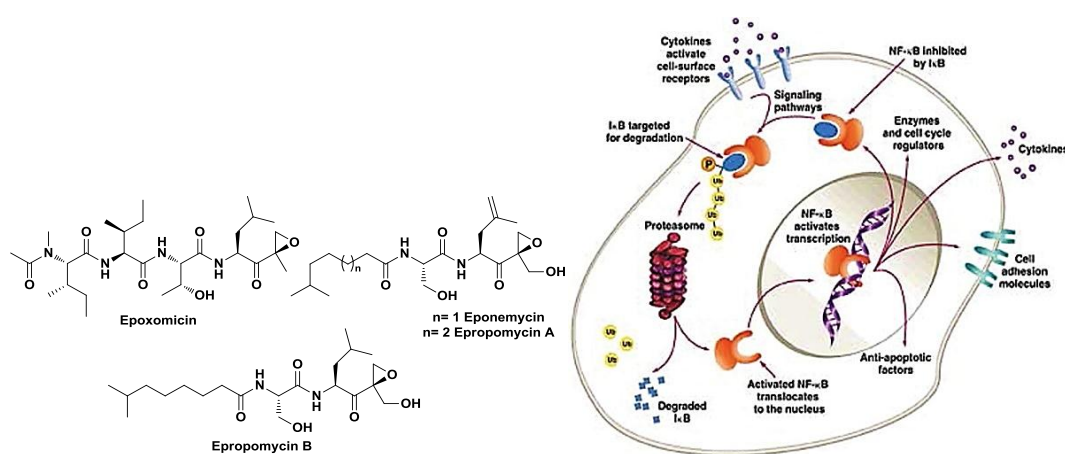


Figure 72: Natural epoxyketone peptides inhibitors of proteasome as anticancer agents.

Such epoxyketone peptides have been naturally designed to bind covalently with Thr of proteasome 20S, thus leading to irreversible inhibitory activity and a potent, but rather selective, cytotoxicity to malign cells. Epoxomicin also served as a scaffold for the generation of a synthetic tetrapeptide epoxyketone with improved activity (Figure 73), YU-101, which became the inspiration for Carfilzomib, the recently approved therapeutic agent for multiple myeloma.<sup>181</sup>

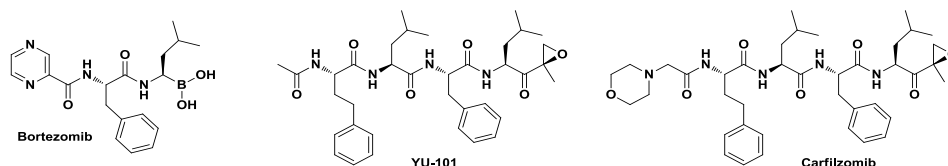
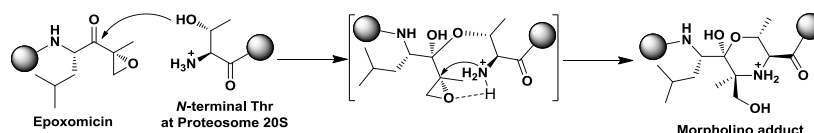


Figure 73: Bortezomib, YU-101 and Carfilzomib proteasome inhibitors.

According to the mechanism described by Hubert and Crews, the unique specificity of epoxomicin is a result of the irreversible formation of a morpholino ring between the amino terminal catalytic Thr-1 of the proteasome 20S and the  $\alpha,\beta'$ -epoxy ketone pharmacophore of

epoxomicin (Scheme 11).<sup>182</sup> A sequential double nucleophilic attack on the epoxy ketone residue of epoxomicin by two nucleophiles of the *N*-terminal Thr (the hydroxyl side chain and the free *N*-terminal) explains the formation of the morpholino ring. Therefore, it is expected that only *N*-terminal nucleophile proteases, such as the proteasome, can form the morpholino ring by reaction with epoxy ketones, thereby rendering epoxomicin an exceptional specificity for the proteasome over alternative mechanism-based proteasome inhibitors.<sup>183</sup>



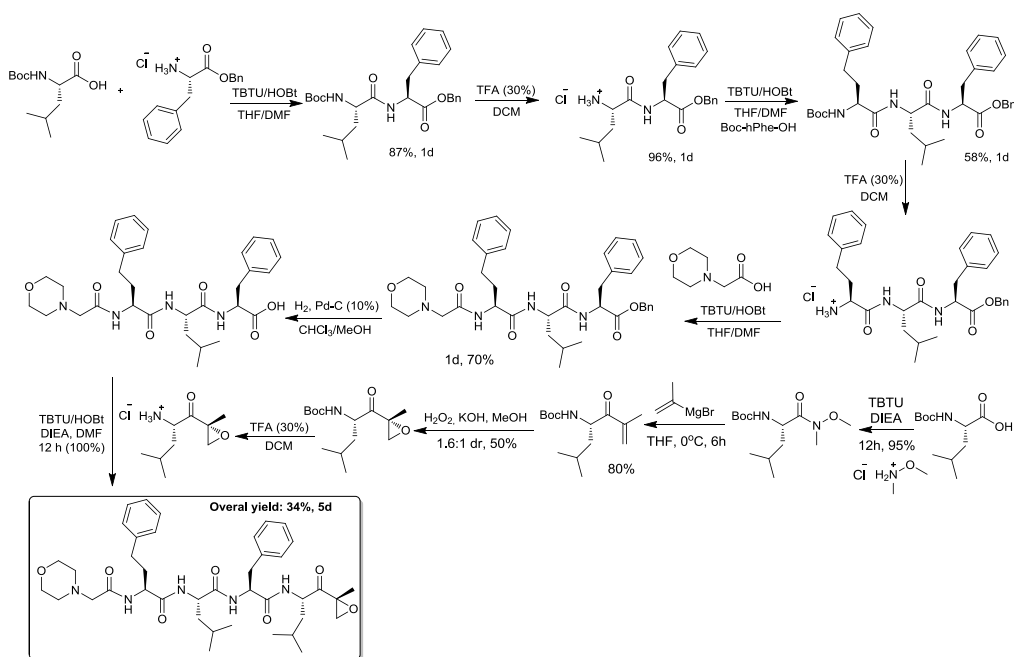
Scheme 11: Mechanism for the formation of a morpholino adduct from epoxy peptides.

## 2.2 Total synthesis of Carfilzomib

The FDA approved Carfilzomib for relapsed and refractory multiple myeloma is marketed under the trade name Kyprolis. Its production uses general approaches of convergent peptide couplings in liquid phase but some differences are observed in the stage of synthesis of the epoxide building block that starts with a vinylketone.<sup>184</sup>

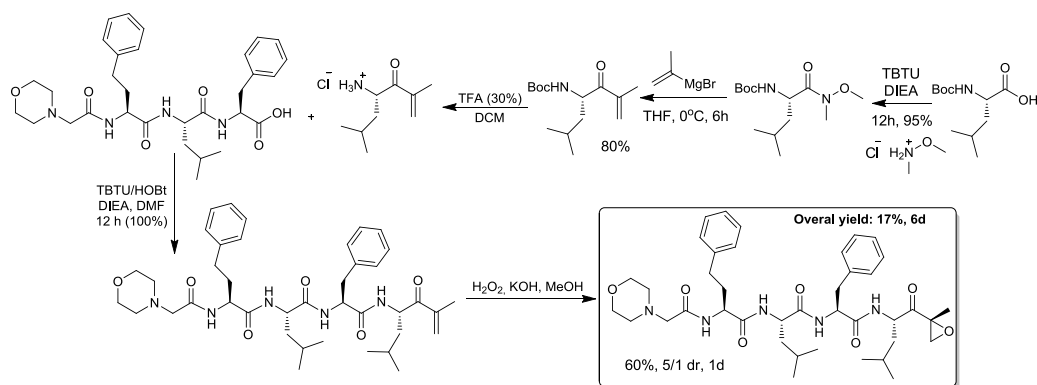
One route leads from the simple Leucine-vinylketone epoxidation, previously synthesized through the Weinreb amide of Boc-Leu-OH and subsequent reaction with the isopropenylmagnesium or the isopropenyllithium organometallic reagent. The subsequent epoxidation of the Boc-Leu-vinylketone with non-stereoselective methods ( $\text{H}_2\text{O}_2$  (1.6:1 *dr*),  $\text{Ca}(\text{ClO})_2$  (2:1 *dr*), etc) leads to mixtures of diastereomers and implies the final chromatography separation of the desired epoxide. Double protection of the Leu-vinylketone, with two Boc, Boc and Cbz or two Cbz and subsequent epoxidation render 9-10:1 *dr* but implies an additional step of protection. The epoxidation of late stage intermediates (Boc-Phe-Leu-vinylketone) with  $\text{H}_2\text{O}_2$  (9:1 *dr*),  $\text{Ca}(\text{OCl})_2$  (3:1 *dr*), mCPBA (1:1 *dr*), *t*-BuOOH, lanthanide BINOL complexes (96.5:3.5 *dr*),  $\text{H}_2\text{O}_2$  and chiral manganese complex (7:1 *dr*) have been also implemented.<sup>184</sup>

The other fragment is synthesized by a linear peptide coupling procedure using the Boc/Bzl chemistry. The morpholine group may be appended in two steps via acylation with chloroacetyl chloride and displacement of chloro with morpholine.<sup>184</sup> In the final step, a tetrapeptide (Morf-Ac-Hph-Leu-Phe-OH) is connected to the Leu-epoxide. Different coupling reagents have been used, with low racemization of the *C*-terminal amino acid (Section 2.4, Chapter 1). The overall process is completed in, at least, five days of work and only with 29% yield (Scheme 12).<sup>184</sup>



Scheme 12: Convergent synthesis of Carfilzomib by early epoxidation.

A second route is a late-stage epoxidation process that includes also the previous linear synthesis of the tetrapeptide left-hand fragment, using liquid phase procedures. Next, a vinylketone analogue of carfilzomib is synthesized by coupling the tetrapeptide left-hand fragment and Leu-vinylketone (Scheme 13). The vinylketone pentapeptide can be epoxidized at late-stage by  $\text{H}_2\text{O}_2/\text{KOH}$  with 5:1 *dr* and yield 60%.<sup>184</sup> However, the diastereomeric mixture has to be purified by column chromatography, with the loss of 20% mass of the desired diastereomer. Hence, the yield of the epoxide building block with the desired configuration is somewhat low. The overall yield after six days of work is only 17%. Further advance of the process could be more simple reaction conditions, the use of readily available starting materials and reagents, the use of solvents that are easily handled and/or removed, the prevention of the use of hazardous and explosive materials and the improvement of stereoselectivity. A Chinese patent application describes epoxidation of the vinylketone pentapeptide using  $\text{NaHCO}_3$ , oxone, and trifluoroacetone in DCM at  $-10\text{ }^\circ\text{C}$ . After chromatography, carfilzomib is isolated in 46% yield and peptidic purity >99%. The *dr* of the reaction is not provided.<sup>184</sup>



Scheme 13: Convergent synthesis of Carfilzomib by late-stage epoxidation.

### 2.3 Antibody drug conjugates (ADCs). Linker technologies, maleimido linkers and carbonylacrylic acid approach.

ADCs are examples of bioconjugates, immunoconjugates and are biopharmaceutical drugs designed as a targeted therapy for treating cancer because intend to target and kill tumor cells while sparing healthy cells. They are complex molecules composed by an antibody linked to a biologically active cytotoxic payload or drug. Until the 2019, 56 pharmaceutical companies have been working in the developed of ADCs.<sup>185</sup>

Antibodies specifically target certain tumor antigen (a protein that, ideally, is only found on tumor cells) and trigger a signal in the tumor cell that activates the internalization of the ADC. After the ADC is internalized, the cytotoxin kills the cancer cell once released. This kind of targeting limits side effects and gives a wider therapeutic window than the traditional chemotherapies.<sup>187</sup>

Mechanisms of resistance to ADCs include low/loss of antigen expression, masking of the antigen, presence of NRG (neuregulins or neuroregulins, part of the EGF family of proteins), truncation of the antigen, poor internalization, impaired lysosomal processing, high rate of recycling, oncogenic alterations, mutations in cytotoxic drug target, role of cell cycle and apoptotic deregulation.<sup>189</sup>

In the development of ADCs or PDCs, the linker is of the same essential importance that the monoclonal antibodies and the cytotoxic drugs used.<sup>187</sup> The linker impacts the efficacy and tolerability of the final bioconjugate and ensures that less of the cytotoxic payload falls off before reaching a tumor cell, improving safety, and limiting dosages.<sup>190</sup>

General linkers are based on chemical motifs including disulfides, hydrazones or peptides (cleavable), or thioethers (noncleavable). Cleavable linkers rely on the physiological stimuli, which mainly includes chemically cleavable linkers (acid-labile linkers and disulfide linkers) and enzymatically cleavable linkers (peptide linkers and  $\beta$ -glucuronide linkers).<sup>191</sup>

Alternatively, noncleavable linkers require proteolytic degradation. They depend on the internalization more than cleavable linkers do. Cleavable linkers take advantage of the antibody-drug conjugate targeting mechanism which involves sequential binding of the antibody-drug conjugate to the cognate antigen on the surface of the target cancer cells, and internalization of the ADC-antigen complexes through the endosomal-lysosomal pathway.<sup>191</sup> For acid-labile linkers (hydrazones and *cis*-aconityl, sometimes with low serum stability), intracellular release of payloads relies on the different pH between endosomes/lysosomes (pH= 7.3-7.5) and blood (pH= 7.3-7.5) (Figure 74). A *cis*-aconityl linkage can be used to conjugate payloads, such as doxorubicin (DOX) and daunomycin (or daunorubicin). This kind of conjugation was achieved through the carbohydrate residues of the mAbs after periodate oxidation, which improved the therapeutic index compared to the unconjugated drug. Hydrazones utilize aminoacid residues on the antibody instead of the carbohydrate moieties for covalent attachment. Gemtuzumab ozogamicin (Mylotarg), the first ADC approved by FDA, is an example that uses the hydrazone linker technology.<sup>191</sup>

Disulfides (Figure 74) are thermodynamically stable at physiological pH and are designed to release the drug upon internalization inside cells by attack/interchange of cytoplasmic thiol cofactors, such as glutathione (GSH) or the intracellular enzyme protein disulfide isomerase. Each linker has their advantages and limitations. Ultimately, the choice of the linker is correlated to the antibody, the drug and the disease to be treated.<sup>192</sup> When drugs already approved by some regulatory agency are used in ADC construction, an important criterion to follow is the use of linkers that not leave traces once liberated from the drug.

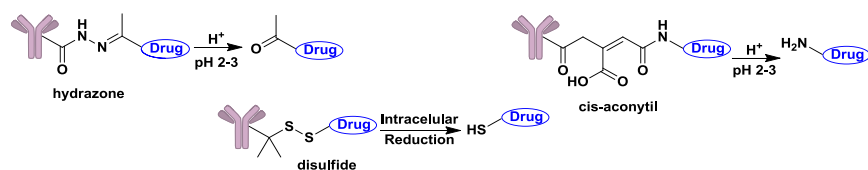


Figure 74: General types of cleavable linkers.

### 2.3.1 Enzymatically cleavable linkers: Peptide linkers. Traceless linkers.

Enzymatically cleavable linkers are sensitive to enzymes located in cytoplasm, providing ADCs with improved plasma stability, comparable to non-cleavable linkers, while boasting a more defined method of drug release. Moreover, the ability to pair these linkers with self-immolative chemical groups allows the release of free drugs with a minimal derivation (traceless procedure). Dipeptide-based linkers Val-Cit and Phe-Lys are examples of them and have been used in ADCs under clinical trials. However, the dipeptide Val-Cit combined with PAB (*p*-aminobenzyl alcohol), a self-immolative linker, is the most popular enzymatic





amine groups and a release without traces. For example, FDA approved drug, Brentuximab vedotin adopts this linker (Figure 76).<sup>197</sup>

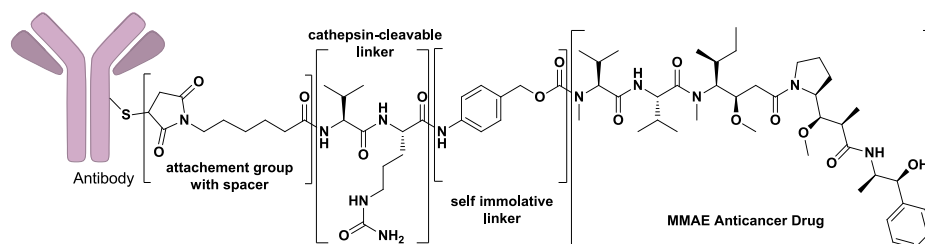
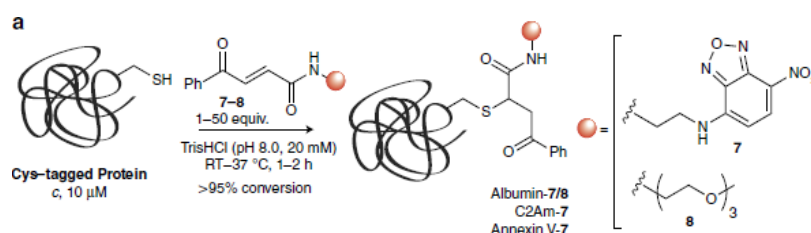


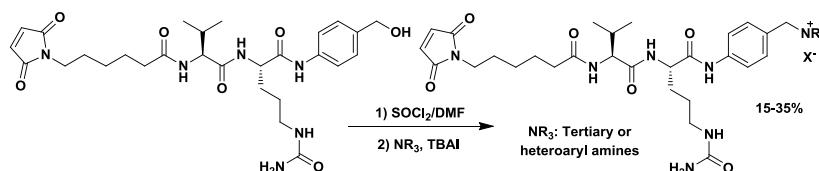
Figure 76: Approved anticancer treatment: Brentuximab vedotin (trade name Adcetris).

Substitutes of maleimidobased linkers include the one-step and irreversible Cys selective bioconjugation using simple carbonylacrylic reagents (Scheme 15). These reagents undergo rapid thiol-Michaeladdition under biocompatible conditions in stoichiometric amounts. The reaction proceeds with a high degree of Cys selectivity using equimolar amounts of synthetically accessible reagents under aqueous, biological friendly conditions. The formed conjugates are fully stable in plasma and retain their function.<sup>198</sup>



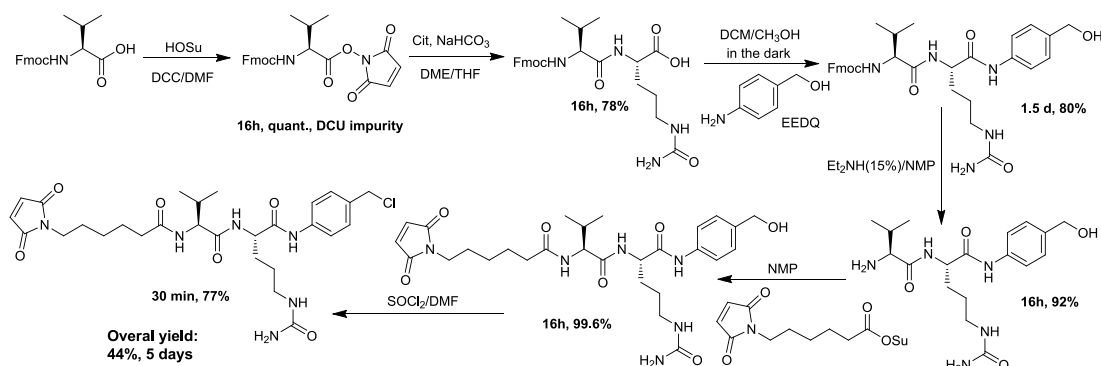
Scheme 15: Irreversible Cys selective bioconjugation using simple carbonylacrylic reagents.

Recently, a new maleimide-traceless linker for bioconjugation of tertiary or heteroaryl amines containing drugs (a common chemical motif in many anticancer compounds) was developed.<sup>199</sup> The linker possess a chlorobenzyl moiety that reacts with this type of drug by  $S_N2$  substitution forming a tetraalkylammonium salt in yields ranging 15-35% (Menshutkin reaction)<sup>200</sup> (Scheme 16).



Scheme 16: Maleimide-Caproil-Val-Cit-PAB-Cl linker for the traceless release of tertiary and heteroaryl amines from ADCs.

This linker is synthesized by a convergent peptide coupling approach and final chlorobenzoylation with tonyl chloride. The overall process is tedious and only 44% of yield is obtained after at least five days of work (Scheme 17).<sup>201</sup>



Scheme 17: Reported Maleimido-Caproic-Val-Cit linker synthesis.

## 2.4 pHLIP peptides and related pHLIP-drug conjugates.

Acidity is a general hallmark of tumors.<sup>202</sup> While normal tissue pH is about 7.4, pH in tumors range from 5.5 to 7. Peptides as GALA,<sup>203</sup> ATRAM<sup>204</sup> or pHLIP (AEQNPIYWARYADWLFTPLLLLDLALLVDADEGT) are synthetic pH-responsive amphipathic peptide that target acidity in biological membranes by formation of a  $\alpha$ -helical transmembrane at pH less than 7.

These peptides can be used to target cancers or conditions as viral infections in the lung, or even arthritis in the knee. Unlike other strategies that are developed to target few specific types of cancer, the approach is extremely simple and relies on a feature that is common to most solid tumors. pHLIP have been used for the release of cargo molecules attached by the C-terminus via a disulfide bond, that is cleaved in the cytoplasm. Disulfide reduction could be effected by several changes in the tumor metabolism and sometimes does not show good results. pHLIP conjugates with DOX,<sup>205</sup> Phalloidin toxin<sup>206</sup> or Amanitin (Figure 77)<sup>207</sup> are recent examples.

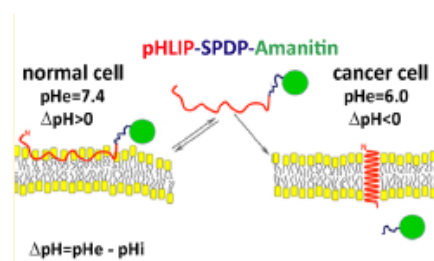


Figure 77: Mechanism of target and intracellular release of the anticancer bioconjugate pHLIP-Amanitin (SPDP: maleimido disulfide linker).

Thévenin's lab uses the pH (low) insertion peptide (pHLIP), a peptide that can selectively target tumors in mice, solely based on their acidity rather than on any specific biomarker. pHLIP

circulates in the blood supply until it anchors to the cell membrane of acidic tissues. Their recent study shows that pHLIP–MMAE combination is effective at killing a breast cancer cell line that is resistant to current targeted therapies, after only two hours of incubation without any apparent disruption of the plasma membrane.<sup>208</sup>

PET Imaging of extracellular pH with <sup>64</sup>Cu- and <sup>18</sup>F-Labeled pHLIP peptide Variant3 (ACDDQNPWRAYLDLLFPTDLLLLDLLT) have been used to target tumors (Figure 78).<sup>209</sup>

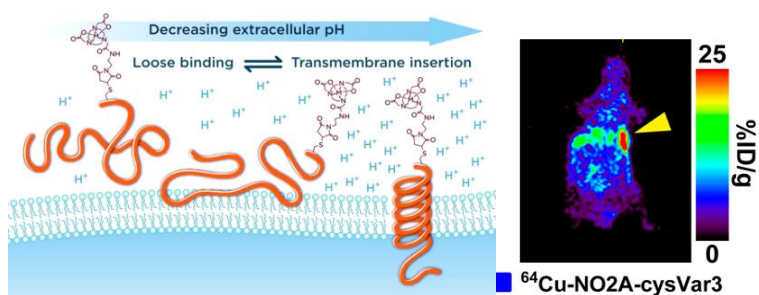


Figure 78: PET Imaging of extracellular pH with <sup>64</sup>Cu labeled pHLIP-Variant3.

The pathway of pHLIP entry into the membrane and the translocation of molecules into cells is not mediated by endocytosis, but by interactions with cell receptors or by formation of pores in the cell membrane. pHLIP demonstrates prolonged circulation in the blood (several hours), which is consistent with the ability to bind weakly to membrane surfaces at neutral and high pH, preventing the rapid clearance by the kidney expected for a small, soluble peptide.<sup>210</sup>

### **3 Results and discussion. Chapter 3**

#### **3.1 Our proposal for the peptide conjugation of Carfilzomib**

Peptide conjugation of Carfilzomib could be realized with many types of peptide-based biomaterials with stimuli-responsive and membrane-active properties. Within these, the use of pHLIP Varian3 is promising because it has been proved to be effective as pH acidity biomarker and in PDCs conjugates due to the easiness of synthesis, covalent modification and good stability during plasma circulation.

Peptides can be prepared in a linear stepwise synthesis in which each amino acid is successively coupled, or in a convergent approach, where short fragments are grown separately, purified and connected. Both strategies can be carried out in solution or in solid support, although solution and solid-phase methods can coexist in convergent approaches. The synthesis in solution is cheaper if it is used to obtain small peptides, but the requirement of purification for each intermediate obtained is a tedious and slow process that requires time, a disadvantage with respect to the solid phase method. Synthesis on solid support is more expensive, so the cost-benefit ratio should be favorable during the application. However, it requires a shorter reaction time, may be automated and peptides with a high degree of peptidic purity are obtained.<sup>9</sup>

Reported synthesis of Carfilzomib is carried out mainly in liquid phase and implies inefficient process of amino acids coupling and intermediate purifications. Solid phase methods for the synthesis of the left-hand fragment of Carfilzomib was recently completed but in low yields (48%). Currently, the conjugation of pHLIP peptides to drugs uses only cleavable disulfide linkers, which sometimes have poor stability in plasma and therefore limited outcomes. The application of enzymatically cleavable linkers to pHLIP-Carfilzomib conjugates could improve the effectiveness of the new anticancer bioconjugate and could be further implemented with other drugs or stimuli-responsive and membrane-active. One of the most used enzymatically cleavable linker (MC-Val-Cit-PAB-Cl) is synthesized inefficiently in liquid phase; it contains a maleimido group for addition of thiols and a PAB moiety functionalized with chloride for the reaction with tertiary amines. Bioconjugates containing maleimido have poor stability in plasma and the reaction of PAB chlorides with tertiary amines have low yield. Therefore, the use of carbonylacrylic instead of maleimido and PAB-iodides instead of PAB-chlorides should be advantageous. The implementation of solid phase peptide synthetic methods in the synthesis of this linker is a novel strategy in this research area.

With these statements in mind, the objectives of this work could be numbered as follow:

- ✓ Develop an improved synthesis of Carfilzomib using peptide synthetic methods in solid

phase.

- ✓ Develop an enzymatically-cleavable linker containing carbonylacrylic and PAB-iodides instead of maleimido and PAB-chlorides to improve both, PDC or ADC effectiveness in-vivo and the yield of coupling to tertiary amine-based drugs.
- ✓ Develop a solid phase peptide synthetic protocol to produce linkers like MC-Val-Cit-PAB-OH.
- ✓ Synthesize pHLIP-Variant3 containing Cys at the N or C-terminal.
- ✓ Synthesize pHLIP Variants3-Linker-Carfilzomib bioconjugates to address biological anticancer effectiveness and reduction of adverse effects of Carfilzomib treatments.

The results obtained in each stage of the experimental work are described below and follow the methodology of peptide characterization described in the section 3.1 of Chapter 1. The small intermediate molecules were characterized by NMR and ESI-MS or ESI-HRMS in some cases. The molecules synthesized in solid phase were characterized by analytical RP-HPLC, ESI-HRMS and NMR in some cases. The small molecules were purified by liquid column chromatography and the others by preparative RP-HPLC.

## 3.2 Carfilzomib Synthesis

### 3.2.1 Solid-phase synthesis of the left-hand fragment of Carfilzomib.

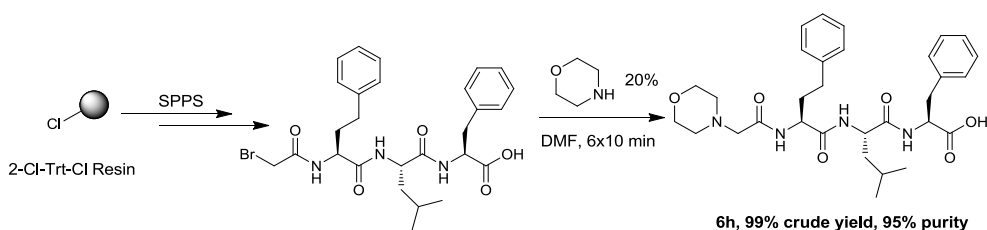
Previous synthetic methods of Carfilzomib include liquid and solid phase approach, some of them with a late-stage epoxidation step. The late-stage epoxidation method developed until today, even though it has more yield, implies the loss of 20% of important and costly advance material during diastereomers separation. For that reason, in this work we decided to use the standard approach of epoxidation at early stage, in which only the aminoacid Leu is lost during separation of the diastereomeric epoxides.

The left hand of carfilzomib is a tetrapeptide containing the non-natural aminoacids Hph and morpholino acetic acid. Both are commercially available but rather expensive (Hph in the form of Fmoc-Hph-OH) and morpholino acetic acid could be easily prepared by liquid phase substitution of the bromo in bromoacetic acid by morpholine. As this peptide have C-terminal in the form of carboxylic acid, it is possible to use Wang or Cl-Trt-Chloride resins to carry out the synthesis. Taking into account that aminoacids in this peptide do not have protected lateral chains, Cl-Trt-Chloride resin is the best option to avoid the extreme cleavage condition of the Wang resin (95% TFA).

The peptide was grown using Cl-Trt-Chloride resin with 1.47 mmol/g of substitution. The first aminoacid (Fmoc-Phe-OH) was coupled in 2 h by unimolecular substitution ( $S_N1$ ) over the Cl-Trt group in the resin, using excess of DIEA as base. The possible remained active sites in the resin were capped with MeOH washings. Peptide synthesis was carried out by sequential deprotection and coupling reaction and checked by ninhydrin test after the final reaction. The combination of DIC/OxymaK as has been reported was an excellent coupling agent due to eradication of early cleavage of the peptide in the presence of weak acids as HOBT or Oxyma. We proved also a reduction in the consumption of aminoacid and OxymaK quantities. The combination of 2equiv. of Fmoc-AA-OH and DIC with 3 equiv. of OxymaK produced comparable efficiency (time and yields) as the coupling with 4 equiv. of excess of all reagents. It also reduced the waste and cost of the overall synthesis. Cl-Trt-Chloride Resin also represents an advance because can be recovered.

Notably, we developed a new procedure for the synthesis of the morpholino acetic acid moiety in the last step. Instead of coupling this compound, we coupled bromoacetic acid and then the treatment with morpholine solution (6x10 min) in DMF afforded the expected product by total bimolecular substitution ( $S_N2$ ) of the bromo atom. Final cleavage with 1% TFA in DCM afforded the expected peptide in the form of TFA salt in almost quantitative yield. The total

synthesis of the left-hand fragment of Carfilzomib was accomplished in solid phase in only 6 h and with excellent yield (95%) (Scheme 18). Our results are substantially superior to the liquid phase procedure that could imply at least one week of coupling reactions, intermediate purifications and less than 35% of yield. Compared with the previously solid phase developed protocol<sup>184</sup> we increased the yield from 48% to 95% due to the use of OxymaK racemization inhibitor. The ESI-HRMS (Figure 79) confirms the expected mass of this tetrapeptide and RP-HPLC the peptidic purity and absence of racemization during the coupling reactions (see experimental part for details, Chapter 3).



Scheme 18: Synthesis of the left-hand fragment of Carfilzomib.

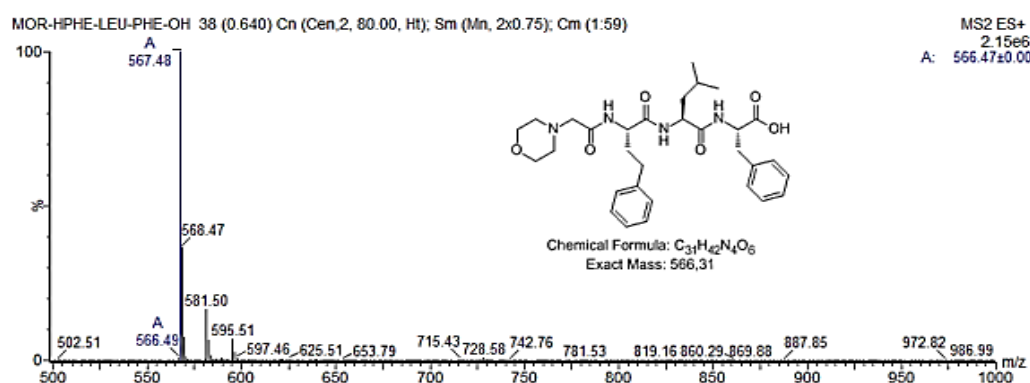


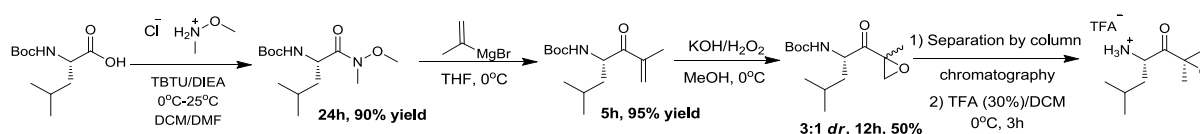
Figure 79: ESI-HRMS of the left-hand fragment of Carfilzomib.

Despite of the use of excess reagents (2equiv.) in the synthesis in solid phase, the gain in time and performance implies reduction of operating costs, laboratory material, payment of qualified personal, environmental harmful residues, energy consumption and health risks due to working conditions. A further improvement may be the substitution of DMF by THF or MeTHF as greener solvents. The implementation of coupling conditions that implies the uses of 2 equiv. of FmocAa-OH/DIC and 3 equiv. of racemization inhibitor are being investigated on other more complex peptides.



### 3.2.2 Synthesis of the right-hand fragment of carfilzomib and coupling to the left-hand fragment.

For the synthesis of the right-hand of carfilzomib we employed a reported procedure that uses Weinreb amide and leucine  $\alpha,\beta$ -unsaturated ketone as intermediates before the final epoxide synthesis. We started protecting (*L*)-Leucine with  $\text{Boc}_2\text{O}$  using a standard protocol. The Weinreb amide of Boc-Leu-OH was prepared in high yield and peptidic purity using TBTU as coupling agent. The following Grignard reaction with commercial *iso*-propenylmagnesium bromide afforded the  $\alpha,\beta$ -unsaturated ketone in high yield and in a simpler procedure compared with the reported *iso*-propenyl lithium. Final stereo uncontrolled epoxidation of the enone afforded a mixture (3:1 *dr* as judge by  $^1\text{H-NMR}$  (Figure 80) and the mass of isolated products) of diastereomeric epoxides in 50% yield, which was separated by *flash* chromatography. The TFA salt of the desired Leu-epoxide aminoacid was obtained in quantitative yield after Boc deprotection in the presence of TFA/DCM 30% (azeotropic removal of TFA with toluene was necessary to get the pure white solid, Scheme 19).



Scheme 19: Synthesis of the right-hand fragment of carfilzomib.

The  $^1\text{H-NMR}$  of Weinreb amide, alkene and epoxide are presented in Figure 80. For the Weinreb amide, the two singlets in 3.77 ppm (*a*, s, 3H) and 3.18 ppm (*b*, s, 3H) indicate the formation of the product. Other important signals come from the Boc protecting group in 1.41 ppm (s, 11H, together with the  $-\text{CH}_2$  of the leucine) and the two doublets in 0.94 ppm (d,  $J = 6.5$  Hz, 3H) and 0.91 ppm (d,  $J = 6.7$  Hz, 3H) corresponding to the  $-\text{CH}_3$  of the leucine amino acid. The  $\alpha,\beta$ -unsaturated ketone system is confirmed by the presence of two singlets in 6.06 ppm (*a*, s, 1H) and 5.86 ppm (*a'*, s, 1H), together with the singlet of the  $-\text{CH}_3$  in 1.88 ppm (*b*, s, 3H). For the epoxide, two doublets in 3.29 ppm (*a*, d,  $J = 4.8$  Hz, 1H) and 2.89 ppm (*a'*, d,  $J = 4.8$  Hz, 1H) and a singlet in 1.51 ppm (*b*, s, 3H) corroborated the structure. The other isomer of the epoxide was isolated and characterized. The main differences are observed for the  $-\text{CH}_2\text{O}$  signals of the epoxide in 3.06 ppm (d,  $J = 5.0$  Hz, 1H) and 2.88 ppm (d,  $J = 5.1$  Hz, 1H) and the  $-\text{CH}_3$  observed in 1.58 (s, 3H) (Figure 102). The obtained spectroscopic data is in accordance with the previously described results in the literature.<sup>14</sup>

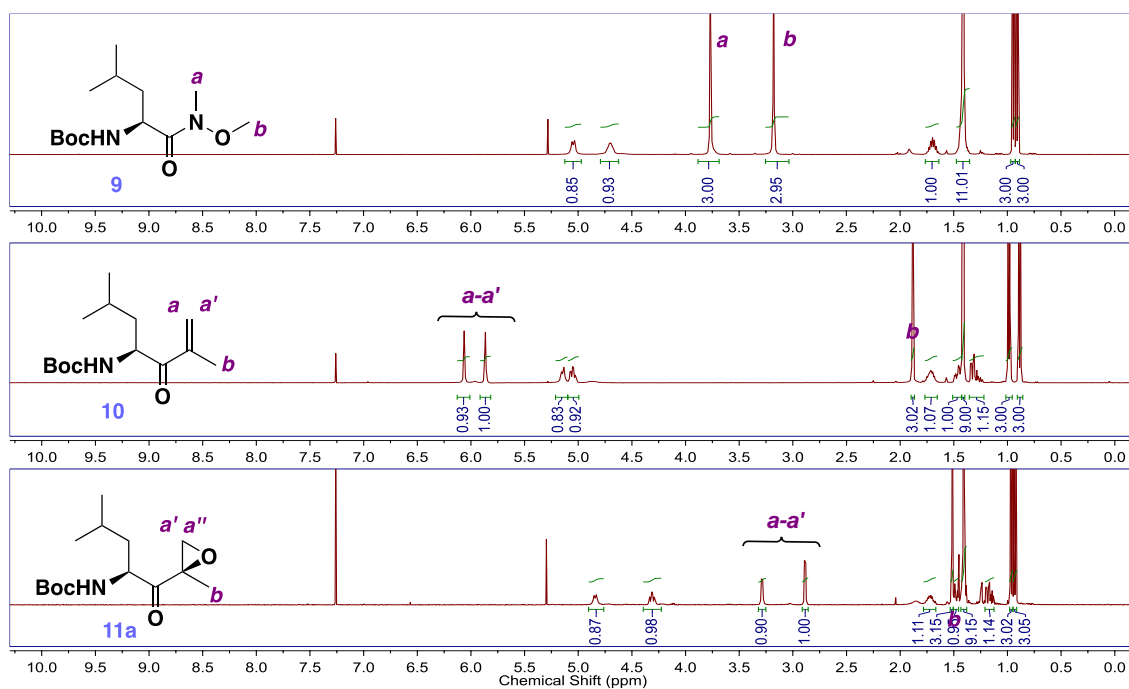
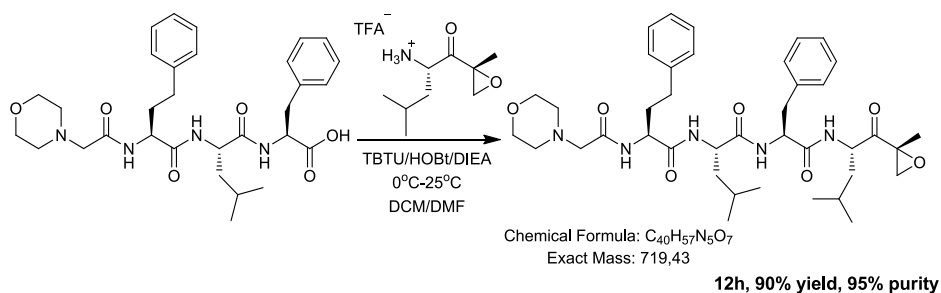


Figure 80:  $^1\text{H}$  NMR spectra of the Boc-protected Leu 9, 10 and 11a ( $\text{CDCl}_3$ , 400 MHz).

The synthesis of the epoxy-drug was finally accomplished by the coupling of leucine-epoxidewith the MorfAc-Hph-Leu-Phe-OH tetrapeptide in the presence of TBTU/HOBt/DIPEA and THF at  $-20^\circ\text{C}$  to room temperature after 12 h (Scheme 20) furnishing Carfilzomib in 90% yield as a white solid after purification by *flash* column chromatography using ethyl acetate as solvent. The  $^1\text{H}$  NMR ( $\text{CDCl}_3$ ) spectrum of Carfilzomib is showed in Figure 81. The incorporation of the Leu-epoxide in the main tripeptide structure can be confirmed by the multiplet in 0.89–0.82 ppm with integration to 12H (2  $\text{CH}_3$  from 2 Leu), together with the epoxide signal in 2.85 ppm ( $\text{CH}_2\text{O}$ , d, 1H,  $J = 4.9$  Hz)/3.22 ppm ( $\text{CH}_2\text{O}$ , d, 1H,  $J = 5.1$  Hz) and the  $-\text{CH}_3$  of the epoxide in 1.48 ppm (s, 3H).



Scheme 20: Final coupling of the left and right hand fragments of Carfilzomib.

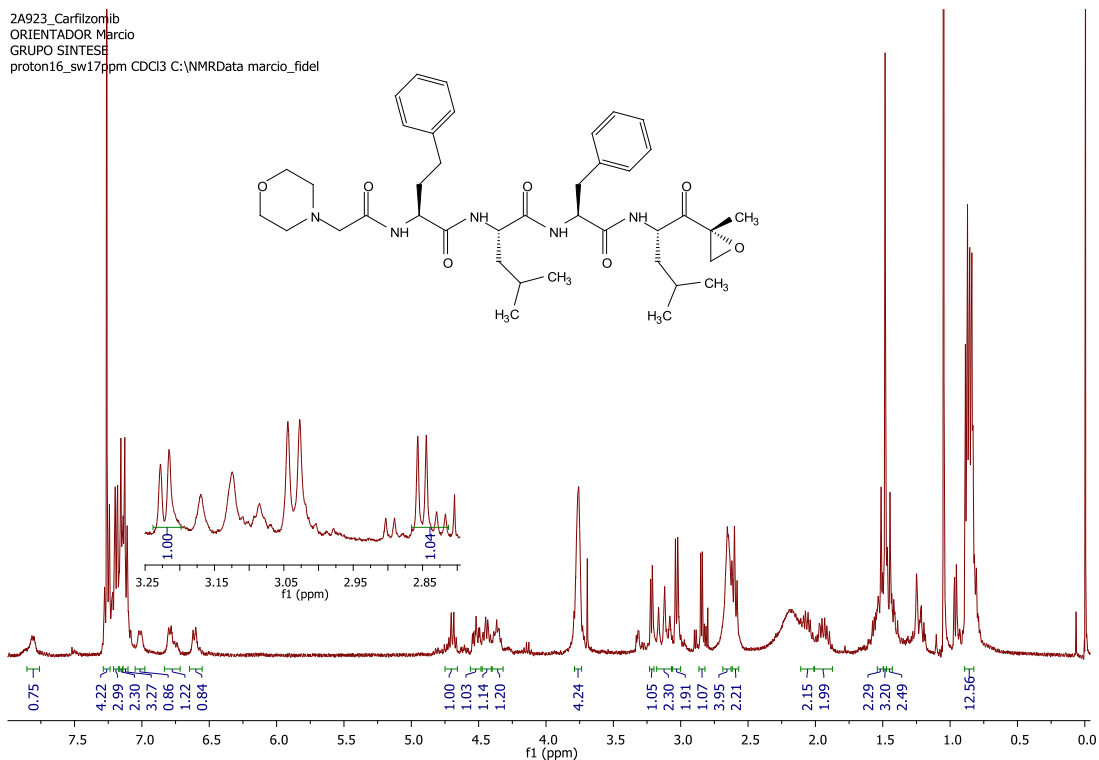


Figure 81:  $^1\text{H}$  NMR of Carfilzomib in  $\text{CDCl}_3$ , 400 MHz.

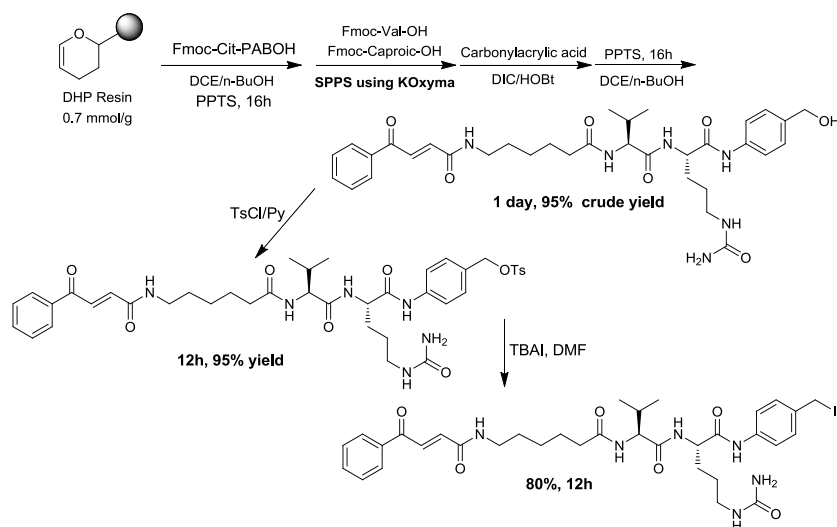
The total synthesis of Carfilzomib was accomplished in an overall yield of only 57% besides the improvement in the left-hand procedure of synthesis, fundamentally because the epoxidation process used was non-stereoselective.

### 3.3 Carbonylacrylic-Caproic-Val-Cit-PABOH linker preparation in solid phase.

As previously shown, the reported synthesis of Maleimido-Caproic-Val-Cit-PABOH linker using convergent solution phase synthesis is laborious and not efficient (5 days and 44% yield). A possible solid phase synthesis of this linker or a similar containing carbonylacrylic moiety instead of maleimido is desired. Carbonylacrylic moiety is preferred instead of maleimide because of the expected physiological instability in biological conditions. Initial attempts employing Cl-Trt-Chloride resin were not good enough because the coupling of alcohol (Fmoc-PAB-OH) to Trt produces only 10% yield (reaction in Py at 60 °C or using AgOTf as catalyst).<sup>211</sup> Accompanying to this, the subsequent coupling of Fmoc-Cit-OH to the deprotected  $\text{H}_2\text{N-PAB-O-Trt-Chloride}$  resin was unsuccessful with any coupling reagent, DIC/OxymaK, BTC/collidine or EEDQ. This could be due to the early cleavage of the PABOH during deprotection of Fmoc with piperidine 20% in DMF or the expected product (Fmoc-Cit-PABOH, attached in only 10%). To solve this problem, Fmoc-Cit-PABOH (90% yield) was prepared in liquid phase by coupling of Fmoc-Cit-OH with PABOH in the presence of the special coupling

reagent EEDQ. The attachment of this compound to Cl-Trt Chloride resin and later coupling of Val, 6-aminocaproic acid and carbonylacrylic acid afforded the expected product in less than 10% yield.

After a literature review, we found a special resin for the attachment of alcohols, named DHP-resin. It contains a dihydropyran linker that after reaction with alcohol in the presence of strong acid catalyst (TsOH, 0.1 equiv.) furnishes the alcohol attached to a tetrahydropyrane forming acetal in high yield. The cleavage is realized by treatment with the weak acid PPTS at 60 °C (pyridinium p-toluensulfonate). The attachment of Fmoc-Cit-PABOH to this resin occurred in almost quantitative yield and the following couplings of Val, caproic acid and carbonylacrylic acid permitted to obtain the expected product (which we will call Linker-OH from now on) in more than 95% yield, in only 2 days (Scheme 21). This route represents a great improvement in the synthesis of this type of linkers and for the first time includes the introduction of the carbonylacryl Michael-acceptor. It is important to mention that the couplings of Val and caproic acid were performed using DIC/OxymaK, but in the last step (attachment of the carbonylacrylic acid), it was necessary to use DIC/Oxyma coupling agent since OxymaK reacted with the double bond of the Michael-acceptor.



Scheme 21: Solid phase synthesis of the Linker-OH using DHP-resin.

The  $^1\text{H-NMR}$  spectra of the Linker-OH is presented in the Figure 82. The signals of the hydrogens **a** and **b** can be confirmed by the presence of two doublets in 7.88 ppm (**a**,  $J = 15.4$  Hz, 1H) and 7.01 ppm (**b**,  $J = 15.4$ , 1H), with a coupling constant of 15.4 Hz for the *trans* geometry of the olefin. The two peptidic  $-N\text{-CH-CO-}$  (**c** and **d**) hydrogens can be identified by the signal in 4.40 ppm (**c**, dd,  $J = 9.0, 4.7$  Hz, 1H) and the doublet in 4.19 ppm (**d**, d,  $J = 7.4$  Hz, 1H). The two  $\text{CH}_3$  groups of the Valaminoacid (**e**) can be confirmed by the doublet of

doublets in 0.98 ppm (dd,  $J = 8.6, 6.8$  Hz, 6H). The multiplets from the aminoacids side chains (Cit and 6-aminohexanoic) are distributed from 3.6 and 1.4 ppm. The aromatic phenyl rings of carbonylacrylic and PABOH appear in 8.08–7.99 ppm (m, 2H), 7.72–7.65 ppm (m, 1H) and 7.61–7.53 ppm (m, 2H). In the  $^{13}\text{C}$  NMR spectra is possible to observe seven carbonyl signals between 191.9 and 162.24 ppm, four aromatic and two olefin signals from 138.0 and 129.9 ppm, two peptidic  $-N\text{-CH-CO-}$  in 60.5 and 53.4 ppm followed by nine singlets between 40.5 and 18.8 ppm corresponding to the Cit, Val, and 6-aminohexanoic acid.

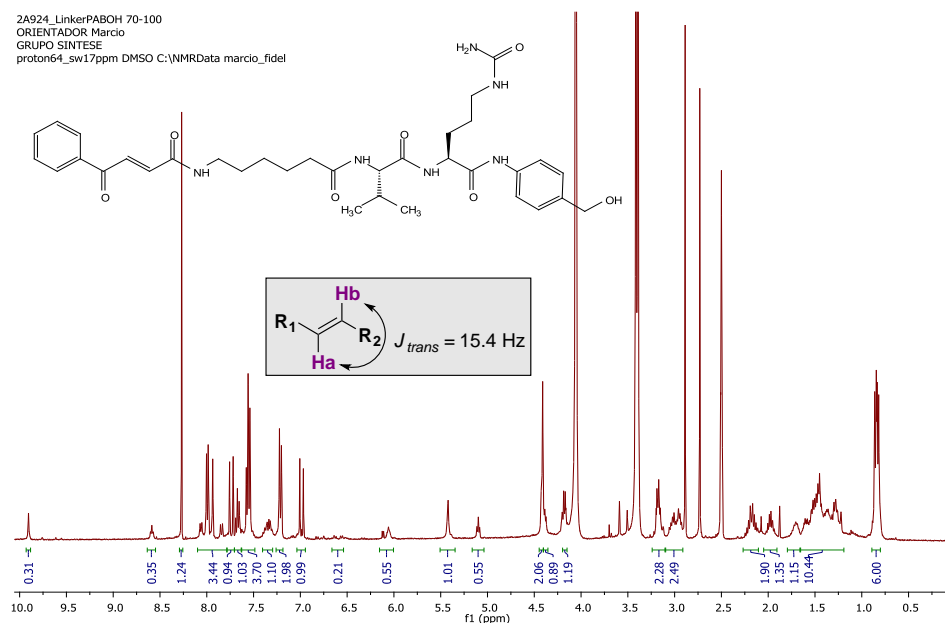


Figure 82:  $^1\text{H}$ -NMR of the Linker-OH in DMSO- $d_6$ .

The ESI-MS of the Linker-OH (crude cleavage product) show masses corresponding to the pyridinium charged molecule due to the presence of PPTS in the cleavage crude material (Figure 83).

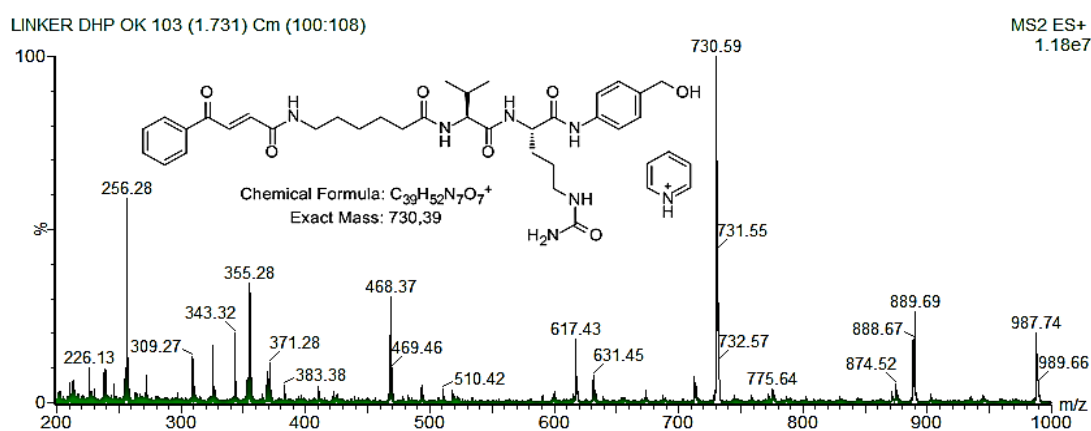


Figure 83: ESI-MS of the crude Linker-OH.

We then proceeded to the chlorination reaction using thionyl chloride and DMF as solvent/catalyst. This reaction proceeds efficiently (70%) and does not affect the carbonylacrylic motif. However, as reported previously,<sup>199</sup> the Menshutkin reaction (formation of quaternary salts by reaction of benzyl chlorides with tertiary amines) of this linker with Carfilzomib gives poor yields (15-30%, in the presence of TBAI as catalyst). It is known that bimolecular substitution reactions ( $S_N2$ ) are influenced by the nature of the leaving group. In some cases, an iodine source is used as catalyst when bromo or chloro should be substituted. The tosylation of the Linker-OH and then substitution with iodide allows to obtain a linker with efficient yield in the reaction with tertiary amine and only implies an additional step in the total process. Tosylation of the Linker-OH was performed quantitatively with tosyl chloride in Py. The ESI-MS of the crude showed the same behavior that in case of Linker-OH, the signal of double charged species produces by the simultaneous protonation and pyridinium was present (Figure 84).

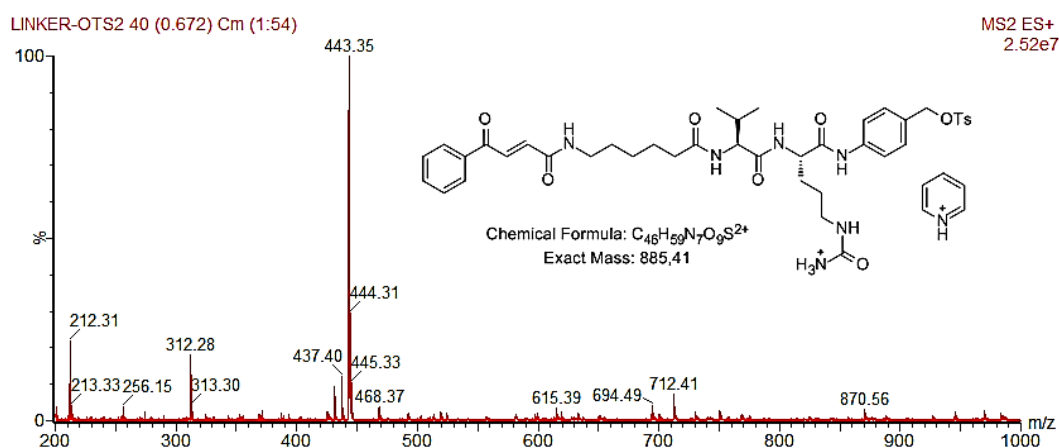


Figure 84: ESI-MS of the Linker-OTs.

The final reaction of the Linker-OTs with TBAI afforded the Linker-I in good yield after 24 h of reaction. The characterization by  $^1H$ -NMR (Figure 85), ESI-MS (Figure 86) and ESI-HRMS (Figure 87) validated the structure after purification by *flash* chromatography.

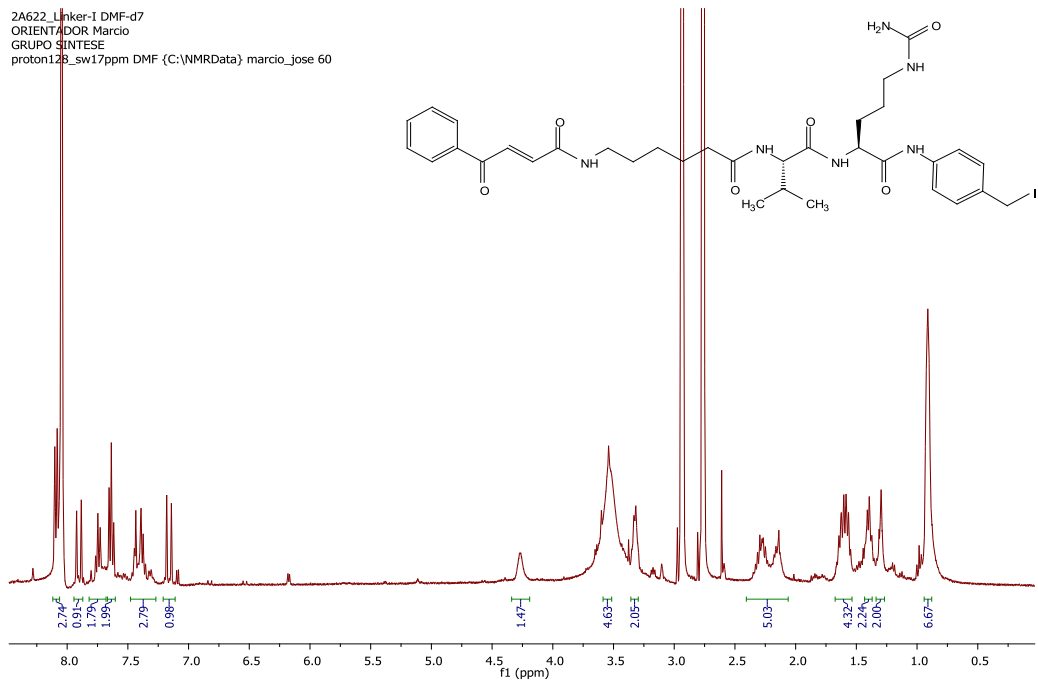


Figure 85:  $^1\text{H-NMR}$  of the Linker-I in DMF-d7, 400 MHz.

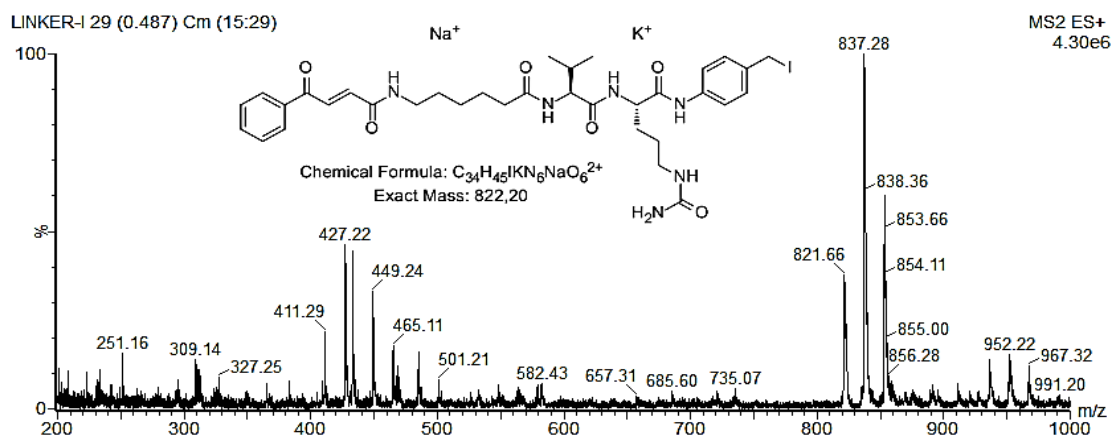


Figure 86: ESI-MS of the Linker-I.

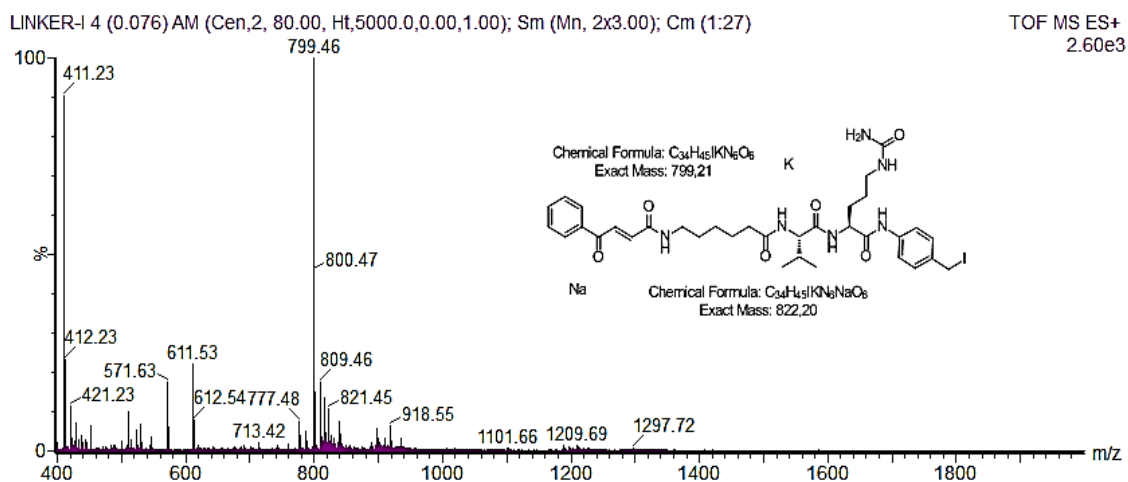


Figure 87: ESI-HRMS of the Linker-I.

### 3.4 pHLIP-Variant3 synthesis containing Cys at *N* or *C*-terminals

Low pH insertion peptide pHLIP-Variant3 (ACDDQNPWRAYLDLLFPTDTLLLDLLW) is a novel marker of acidic malignant lesions. By using  $^{31}\text{P}$  magnetic resonance spectroscopy (MRS), Tapmeier et al. demonstrated that pHLIP-Variant3 was retained in tumors of pH equal to or less than 6.7, but not in tissues of higher pH. Acidic pH may distinguish aggressive from more indolent cancers. Using pHLIP Variant3, they showed the ability to detect cancer with a low false-positive rate in a genetically engineered model of murine breast cancer, paving the way for testing this probe in clinical situations.

pHLIP-Variant3 peptide possesses a Cys residue at the *N*-terminal, making it a special candidate for the conjugation to anticancer drugs through sulphur addition to carbonylacryl containing linkers. This construct could target cancer cells by the characteristic low pH that presents. After insertion of the pHLIP-Variant3 peptide into the membrane by the *C*-terminal, linker-drug at the *N*-terminal stays outside the membrane. Besides the final cleavage of the drug from the linker occurs in lysosomes after the total internalization, a pHLIP variant containing Cys at *C*-terminal is desired, although that it could affect the insertion of pHLIP into the membrane. We decided to synthesize the two variants, Cys at *C*-terminal or at *N*-terminal and finally determine the best by biological tests.

The synthesis was carried out by successive coupling of aminoacids with DIC/Oxyma in the Wang-Resin to obtain the free carboxylic acid at the *C*-terminal of peptides. Cleavage in the presence of EDT was needed to avoid oxidation of Cys during concentrated TFA treatment. RP-HPLC of the crude product showed more than 80% peptidic purity (70% yield) for both cases (Figure 112) and retention times of 33 min for pHLIP-Variant3 containing Cys at *N*-terminal and 34.7 min for the variant containing Cys at *C*-terminal. ESI-HRMS spectra indicated the expected molar mass of the products and two fragments due to inevitable ionization cleavage at the second Pro of the sequences. MALDI (soft ionization technique) analysis corroborated the existence of both structures without fragmentation (Figure 88, Figure 89).



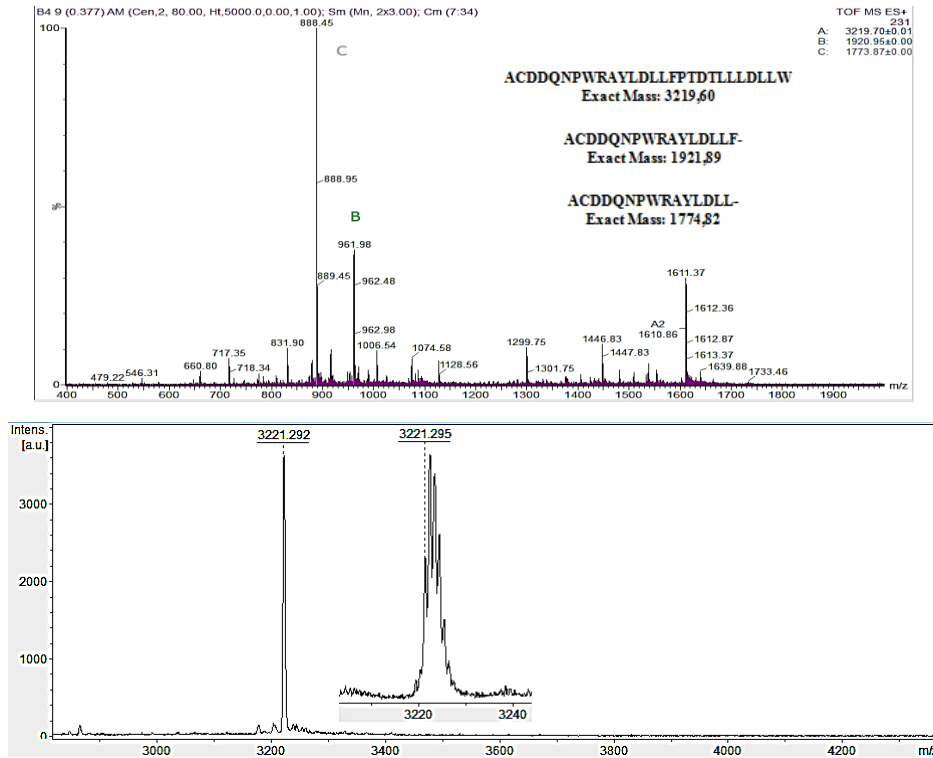


Figure 88: ESI-HRMS (upper panel) and MALDI (lower panel) spectra of the pHLIP peptide containing Cys at C-terminal (AADDQNPWRAYLDLLFPTDLLLLDLCW).

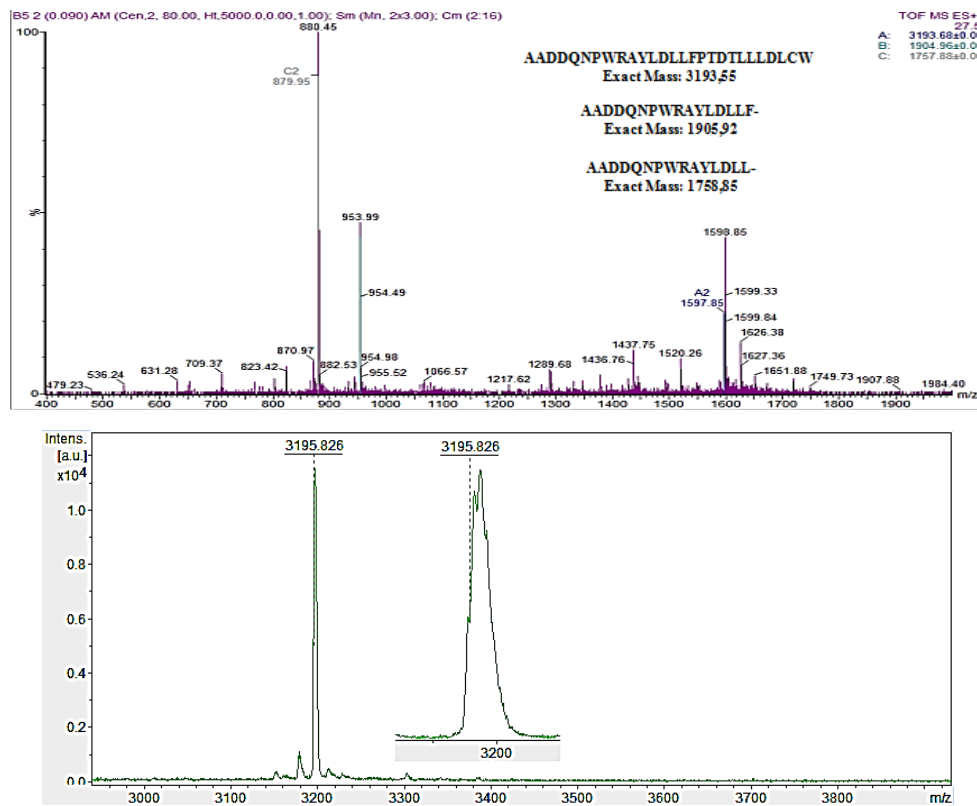
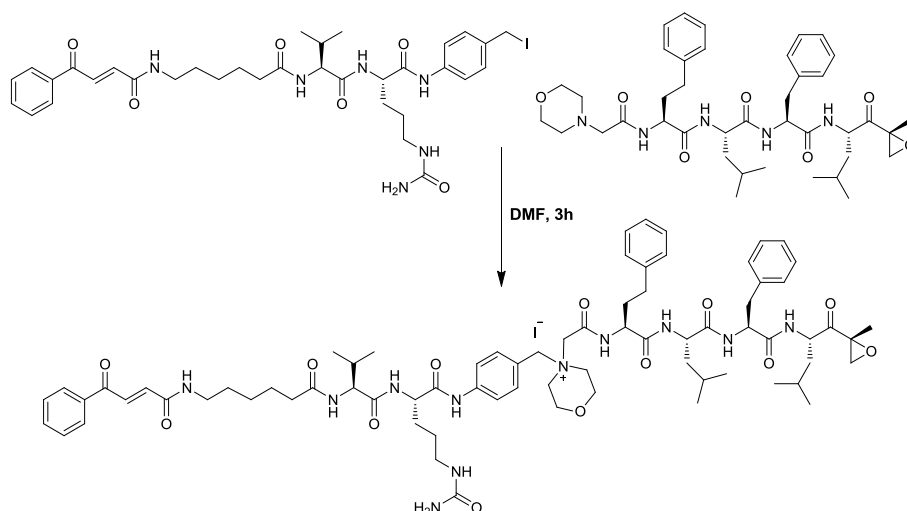


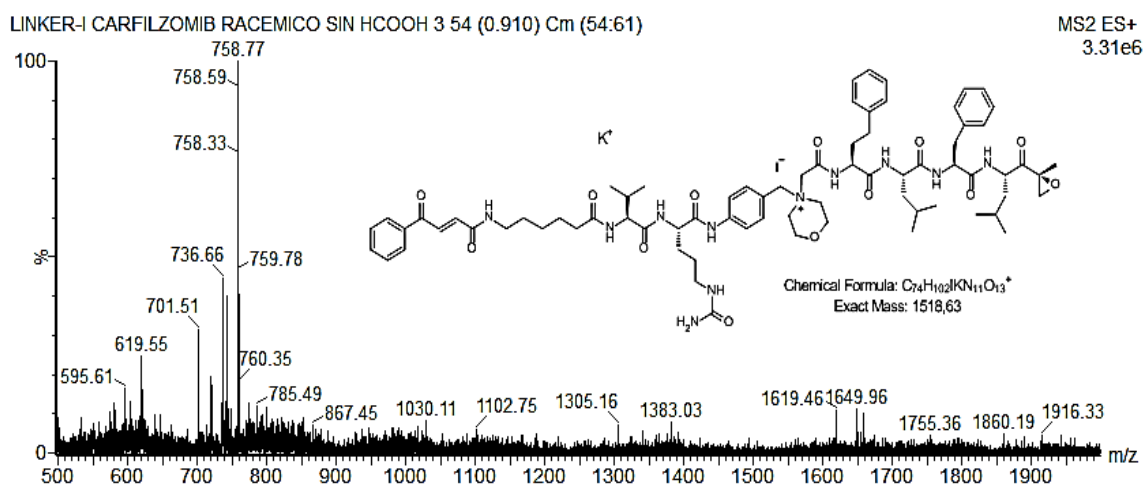
Figure 89: ESI-HRMS (upper panel) and MALDI (lower panel) spectra of the pHLIP peptide containing Cys at N-terminal (ACDDQNPWRAYLDLLFPTDLLLLDLLW).

### 3.5 Carfilzomib coupling to Linker-I

With the pure Carfilzomib and Linker-I in hand, we developed the Menshutkin reaction between them in DMF at room temperature (Scheme 22). After 3 h of reaction, we observed the total consumption of Carfilzomib in TLC analysis but after precipitation in diethylether, only 48 % yield was obtained. This represents a great advance in reaction time and conversion when is compared with the previously reported method using Linker-Cl. The ESI-MS confirmed the expected molecular mass of the product (Figure 90) and indicate good stability when ionization is achieved in presence of HCOOH, besides showed different ionization behavior.



Scheme 22: Coupling of the Linker-I to Carfilzomib.



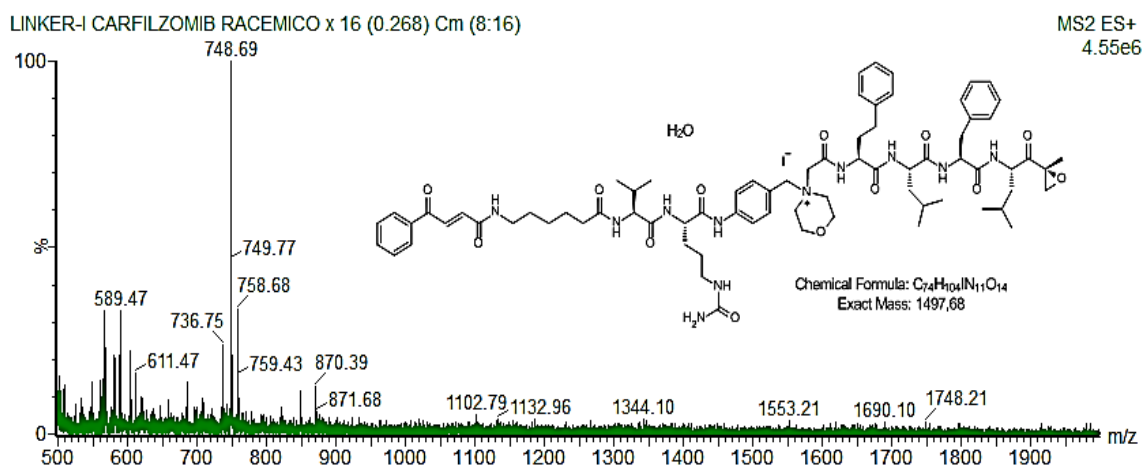


Figure 90: ESI-MS of the Linker-Carfizomib salt in presence of HCOOH (upper panel) or without HCOOH (lower panel).

### 3.6 Final coupling of pHLIP to Linker-Carfizomib by thiol-Michael addition.

Treating carbonylacrylic derivatives Linker-I in a solution of MeCN/sodium phosphate buffer (NaPi) (pH 8.0, 50 mM) at room temperature, for 12 h and inert atmosphere to avoid the Cys oxidation by oxygen, gave excellent isolated yield of the desired cysteine-conjugates (Scheme 23). RP-HPLC analysis (Figure 91) showed more than 60% of conversion and a change in retention time (from 39 min to 41 min) of the starting material, pHLIP-Variant3 (Cys at the *N*-terminal, B5 in Experimental Seccion, Figure 112). ESI-HRMS (Figure 92), show fragmentations similar to pHLIP peptides and MALDI analysis will be performed in future experiments.

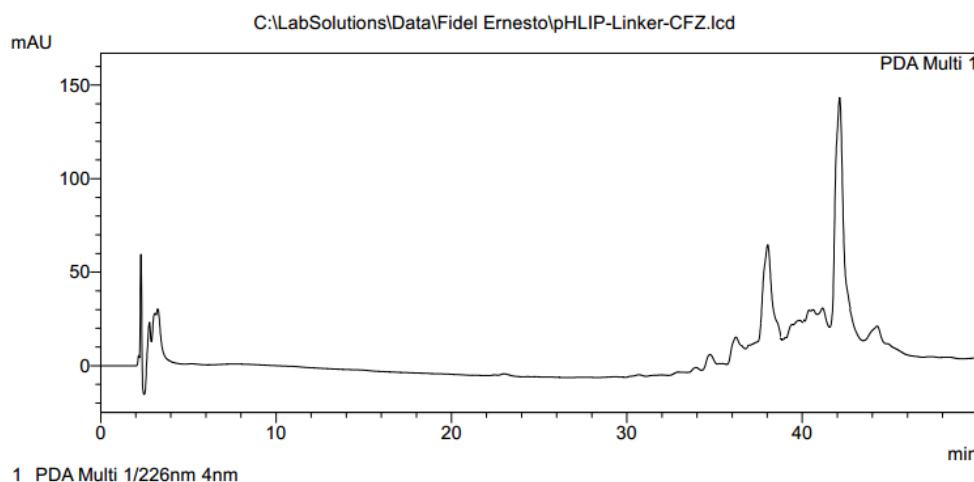
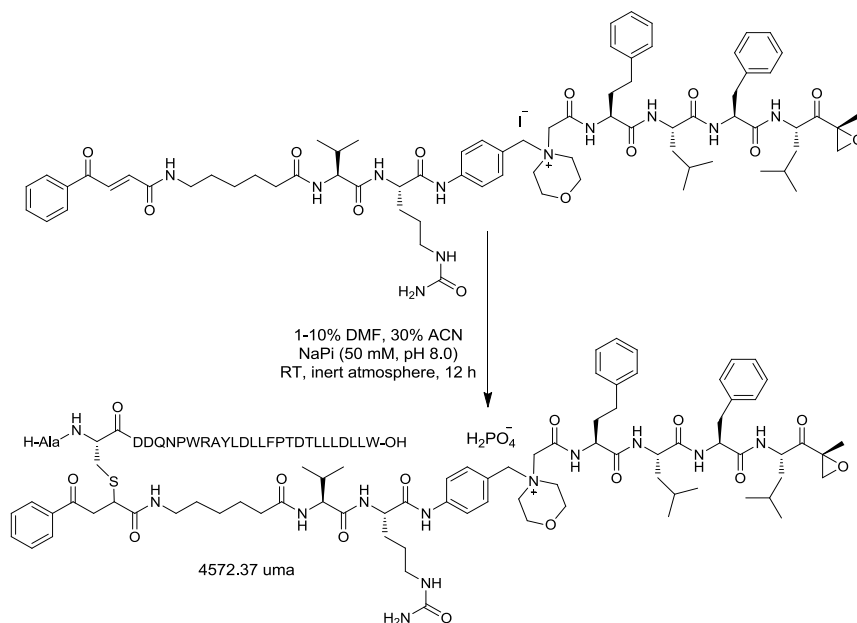


Figure 91: RP-HPLC of the bioconjugation of Linker-CFZ salt with pHLIP-Variant3 containing Cys at the *N*-terminal.

The binding of Carfizomib to pHLIP instead of an antibody eliminates all the disadvantages of ADCs, especially those related to the masking of tumor cells. On the other hand, the production

of pHLIP is simpler, less expensive and has shown to be proteolytically stable. The linker guarantees, together with pHLIP peptide, the targeted release of the drug, in addition to releasing it without chemical modifications (traceless approach).



Scheme 23: Final conjugation of Linker-CFZ salt to pHLIP-Variant3 peptide containing Cys at the *N*-terminal. NaPi should cause the interchange of iodo by dihydrogenphosphate.

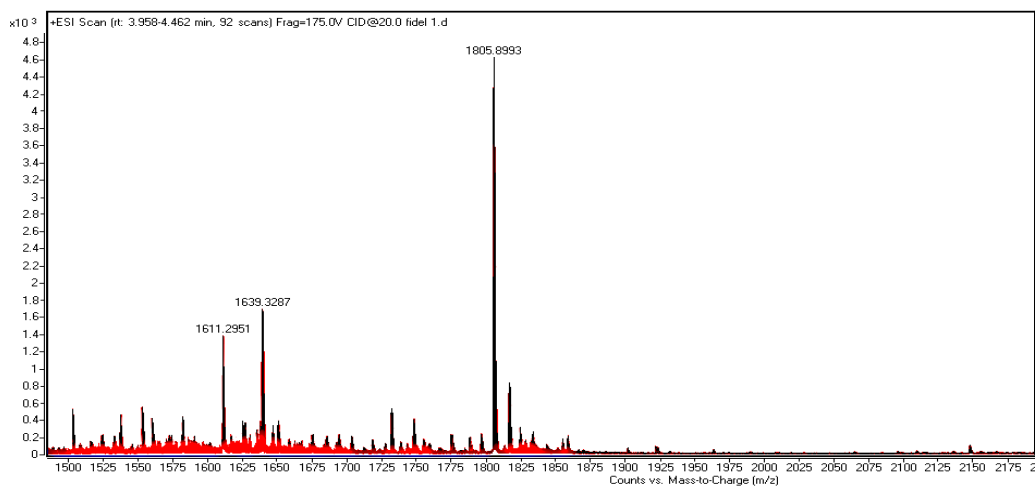


Figure 92: ESI-HRMS of the bioconjugate pHLIP-Variant3-Linker-CFZ.

### Conclusions. Chapter 3

✓ Carfilzomib was synthesized in 45% yield by combination of SPPS using OxymaK (including the synthesis of morpholino acetyl by morpholine bimolecular substitution of bromoacetyl) and final coupling of Leu-epoxide.

✓ A new carbonylacrylic-traceless-linker solid phase synthetic method was developed; in which iodo was used as leaving group to improve the yield during reaction with tertiary amine drugs (Carfilzomib).

✓ pHLIP peptide containing Cys at the *C* and *N* terminals was synthesized in solid phase with good yield and peptidic purity.

✓ For the first time, a PDCs containing pHLIP, Carfilzomib and a carbonylacrylic container linker (self-immolative and enzymatically cleavable) were obtained.

### **Future works. Chapter 3**

- ✓ Evaluate the anticancer effectiveness and reduction of adverse effect of Carfilzomib using the pHLIP-Variant3-Linker-CFZ conjugate of our work.

## **4 Experimental Section. Chapter 3**

### **4.1 General Remarks**

#### **4.1.1 Materials**

In this section was used the same materials, method of peptide synthesis, peptide cleavage, analytical RP-HPLC, ESI-HRMS and semipreparative RP-HPLC as described in sections 4.1.1-4.1.3 and 4.1.6-4.1.8 of Chapter 1 and section 4.1.2 for NMR conditions of Chapter 2.

Cl-Trt Chloride Polystyrene Resin (1.47 mmol/g), Wang Polystyrene Resin (1.7 mmol/g) and DHP-Polystyrene Resin (1.56 mmol/g) were obtained from commercial suppliers.

#### **4.1.2 MALDI-TOF**

Low-energy MALDI spectra were obtained in the LaBioMI, UFSCar, Brazil. All spectra were obtained with the sample deposited on a MALDI ground steel target plate (MTP 384, Bruker Daltonics®) loaded onto a MALDI-TOF MS AutoFlex Speed (Bruker Daltonics®) and  $\alpha$ -cyano-4-hydroxycinnamic acid as matrix. The MALDI-TOF MS equipment was operated using Flex Control 3.3 software (Bruker Daltonics®). The positively-charged ions were generated with a Smartbeam™ laser at 355 nm, 50 Hz frequency, PIE (Pulsed Ion Extraction) of 120 ns and voltage of 2.60 kV lenses. The voltage of the ion sources was 5.99 kV in the first ion source and 5.23 kV in the second. The ions were separated using the TOF operating in linear mode. The spectra were generated with an average of 10,000 laser shots per spectrum, with power ranging between 70% and 90%, with attenuations (laser offset) of 15–28%. For peak position, a 75% cut off above the base line level (percent height) was specified. For the exportation of the raw spectra, the Flex Analysis 3.3 software (Bruker Daltonics®) was used. The calibration was performed using Protein Calibration Standard I (Insulin,  $[M+H]^+$  at  $m/z$  5734.51, Ubiquitin I,  $[M+H]^+$  at  $m/z$  8565.76) from Bruker Daltonics®, in a mass range of 2 to 10 kDa.

#### **4.1.3 ESI-MS**

Low-energy ESI-MS spectra were obtained in the CERSusChem, UFSCar, Brasil, by using a time-of-flight TOF instrument (Waters, Milford, MA, USA) equipped with a electrospray ion source in positive ion mode. Peptide solutions were prepared dissolving the crude of reaction in a solution of HCOOH 1% in MeOH and loaded into a metal-coated borosilicate capillary tip (Proxeon, Denmark), inserted into the Z-spray flow electrospray ion source, and slightly pressured with nitrogen to guarantee their stable spray during measurement. The capillary and cone voltage were set to 100 to 300 and 5 to 50 eV, respectively. Mass spectra were acquired in the  $m/z$  range of 200–1000 Th. Electrospray ionization mass spectrometry spectra were

processed using the MassLynx version 4.1 program (Micromass, England). Protonated molecular ions (M+H)<sup>+</sup>, sodium adducts (M+Na)<sup>+</sup> or potassium adducts (M+K)<sup>+</sup> were used for empirical formula confirmation.

## 4.2 Synthesis of the left-hand fragment of Carfilzomib: Morf-Ac-Hph-Leu-Phe-OH

### 4.2.1 Loading of Fmoc-Phe-OH to Cl-Trt Chloride resin (1.47 mmol/g)

NOTE: It is important to dry all solvents and glassware before use. Fmoc-aminoacids are best dried before use by repeated evaporation from dioxane. The carboxylic acid (1.2 eq. relative to the resin) and DIPEA (4 eq) is dissolved in dry DCM (approx. 10 mL per gram of resin) containing, if necessary, a small amount of dry DMF (just enough to facilitate dissolution of the acid). This mixture is added to the pre-swelled resin and stir for 1-2 h. At the end of this time, the resin was washed with 3x DCM/MeOH/DIPEA (17:2:1), 3x DCM; 2x DMF, 2x DCM, dried in vacuum and weigh to check the quantity of Fmoc-aminoacid loading (95% loading).

Subsequent couplings of Fmoc-Leu-OH, Fmoc-Hph-OH, BrHAc and substitution of bromo by morpholino were conducted followig the general peptide synthesis protocol in Section 4.1.2, Chapter 1. The only difference was the use of OxymaK racemization inhibitor instead of Oxyma in aim of delimitate the early cleavage from the resin. Bromo substitution by morpholino was performed similarly to the deprotection of the Fmoc group by piperidine 20% in DMF.

### 4.2.2 Cleavage of Morf-Ac-Hph-Leu-Phe-OH with TFA/DCM

The peptidyl Cl-Trt Chloride resin was treated at room temperature with TFA 1% in DCM (2:8) (10 x 2 min). After the appropriate time, the resin was removed by filtration, washed with MeOH and Et<sub>2</sub>O and dried in vacuum to check the loss of mass (100% losses). Combined filtrates are evaporated to dryness. TFA sal of the product is obtained.

**ESI-HRMS *m/z***: 567.47±0.00 [M+H]<sup>+</sup>, calcd. for [C<sub>31</sub>H<sub>42</sub>N<sub>4</sub>O<sub>6</sub>]<sup>+</sup>: 567.31

**<sup>1</sup>H NMR** (400 MHz, CDCl<sub>3</sub>) δ: 7.26 – 7.21 (m, 4H), 7.21 – 7.15 (m, 4H), 7.11 (d, *J* = 6.9 Hz, 2H), 4.66 (dd, *J* = 14.0, 8.8 Hz, 1H), 4.37 (dd, *J* = 14.2, 8.4 Hz, 1H), 4.26 (dd, *J* = 13.5, 6.9 Hz, 1H), 4.03 – 3.86 (m, 6H), 3.49 (s, 2H), 3.23 (dd, *J* = 14.0, 4.6 Hz, 2H), 3.13 – 3.00 (m, 1H), 2.94 (dd, *J* = 13.7, 9.4 Hz, 1H), 2.80 – 2.57 (m, 2H), 2.15 – 1.95 (m, 2H), 1.53 – 1.38 (m, 2H), 1.37 – 1.21 (m, 2H), 0.78 (d, *J* = 6.2 Hz, 3H), 0.71 (d, *J* = 6.0 Hz, 3H).

**<sup>13</sup>C NMR** (100 MHz, CDCl<sub>3</sub>) δ: 174.42, 173.39, 172.93, 164.34, 140.06, 136.22, 129.27 (2xCH), 128.59 (2xCH), 128.52, 128.35, 127.03, 126.43, 63.61, 63.27, 57.46, 55.80, 53.76, 53.48, 53.11, 40.42, 37.42, 33.46, 32.12, 24.73, 22.45, 21.55, 17.67 (2xCH<sub>3</sub>), 12.25.



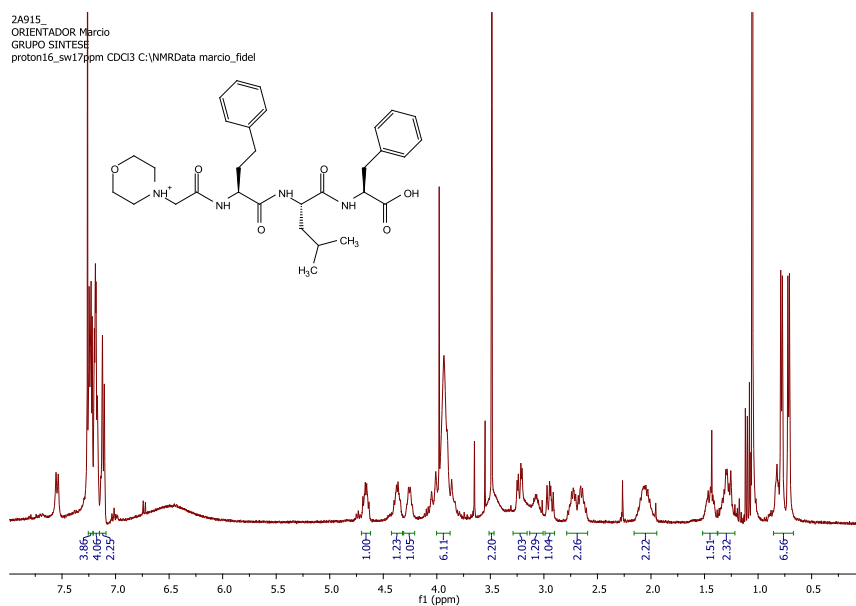


Figure 93:  $^1\text{H}$  NMR of the left hand fragment of Carfilzomib in  $\text{CDCl}_3$ , 400 MHz.

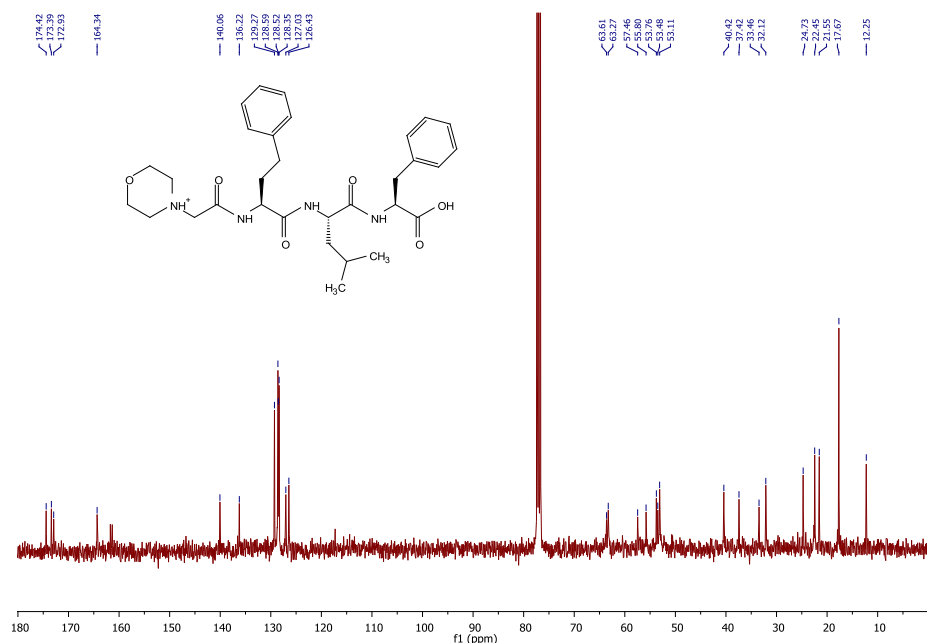


Figure 94:  $^{13}\text{C}$  NMR of the left hand fragment of Carfilzomib in  $\text{CDCl}_3$ , 100 MHz.

### 4.3 Synthesis of the left-hand fragment of Carfilzomib

#### 4.3.1 Synthesis of Boc-Leu-derived Weinreb amide

To a solution of Boc-Leu-OH (336 mg, 1.26 mmol) and TBTU (497 mg, 1.54 mmol) in THF (10 mL) at  $0^\circ\text{C}$  was added a solution of HCl salt of *N,O*-dimethylhydroxylamine (350 mg, 1.26 mmol) in THF (3 mL) followed by DIPEA (660  $\mu\text{L}$ , 3 mmol). The mixture was stirred at  $-20^\circ\text{C}$  to rt for 12h, quenched by the addition of saturated HCl (5% aq) and extracted with EtOAc. The organic layer was washed one more time with HCl (5% aq), two times with saturated  $\text{NaHCO}_3$

(aq), brine, dried over Na<sub>2</sub>SO<sub>4</sub> and the solvent was removed under reduced pressure. Column chromatography (10:1 to 5:1 Hexane:EtOAc) gave 470 mg (93%) of Boc-Leu-derived Weinreb amide.

**R<sub>f</sub>** = 0.58 (Hexane/EtOAc 8:2)

**<sup>1</sup>H NMR** (400 MHz, CDCl<sub>3</sub>) δ: 5.06 (d, *J* = 8.9 Hz, 1H), 4.73 (td, *J* = 9.2, 2.9 Hz, 1H), 3.79 (s, 3H), 3.20 (s, 3H), 1.82 – 1.65 (m, 2H), 1.43 (s, 10H), 0.97 (d, *J* = 6.5 Hz, 3H), 0.93 (d, *J* = 6.7 Hz, 3H).

**<sup>13</sup>C NMR** (100 MHz, CDCl<sub>3</sub>) δ: 173.90, 155.65, 79.46, 61.59, 48.97, 42.09, 32.14, 28.35, 24.72, 23.35, 21.57.

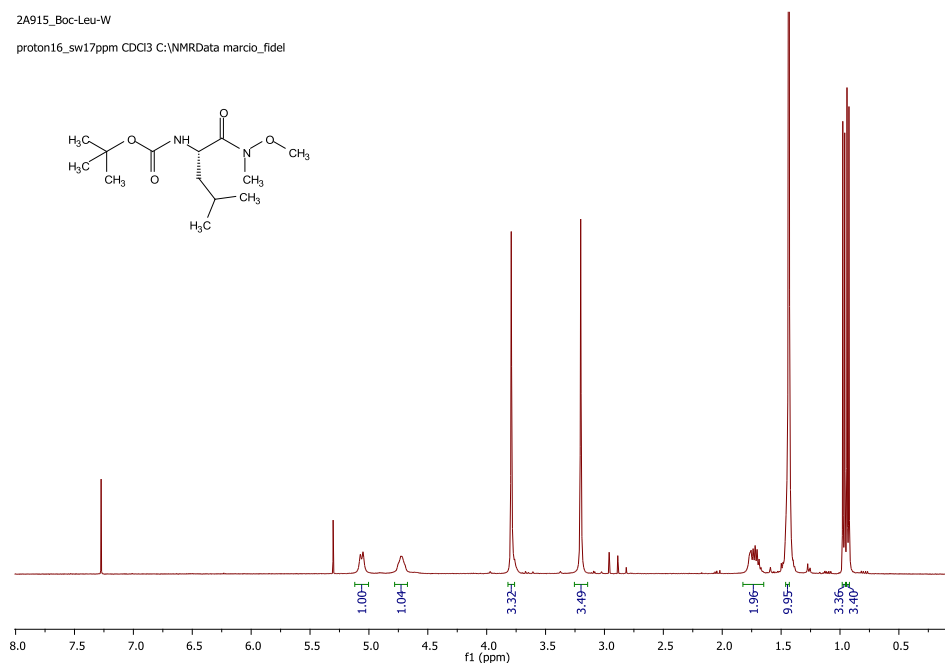


Figure 95: <sup>1</sup>H NMR of Boc-Leu-Weinreb amide derivative in CDCl<sub>3</sub>, 400 MHz.

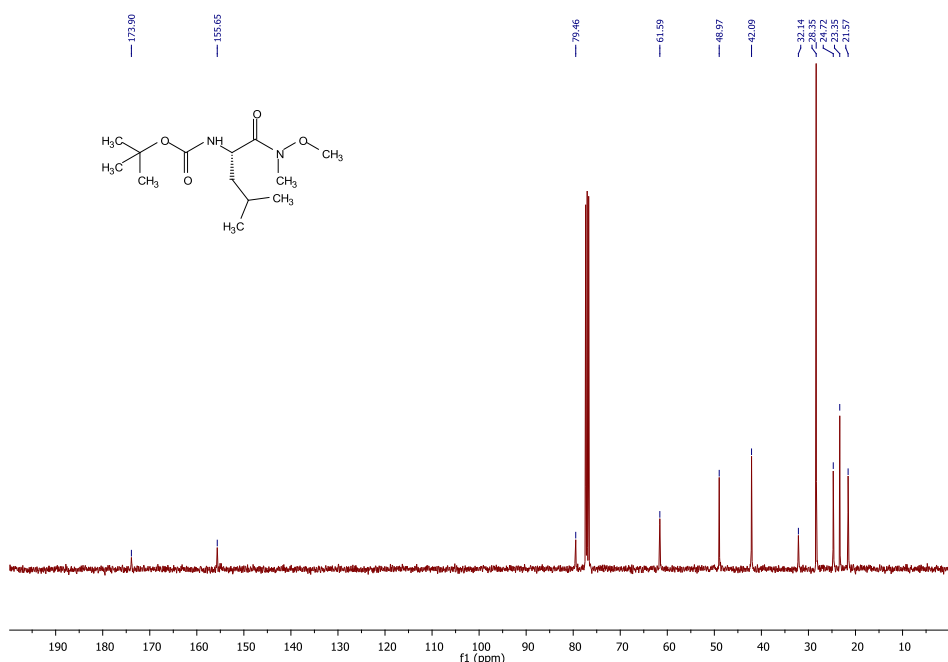


Figure 96:  $^{13}\text{C}$  NMR of Boc-Leu-Weinreb amide derivative in  $\text{CDCl}_3$ , 100 MHz.

#### 4.3.2 Synthesis of Boc-Leu-derived *iso*-propenyl ketone

In a Schlenk tube equipped with septum and magnetic stirring bar, Boc-Leu-Weinreb amide (470 mg, 1.71 mmol) was cooled to  $0\text{ }^\circ\text{C}$ . A solution of isopropenylmagnesium bromide in THF (0.5 M, 10.3 mL, 5.14 mmol, 3 equiv.) was added dropwise. The reaction was maintained at  $0\text{ }^\circ\text{C}$  for one hour, warmed to rt and stirred for 5-6 hours until full conversion was detected by TLC (Hexane/EtOAc 9:1). The reaction was cooled to  $0\text{ }^\circ\text{C}$  and quenched by addition of saturated  $\text{NH}_4\text{Cl}$  (5 mL) and water (10 mL). The mixture was extracted with 3x10 mL of  $\text{Et}_2\text{O}$ . Layers were separated and the aqueous phase was extracted with EtOAc (2x250 mL). The combined organic layer was washed with HCl (5% aq), saturated  $\text{NaHCO}_3$ , brine, dried over  $\text{Na}_2\text{SO}_4$  and the solvent was removed under reduced pressure to afford 500 mg of crude product. Purification by *flash* chromatography using a gradient elution mixture (10:1 to 8:2 hexane/EtOAc) gave 349 mg (80%) of the product, which solidifies upon standing at  $8\text{ }^\circ\text{C}$ .

$R_f$  = 0.43 (Hexane/EtOAc 9:1)

$^1\text{H}$  NMR (400 MHz,  $\text{CDCl}_3$ )  $\delta$ : 6.07 (s, 1H), 5.87 (s, 1H), 5.13 (d,  $J$  = 8.1 Hz, 1H), 5.05 (td,  $J$  = 9.2, 2.9 Hz, 3H), 1.89 (s, 3H), 1.78 – 1.66 (m, 1H), 1.42 (s, 10H), 1.36 – 1.28 (m, 1H), 0.99 (d,  $J$  = 6.5 Hz, 3H), 0.90 (d,  $J$  = 6.7 Hz, 3H).

$^{13}\text{C}$  NMR (100 MHz,  $\text{CDCl}_3$ )  $\delta$ : 201.64, 155.55, 142.28, 126.09, 79.57, 52.56, 43.18, 28.33, 24.95, 23.37, 21.74, 17.84.

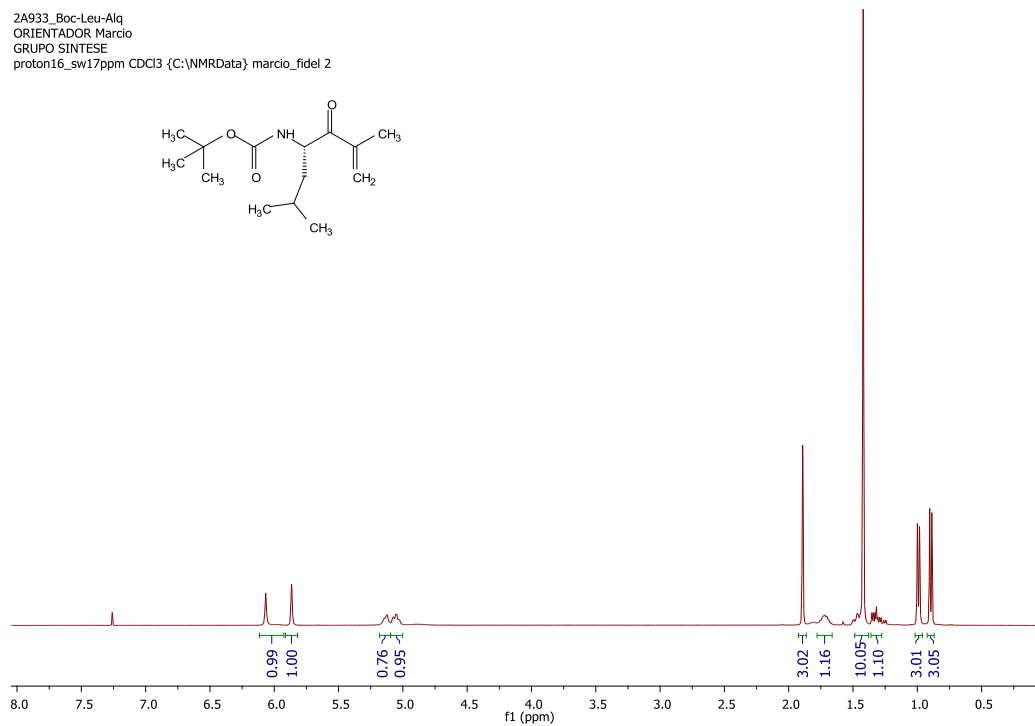


Figure 97:  $^1\text{H}$  NMR of Boc-Leu-Alkene in  $\text{CDCl}_3$ , 400 MHz.

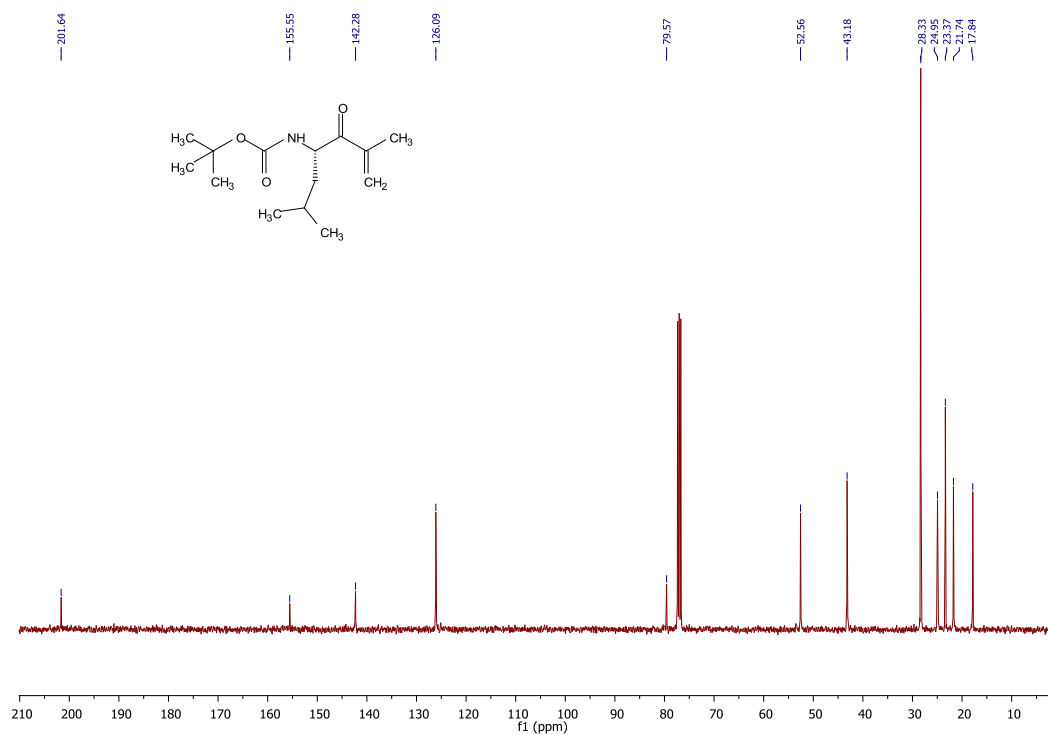


Figure 98:  $^{13}\text{C}$  NMR of Boc-Leu-Alkene in  $\text{CDCl}_3$ , 100 MHz.

### 4.3.3 Epoxidation of Boc-Leu-derived *iso*-propenyl ketone

349 mg of the vinylketone (1.36 mmol) were dissolved in 10 mL of MeOH and the solution was cooled to 0°C. Subsequently 400 µL of 30% H<sub>2</sub>O<sub>2</sub> (ac) (2.6 eq) in 1 mL of MeOH and 45 mg KOH (0.5 eq) dissolved in 1 mL of MeOH was added drop wise. The mixture was stirred overnight and then allowed to reach room temperature. The mixture was hydrolyzed with 15 mL of water and the product was extracted with 2x50 mL of DCM. The combined organic phases were washed with 50 mL of 1M Na<sub>2</sub>S<sub>2</sub>O<sub>3</sub> (ac) and brine. After evaporation to dryness 200 mg (50%) of a white solid was isolated, which contains an approximate 4:1 ratio of two diastereomers of the desired product as judged by <sup>1</sup>H-NMR (Figure 99). Purification by *flash* chromatography using a gradient elution mixture (10:1 to 8:2 hexane:EtOAc) gave 150 mg of the BocLeu-Epoxide-A (Figure 100, Figure 101) and 40 mg of the BocLeu-Epoxide-B (Figure 102), which crystallizes upon standing at 8 °C.

R<sub>f</sub> = 0.4 (Hexane/EtOAc 9:1)

<sup>1</sup>H NMR (400 MHz, CDCl<sub>3</sub>) δ: 4.84 (d, *J* = 7.7 Hz, 1H), 4.32 (t, *J* = 8.8 Hz, 1H), 3.29 (d, *J* = 4.8 Hz, 1H), 2.88 (d, *J* = 5.0 Hz, 1H), 1.79 – 1.60 (m, 1H), 1.51 (s, *J* = 8.2 Hz, 1H), 1.41 (s, 1H), 1.22 – 1.12 (m, 1H), 0.95 (dd, *J* = 12.9, 6.6 Hz, 1H).

<sup>13</sup>C NMR (100 MHz, CDCl<sub>3</sub>) δ: 209.57, 155.46, 79.74, 58.97, 52.32, 51.40, 40.45, 28.31, 25.08, 23.39, 16.77.

2A929\_Boc-Leu-Epox  
 ORIENTADOR Marcio  
 GRUPO SINTESIS  
 proton16\_sw17ppm CDCl3 {C:\NMRData} marcio\_fidel 29

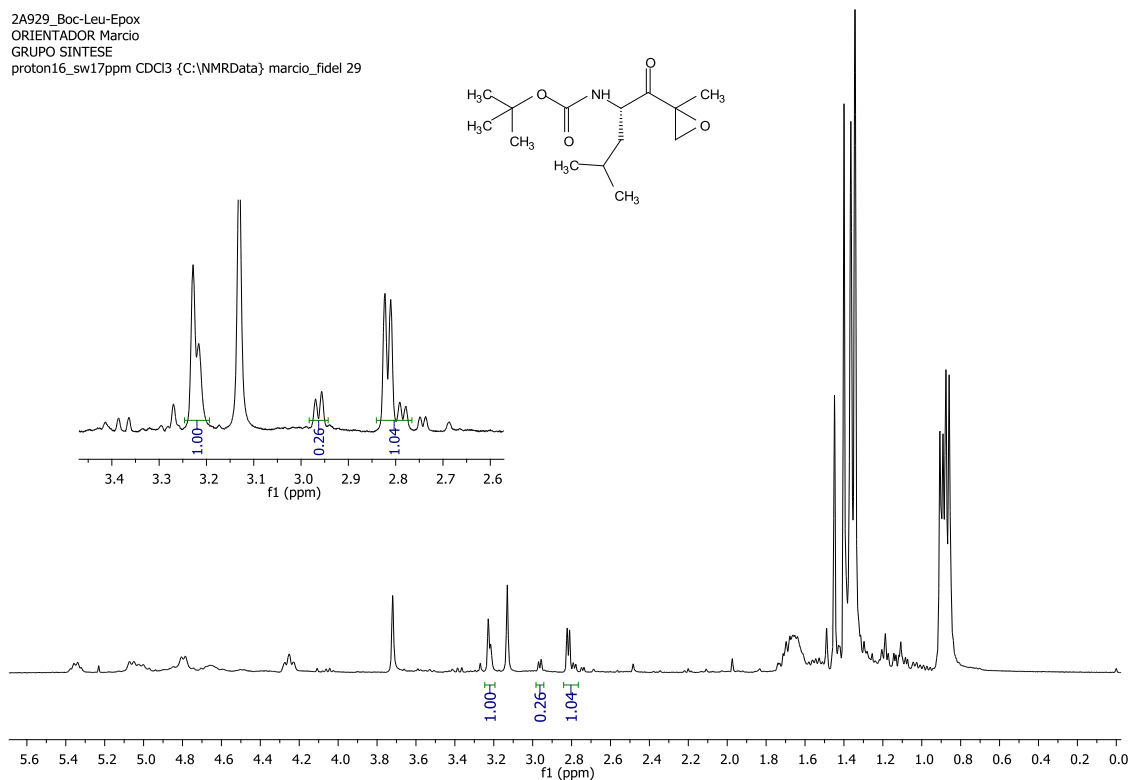


Figure 99:  $^1\text{H}$  NMR of the crude mixture of diastereomeric Boc-Leu-Epoxides in  $\text{CDCl}_3$ , 400 MHz.

2A929\_BocLeuEpox a  
 ORIENTADOR Marcio  
 GRUPO SINTESIS  
 proton16\_sw17ppm CDCl3 {C:\NMRData} marcio\_fidel 39

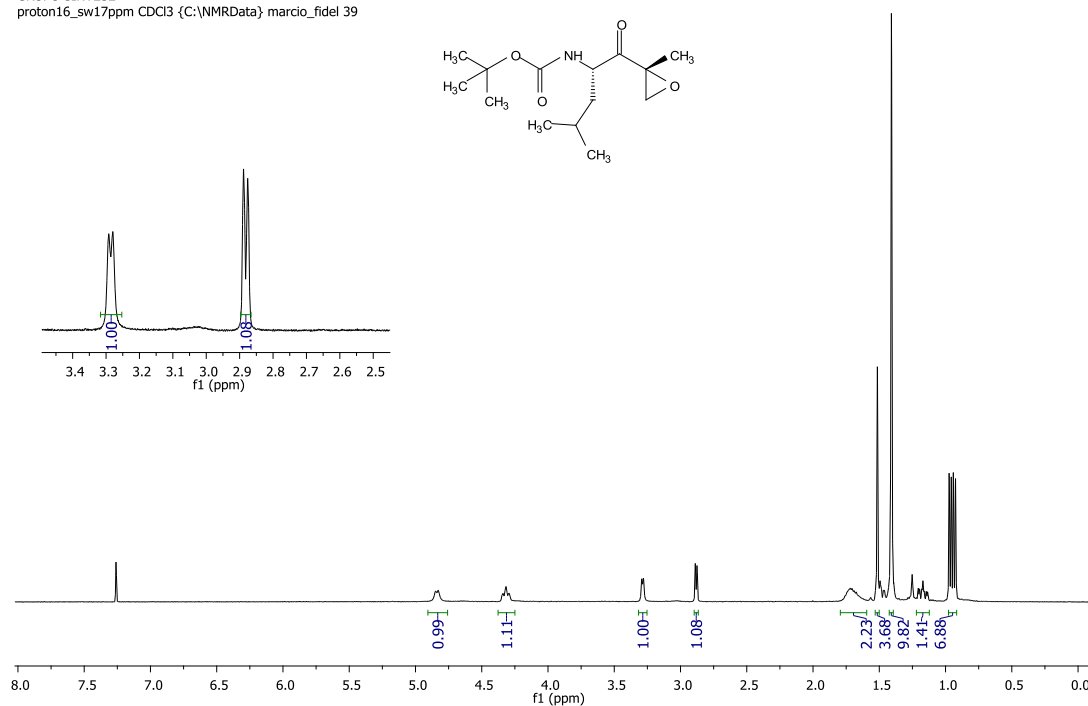


Figure 100:  $^1\text{H}$  NMR of Boc-Leu-Epoxide-A in  $\text{CDCl}_3$ , 400 MHz.

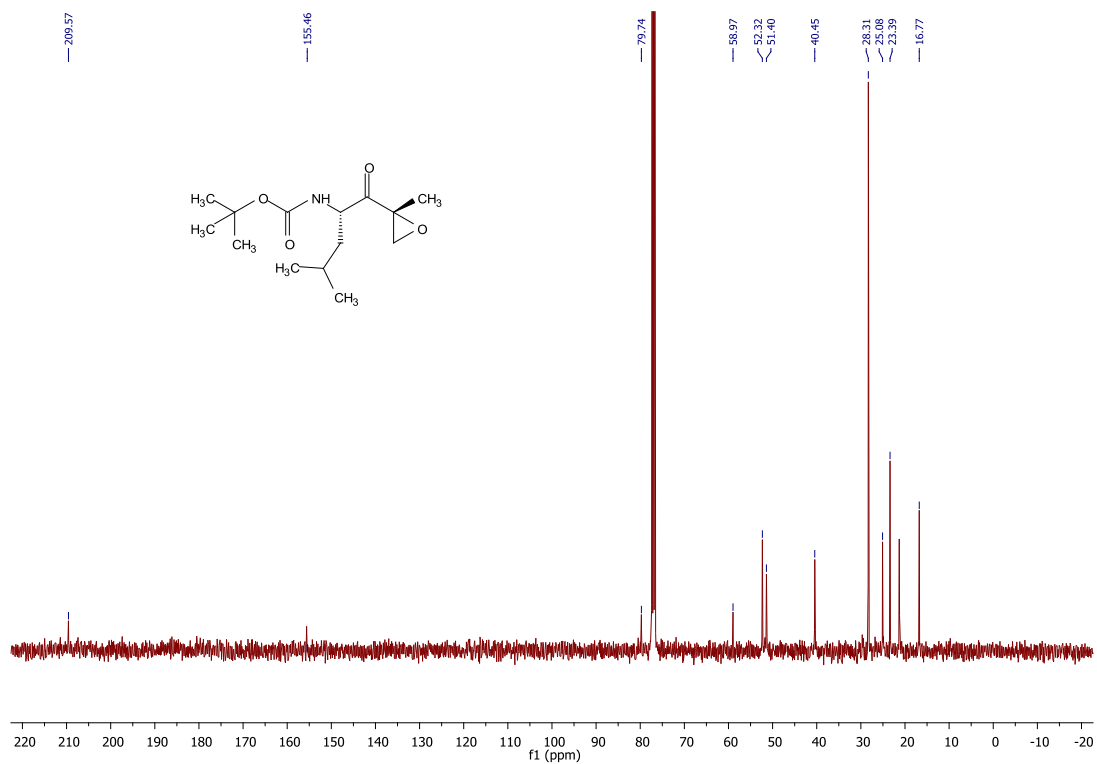


Figure 101: <sup>13</sup>C NMR of Boc-Leu-Epoxyde-A in CDCl<sub>3</sub>, 100 MHz.

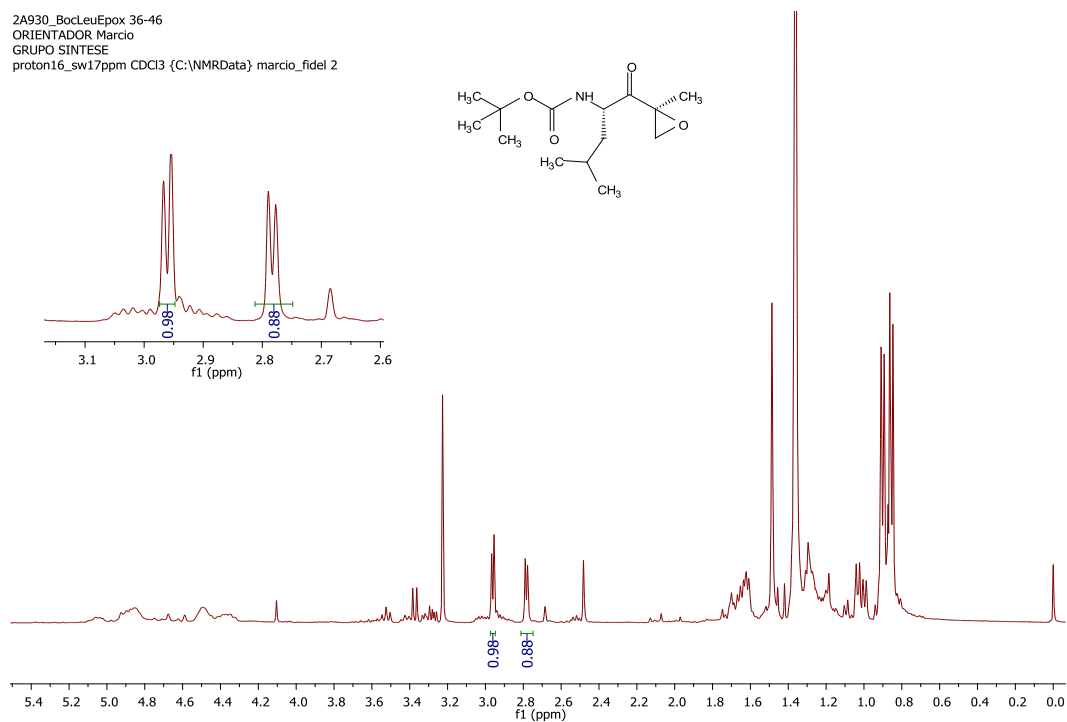


Figure 102: <sup>1</sup>H-NMR of Boc-Leu-Epoxyde-B (impure) in CDCl<sub>3</sub>, 400 MHz. R<sub>f</sub> = 0.37 (Hexane/EtOAc 9:1).

#### 4.3.4 Deprotection of Boc-Leu-Epoxy ketone

To a solution of Boc-Leu-Epoxy ketone (2 g, 7.8 mmol) in DCM (30 mL) at 0°C was added TFA (10 mL). The reaction was warmed to room temperature and stirred for 6 h (completion checked by TLC). The solvent was removed and the TFA salt precipitated with ter-butyl methyl ether (TBME) and hexane at low temperature to give 1.5 g (75%) of the product after filtration and drying under vacuum.

**<sup>1</sup>H NMR** (400 MHz, CDCl<sub>3</sub>) δ: <sup>1</sup>H NMR (400 MHz, CDCl<sub>3</sub>) δ 7.96 (s, *J* = 37.8 Hz, 3H), 4.08 (d, *J* = 9.0 Hz, 1H), 3.11 (d, *J* = 4.2 Hz, 1H), 2.94 (d, *J* = 4.4 Hz, 1H), 1.84 – 1.75 (m, 1H), 1.71 (t, *J* = 11.8 Hz, 1H), 1.58 – 1.47 (m, 4H), 0.97 (d, *J* = 4.4 Hz, 6H).

**<sup>13</sup>C NMR** (100 MHz, CDCl<sub>3</sub>) δ: 205.56, 161.88, 161.51, 58.79, 52.74, 52.49, 39.02, 24.56, 22.95, 20.63, 16.54.

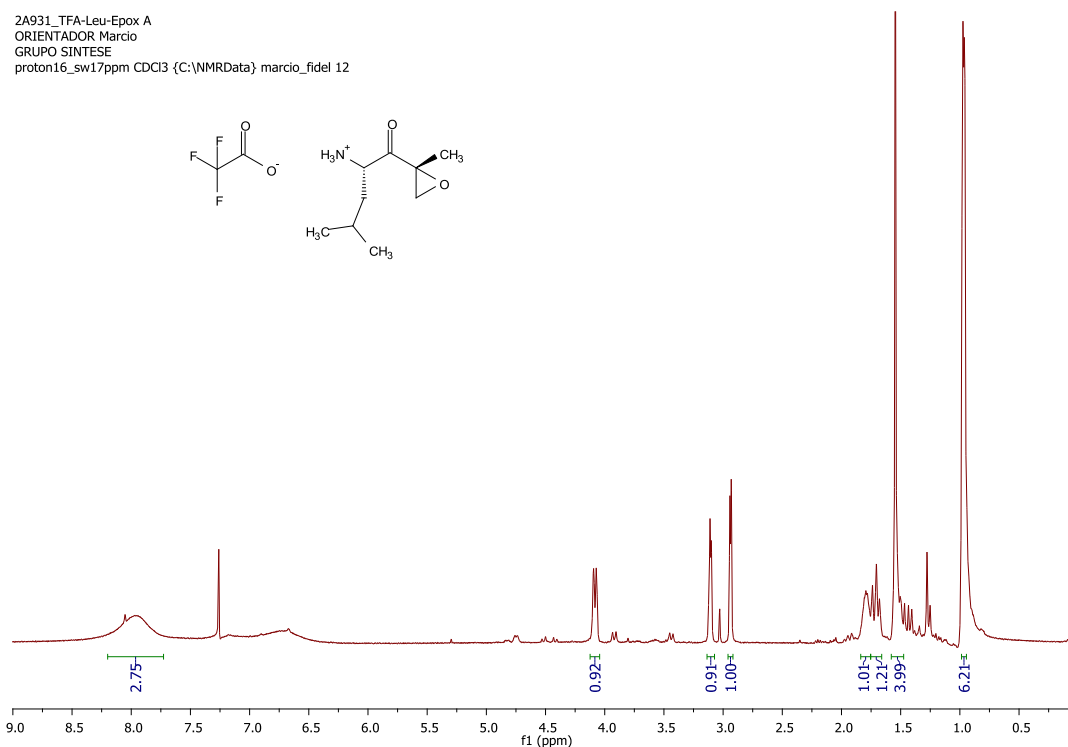


Figure 103: <sup>1</sup>H NMR of trifluoroacetate salt of Leu-Epoxy-A in CDCl<sub>3</sub>, 400 MHz.



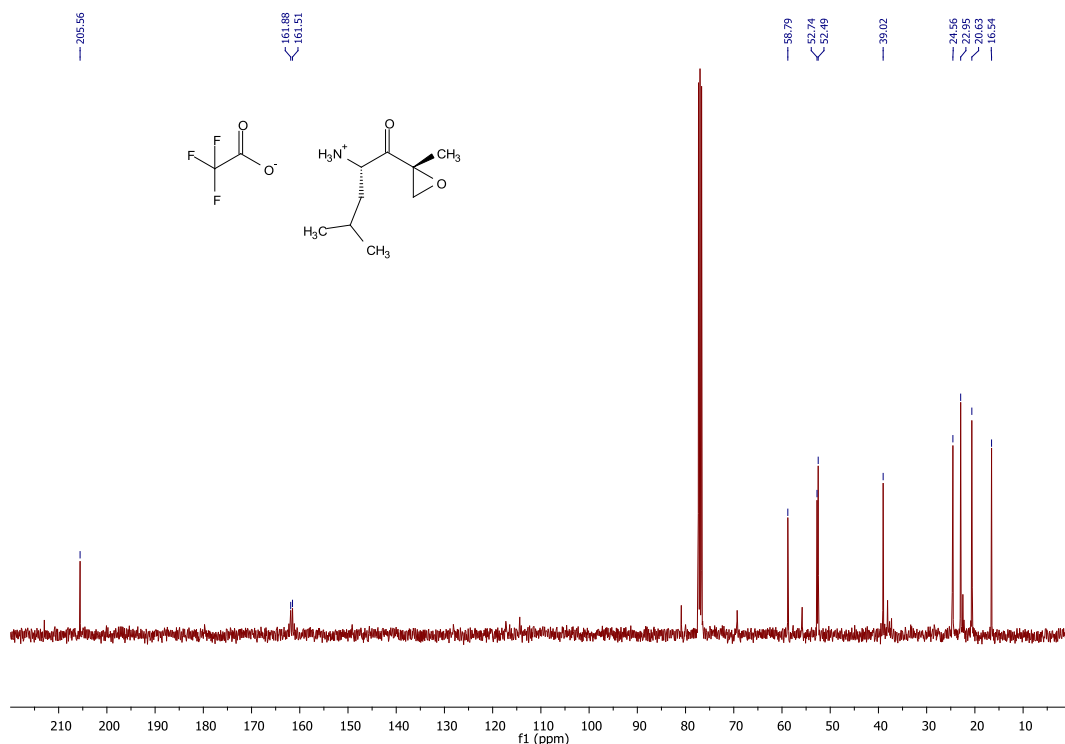


Figure 104:  $^{13}\text{C}$  NMR of trifluoroacetate salt of Leu-Epoxy-A in  $\text{CDCl}_3$ , 100 MHz.

### 4.3.5 Coupling of the left- and right-hand fragments of Carfilzomib

To the tetrapeptide Morf-Ac-Hph-Leu-Phe-OH (100 mg, 0.176 mmol), TBTU (70 mg 0.211 mmol) and HOBt (29 mg, 0.211 mmol) in THF (2.5 mL) was added DIPEA (90  $\mu\text{L}$ , 0.53 mmol) at  $-20^\circ\text{C}$ . Then the HCl salt of Leu-Epoxy ketone (34 mg, 0.176 mmol) in THF (1 mL) was added. After stirring the mixture for 12 h at room temperature, saturated  $\text{NaHCO}_3$  was added and extracted with EtOAc. The organic layer was washed with saturated  $\text{NaHCO}_3$ , brine, dried over  $\text{Na}_2\text{SO}_4$  and the solvent removed under reduced pressure to give 124 mg (100%) of crude product.

$R_f = 0.65$  (EtOAc)

**ESI-MS  $m/z$**  (of the pure product):  $720.42 \pm 0.00$   $[\text{M}+\text{H}]^+$ , calcd. for  $[\text{C}_{40}\text{H}_{57}\text{N}_5\text{O}_7]^+$ : 720.43

**$^1\text{H}$  NMR** (400 MHz,  $\text{CDCl}_3$ )  $\delta$ : 7.29 – 7.21 (m, 2H), 7.19 (dd,  $J = 7.0, 1.3$  Hz, 3H), 7.15 (dd,  $J = 8.1, 3.0$  Hz, 2H), 7.13 (dd,  $J = 6.6, 5.2$  Hz, 4H), 7.01 (d,  $J = 7.7$  Hz, 1H), 4.69 (dd,  $J = 14.8, 7.0$  Hz, 1H), 4.56 – 4.48 (m, 1H), 4.48 – 4.41 (m, 1H), 4.40 – 4.32 (m, 1H), 3.80 – 3.73 (m, 4H), 3.22 (d,  $J = 4.9$  Hz, 1H), 3.12 (t,  $J = 16.9$  Hz, 2H), 3.03 (d,  $J = 6.8$  Hz, 2H), 2.85 (d,  $J = 5.0$  Hz, 1H), 2.69 – 2.62 (m, 4H), 2.60 (t,  $J = 7.5$  Hz, 3H), 2.11 – 2.02 (m, 2H), 2.00 – 1.88 (m, 2H), 1.51 (t,  $J = 5.5$  Hz, 2H), 1.48 (s, 3H), 1.45 (t,  $J = 6.5$  Hz, 2H), 0.89 – 0.82 (m, 12H).

$^{13}\text{C}$  NMR (100 MHz,  $\text{CDCl}_3$ )  $\delta$ : 207.91, 171.46, 171.36, 170.57, 170.47, 140.57, 136.34, 129.28, 128.62, 128.53, 128.32, 126.98, 126.32, 66.88, 61.79, 58.99, 53.89, 53.79, 52.41, 52.28, 52.17, 49.99, 40.94, 39.95, 37.94, 33.44, 31.94, 25.02, 24.75, 23.31, 22.91, 21.83, 21.27, 16.66.

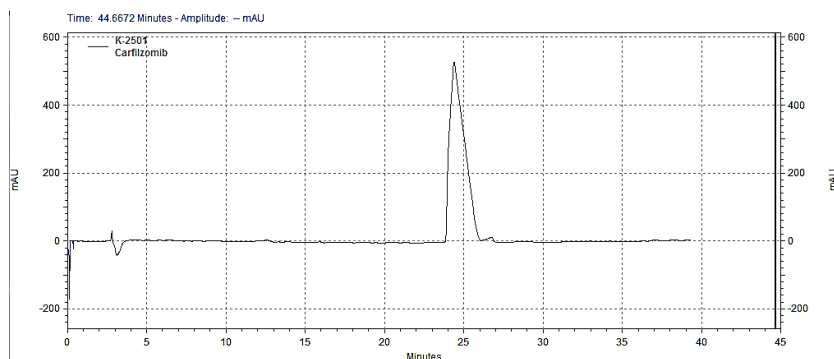


Figure 105: RP-HPLC of Carfilzomib.

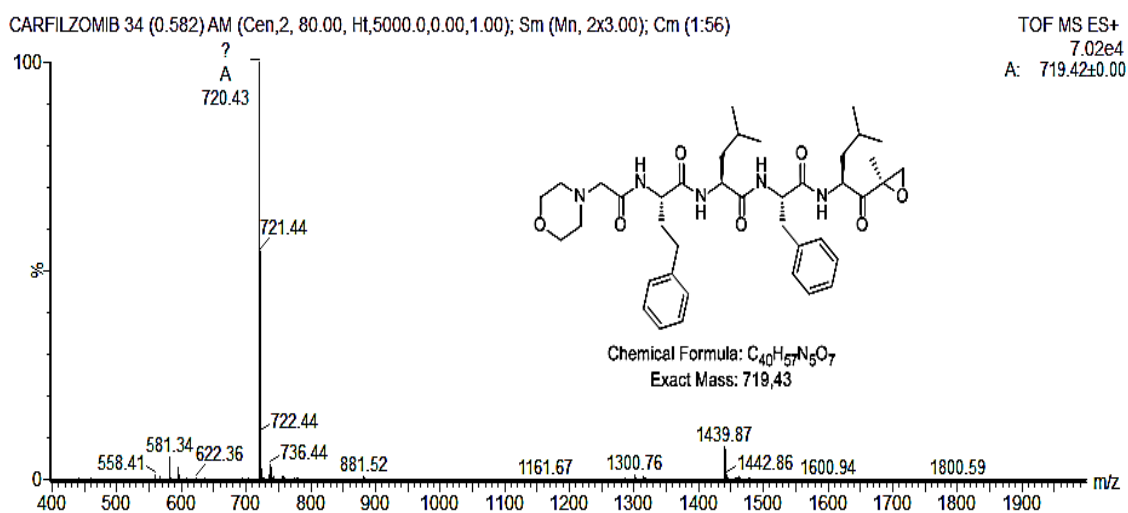


Figure 106: ESI-HRMS of Carfilzomib.

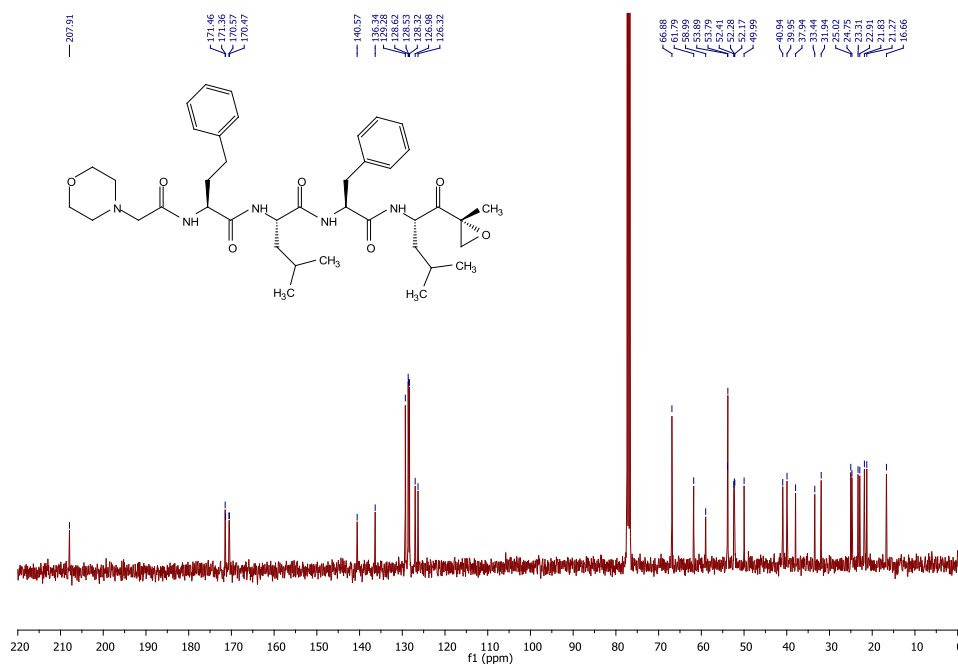


Figure 107: <sup>13</sup>C NMR of Carfilzomib in CDCl<sub>3</sub>, 100 MHz.

## 4.4 Carbonylacrylic-Caproic-Val-Cit-PABOH linker preparation in solid phase

### 4.4.1 Synthesis of Fmoc-Cit-PABOH

A solution of Fmoc-Cit-OH (500 mg, 1.27 mmol) and PABOH (234 mg, 1.9 mmol) in DCM (10 ml) and MeOH (4 ml) was treated with EEDQ (470 mg, 1.9 mmol) and stirred for 15 h. The solid product was triturated three times with ether, then filtered and dried. The yield was 570 mg (90%).

**<sup>1</sup>H NMR** (400 MHz, DMSO)  $\delta$ : 7.86 (d,  $J = 7.3$  Hz, 2H), 7.74 – 7.66 (m, 2H), 7.54 (d,  $J = 8.4$  Hz, 2H), 7.38 (t,  $J = 7.2$  Hz, 2H), 7.34 – 7.26 (m, 2H), 7.21 (d,  $J = 8.1$  Hz, 2H), 6.08 – 5.87 (m, 1H), 5.51 – 5.32 (m, 2H), 5.09 (t,  $J = 5.6$  Hz, 1H), 4.40 (d,  $J = 5.4$  Hz, 2H), 4.32 – 4.05 (m, 4H), 3.10 – 2.86 (m, 2H), 1.75 – 1.52 (m, 2H), 1.51 – 1.28 (m, 2H).

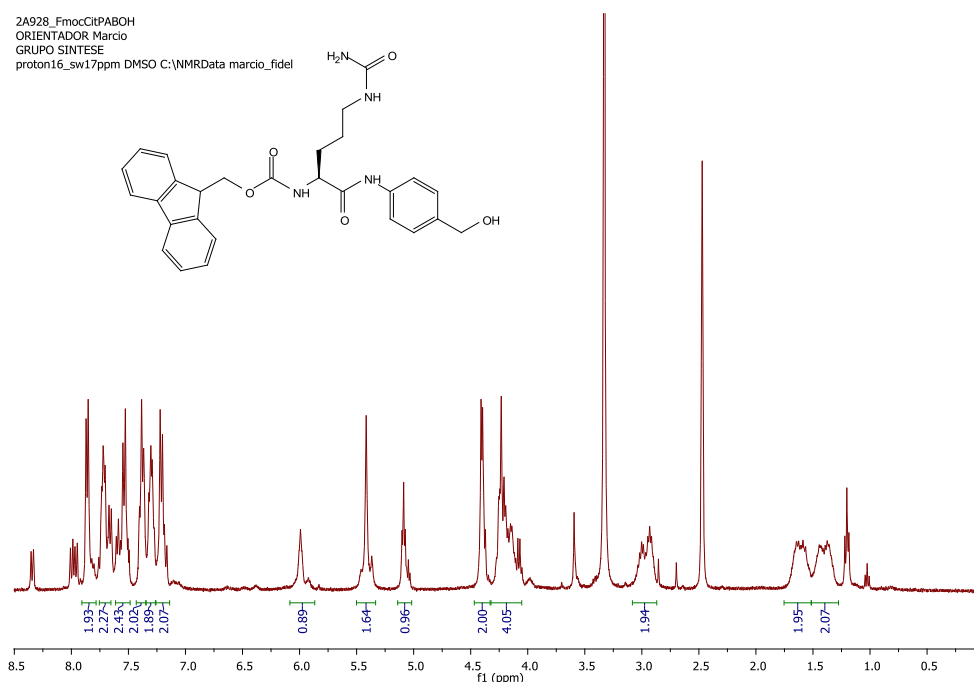


Figure 108: <sup>1</sup>H NMR of Fmoc-Cit-PABOH in DMSO-d<sub>6</sub>, 400 MHz.

#### 4.4.2 Loading of Fmoc-Cit-PABOH to DHP Polystyrene resin and Linker-OH synthesis

The resin (1g, 0.7 mmol) is solvated in 7.8 mL of DCE at room temperature for 15 min. The alcohol (5 equiv.) is then added and the mixture is chilled to 0 °C, followed by addition of p-TsOH (134 g, 0.70 mmol) in one portion. The resulting slurry is stirred at 0 °C for 16 h. The resin is then washed with DCM (1x), DMF, DCM (3x) and dried in vacuum. Subsequent couplings of Fmoc-Val-OH, Fmoc-6-aminohexanoic acid, was conducted following the general peptide synthesis protocol in Section 4.1.2, Chapter 1. The only difference was the use of OxymaK racemization inhibitor instead of Oxyme to limitate the early cleavage from the resin. Final coupling of carbonylacrylic acid was realized with DIC/HOBt because Oxyma or OxymaK react with the Michael-acceptor.

#### 4.4.3 General conditions for cleaving the Linker-OH from the DHP Polystyrene Resin

Peptide-alcohol derivatized resin (1g, 0.74 mmol) is solvated in 20 mL of 1:1 n-butanol/1,2-dichloroethane, and PPTS (370 mg, 1.48 mmol) is then added. The flask is stoppered and heated to 60°C for 16 h. The solution is isolated by filtration and concentrated *in-vacuum*. The resulting material can be separated from the PPTS by *flash* chromatography (EtOAc/MeOH 10:1).

**R<sub>f</sub>**: 0.4 (EtOAc/MeOH 10:1)

**ESI-MS *m/z*** (of the crude product): 730.59 [M+PyH]<sup>+</sup>, calcd. for [C<sub>39</sub>H<sub>52</sub>N<sub>7</sub>O<sub>7</sub>]<sup>+</sup>: 730.39

**ESI-MS  $m/z$**  (of the pure product): 673.5  $[M+Na]^+$ , calcd. for  $C_{34}H_{46}N_6NaO_7$ : 673.33

**$^1H$  NMR** (400 MHz, DMSO)  $\delta$ : 9.91 (s, 1H), 8.59 (s, 1H), 8.27 (s, 1H), 8.10 – 7.80 (m, 3H), 7.74 (d,  $J = 15.3$  Hz, 1H), 7.67 (t,  $J = 7.4$  Hz, 1H), 7.56 (t,  $J = 7.7$  Hz, 4H), 7.41 – 7.29 (m, 1H), 7.21 (d,  $J = 8.5$  Hz, 2H), 6.99 (d,  $J = 15.3$  Hz, 1H), 6.59 (dd,  $J = 26.5, 9.5$  Hz, 1H), 6.16 – 6.01 (m, 1H), 5.42 (s, 2H), 5.10 (t,  $J = 5.8$  Hz, 1H), 4.38 (d,  $J = 5.4$  Hz, 1H), 4.18 (dd,  $J = 10.9, 4.2$  Hz, 1H), 3.24 – 3.10 (m, 2H), 3.10 – 2.91 (m, 2H), 2.28 – 2.10 (m, 2H), 2.04 – 1.91 (m, 1H), 1.81–1.65 (m, 1H), 1.65 – 1.20 (m, 9H), 0.84 (dd,  $J = 10.2, 6.8$  Hz, 6H).

**$^{13}C$  NMR** (100 MHz, DMSO)  $\delta$ : 189.76, 172.38, 171.24, 170.32, 163.25, 162.52, 137.43, 136.59, 133.58, 131.53, 128.88 (3CH), 128.52 (3 CH), 126.92, 126.82, 118.80, 118.71, 62.60, 57.65, 52.96, 47.73, 35.72, 35.02, 30.24, 28.56, 26.67, 26.05, 25.05, 19.16, 18.12.

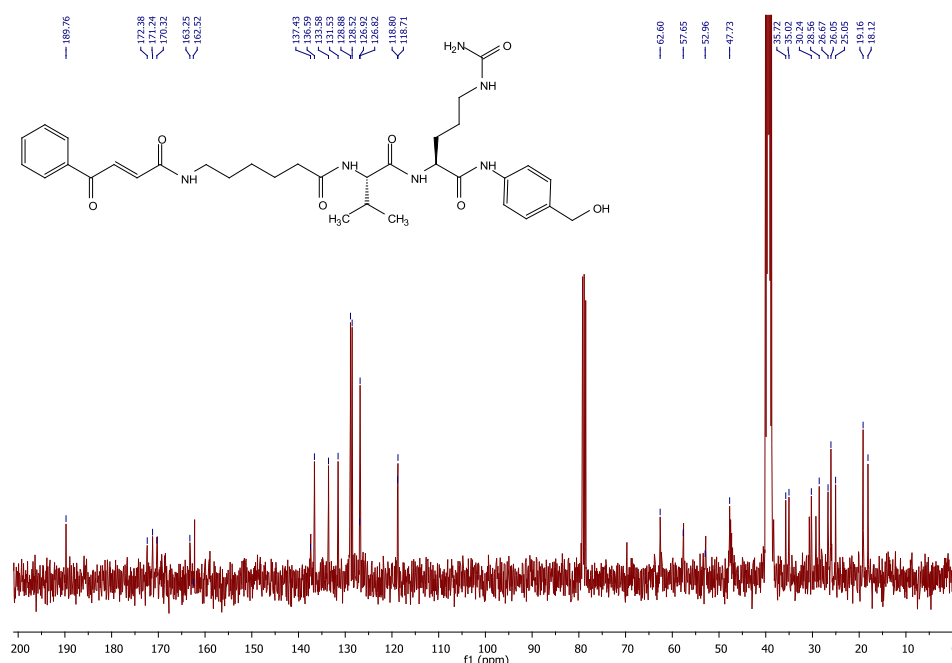


Figure 109:  $^{13}C$  NMR of Linker-OH in DMSO- $d_6$ , 100 MHz.

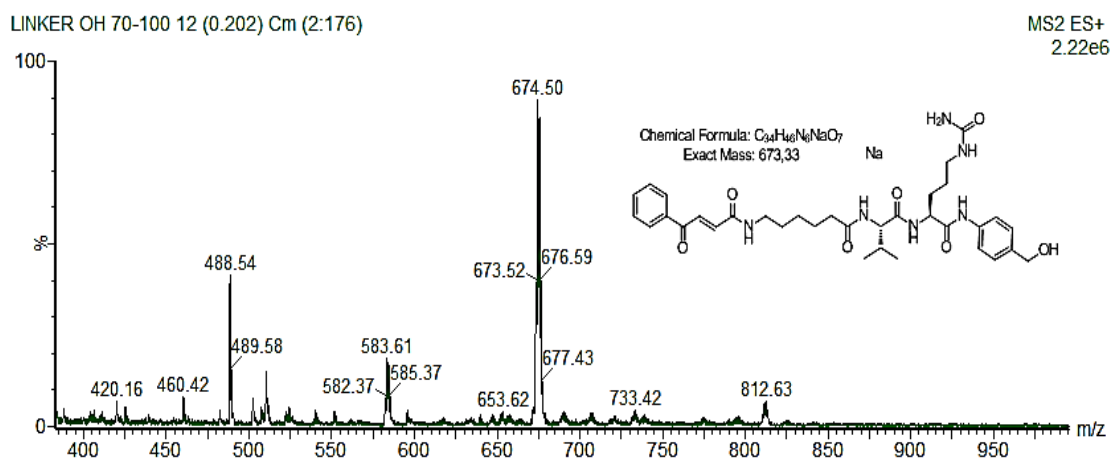


Figure 110: ESI-MS of the pure Linker-OH.

#### 4.4.4 Tosylation of Linker-OH

In a three-neck balloon, 0.6 g (12.8 mmol) of linker-OH are dissolved in 20 mL of Py and 3.68 g (19.3 mmol) of TsCl are added. The air is removed under reduced pressure, the mixture is stirred at room temperature under inert atmosphere (N<sub>2</sub>) and protected from light until the total disappearance of the starting material (approximately 24h, followed by TLC, hexane/EtOAc 3:7, R<sub>f</sub>= 0.9). Some drops of water is added to quench the excess of TsCl. The Py is removed by azeotropic evaporation with toluene (3x) to obtain the desired tosylate in 91% yield (0.50 g) after *flash* chromatographic purification (Hexane:EtOAc 1:1).

**ESI-MS *m/z*** (of the crude product): 443.35 [M+PyH]<sup>+</sup>, calcd. for [C<sub>43</sub>H<sub>59</sub>N<sub>7</sub>O<sub>9</sub>S]<sup>2+</sup>: 855.41

#### 4.4.5 Iodination of Linker-OTs

In a small vial, the Linker-OTs (1 equiv.) were combined in DMF (0.25 M) at room temperature with 1.1 eq of TBAI and the mixture stirred until all starting material was consumed TLC (EtOAc, 24h). The mixture is then treated slowly with water (130 mL) to precipitate a yellow solid, which was collected by filtration. The solid was washed sequentially with water, ACN, and MTBE. After drying under vacuum, 0.5 g (50% yield) of yellow solid was recovered.

R<sub>f</sub>= 0.8 (EtOAc)

**ESI-MS *m/z*** (of the pure product): 411.23 [M+NaK]<sup>2+</sup>, calcd. for [C<sub>34</sub>H<sub>45</sub>IKN<sub>6</sub>NaO<sub>6</sub>]<sup>2+</sup>: 822.20 and 799.46 [M+K]<sup>+</sup>, calcd. for [C<sub>34</sub>H<sub>45</sub>IKN<sub>6</sub>O<sub>6</sub>]<sup>+</sup>: 799.21

**<sup>1</sup>H NMR** (400 MHz, DMF) δ: 8.09 (d, *J* = 7.9 Hz, 2H), 7.90 (d, *J* = 15.3 Hz, 1H), 7.82–7.68 (m, 2H), 7.64 (t, *J* = 7.6 Hz, 2H), 7.49 – 7.26 (m, 3H), 7.16 (d, *J* = 15.2 Hz, 1H), 4.26 (s, 2H), 3.66 – 3.40 (m, 4H), 3.32 (d, *J* = 6.4 Hz, 2H), 2.42–2.06 (m, 5H), 1.70–1.51 (m, 4H), 1.40 (dd, *J* = 14.1, 7.8 Hz, 2H), 1.30 (t, *J* = 5.2 Hz, 2H), 0.94–0.88 (m, 6H).

**<sup>13</sup>C NMR** (100 MHz, DMF) δ: 202.73, 190.29, 179.35, 172.83, 168.86, 164.00, 137.36, 137.02, 134.00, 132.16, 129.10 (2C), 128.75 (2C), 128.48, 128.39, 126.02, 125.09, 58.27, 57.01, 39.94, 39.73, 39.48, 38.87, 35.71, 30.72, 28.52, 26.86, 26.67, 25.66, 22.58, 19.25, 17.77, 13.01.

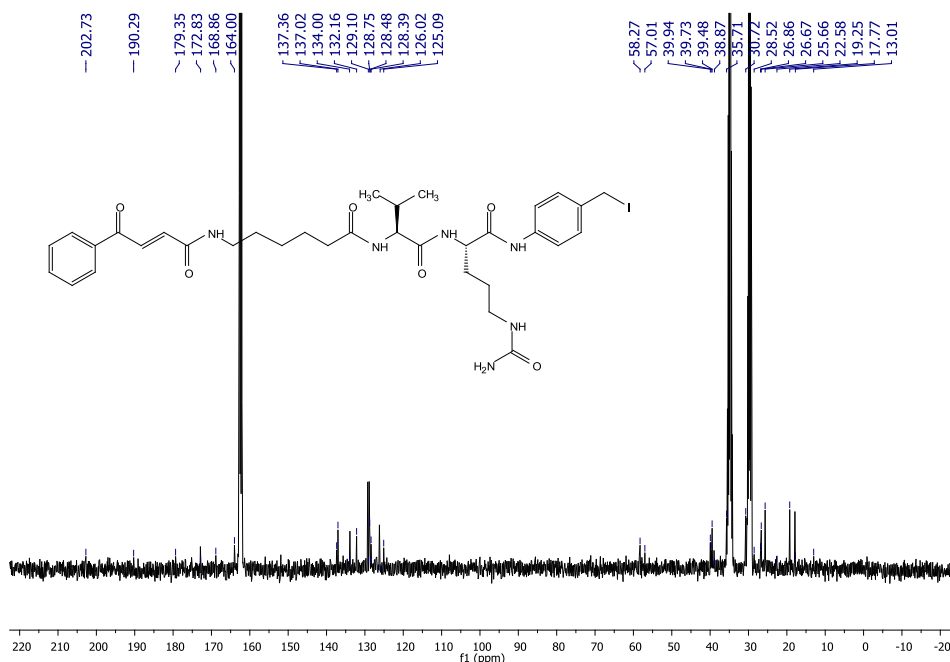


Figure 111: <sup>13</sup>C NMR of the Linker-I in DMF-d<sub>7</sub>, 100 MHz.

## 4.5 Synthesis of pHLIP-Variant3 peptide containing Cys at C and N terminal.

### 4.5.1 Loading of the first aminoacid to Wang-Resin (Steglich sterification)

The resin (1g) is placed in a clean, dry flask, and sufficient DMF is added to just cover and allow swelling for 30 min. If necessary extra DMF is added, just to cover the resin. Fmoc-Trp (Boc)-OH (10 equiv. relative to resin loading) is dissolved in dry DCM. One or two drops of DMF may be needed to aid complete dissolution. A solution of DIC (5 equiv. relative to resin loading) in dry DCM is added to the aminoacid solution. The mixture is stirred for 20 min at 0°C, keeping the reaction mixture free of moisture with a calcium chloride drying tube. DCM is removed by evaporation under reduced pressure using a rotary evaporator. The residues dissolved the minimum amount of DMF and the solution is added to the resin. DMAP (0.1 equiv. relative to resin loading) is dissolved in DMF and this solution is added to the resin/aminoacid mixture. The flask is stoppered and the mixture is allowed to stand at room temperature for 2h with swirling. Subsequent couplings of Fmoc-aminoacids and cleavage are conducted follow the general peptide synthesis protocol in Section 4.1.2-4.1.4, Chapter 1.

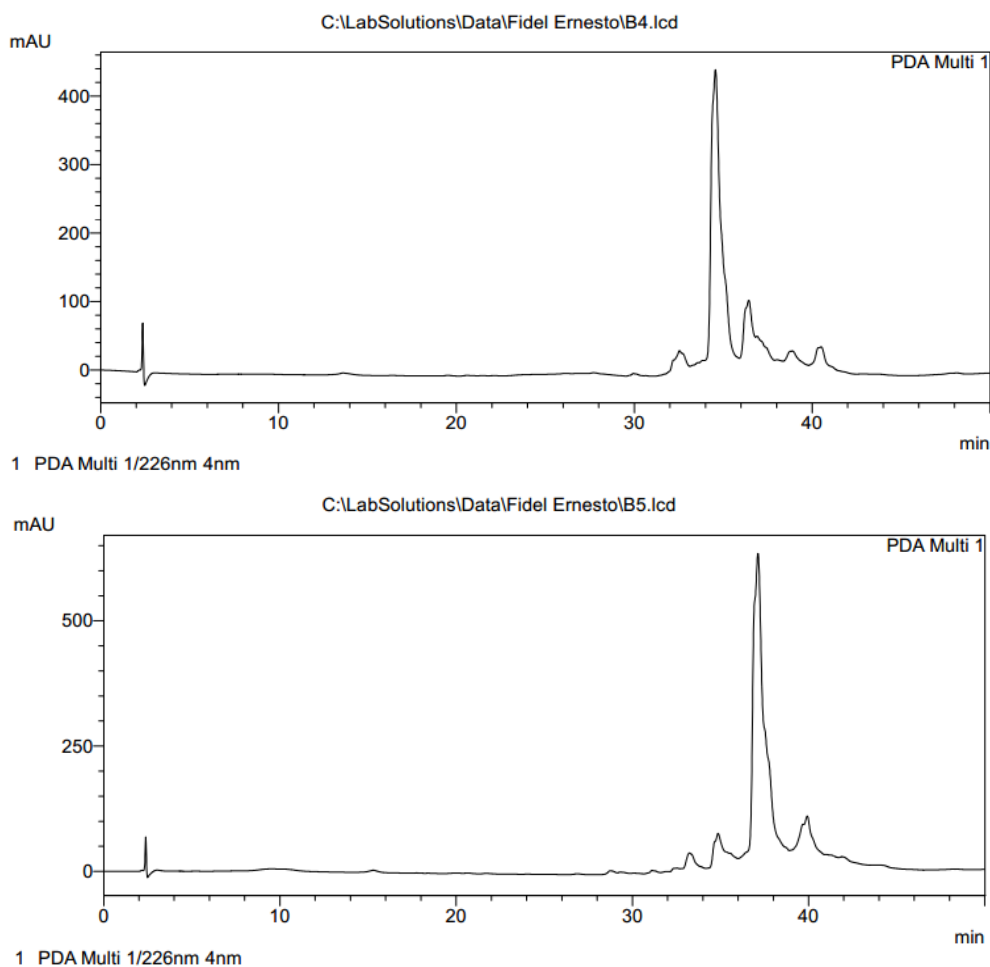


Figure 112: RP-HPLC of pHLIP-Variant3 containing Cys at *N*-terminal (upper panel) or *C*-terminal (lower panel).

#### 4.6 Coupling of the Linker-I to Carfilzomib

In a small vial, Carfilzomib (40 mg, 1 equiv.) and Linker-I (46 mg, 1.1 equiv.) was dissolved in DMF (2.5 M) at room temperature and the mixture is stirred until all starting material was consumed, TLC (EtOAc, 3h). The mixture was precipitated in freezing Et<sub>2</sub>O, centrifuged and and lyophilized to afford 42 mg (49 % yield) of the desired product (Linker-CFZ-I).

**ESI-MS *m/z*** (of the lyophilized product): 758.33 [M+K]<sup>2+</sup>, calcd. for [C<sub>74</sub>H<sub>102</sub>IKN<sub>11</sub>O<sub>13</sub>]<sup>2+</sup>: 1518.63 and 748.69 [M+H<sub>2</sub>O]<sup>2+</sup>, calcd. for [C<sub>74</sub>H<sub>104</sub>IN<sub>11</sub>O<sub>14</sub>]<sup>2+</sup>: 1497.68

#### 4.7 Conjugation of pHLIP-Variant3 to Linker-Carfilzomib-I

To a solution of pHLIP (43 mg, 0.013 mmol, 1 equiv.) in 3 mL of sodium phosphate buffer (pH 8.0, 50 mM) containing 30% of MeCN was generated inert atmosphere of N<sub>2</sub>. Followed, a solution of Linker-CFZ-I (20 mg, 0.014 mmol, 1.1 equiv.) in DMF (0.2 mL) was added at room temperature. After 12 h of reaction the solvent was removed under reduced pressure and the



resulting mixture was precipitated in freezing Et<sub>2</sub>O, centrifugated and lyophilized to afford 52 mg (82 % yield) of the desired product (pHLIP-Variant3-Linker-CFZ-I).

## References

1. Kriengkauykiat, J.; Ito, J.; Dadwal, S. S., Epidemiology and treatment approaches in management of invasive fungal infections. *Clinical Epidemiology* **2011**, *3*, 175-191.
2. (a) Arnold, T. M.; Dotson, E.; Sarosi, G. A.; Hage, C. A., Traditional and emerging antifungal therapies. *Proceedings of the American Thoracic Society* **2010**, *7* (3), 222-228; (b) Steinbach, W. J.; Juvvadi, P. R.; Fortwendel, J. R.; Rogg, L. E., Newer combination antifungal therapies for invasive aspergillosis. *Medical mycology* **2011**, *49* (Supplement 1), S77-S81.
3. Di Marino, S.; Scrima, M.; Grimaldi, M.; D'Errico, G.; Vitiello, G.; Sanguinetti, M.; De Rosa, M.; Soriente, A.; Novellino, E.; D'Ursi, A. M., Antifungal peptides at membrane interaction. *European Journal of Medicinal Chemistry* **2012**, *51*, 154-162.
4. Sun, Z. J.; Heffron, G.; Mcbeth, C.; Wagner, G.; Otero-González, A. J.; Starnbach, M. N., Solution structure of a potent antifungal peptide Cm-p5 derived from *C. muricatus*. *Deposit PDB: 2014-05-14, Status HPUB, entrance code 2MP9* 2014.
5. López-Abarrategui, C.; McBeth, C.; Zhen-Yu, J. S.; Heffron, G.; García, M.; Alba-Menéndez, A.; Migliolo, L.; Reyes-Acosta, O.; Campos-Dias, S.; Brandt, W.; Porzel, A.; Wessjohann, L.; Starnbach, M.; Franco, O. L.; Otero-González, A. J., Cm-p5: an antifungal hydrophilic peptide derived from the coastal mollusk *Cenchritis muricatus* (Gastropoda: Littorinidae). *FASEB Journal* **2015**, *29* (8), 3315-3325.
6. González-García, M.; Valdés, M. E.; Freitas, C. G.; Alba-Menéndez, A.; López-Abarrategui, C.; Juan-Galan, J. S.; Campos, S. D.; Franco, O. L.; Otero-Gonzalez, A. J., In vitro complementary biological activity of the antifungal peptide Cm-p5 and in silico prediction of its functional regions. *Rev Cubana Med Tropical* **2017**, *69* (1), 1-15.
7. Clancy, C. J.; Yu, L. V.; Morris, A. J.; Snyderman, D. R.; Nguyen, H. M., Fluconazole MIC and the Fluconazole Dose/MIC Ratio Correlate with Therapeutic Response among Patients with Candidemia. *Antimicrobial Agents and Chemotherapy* **2005**, *49* (8), 3171-3177.
8. Szabo, Z.; Soczo, G.; Miszti, C.; Hermann, P.; Rozgonyi, F., In vitro activity of fluconazole and amphotericin B against *Candida inconspicua* clinical isolates as determined by the time-kill method. *Acta Microbiol. Immunol. Hung.* **2008**, *55* (1), 53-61.
9. Schmidt, N. W.; Mishra, A.; Hwee, G. L.; Davis, M.; Sanders, L. K.; Tran, D.; Garcia, A.; Tai, K. P.; McCray Jr, P. B.; Ouellette, A. J.; Selsted, M. E.; Wong, G. C. L., Criterion for Amino Acid Composition of Defensins and Antimicrobial Peptides Based on Geometry of Membrane Destabilization. *J. Am. Chem. Soc.* **2011**, *133* (17), 6720-6727.
10. Vazquez, J. A., Anidulafungin: A new echinocandin with a novel profile. *Clinical Therapeutics* **2005**, *27* (6), 657-673.
11. Ghannoum, M. A.; Rice, L. B., Antifungal Agents: Mode of Action, Mechanisms of Resistance, Correlation of These Mechanisms with Bacterial Resistance. *Clin. Microbiol. Rev.* **1999**, *12* (4), 501-517.
12. Elewski, B. E., Mechanisms of action of systemic antifungal agents. *Journal of the American Academy of Dermatology* **1993**, *28* (5), S29-S34.
13. Henninot, A.; Collins, J. C.; Nuss, J. M., The Current State of Peptide Drug Discovery: Back to the Future? . *Journal of Medicinal Chemistry* **2018**, *61* (4), 1382-1414.
14. Milton, H. J.; Chess, R. B., Effect of pegylation on pharmaceuticals. *Nature Reviews, Drug Discovery* **2003**, *2*, 214-221.
15. Lien, S.; Lowman, H. B., Therapeutic peptides. *Trends in Biotechnology* **2003**, *21* (12), 556-562.
16. Bray, B. L., Large-scale manufacture of peptide therapeutics by chemical synthesis. *Nature Reviews Drug Discovery* **2003**, *2* (587-593).

17. Ayoub, M.; Scheidegger, D., Peptide drugs, overcoming the challenges, a growing business. *Chemistry Today, Peptides* **2006**, 24 (4), 46-48.
18. Sewald, N.; Jakubke, H. D., *Peptides: Chemistry and Biology*. Wiley-VCH Verlag GmbH & Co. KGaA: Weinheim, Germany, **2002**.
19. Lopez-Abarrategui, C. L.; Alba, A.; Silva, O. N.; Acosta, O. R.; Vasconcelos, I. M.; Oliveira, J. T. A.; Migliolo, L.; Costa, M. P.; Costa, C. R.; Silva, M. R. R.; Garay, H. E.; Dias, S. C.; Franco, O. L.; Otero-González, A. J., Functional characterization of a synthetic hydrophilic antifungal peptide derived from the marine snail *Cenchritis muricatus*. *Biochimie* **2012**, 94 (4), 968-974.
20. Gracia, S. R.; Gaus, K.; Sewald, N., Synthesis of chemically modified bioactive peptides: recent advances, challenges and developments for medicinal chemistry. *Future medicinal chemistry* **2009**, 1 (7), 1289-1310.
21. Voet, D.; Voet, J. G., *Biochemistry*. 3 ed.; John Wiley and Sons, Inc.: Hoboken, New Jersey, **2004**; Vol. 1.
22. (a) Castañeda-Casimiro, J.; Ortega-Roque, J. A.; Venegas-Medina, A. M.; Aquino-Andrade, A.; Serafín-López, J.; Estrada-Parra, S.; Estrada, I., Péptidos antimicrobianos: péptidos con múltiples funciones. *Asma, Alergías e Inmunología Pediátricas* **2009**, 18, 16-29; (b) Otero-Gonzalez, A. J.; Magalhaes, B. S.; Garcia-Villarino, M.; Lopez-Abarrategui, C.; Sousa, D. A.; Dias, S. C.; Franco, O. L., Antimicrobial peptides from marine invertebrates as a new frontier for microbial infection control. *FASEB J.* **2010**, 24 (5), 1320-34.
23. Guani-Guerra, E.; Santos-Mendoza, T.; Lugo-Reyes, S. O.; Teran, L. M., Antimicrobial peptides: general overview and clinical implications in human health and disease. *Clin. Immunol.* **2010**, 135 (1), 1-11.
24. Sanchez, M. L., Mecanismos de acción de péptidos antimicrobianos y mecanismos de resistencia de los patógenos. *Bioquímica y Patología Clínica* **2016**, 80 (1), 36-43.
25. Wang, G.; Zhou, P.; Huang, J., *Computational Peptidology, Methods in Molecular Biology*. Springer Science+Business Media: New York, **2015**; p 44-66.
26. Lopez-Abarrategui, C.; Figueroa-Espi, V.; Reyes-Acosta, O.; Reguera, E.; Otero-Gonzalez, A. J., Magnetic nanoparticles: new players in antimicrobial peptide therapeutics. *Curr. Protein. Pept. Sci.* **2013**, 14 (7), 595-606.
27. Kumar, P.; Kizhakkedathu, J. N.; Straus, S. K., Antimicrobial Peptides: Diversity, Mechanism of Action and Strategies to Improve the Activity and Biocompatibility in Vivo. *Biomolecules* **2018**, 8 (1), 1-24.
28. Hancock, R. E.; Haney, E. F.; Gill, E. E., The immunology of host defence peptides: beyond antimicrobial activity. *Nature Reviews Immunology* **2016**, 16 (5), 321-334.
29. De la Fuente, N. M.; Villarreal, J.; Díaz, M. A.; García, A. P., Evaluación de la actividad de los agentes antimicrobianos ante el desafío de la resistencia bacteriana. *Revista Mexicana de Ciencias Farmacéuticas.* **2016**, 46 (2), 7-16.
30. Nuding, S.; Frasc, T.; Schaller, M.; Stange, E. F.; Zabel, L. T., Synergistic Effects of Antimicrobial Peptides and Antibiotics against *Clostridium difficile*. *Antimicrob. Agents Chemother.* **2014**, 58 (10), 5719-5725.
31. Zhang, L.; Falla, T. J., Host defense peptides for use as potential therapeutics. *Curr. Opin. Investig. Drugs* **2009**, 10 (2), 164-171.
32. Fan, X.; Reichling, J.; Wing, M., Antibacterial activity of the recombinant antimicrobial peptide Ib-AMP4 from *Impatiens balsamina* and its synergy with other antimicrobial agents against drug resistant bacteria. *Pharmazie* **2013**, 68, 628-630.
33. Zhang, Z.; Mu, L.; Tang, J.; Duan, Z.; Wang, F.; Wei, L., A small peptide with therapeutic potential for inflammatory acne vulgaris. *PLoS One* **2013**, 8 (8).

34. Hossen, S.; Hua, S. G.; Khalil, I., Melittin, a Potential Natural Toxin of Crude Bee Venom: Probable Future Arsenal in the Treatment of Diabetes Mellitus. *Journal of Chemistry* **2017**, 1-7.
35. Porto, W. F.; Irazazabal, L.; Alves, E. S. F.; Ribeiro, S. M.; Matos, C. O.; Pires, A. S.; Fensterseifer, I. C. M.; Miranda, V. J.; Haney, E. F.; Humblot, V.; Torres, M. D. T.; Hancock, R. E. W.; Liao, L. M.; Ladram, A.; Lu, T. K.; Fuente-Nunez, C.; Franco, O. L., In silico optimization of a guava antimicrobial peptide enables combinatorial exploration for peptide design. *Nature Communicatios* **2018**, 9 (1490), 1-12.
36. Vijayaraghavan, R.; Mahesh, M.; Alagappan, M.; Sundaram, M.; Karunakaran, R.; Vinodh, S., Triple antibiotic paste in root canal therapy. *Journal of Pharmacy and Bioallied Sciences* **2012**, 4 (2), S230–S233.
37. Amabile-Cuevas, C., Society must seize control of the antibiotics crisis: pressure from the public could force firms to develop new drugs that treat resistant infections. *Nature* **2016**, 533 (7604), 439.
38. Arias, C. A.; Murray, B. E., Antibiotic-Resistant Bugs in the 21st Century-A Clinical Super Challenge. *N. Engl. J. Med.* **2009**, 360 (5), 439-443.
39. French, P. M., Are Fungal Infections the Cause of Motor Neuron Disease? In *Biotechnology Innovator*, **2011**; Vol. 2018.
40. (a) Alonso, R.; Pisa, D.; Marina, A. I.; Morato, E.; Rábano, A.; Rodal, I.; Carrasco, L., Evidence for Fungal Infection in Cerebrospinal Fluid and Brain Tissue from Patients with Amyotrophic Lateral Sclerosis. *Int. J. Biol. Sci.* **2015**, 11 (5), 546-558; (b) Alonso, R.; Pisa, D.; Fernández-Fernández, A. M.; Rábano, A.; Carrasco, L., Fungal Infection in neural tissue of patients with amyotrophic lateral sclerosis. *Neurobiol Dis.* **2017**, 108, 249-260; (c) Alonso, R.; Pisa, D.; Fernández-Fernández, A. M.; Carrasco, L., Infection of Fungi and Bacteria in Brain Tissue From Elderly Persons and Patients With Alzheimer's Disease. *Frontiers in Aging Neuroscience* **2018**, 10, 1-20.
41. (a) Huang, R.; Li, L.; Gregory, R. L., Bacterial interactions in dental biofilm. *Virulence* **2011**, 2 (5), 435-444; (b) Akyıldız, I.; Take, G.; Uygur, K.; Kızıl, Y.; Aydil, U., Bacterial Biofilm Formation in the Middle-Ear Mucosa of Chronic Otitis Media Patients. *Indian J. Otolaryngol Head Neck Surg* **2012**, 65 (3), 557-561.
42. Burke, A. C., Antibiotic side effects. *Medical Clinics of North America* 2001, 85 (1), 149-185.
43. Butler, M. S.; Cooper, M. A., Antibiotics in the clinical pipeline in 2011. *The Journal of antibiotics* **2011**, 64 (6), 413-425.
44. (a) Menzin, J.; Meyers, J. L.; Friedman, M.; Korn, J. R.; Perfect, J. R.; Langston, A. A.; Danna, R. P.; Papadopoulos, G., The economic costs to United States hospitals of invasive fungal infections in transplant patients. *American journal of infection control* **2011**, 39 (4), e15-e20; (b) Hennen, C. R., Pharmacoeconomic evaluations of antifungal therapies. *Curr Med Res Opin* **2009**, 25 (7), 1751-1758.
45. (a) Duncan, V. M.; O'Neil, D. A., Commercialization of antifungal peptides. *Fungal Biology Reviews* **2013**, 26, 156-165; (b) Duncan, V. M.; O'Neil, D. A., Commercialization of antifungal peptides. *Fungal Biology Reviews* **2013**, 26 (4), 156-165.
46. Van der Does, A. M.; Hensbergen, P. J.; Bogaards, S. J.; Cansoy, M.; Deelder, A. M.; van Leeuwen, H. C.; Drijfhout, J. W.; van Dissel, J. T.; Nibbering, P. H., The human lactoferrin-derived peptide hLF1-11 exerts immunomodulatory effects by specific inhibition of myeloperoxidase activity. *The Journal of Immunology* **2012**, 188 (10), 5012-5019.
47. Van der Velden, W. J.; Van Iersel, T. M.; Blijlevens, N. M.; Donnelly, J. P., Safety and tolerability of the antimicrobial peptide human lactoferrin 1-11 (hLF1-11). *BMC Medicine* **2009**, 7, 44.

48. Vlieghe, P.; Lisowski, V.; Martinez, J.; Khrestchatsky, M., Synthetic therapeutic peptides: science and market. *Drug discovery today* **2010**, *15* (1), 40-56.
49. (a) Pérez-Escoda, M. T. Diseño y síntesis de péptidos para el diagnóstico de la infección por el virus de la hepatitis G (GBV-C/HGV). México, **2009**; (b) Marder, O.; Albericio, F., Industrial application of coupling reagents in peptides. *Chim. Oggi* **2003**, 6-11.
50. Sewald, N.; Jakubke, H. D., Peptide Synthesis. In *Peptides: Chemistry and Biology*, Wiley-VCH Verlag GmbH & Co. KGaA: Weinheim, Germany, **2002**; Vol. , pp 135-267.
51. Vlieghe, P.; Lisowski, V.; Martinez, J.; Khrestchatsky, M., Synthetic therapeutic peptides: science and market. *Drug Discov. Today* **2010**, *15* (1/2), 40-56.
52. Merrifield, B., Solid Phase Peptide Synthesis. I. The Synthesis of a Tetrapeptide'. *J. Am. Chem. Soc.* **1963**, *85*, 2149-2154.
53. Garay, H. E. Síntesis de péptidos modificados químicamente con posibles aplicaciones farmacéuticas. Doctorado, Universidad de La Habana, La Habana, Cuba, **2012**.
54. Bruckdorfer, T.; Marder, O.; Albericio, F., From production of peptides in milligram amounts for research to multi-tons quantities for drugs of the future. *Curr Pharm Biotechnol.* **2004**, *5* (3), 29-43.
55. Morales, F. E. Síntesis de híbridos péptido-esteroidales por conjugación multicomponente de péptidos a isocianoesteroides. Diploma, CEPN, Universidad de La Habana, La Habana, **2012**.
56. Merrifield, B., Solid phase synthesis. *Science* **1986**, *232*, 341-347.
57. Fields, G. B.; Noble, R. L., Solid phase peptide synthesis utilizing 9-fluorenylmethoxycarbonyl amino acids. *Int J. Pept. Protein Res.* **1990**, *35*, 161-214.
58. Soriano, J. M. Nuevos reactivos poliméricos para el acoplamiento y protección de aminoácidos. Doctorado, Universidad de Alicante, Alicante, España, **2002**.
59. (a) Paquet, A., Introduction of 9-fluorenylmethyloxycarbonyl, trichloroethoxycarbonyl, and benzyloxycarbonyl amine protecting groups into 0-unprotected hydroxyamino acids using succinimidyl carbonates. *Can. J.Chem.* **1982**, *60*, 976-980; (b) Kaiser, E.; Colescott, R. L.; Bossinger, C. D.; Cook, P. I., Color test for detection of free terminal amino groups in the solid-phase synthesis of peptides. *Anal. Biochem.* **1970**, *34*, 595-598.
60. Merrifield, B., Solid Phase Peptide Synthesis. *World Scientific Publishing Co.* **1992**, *9* (3), 2149-2154.
61. (a) Doherty-Kirby, A. L.; Lajoie, G. A., Side-Chain Protecting Groups. In *Solid-Phase Synthesis. A practical guide*, Kates, S.; Albericio, F., Eds. Marcel Dekker: New York, **2000**; pp 129-197; (b) Henklein, P.; Heyne, H. U.; Halatsch, W. R.; Niedrich, H., 5-Norbornene-2,3-dicarboximido Carbonochloridate. A New Stable Reagent for the Introduction of Amino-Protecting Groups. *Synthesis* **1987**, *2*, 166-167.
62. Pennington, M. W., *Peptide Synthesis Protocols* Humana Press: Totowa, New Jersey, **1994**.
63. Martínez, C. P.; Ortiz, P., *Espectroscopía*. Ed. Universidad de La Habana: La Habana, Cuba, **2010**; Vol. 1, 2, p 95-260, 261-397.
64. (a) Mayne, L.; Englander, S. W.; Qiu, R.; Yang, J.; Gong, Y.; Spek, E. J.; Kallenbach, N. R., Stabilizing Effect of a Multiple Salt Bridge in a Prenucleated Peptide. *Journal of the American Chemical Society* **1998**, *120*, 10643-10645; (b) Baker, E. G.; Bartlett, G. J.; Crump, M. P.; Sessions, R. B.; Linden, N.; Faul, C. F. J.; Woolfson, D. N., Local and macroscopic electrostatic interactions in single  $\alpha$ -helix. *Nature chemical biology* **2015**, *11* (3), 221-228.
65. Sandeep, K.; Ruth, N., Close-Range Electrostatic Interactions in Proteins. *ChemBioChem* **2002**, *3*, 604-617.
66. Scholtz, J. M.; Qian, H.; Robbins, V. H.; Baldwin, R. L., The energetics of ion-pair and hydrogen-bonding interactions in a helical peptide. *Biochemistry* **1993**, *32*, 9668-9676.

67. Hruby, V. J., Designing peptide receptor agonists and antagonists. *Nature Reviews Drug Discovery* **2002**, *1* (11), 847-858.
68. Alexopoulos, C.; Krikorian, D.; Panou-Pomonis, E.; Sakarellos-Daitsiotis, M.; Sakarellos, C., Innovative, Multifunctional Sequential Oligopeptide Carriers Socn-I and SOcn-II: Functions-Technology-Perspectives. *Protein Pept. Lett.* **2005** *12* (6), 601-607.
69. Wessjohann, L. A.; Andrade, C. K. Z.; Vercillo, O. E.; Rivera, D. G., Macrocyclic Peptoids: *N*-Alkylated Cyclopeptides and Depsipeptides. In *Targets Heterocyclic Systems. Chemistry and Properties*, Attanasi, O. A.; Spinelli, D., Eds. Societa Chimica Italiana: Italy, **2006**; Vol. 10, pp 24-53.
70. Silva-Flannery, L. M.; Cabrera-Mora, M.; Dickherber, M.; Moreno, A., Polymeric Linear Peptide Chimeric Vaccine-Induced Antimalaria Immunity Is Associated with Enhanced In Vitro Antigen Loading. *Infect. Immun.* **2009**, *77* (5), 1798-1806.
71. Nadolski, M. J.; Linder, M. E., Protein lipidation. *FEBS Journal* **2007**, *274*, 5202–5210.
72. Rivera, D. G.; León, F.; Concepción, O.; Morales, F. E.; Wessjohann, L. A., A Multiple Multicomponent Approach to Chimeric Peptide–Peptoid Podands. *Chem. Eur. J.* **2013**, 1-14.
73. Purcell, A. W.; McCluskey, J.; Rossjohn, J., More than one reason to rethink the use of peptides in vaccine design. *Nature Reviews Drug Discovery* **2007**, *6* (5), 404-414.
74. Wu, F.; Mayer, J. P.; Gelfanov, V. M.; Liu, F.; DiMarchi, R. D., Synthesis of Four-Disulfide Insulin Analogs via Sequential Disulfide Bond Formation. *The Journal of Organic Chemistry* **2017**, *82* (7), 3506-3512.
75. Garay Pérez, H. E. Síntesis de péptidos modificados químicamente con posibles aplicaciones farmacéuticas. Tesis de Doctorado, Universidad de La Habana, **2012**.
76. Bulaj, G., Formation of disulfide bonds in proteins and peptides. *Biotechnology advances* **2005**, *23* (1), 87-92.
77. Hossain, M. A.; Belgi, A.; Lin, F.; Zhang, S.; Shabanpoor, F.; Chan, L.; Belyea, C.; Truong, H.-T.; Blair, A. R.; Andrikopoulos, S., Use of a temporary “solubilizing” peptide tag for the Fmoc solid-phase synthesis of human insulin glargine via use of regioselective disulfide bond formation. *Bioconjugate chemistry* **2009**, *20* (7), 1390-1396.
78. Taylor, J. W., The synthesis and study of side chain lactam bridged peptides. *Peptide Science* **2002**, *66* (1), 49-75.
79. Monincová, L.; Slaninová, J.; Fučík, V.; Hovorka, O.; Voburka, Z.; Bednárová, L.; Maloň, P.; Štokrová, J.; Čerovský, V., Lasiocepsin, a novel cyclic antimicrobial peptide from the venom of eusocial bee *Lasioglossum laticeps* (Hymenoptera: Halictidae). *Amino acids* **2012**, *43* (2), 751-761.
80. Mochizuki, M.; Tsuda, S.; Tanimura, K.; Nishiuchi, Y., Regioselective Formation of Multiple Disulfide Bonds with the Aid of Postsynthetic S-Tritylation. *Organic Letters* **2015**, *17* (9), 2202-2205.
81. Albericio, F.; Annis, I.; Royo, M.; Barany, G., Preparation and handling of peptides containing methionine and cysteine. *ChemInform* **2000**, *31* (43).
82. Tang, J.-G.; Wang, Z.-H.; Tregear, G. W.; Wade, J. D., Human gene 2 relaxin chain combination and folding. *Biochemistry* **2003**, *42* (9), 2731-2739.
83. Bathgate, R. A.; Lin, F.; Hanson, N. F.; Otvos, L.; Guidolin, A.; Giannakis, C.; Bastiras, S.; Layfield, S. L.; Ferraro, T.; Ma, S., Relaxin-3: improved synthesis strategy and demonstration of its high-affinity interaction with the relaxin receptor LGR7 both in vitro and in vivo. *Biochemistry* **2006**, *45* (3), 1043-1053.
84. Góngora-Benítez, M.; Tulla-Puche, J.; Paradís-Bas, M.; Werbitzky, O.; Giraud, M.; Albericio, F., Optimized Fmoc solid-phase synthesis of the cysteine-rich peptide linacotide. *Peptide Science* **2011**, *96* (1), 69-80.
85. Hossain, M. A.; Lin, F.; Zhang, S.; Ferraro, T.; Bathgate, R. A.; Tregear, G. W.; Wade, J. D., Regioselective disulfide solid phase synthesis, chemical characterization and in vitro

receptor binding activity of equine relaxin. *International Journal of Peptide Research and Therapeutics* **2006**, *12* (3), 211-215.

86. Moroder, L.; Musiol, H. J.; Götz, M.; Renner, C., Synthesis of single- and multiple-stranded cystine-rich peptides. *Peptide Science* **2005**, *80* (2-3), 85-97.

87. Ellman, G. L., A colorimetric method for determining low concentrations of mercaptans. *Archives of biochemistry and Biophysics* **1958**, *74* (2), 443-450.

88. Aguilar, M.-I.; Hearn, M. T. W., High-resolution reversed-phase high-performance liquid chromatography of peptides and proteins. *Methods in enzymology* **1996**, *270*, 3-26.

89. Ambulos, N.; Bibbs, L.; Bonewald, L.; Kates, A.; Khatri, A.; Weintraub, S., Analysis of Synthetic Peptide. *Solid-Phase Synthesis. A Practical Guide* **2000**, *1*, 751-789.

90. Galande, A. K.; Trent, J. O.; Spatola, A. F., Understanding Base-Assisted Desulfurization Using a Variety of Disulfide-Bridged Peptides. *Biopolymers (Peptide Science)* **2003**, *71*, 534-551.

91. Edelheit, O.; Hanukoglu, I.; Dascal, N.; Hanukoglu, A., Identification of the roles of conserved charged residues in the extracellular domain of an epithelial sodium channel (ENaC) subunit by alanine mutagenesis. *Am. J. Physiol. Renal Physiol.* **2011** *300* (4), 887–897.

92. Marcos, J. F.; Muñoz, A.; Pérez-Payá, E.; Misra, S.; López-García, B., Identification and Rational Design of Novel Antimicrobial Peptides for Plant Protection. *Annu. Rev. Phytopathol.* **2008**, *46*, 273–301.

93. Helmerhors, E. J.; Breeuwer, P.; Van 't Hof, W.; Walgreen-Weterings, E.; Oomeni, L. C.; Veerman, E. C. I.; Amerongen, N. A. V.; Abee, T., The Cellular Target of Histatin 5 on *Candida albicans* Is the Energized Mitochondrion. *Journal of Biological Chemistry* **1999**, *274* (11), 7286-7291.

94. Epanand, R. M.; Vogel, H. J., Diversity of antimicrobial peptides and their mechanisms of action. *Biochim. Biophys. Acta* **1999**, *1462* (1-2), 11–28.

95. Chan, D. I.; Prenner, E. J.; Vogel, H. J., Tryptophan- and arginine-rich antimicrobial peptides: Structures and mechanisms of action. *Biochim. Biophys. Acta* **2006**, *1758* (9), 1184–1202.

96. Van Loon, L. C.; Rep, M.; Pieterse, C. M. J., Significance of inducible defense-related proteins in infected plants. *Annu. Rev. Phytopathol.* **2006**, *44*, 135–162.

97. Dathe, M.; Wieprecht, M., Structural features of helical antimicrobial peptides: their potential to modulate activity on model membranes and biological cells. *Biochimica et Biophysica Acta* **1999**, *71*-78.

98. Eisenberg, D.; Weiss, R. M.; Terwilliger, T. C., The helical hydrophobic moment: a measure of the amphiphilicity of  $\alpha$ -helix. *Nature* **1982**, *299* (5881), 371-374.

99. Gautier, R.; Douguet, D.; Antony, B.; Drin, G., HELIQUEST: a web server to screen sequences with specific  $\alpha$ -helical properties. *Bioinformatics* **2008**, *24* (18), 2101-2102.

100. Tam, J. P.; Lu, Y.-A.; Yang, J.-L., Antimicrobial dendrimeric peptides. *Eur. J. Biochem.* **2002**, *269* (3), 923-932.

101. Subirós-Funosas, R.; Prohens, R.; Barbas, R.; El-Faham, A.; Albericio, F., Oxyma: An efficient additive for peptide synthesis to replace the benzotriazole-based HOBt and HOAt with a lower risk of explosion. *Chem. Eur. J.* **2009**, *15* (37), 9394–9403.

102. Dougherty, D. A., *Modern Physical Organic Chemistry*. 2006.

103. (a) Anderson, D. E.; Becktel, W. J.; Dahlquist, F. W., pH-Induced Denaturation of Proteins: A Single Salt Bridge Contributes 3-5 kcal/mol to the Free Energy of Folding of T4 Lysozyme. *Biochemistry* **1990**, *29* (9), 2403–2408; (b) Horovitz, A.; Serrano, L.; Avron, B.; Bycroft, M.; Fersht, A. R., Strength and Co-operativity of Contributions of Surface Salt Bridges to Protein Stability. *J. Mol. Biol.* **1990**, *216* (4), 1031–1044.

104. Mihailescu, E.; Worcester, D.; Castro-Roman, F.; Fernandez-Vidal, M.; White, S. H., Determining the Water Content of Lipid Membranes by Neutron Diffraction. *Biophysical Journal* **2010**, *98* (3), 286A.
105. Liang, M.; Patwardhan, S. V.; Danilovtseva, E. N.; Annenkov, V. V.; Perry, C. C., Imidazole catalyzed silica synthesis: Progress toward understanding the role of histidine in (bio) silicification. *Journal of Materials Research* **2009**, *24* (5), 1700-1708.
106. Henchey, L. K.; Jochim, A. L.; Arora, P. S., Contemporary strategies for the stabilization of peptides in the  $\alpha$ -helical conformation. *Current Opinion in Chemical Biology* **2008**, *12* (6), 692–697.
107. Garay, H.; Espinosa, L. A.; Perera, Y.; Sánchez, A.; Diago, D.; Perea, S. E.; Besada, V.; Reyes, O.; González, L. J., Characterization of low-abundance species in the active pharmaceutical ingredient of CIGB-300: A clinical-grade anticancer synthetic peptide. *J. Pep. Sci.* **2018**, *24* (6), e3081.
108. Larsen, R. A.; Bauer, M.; Thomas, A. M.; Graybill, J. R., Amphotericin B and Fluconazole, a Potent Combination Therapy for Cryptococcal Meningitis. *Antimicrobial Agents and Chemotherapy* **2004**, *48* (3), 985-991.
109. Richardson, M. D., Changing patterns and trends in systemic fungal infections. *Journal of Antimicrobial Chemotherapy* **2005**, *56* (1), i5-i11.
110. Sieprawska-Lupa, M.; Mydel, P.; Krawczyk, K.; Wójcik, K.; Puklo, M.; Lupa, B.; Suder, P.; Silberring, J.; Reed, M.; Pohl, J.; Shafer, W.; McAleese, F.; Foster, T.; Travis, J.; Potempa, J., Degradation of human antimicrobial peptide LL-37 by *Staphylococcus aureus*-derived proteinases. *Antimicrob Agents Chemother* **2004**, *48* (12), 4673-4679.
111. Steinberg, D. A.; Lehrer, R. I., Designer assays for antimicrobial peptides. Disputing the "one-size-fits-all" theory. *Methods Mol Biol* **1997**, *78*, 169-186.
112. Turner, J.; Cho, Y.; Dinh, N. N.; Waring, A. J.; Lehrer, R. I., Activities of LL-37, a Cathelin-Associated Antimicrobial Peptide of Human Neutrophils. *Antimicrobial Agents and Chemotherapy* **1998**, *42* (9), 2206-2214.
113. Ramaswamy, V.; Cresence, V. M.; Rejitha, J. S.; Lekshmi, M. U.; Dharsana, K. S.; Prasad, S. P.; Vijila, H. M., *Listeria*—review of epidemiology and pathogenesis. *J. Microbiol. Immunol. Infect.* **2007**, *40* (1), 4-13.
114. Balcht, A.; Smith, R., *Pseudomonas aeruginosa: Infections and Treatment. Informa Health Care* **1994**, 83-84.
115. Wu, M.; Hancock, R. E., Improved derivatives of bactenecin, a cyclic dodecameric antimicrobial cationic peptide. *Antimicrob. Agents Chemother.* **1998**, *43* (5), 1274-1276.
116. Ashrafuzzaman, M. D.; Andersen, O. S.; McElhaney, R. N., The antimicrobial peptide gramicidin S permeabilizes phospholipid bilayer membranes without forming discrete ion channels. *Biochimica et Biophysica Acta* **2008**, *1778* (12), 2814-2822.
117. Koyama, Y.; Motobu, M.; Hikosaka, K.; Yamada, M.; Nakamura, K.; Saido-Sakanaka, H.; Asaoka, A.; Yamakawa, M.; Isobe, T.; Shimura, K.; Kang, C. B.; Hayashidani, H.; Nakai, Y.; Hirota, Y., Cytotoxicity and antigenicity of antimicrobial synthesized peptides derived from the beetle *Allomyrina dichotoma* defensin in mice. *Int Immunopharmacol* **2006**, *6* (11), 1748-1753.
118. Pick, N.; Cameron, S.; Arad, D.; Av-Gay, Y., Screening of Compounds Toxicity against Human Monocytic cell line-THP-1 by Flow Cytometry. *Biol. Proced Online* **2004**, *6*, 220-225.
119. Micsonai, A.; Wienb, F.; Kernya, L.; Lee, Y. H.; Goto, Y.; Réfrégiers, M.; Kardos, J., Accurate secondary structure prediction and fold recognition for circular dichroism spectroscopy. *PNAS* **2015**, *112* (24), E3095-103.
120. Satoh, K.; Makimura, K.; Hasumi, Y.; Nishiyama, Y.; Uchida, K.; Yamagu-chi, H., *Candida auris* sp. nov., a novel ascomycetous yeast isolated from the external ear canal of an inpatient in a Japanese hospital. *Microbiol Immunol* **2009**, *53* (1), 41–44.



121. Reference method for broth dilution antifungal susceptibility testing of yeasts; approved standard In *CLSI document M27-A3*, Third edition ed.; **2008**; pp 1-25.
122. Lambert, R. J. W.; Pearson, J., Susceptibility testing: Accurate and reproducible minimum inhibitory concentration (MIC) and non-inhibitory concentration (NIC) values. *J. Appl. Microbiol.* **2000**, *88* (5), 784–790.
123. Case, D. A.; Darden, T. A.; Cheatham, T. E.; Simmerling, C. L.; Wang, J., AMBER11. University of California, San Francisco, **2010**.
124. Malina, A.; Shai, Y., Conjugation of fatty acids with different lengths modulates the antibacterial and antifungal activity of a cationic biologically inactive peptide. *Biochemical Journal* **2005**, *390* (3), 695-702.
125. (a) Zhang, L., Bulaj, G. , Converting Peptides into Drug Leads by Lipidation. *Current Medicinal Chemistry* **2012**, *19*, 1602-1618; (b) Irwin, N.; Green, B. D.; Gault, V. A.; Greer, B.; Harriott, P.; Bailey, C. J.; Flatt, P. R.; O'Harte, F. P., Degradation, insulin secretion, and antihyperglycemic actions of two palmitate-derivitized *N*-terminal pyroglutamyl analogues of glucose-dependent insulinotropic polypeptide. *J. Med. Chem.* **2005**, *48* (4), 1244-1250.
126. Meena, K. R.; Kanwar, S. S., Lipopeptides as the Antifungal and Antibacterial Agents: Applications in Food Safety and Therapeutics. *BioMed Research International* 2014, **2015**, 1-9.
127. Mandal, S. M.; Sharma, S.; Pinnaka, A. K.; Kumari, A.; Korpole, S., Isolation and characterization of diverse antimicrobial lipopeptides produced by *Citrobacter* and *Enterobacter*. *BMC Microbiology* **2013**, *13* (152).
128. (a) Emmert, E. A. B.; Handelsman, J., Biocontrol of plant disease: a (Gram-) positive perspective. *FEMS Microbiology Letters* **1999**, *1*, 1–9; (b) Roongsawang, N.; Washio, K.; Morikawa, M., Diversity of nonribosomal peptide synthetases involved in the biosynthesis of lipopeptide biosurfactants. *International Journal of Molecular Sciences* **2011**, *12*, 141–172.
129. Ongena, M.; Jacques, P., Bacillus lipopeptides: versatile weapons for plant disease biocontrol. *Trends in Microbiology* **2008**, *16*, 115–125.
130. Sharma, D.; Mandal, S. M.; Manhas, R. K., Purification and characterization of a novel lipopeptide from *Streptomyces amritsarensis* sp.nov.active against methicillin-resistant *Staphylococcus aureus*. *AMB Express* **2014**, *4*, 50.
131. Deris, Z. Z.; Swarbrick, J. D.; Roberts, K. D., Probing the penetration of antimicrobial polymyxin lipopeptides into gram-negative bacteria. *Bioconjugate Chemistry* **2014**, *25*, 750–760.
132. Kaiser, A.; Gaidzik, N.; Becker, T.; Menge, C.; Groh, K.; Cai, H.; Yan-Mei, L.; Gerlitzki, B.; Schmitt, E.; Kunz, H., Fully Synthetic Vaccines Consisting of Tumor-Associated MUC1 Glycopeptides and a Lipopeptide Ligand of the Toll-like Receptor 2. *Angew. Chem. Int. Ed.* **2010**, *49*, 3688 –3692.
133. Rescigno, M.; Urbano, M.; Rimoldi, M.; Valzasina, B.; Rotta, G.; Granucci, F. P., Toll-like receptor 4 is not required for the full maturation of dendritic cells or for the degradation of Gram-negative bacteria *European journal of immunology* **2002**, (32), 2800–2806.
134. Tarwadi; Jazayeri, J. A.; Prankerd, R. J.; Pouton, C. W., Preparation and in Vitro Evaluation of Novel Lipopeptide Transfection Agents for Efficient Gene Delivery. *Bioconjugate Chem.* **2008**, *19* (4), 940–950.
135. Kaya, K.; Mahakhant, A.; Keovara, L.; Sano, T.; Kubo, T.; Takagi, H., Spiroidesin, a Novel Lipopeptide from the Cyanobacterium *Anabaena spiroides* That Inhibits Cell Growth of the Cyanobacterium *Microcystis aeruginosa*. *J. Nat. Prod.* **2002**, *65* (6), 920-921.
136. Olsen, H. B.; Kaarsholm, N. C., Structural Effects of Protein Lipidation as Revealed by LysB29-myristoyl, des(B30) Insulin. *Biochemistry* **2000**, *39* (39), 11893-11900.

137. Sarwar, A.; Brader, G.; Corretto, E.; Aleti, G.; Abaidullah, M.; Sessitsch, A.; Hafeez, F. Y., Qualitative analysis of biosurfactants from *Bacillus* species exhibiting antifungal activity. *PLOS ONE* **2018**, *13* (6), 1-15.
138. Hang, H. C.; Linder, M. E., Exploring Protein Lipidation with Chemical Biology. *Chem. Rev.* 2011, *111*, 6341–6358.
139. Wittmann, M.; Linne, U.; Pohlmann, V.; Marahiel, M. A., Role of DptE and DptF in the lipidation reaction of daptomycin. *FEBS Journal* **2008**, *275*, 5343-5354.
140. Nadolski, M. J.; Linder, M. E., Protein lipidation. . *FEBS Journal* **2007**, *274*, 5202–5210.
141. James P. Tam, Y.-A. L., Jin-Long Yang, Antimicrobial dendrimeric peptides. *Eur. J. Biochem.* **2002**, *269*, 923–932.
142. Baltz, R. H.; Nguyen, K. T.; Alexander, D. C., Reprogramming Daptomycin and A54145 Biosynthesis to produce novel lipopeptide antibiotics. In *Enzyme Technologies: Metagenomics, Evolution, Biocatalysis and Biosynthesis*, John Wiley & Sons, Inc.: Lexington, Massachusetts, **2010**; pp 285-308.
143. Kragol, G.; Lumbierres, M.; Palomo, J. M.; Waldmann, H., Solid-Phase Synthesis of Lipidated Peptides. *Angew. Chem. Int. Ed.* **2004**, *43*, 5839–5842.
144. Douat, C.; Heitz, A.; Paris, M.; Martínez, J.; Fehrentz, J., Post-synthesis Incorporation of a Lipidic Side Chain into a Peptide on Solid Support. *J. Peptide Sci.* **2002**, *8* (5), 601–614.
145. Alsina, J.; Albericio, F., Solid-Phase Synthesis of C-Terminal Modified Peptides. *Biopolymers (Peptide Science)* **2003**, *71*, 454-477.
146. Morales, F. E.; Garay Pérez, H. E.; Muñoz, D. F.; Augusto, Y. E.; Otero-González, A. J.; Reyes Acosta, O.; Rivera, D. G., Aminocatalysis-Mediated on-Resin Ugi Reactions: Application in the Solid-Phase Synthesis of N-Substituted and Tetrazolo Lipopeptides and Peptidosteroids. *Organic letters* **2015**.
147. (a) Zhu, J.; Bienaymé, H., *Multicomponent Reactions*. WILEY-VCH Verlag GmbH & Co. KGaA: Weinheim, Germany, **2005**; (b) El Kaim, L.; Grimaud, L., Beyond the Ugi reaction: less conventional interactions between isocyanides and iminium species. *Tetrahedron* **2009**, *65*, 2153-2171.
148. Rotstein, B. H.; Zaretsky, S.; Rai, V.; Yudin, A. K., Small heterocycles in multicomponent reactions. *Chemical Reviews* **2013**, 1-116.
149. Dömling, A.; Ugi, I., Multicomponents reaction with isocyanides. *Angew. Chem. Int. Ed.* **2000**, *39*, 3168-3210.
150. Ugi, I.; Werner, B.; Dömling, A., The Chemistry of Isocyanides, their Multicomponent Reactions and their Libraries. *Molecules* **2003**, *8*, 53-66.
151. Banfi, L.; Basso, A.; Guanti, G.; Riva, R., Asymmetric Isocyanide-based MCRs. In *Multicomponent Reactions* Zhu, J.; Bienaymé, H., Eds. WILEY-VCH Verlag GmbH & Co. KGaA: Weinheim, Germany, **2005**; pp 1-33.
152. (a) Short, K. M.; Ching, B. W.; Mjalli, A. M. M., The Synthesis of Hydantoin 4-Imides on Solid Support. *Tetrahedron Letters* **1996**, *37* (42), 7489-7492; (b) Arshady, R.; Ugi, I., Solid Phase Peptide Synthesis by Four Component Condensation: Peptide Formation on an Isocyanide Polymer Support. *Naturforschung* **1981**, *36b*, 1202-1203.
153. (a) Kim, S. W.; Bauer, S. M.; Armstrong, R. W., Construction of Combinatorial Chemical Libraries Using a Rapid and Efficient Solid Phase Synthesis Based on a Multicomponent Condensation Reaction. *Tetrahedron Letters* **1998**, *39*, 6993-6996; (b) Oertel, K.; Zech, G.; Kunz, H., Stereoselective Combinatorial Ugi-Multicomponent Synthesis on Solid Phase. *Angew. Chem. Int. Ed.* **2000**, *39* (8), 1431-1433.
154. (a) Zhang, C.; Moran, E. J.; Woiwode, T. F.; Short, K. M.; Mjalli, A. M. M., Synthesis of Tetrasubstituted Imidazoles via  $\alpha$ -(N-acyl-N-alkylamino)- $\beta$ -ketoamides on Wang Resin. *Tetrahedron Letters* **1996**, *37* (6), 751-754; (b) Strocker, A. M.; Keating, T. A.; Tempest, P. A.;

- Amstrong, R. W., Use of a Convertible Isocyanide for Generation of Ugi Reaction Derivatives on Solid Support: Synthesis of  $\alpha$ -Acylaminoesters and Pyrroles. *Tetrahedron Letters* **1996**, 37 (8), 1149-1152.
155. Hulme, C.; Peng, J.; Morton, G.; Salvino, J. M.; Herpin, T.; Labaudiniere, R., Novel Safety-Catch Linker and its Application with a Ugi/De-BOC/Cyclization (UDC) Strategy to access Carboxylic acids, 1,4-Benzodiazepines, Diketopiperazines, Ketopiperazines and Dihydroquinoxalinones. *Tetrahedron Letters* **1998**, 39, 7227-7230.
156. (a) Hoel, A. M.; Neilsen, J., Microwave Assisted Solid-Phase Ugi Four Component Condensation. *Tetrahedron Lett.* 1999, 40, 3941-3944; (b) Lew, A.; Krutzik, P. O.; Hart, M. E.; Chamberlin, A. R., Increasing Rates of Reaction: Microwave-Assisted Organic Synthesis for Combinatorial Chemistry. *Journal of Combinatorial Chemistry* **2002**, 4 (2), 45-63.
157. Bisai, V.; Bisai, A.; Singh, V. K., Enantioselective organocatalytic aldol reaction using small organic molecules. *Tetrahedron* **2012**, 68 (24), 4541-4580.
158. Pierson, N. A.; Chen, L.; Russell, D. H.; Clemmer, D. E., Cis-Trans Isomerizations of Proline Residues are Key to Bradykinin Conformations. *J Am Chem Soc* **2014**, 135 (8), 3186-3192.
159. Krieger, F.; Moglich, A.; Kiefhaber, T., Effect of Proline and Glycine Residues on Dynamics and Barriers of Loop Formation in Polypeptide Chains. *J. Am. Chem. Soc.* **2005**, 127, 3346-3352.
160. Florance, H. V.; Stopford, A. P.; Kalapothakis, J. M.; McCullough, B. J.; Bretherick, A.; Barran, P. E., Evidence for  $\alpha$ -helices in the gas phase: A case study using Melittin from honey bee venom. *Analyst* **2011**, 136, 3446-3452.
161. Wolffe, A. P.; Khochbin, P. S.; Dimitrov, S., What do linker histones do in chromatin? *BioEssays* **1997**, 19, 249-255.
162. Hartman, P. G.; Chapman, G. E.; Moss, T.; Bradbury, E. M., Studies on the role and mode of operation of the very-lysine-rich histone H1 in eukaryotic chromatin: The three structural regions of the histone H1 molecule. *Eur. J. Biochem.* **1977**, 77, 45-51.
163. Vila, R.; Ponte, I.; Jimenez, M. A.; Rico, M.; Suau, P., An inducible helix-Gly-Gly-helix motif in the N-terminal domain of histone H1e: A CD and NMR study. *Protein Science* **2002**, 11, 214-220.
164. Jeanteur, D.; Lakey, J. H.; Pattus, F., The bacterial porin superfamily: Sequence alignment and structure prediction. *Mol. Microbiol.* **1991**, 5, 2153-2164.
165. Van Gelder, P.; Saint, N.; van Boxtel, R.; Rosenbusch, J. P.; Tommassen, J., Pore functioning of outer membrane protein PhoE of Escherichia coli: Mutagenesis of the constriction loop L3. *Protein Eng.* **1997**, 10, 699-706.
166. Khan, A. R.; Johnson, K. A.; Braam, J.; James, M. N. G., Comparative modeling of the three-dimensional structure of the calmodulin-related TCH2 protein from Arabidopsis. *Prot. Struc. Func. Genet.* **1997**, 27, 144-153.
167. Salam, N. K.; Adzhigirey, M.; Sherman, W.; Pearlman, D. A., Structure-based approach to the prediction of disulfide bonds in proteins. *Protein Engineering Design and Selection* **2014**, 27 (10), 365-374.
168. González-García, M. Caracterización funcional complementaria del péptido antifúngico Cm-p5 y de sus análogos sintéticos. Tesis de Diploma, Universidad de La Habana, **2016**.
169. Oddo, A.; Hansen, P. R., Hemolytic Activity of Antimicrobial Peptides. *Methods Mol Biol.* **2017**, 1548, 427-435.
170. Wright, L. R.; Borkman, R. F., Ab Initio Self-Consistent Field Studies of the Peptides Gly-Gly, Gly-Ala, Ala-Gly, GI y-Gly-Gly. *J. Phys. Chem. B* **1982**, 86, 3956-3962.
171. Morejón, M. C.; Laub, A.; Westermann, B.; Rivera, D. G.; Wessjohann, A., Solution and Solid-Phase Macrocyclization of Peptides by the Ugi-Smiles Multicomponent Reaction: Synthesis of N-Aryl-Bridged Cyclic Lipopeptides. *Organic letters* **2016**, 18 (16), 4096-4099.

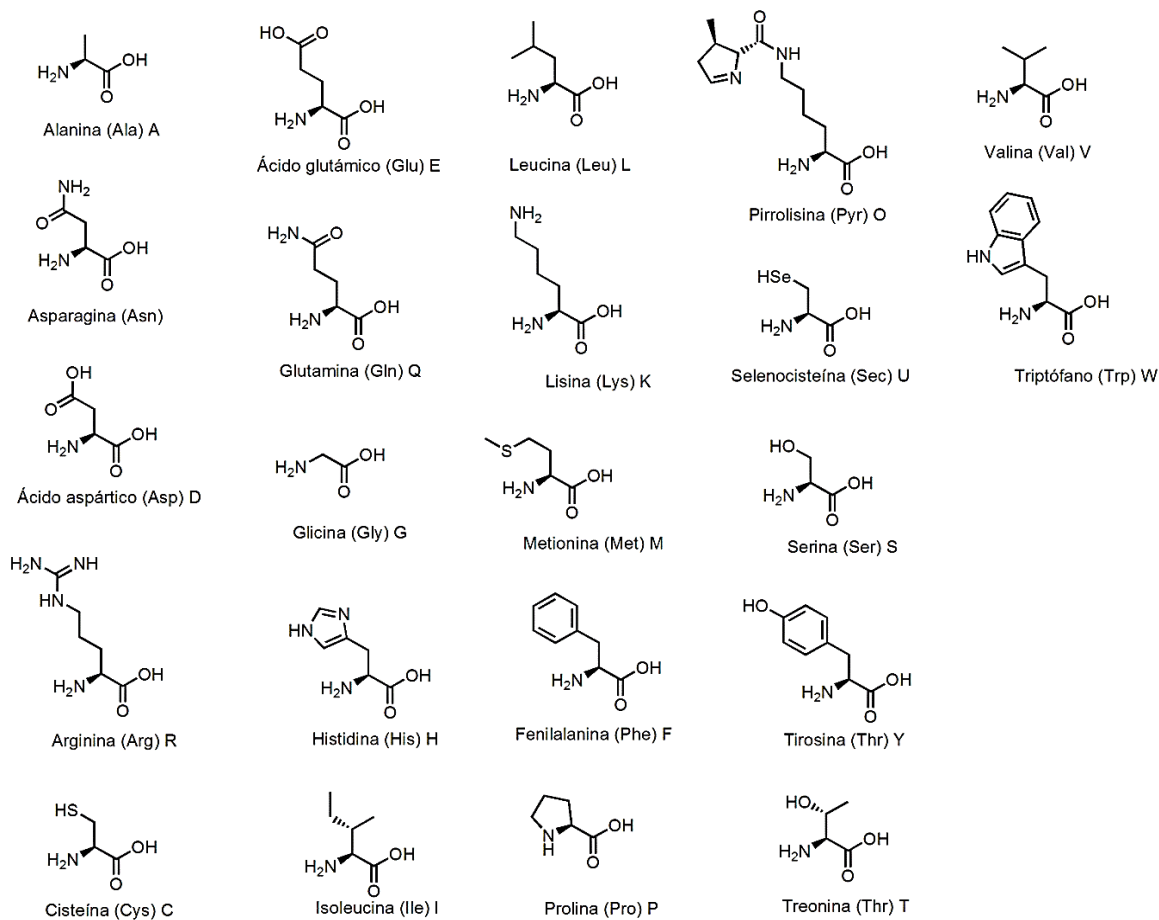
172. He, R.; Finan, B.; Mayer, J. P.; DiMarchi, R. D., Peptide conjugates with small molecules designed to enhance efficacy and safety. *Molecules* **2019**, *24* (10), 1855.
173. Ma, L.; Wang, C.; He, Z.; Cheng, B.; Zheng, L.; Huang, K., Peptide-drug conjugate: a novel drug design approach. *Current medicinal chemistry* **2017**, *24* (31), 3373-3396.
174. Aluri, S.; Janib, S. M.; Mackay, J. A., Environmentally responsive peptides as anticancer drug carriers. *Advanced drug delivery reviews* **2009**, *61* (11), 940-952.
175. Scott, C. J.; Taggart, C. C., Biologic protease inhibitors as novel therapeutic agents *Biochimie* **2010**, *92* 1681-1688.
176. Ji Eun, P.; Joonyoung, P.; Yearin, J.; Yunseok, O.; Gongmi, R.; Yoo-Seong, J.; G., H. H.; Jee Sun, M.; Jung Hwan, J., Expanding therapeutic utility of carfilzomib for breast cancer therapy by novel albumin-coated nanocrystal formulation. *Journal of Controlled Release* **2019**, *302*, 148-159.
177. Staudacher, A. H.; Brown, M. P., Antibody drug conjugates and bystander killing: is antigen-dependent internalisation required. *British Journal of Cancer* **2017**, *117* 1736-1742.
178. Guerrero-Garcia, T. A.; Gandolfi, S.; Laubach, J. P.; Hideshima, T.; Chauhan, D.; Mitsiades, C.; Anderson, K.; Richardson, P. G., The power of proteasome inhibition in multiple myeloma. *Expert Review of Proteomics* **2018**, *15* (22), 1033-1052.
179. Efentakis, P.; Kremastiotis, G.; Varela, A.; Nicolau, P. E.; Papanagnou, E. D.; Davos, C. H.; Tsoumani, M.; Agrogiannis, G.; Konstantinidou, A., Molecular mechanisms of carfilzomib-induced cardiotoxicity in mice and the emerging cardioprotective role of metformin. *Blood* **2018**, *133* (7), 710-723.
180. Meng, L.; Mohan, R.; Kwok, B. H.; Elofsson, M.; Sin, N.; Crews, C. M., Epoxomicin, a potent and selective proteasome inhibitor, exhibits in vivo antiinflammatory activity. *Proc. Natl. Acad. Sci. U. S. A.* **1999**, *96* (18), 10403-10408
181. Sin, N.; Kim, K. B.; Elofsson, M.; Meng, L.; Auth, H.; Kwok, B. H.; Crews, C. M., Total synthesis of the-potent proteasome inhibitor epoxomicin: a useful tool for understanding proteasome biology *Bioorg. Med. Chem. Lett.* **1999**, *9* (15), 2283-2288.
182. Kim, K. B.; Crews, C. M., From epoxomicin to carfilzomib: chemistry, biology, and medical outcomes. *Nat. Prod. Rep.* **2013**, *30* 600-604.
183. Groll, M.; Kim, K. B.; Kairies, N.; Huber, R.; Crews, C. M., Crystal Structure of Epoxomicin: 20S Proteasome Reveals a Molecular Basis for Selectivity of  $\alpha'$ ,  $\beta'$ -Epoxyketone Proteasome Inhibitors *J. Am. Chem. Soc.* **2000**, *122* 1237-1238.
184. Hughes, D. L., Patent Review of Manufacturing Routes to Oncology Drugs: Carfilzomib, Osimertinib, and Venetoclax. *Org. Process Res.* **2016**, *20* (12), 2028-2042.
185. Mullard, A., Maturing antibody-drug conjugate pipeline hits 30. *Nature Reviews Drug Discovery* **2013**, *12* (5), 329-332.
186. Lu, J.; Jiang, F.; Lu, A.; Zhang, G., Linkers having a crucial role in antibody-drug conjugates. *International journal of molecular sciences* **2016**, *17* (4), 561.
187. Chari, R. V. J.; Martell, B. A.; Gross, J. L.; Cook, S. B.; Shah, S. A.; Blättler, W. A.; McKenzie, S. J.; Goldmacher, V. S., Immunoconjugates containing novel maytansinoids: promising anticancer drugs. *Cancer Research* **1992**, *52* (1), 127-131.
188. Axup, J. Y.; Bajjuri, K. M.; Ritland, M., Synthesis of site-specific antibody-drug conjugates using unnatural amino acids. *Proc. Natl. Acad. Sci. U.S.A.* **2012**, *109* (40), 16101-16106.
189. García-Alonso, S.; Ocana, A.; Pandiella, A., Resistance to Antibody-Drug Conjugates. *Cancer Res* **2018**, 1-7.
190. Beck, A.; Goetsch, L.; Dumontet, C.; Corvaia, N., Strategies and challenges for the next generation of antibody-drug conjugates. *Chem. Soc. Rev.* **2017**, *19* (16), 315-337.
191. McCombs, J. R.; Owen, S. C., Antibody drug conjugates: design and selection of linker, payload and conjugation chemistry. *The AAPS journal* **2015**, *17* (2), 339-351.

192. Nolting, B., Linker technologies for antibody–drug conjugates. In *Antibody-Drug Conjugates*, Springer: **2013**; pp 71-100.
193. Anurag, A. J. R.; Weiskopf, A.; Rathore, S., Defining critical quality attributes for monoclonal antibody therapeutic products. *BioPharm International* **2014**, *27* (7), 1-3.
194. Tsuchikama, K.; An, Z., Antibody-drug conjugates: recent advances in conjugation and linker chemistries. *Protein & cell* **2018**, *9* (1), 33-46.
195. Lyon, R. P.; Setter, J. R.; Bovee, T. D.; Doronina, S. O.; Hunter, J. H.; Anderson, M. E.; Balasubramanian, C. L.; Duniho, S. M.; Leiske, C. I.; Li, F., Self-hydrolyzing maleimides improve the stability and pharmacological properties of antibody-drug conjugates. *Nature Biotechnology* **2014**, *32* (10), 1059.
196. Baldwin, A. D.; Kiick, K. L., Tunable degradation of maleimide–thiol adducts in reducing environments. *Bioconjugate chemistry* **2011**, *22* (10), 1946-1953.
197. Francisco, J. A.; Cervený, C. G.; Meyer, D. L.; Mixan, B. J.; Klussman, K.; Chace, D. F.; Rejniak, S. X.; Gordon, K. A.; DeBlanc, R.; Toki, B. E., cAC10-vcMMAE, an anti-CD30–monomethyl auristatin E conjugate with potent and selective antitumor activity. *Blood* **2003**, *102* (4), 1458-1465.
198. Bernardim, B.; Cal, P.; Matos, M. J.; Oliveira, B. L.; Martínez-Sáez, N.; Albuquerque, I. S.; Perkins, E.; Corzana, F.; Burtoloso, A. C. B.; Jiménez-Osés, G., Stoichiometric and irreversible cysteine-selective protein modification using carbonylacrylic reagents. *Nature Communications* **2016**, *7*, 13128.
199. Staben, L. R.; Koenig, S. G.; Lehar, S. M.; Vandlen, R.; Zhang, D.; Chuh, J.; Yu, S.-F.; Ng, C.; Guo, J.; Liu, Y.; Fourie-O'Donohue, A.; Go, M.; Linghu, X.; Segraves, N. L.; Wang, T.; Chen, J.; Wei, B.; Lewis, G. D.; Xu, K.; Kozak, K. R.; Mariathasan, S.; Flygare, J. A.; Pillow, T. H., Targeted drug delivery through the traceless release of tertiary and heteroaryl amines from antibody–drug conjugates. *Nat. Chem.* **2016**, *8*, 1112–1119.
200. Menshutkin, N., Über die Affinitätskoeffizienten der Alkylhaloide und der Amine. *Zeitschrift für Physikalische Chemie* **1890**, *6* (1), 41-57.
201. Nicolaou, K. C.; Rigol, S., The Role of Organic Synthesis in the Emergence and Development of Antibody-Drug Conjugates as Targeted Cancer Therapies. *Angew. Chem. Int. Ed.* **2019**, *58*, 2–38.
202. He, X.; Li, J.; An, S.; Jiang, C., pH-sensitive drug-delivery systems for tumor targeting. *Therapeutic delivery* **2013**, *4* (12), 1499-1510.
203. Li, W.; Nicol, F.; Szoka Jr, F. C., GALA: a designed synthetic pH-responsive amphipathic peptide with applications in drug and gene delivery. *Advanced drug delivery reviews* **2004**, *56* (7), 967-985.
204. Nguyen, V. P.; Alves, D. S.; Scott, H. L.; Davis, F. L.; Barrera, F. N., A Novel Soluble Peptide with pH-Responsive Membrane Insertion. *Biophysical Journal* **2016**, *110* (3), 252a.
205. Song, Q.; Chuan, X.; Chen, B.; He, B.; Zhang, H.; Dai, W.; Wang, X.; Zhang, Q., A smart tumor targeting peptide–drug conjugate, pHLIP-SS-DOX: synthesis and cellular uptake on MCF-7 and MCF-7/Adr cells. *Drug delivery* **2016**, *23* (5), 1734-1746.
206. An, M.; Wijesinghe, D.; Andreev, O. A.; Reshetnyak, Y. K.; Engelman, D. M., pH-(low)-insertion-peptide (pHLIP) translocation of membrane impermeable phalloidin toxin inhibits cancer cell proliferation. *Proceedings of the National Academy of Sciences* **2010**, *107* (47), 20246-20250.
207. Moshnikova, A.; Moshnikova, V.; Andreev, O. A.; Reshetnyak, Y. K., Antiproliferative effect of pHLIP-amanitin. *Biochemistry* **2013**, *52* (7), 1171-1178.
208. Burns, K. E.; Hensley, H.; Robinson, M. K.; Thévenin, D., Therapeutic Efficacy of a Family of pHLIP–MMAF Conjugates in Cancer Cells and Mouse Models. *Molecular pharmaceutics* **2017**, *14* (2), 415-422.

209. Demoin, D. W.; Wyatt, L. C.; Edwards, K. J.; Abdel-Atti, D.; Sarparanta, M.; Pourat, J.; Longo, V. A.; Carlin, S. D.; Engelman, D. M.; Andreev, O. A., PET imaging of extracellular pH in tumors with <sup>64</sup>Cu- and <sup>18</sup>F-labeled pHLIP peptides: a structure–activity optimization study. *Bioconjugate chemistry* **2016**, *27* (9), 2014-2023.
210. Thévenin, D.; An, M.; Engelman, D. M., pHLIP-mediated translocation of membrane-impermeable molecules into cells. *Chemistry & Biology* **2009**, *16* (7), 754-762.
211. Lundquist, I. V.; Joseph, T.; Satterfield, A. D.; Pelletier, J. C., Mild and adaptable silver triflate-assisted method for trityl protection of alcohols in solution with solid-phase loading applications. *Organic Letters* **2006**, *8* (18), 3915-3918.

## Annexes

### Annex 1: Structure, name and three and one letter code of the 22 essential aminoacids.



### Annex 2: Relative swelling capacity of some solvents related to poliestirene resins.

Solvent	Relative swelling capacity	Solvent	Relative swelling capacity
THF	5,5	DMA	3,4
DCM	5,1	Et <sub>2</sub> O	2,5
Dioxane	4,6	ACN	2,0
Toluene	4,5	EtOH	1,05
DMF	3,5	MeOH	0,95

**Annex 3:  $^1\text{H}$ -NMR of peptides 6 (upper panel, FMV025) and 8 (lowerpanel, FMV034)in DMSO-d6.**

